

**BIOSORPTION OF PRECIOUS METALS FROM SYNTHETIC
AND REFINERY WASTEWATERS BY IMMOBILIZED
*SACCHAROMYCES CEREVISIAE***

By

CHERIE-LYNN MACK

March 2008

ABSTRACT

The process of precious metal refining can be up to 99.99 % efficient at best, and although it may seem small, the amount of valuable metal lost to waste streams is appreciable enough to warrant recovery. The method currently used to remove entrained metal ions from refinery wastewaters, chemical precipitation, is not an effective means for selective recovery of precious metals from a wastewater. Biosorption, the ability of certain types of biomass to bind and concentrate metals from even very dilute aqueous solutions, may be an effective point-source metal recovery strategy. The yeast, *Saccharomyces cerevisiae*, has been found capable of sorbing numerous precious and base metals, and is a cheap and abundant source of biomass. As such, it represents a possible precious metal sorbent for application to refining wastewaters. In this investigation, *S. cerevisiae* biomass was immobilized, using polyethyleneimine and glutaraldehyde, to produce a suitable sorbent, which was found to be capable of high platinum uptake (150 to 170 mg/g) at low pH (< 2). The sorption mechanism was elucidated and found to be a chemical reaction, which made effective desorption impossible. The sorption process was investigated in a packed bed column conformation, the results of which showed that the diameter and height of the column require further optimization in order to attain the metal uptake values achieved in the batch studies. When applied to a refinery wastewater, two key wastewater characteristics limited the success of the sorption process; the high inorganic ion content and the complex speciation of the platinum ions. The results proved the concept principle of platinum recovery by immobilized yeast biosorption and indicated that a more detailed understanding of the platinum speciation within the wastewater is required before the biosorption process can be applied. Overall, the sorption of platinum by the *S. cerevisiae* sorbent was demonstrated to be highly effective in principle, but the complexity of the wastewater requires that pretreatment steps be taken before the successful application of this process to an industrial wastewater.

CURRICULUM VITAE

I am an environmental biotechnologist. My main interest lies in the mining industry with particular emphasis on the implementation of technologies aimed at reducing the environmental footprint associated with mining activities.

Research outputs based on PhD research project:

Mack, C., Wilhelmi, B., Duncan, J.R. and Burgess, J.E. (2008) A kinetic study of the recovery of platinum ions from an artificial aqueous solution by immobilized *Saccharomyces cerevisiae* biomass. *Minerals Engineering*. **21**, 31-37. (CHAPTER 6)

Mack, C., Wilhelmi, B., Duncan, J.R. and Burgess, J.E. (2007) Biosorption of precious metals. *Biotechnology Advances* **25(3)**, 264-271. (CHAPTER 2)

Mack, C., Wilhelmi, B., Duncan, J.R. and Burgess, J.E. (XXXX) Platinum biosorption from aqueous solution by immobilized *Saccharomyces cerevisiae*. *Process Biochemistry*. Submission under review. (CHAPTER 5)

Mack, C., Wilhelmi, B., Duncan, J.R. and Burgess, J.E. The influence of refining wastewater conditions on the sorption of platinum by immobilized *Saccharomyces cerevisiae* biomass. In preparation. (CHAPTERS 8 and 9)

Mack, C., Wilhelmi, B., Duncan, J.R. and Burgess, J.E. Immobilization of *Saccharomyces cerevisiae* to produce a biosorbent for platinum(IV) recovery from aqueous solutions. In preparation. (CHAPTER 4)

Conference outputs based on PhD research project:

Mack, C.L., Wilhelmi, B., Duncan, J.R. and Burgess, J.E. (2007) Kinetic evaluation of the sorption of platinum ions from aqueous solution by immobilized *Saccharomyces cerevisiae* biomass. *Bio- & Hydrometallurgy '07*, Falmouth, UK, May 1-2.

Mack, C.L., Wilhelmi, B., Duncan, J.R. and Burgess, J.E. (2006). Waste yeast for cost reduction of precious metal recovery from aqueous wastewaters: pH and temperature analysis. *Material, Minerals and Metal Ecology '06*, Cape Town, South Africa. November 14-15.

Confidential technical reports based on PhD research project:

Bioremediation Research Group (2007) Confidential Reports (1-4) to Anglo Platinum PLC

Bioremediation Research Group (2006) Confidential Reports (1-4) to Anglo Platinum PLC

Bioremediation Research Group (2005) Confidential Reports (1-4) to Anglo Platinum PLC

TABLE OF CONTENTS

Abstract	ii
<i>Curriculum Vitae</i>	iii
Table of contents	v
List of figures	x
List of tables	xv
List of abbreviations	xvi
Acknowledgements	xvii
Chapter 1 Introduction and synopsis	1
1.1 INTRODUCTION	1
1.2 SYNOPSIS	3
1.3 MATERIALS AND METHODS OVERVIEW	5
Chapter 2 Literature review	6
2.1 PLATINUM GROUP METALS	6
2.2 RECOVERY OF METALS FROM REFINING WASTEWATERS	9
2.3 BIOSORPTION OF METAL IONS	13
2.4 METAL BINDING MECHANISMS	15
2.4.1 Environmental factors affecting the biosorption mechanism	16
Solution pH	16
Solution temperature	18
Competing ions	19
2.4.2 Precious metal biosorption mechanisms	20
Gold	21
Platinum and palladium	22
2.5 YEAST BIOSORPTION	24
2.5.1 <i>Saccharomyces cerevisiae</i> biosorption	27
2.6 PRELIMINARY SUMMARY AND CONCLUSIONS	29
Chapter 3 Hypothesis, aims and objectives	32
3.1 HYPOTHESIS	32
3.2 AIM AND OBJECTIVES	32
3.2.1 Aim	32

3.2.2 Objectives	32
Chapter 4 Immobilization of <i>Saccharomyces cerevisiae</i> biomass	33
4.1 INTRODUCTION	33
4.1.1 The <i>Saccharomyces cerevisiae</i> cell wall	34
4.2 CHOICE OF IMMOBILIZATION TECHNIQUE	36
4.2.1 Common immobilization techniques	37
4.3 MATERIALS AND METHODS	39
4.3.1 Immobilization procedures	40
Carboxymethyl cellulose (CMC) beads	40
Silica granules	40
Polyethyleneimine modification and glutaraldehyde crosslinking	40
Calcium alginate entrapment	41
Alternate PEIGA sorbent production method	43
4.4 RESULTS	43
4.4.1 Immobilization procedure comparison	43
Carboxymethyl cellulose beads	43
Silica granules	44
PEIGA granules	45
Calcium alginate beads	46
4.4.2 Metal sorption analysis	47
4.4.3 PEIGA sorbent	50
4.5 DISCUSSION	53
4.5.1 Immobilization procedure analysis	53
4.5.2 Metal sorption analysis	54
4.5.3 PEIGA sorbent	55
4.6 SUMMARY	57
4.7 CONCLUSIONS	58
Chapter 5 Sorption of platinum by PEIGA-immobilized <i>S. cerevisiae</i> sorbent	59
5.1 INTRODUCTION	59
5.2 MATERIALS AND METHODS	59

5.2.1 Surface characterization	59
Scanning electron microscopy	59
Fourier Transform Infrared-Attenuated Total Reflectance (FTIR-ATR)	59
Calculation of surface area	60
Potentiometric titration	60
5.2.2 Sorption optimization	61
Batch sorption analysis	61
5.3 RESULTS	62
5.3.1 Surface characterization	62
Scanning electron microscopy	62
Fourier Transform Infrared-Attenuated Total Reflectance analysis	64
Surface area calculation	65
Potentiometric titration	68
5.3.2 Sorption optimization	69
Batch sorption analysis	69
5.4 DISCUSSION	72
5.4.1 Surface characterization	72
5.4.2 Sorption optimization	75
5.5 SUMMARY	77
5.6 CONCLUSIONS	78
Chapter 6 Equilibrium and kinetic modelling of platinum sorption	79
6.1 INTRODUCTION	79
6.2 SORPTION KINETICS	80
6.2.1 Kinetic modelling	80
6.2.2 Intraparticle diffusion model	82
6.2.3 Materials and Methods	82
6.2.4 Results	83
Effect of initial platinum concentration	83
Effect of sorbent dose	85
Effect of temperature	88
6.2.5 Discussion	90
6.3 SORPTION ISOTHERMS AND THERMODYNAMICS	93

6.3.1 Materials and Methods	94
6.3.2 Results	94
Effect of initial solution pH on sorption	94
Effect of solution temperature on sorption	95
6.3.3 Discussion	98
6.5 SUMMARY	101
6.6 CONCLUSIONS	103
Chapter 7 Application considerations	105
7.1 INTRODUCTION	105
7.2 MATHEMATICAL MODELLING OF BREAKTHROUGH CURVES	106
7.2.1 Materials and Methods	109
7.2.2 Results	110
7.2.3 Discussion	119
7.3 DESORPTION OF PLATINUM FROM THE SORBENT	122
7.3.1 Materials and Methods	122
7.3.2 Results	123
7.3.3 Discussion	125
7.4 SUMMARY	127
7.5 CONCLUSIONS	128
Chapter 8 Inhibition of platinum sorption	129
8.1 INTRODUCTION	129
8.2 INHIBITION OF PLATINUM SORPTION	129
8.2.1 Materials and Methods	130
8.2.2 Results	131
8.2.3 Discussion	133
8.3 SUMMARY	136
8.4 CONCLUSIONS	137
Chapter 9 Sorption of platinum from PMR wastewater	138
9.1 INTRODUCTION	139
9.2 BATCH SORPTION OF PLATINUM FROM WASTEWATER	139

9.2.1 Materials and Methods	139
9.2.2 Results	140
9.3 COLUMN SORPTION OF PLATINUM FROM WASTEWATER	141
9.3.1 Materials and Methods	141
9.3.2 Results	142
9.4 DISCUSSION	144
9.5 SUMMARY	147
9.6 CONCLUSIONS	148
Chapter 10 Conclusions	148
10.1 CONCLUSIONS	149
10.1.1 Objective 1: Production of an <i>S. cerevisiae</i> -based sorbent suitable for use in the recovery of precious metals from PMR wastewaters.	150
10.1.2 Objective 2: Determination of the precious metal for which the sorbent has the highest affinity.	151
10.1.3 Objective 3: Optimization of the physical and chemical parameters affecting metal sorption in order to maximize metal recovery.	152
10.1.4 Objective 4: Investigation of the mechanisms or processes governing metal sorption in this system.	153
10.1.5 Objective 5: Comparison of the sorption process efficiency in a stirred batch system to that in a fixed-bed column system.	155
10.1.6 Objective 6: Determination of the effect of wastewater composition on the sorption of the metal from wastewater.	156
10.2 FINAL REMARKS	157
Chapter 11 Further recommendations	159
References	161
Appendices	173

LIST OF FIGURES

Figure 1.1 Flow diagram outlining the methodology to be used in the project.	5
Figure 2.1. Simple overview of the PGM production process (Robinson, 2002, pers. comm).	7
Figure 2.2. Overview of Anglo Platinum Precious Metal Refinery (PMR) flow sheet. SX: Solvent extraction, DT: Distillation, IX: Liquid ion exchange (Robinson, 2002, pers. comm.).	8
Figure 4.1 Structure of the yeast cell wall (Adapted from Kapteyn <i>et al</i> , 1996 and Grun, 2003).	35
Figure 4.2 Yeast cells immobilized within carboxymethyl cellulose. Arrows indicate ruptured and broken beads. The match provides a size scale (1.2× magnification).	44
Figure 4.3 Yeast cells immobilized on the surface of silica gel particles. The match provides a size scale (1.2× magnification).	44
Figure 4.4 Scanning electron micrographs of silica-immobilized yeast granules. A: free silica gel granules. B: Yeast immobilized on silica gel granules. C: View of the layering of yeast cells on the silica surface. D: Indication of the dense layers of yeast immobilized on a silica granule.	45
Figure 4.5 Yeast cells modified with polyethyleneimine and crosslinked with glutaraldehyde. The match provides a size scale (1.2× magnification).	46
Figure 4.6 Yeast cells immobilized within calcium alginate matrix (A) beads maintained in 0.1 M CaCl ₂ , (B) beads maintained in 0.1 M HCl. The match provides a size scale (1.2× magnification).	46
Figure 4.7 Precious metal removal efficiency of calcium alginate-immobilized yeast at low (pH 1) and more neutral pH (4). (200 μM metal solution, 3 hour incubation, 1 g/l sorbent dose, room temperature). Error bars represent standard deviation from the mean ($n = 3$).	47
Figure 4.8 Metal uptake (q) of precious metals by PEIGA granules and silica granules. The error bars represent the standard deviation from the mean ($n = 3$).	48
Figure 4.9 Removal efficiency (%) of PEIGA and silica granules after three hours and twenty four hours of incubation with platinum and gold solutions (200 μM). Error bars represent standard deviation from the mean ($n = 3$).	48
Figure 4.10 Metal uptake (q) by both protonated and unprotonated sorbents. Error bars represent standard deviation from the mean ($n = 3$).	49
Figure 4.11 Scanning electron micrographs of the silica sorbent surface showing, at increasing magnification, the damage inflicted on the immobilized yeast layers by mechanical shear caused by agitation.	50
Figure 4.12 Sorption isotherm curves of platinum, rhodium and gold on PEIGA sorbent.	51
Figure 4.13 Sorption isotherm curves describing the sorption of platinum by the three components that make up the PEIGA sorbent.	52

- Figure 4.14 A comparison between two methods for the production of PEIGA sorbent granules. A: initial process (described in section 4.2.2), B: alternate process (described in section 4.4.1). 53
- Figure 5.1 Scanning electron micrographs of the sorbent showing granule macrostructure (A and B) and surface structure (C and D). 63
- Figure 5.2 Scanning electron micrographs of the sorbent, showing the sorbent macrostructure (A and B) and the sorbent surface (C and D) after incubation with platinum. 64
- Figure 5.3 Energy dispersive x-ray (EDX) analysis of white (A) and dark (B) areas of Figure 5.2D, confirming the adsorption of platinum chloride ions to the white area of the sorbent. 66
- Figure 5.4 FTIR-ATR analyses of (A) native dried yeast, (B) immobilized dried yeast, and (C) platinum-bound immobilized dried yeast. 67
- Figure 5.5 Sorption isotherm showing the sorption of methylene blue onto the *S. cerevisiae* sorbent. Error bars represent the standard deviation from the mean, and in most cases are too small to be visible ($n = 3$). 68
- Figure 5.6 A half-reciprocal plot used to calculate the sorbent maximum specific uptake of methylene blue. 68
- Figure 5.7 Potentiometric titration curve of *S. cerevisiae* sorbent. Arrows indicate inflection points at pH 7.3 (A) and 9.7 (B). 69
- Figure 5.8 Metal uptake (q) values at intervals throughout a six hour platinum biosorption reaction using initial platinum concentrations of 10 – 200 mg/l, a sorbent dose of 1 g/l, and at pH 1.5. Error bars represent standard deviation from the mean ($n = 3$). 70
- Figure 5.9 Effect of pH on the platinum sorption capacity of the *S. cerevisiae* sorbent. Error bars represent the standard deviation from the arithmetic mean, and in some cases are too small to be visible ($n = 3$). 70
- Figure 5.10 The effect of sorbent concentration on platinum removal (%) and metal uptake (q) in 20 mg/l and 50 mg/l platinum solutions. Error bars represent the standard deviation from the arithmetic mean ($n = 3$). 71
- Figure 5.11 Distribution coefficient as a function of sorbent concentration. 72
- Figure 6.1 Kinetics of platinum uptake by immobilized *S. cerevisiae* at various initial platinum concentrations. Error bars represent standard deviation from the mean ($n = 3$). 83
- Figure 6.2 Fit of the data describing the effect of initial platinum concentration on sorption kinetics to (A) the pseudo-first order kinetic model, (B) the pseudo-second order kinetic model and (C) the intraparticle diffusion model. 85
- Figure 6.3 Kinetics of platinum uptake by immobilized *S. cerevisiae* at various sorbent doses. Error bars represent standard deviation from the mean ($n = 3$). 86

- Figure 6.4 Fit of the data describing the effect of sorbent dose on sorption kinetics to (A) the pseudo-first order, (B) the pseudo-second order and (C) the intraparticle diffusion model. 87
- Figure 6.5 Kinetics of platinum uptake by immobilized *S. cerevisiae* at various temperatures. Error bars represent standard deviation from the mean ($n = 3$), and are sometimes too small to be visible. 88
- Figure 6.6 Plot of $\ln k_2$ against reciprocal temperature for sorption of platinum onto yeast sorbent. The solid line represents the exothermic stage, and the dotted line is the endothermic stage. 90
- Figure 6.7 Sorption isotherms showing the sorption of platinum onto *S. cerevisiae* sorbent at increasing pH (Temp =20 °C). Error bars represent the standard deviation from the mean ($n = 3$), and in most cases are too small to be visible. 95
- Figure 6.8 Equilibrium metal uptake (q_e) after incubation with sorbent at controlled temperatures (100 mg/l initial platinum concentration, pH 1.5). Error bars represent standard deviation from the mean ($n = 3$). 96
- Figure 6.9 Sorption isotherms showing the sorption of platinum onto *S. cerevisiae* sorbent at various temperatures. Error bars represent the standard deviation from the mean, and in all cases are too small to be visible ($n = 3$). 97
- Figure 6.10 Linearization of the temperature affinity data in order to determine thermodynamic characteristics of the sorption reaction. 98
- Figure 7.1 A typical sorption breakthrough curve (Adapted from Chu, 2004). 106
- Figure 7.2 Schematic diagram of experimental column setup: (1) Influent reservoir holding platinum solution, (2) peristaltic pump, (3) porous material, (4) packed column, (5) fraction collector and effluent storage. 110
- Figure 7.3 Breakthrough curves for the sorption of platinum by a 1 cm column at four flow rates. Error bars represent standard deviation between duplicate samples. 110
- Figure 7.4 The Thomas Model for continuous sorption of platinum by a 1 cm column of immobilized yeast sorbent. The transformed data are not linear, indicating that they do not fit the model. 111
- Figure 7.5 The Adams-Bohart model for the continuous sorption of platinum by a 1 cm column of immobilized yeast sorbent. The distance of the data points from the lines indicates poorness of fit. 114
- Figure 7.6 The Yoon-Nelson model for the continuous sorption of platinum by a 1 cm column of immobilized yeast sorbent. 115
- Figure 7.7 Breakthrough curves for the sorption of platinum by a 5 cm column at two flow rates. Error bars represent standard deviation from the mean ($n = 3$) and are presented only to indicate variation between columns. 116

- Figure 7.8 The Thomas model for the continuous sorption of platinum by 5 cm columns of immobilized yeast sorbent. 117
- Figure 7.9 The Adams-Bohart model for the continuous sorption of platinum by 5 cm columns of immobilized yeast sorbent. 118
- Figure 7.10 The Yoon-Nelson model for the continuous sorption of platinum by 5 cm columns of immobilized yeast sorbent. 119
- Figure 7.11 Desorption ratio attained by desorption of platinum from metal-laden sorbent by an acid (HNO₃), an alkali (NaOH) and acidified thiourea (TU) in a column setup with a desorbent flow rate of 5 ml/min. Error bars illustrate the standard deviation from the mean (Provided as a visual guideline only, $n = 2$). 124
- Figure 7.12 Effect of varying flow rate and direction on the desorption ratio attained by acidified thiourea on desorption of platinum from the metal-laden sorbent. UF: upflow, DF: downflow. Error bars illustrate the standard deviation from the mean (Provided as a visual guideline only, as $n = 2$). 125
- Figure 8.1 The effect of the presence of anionic ligands at 0.01 M, 0.1 M and 1.0 M on the efficiency of platinum sorption by immobilized *S. cerevisiae*. The error bars indicate standard deviation from the mean ($n = 3$). 131
- Figure 8.2 The effect of different concentrations of light metal ions on the efficiency of platinum sorption by immobilized *S. cerevisiae*. Error bars represent standard deviation from the mean ($n = 3$). 132
- Figure 8.3 The effect of varying concentrations of base metal ions on the efficiency of platinum sorption by immobilized *S. cerevisiae*. Error bars represent the standard deviation from the mean ($n = 3$). 132
- Figure 8.4 The effect of different concentrations of precious metal anions on the efficiency of platinum sorption by immobilized *S. cerevisiae*. Error bars represent standard deviation from the mean ($n = 3$). 133
- Figure 9.1 A comparison of the platinum removal efficiency and specific uptake capacity of the sorbent in synthetic solution and in wastewater. Error bars represent standard deviation from the mean ($n = 3$). 140
- Figure 9.2 The effect of increased sorbent dose on the removal efficiency and specific uptake capacity of the sorbent in wastewater. Error bars represent the standard deviation from the mean (SD < 1%) and are all too small to be visible ($n = 3$). 141
- Figure 9.3 Breakthrough curves describing the normalized concentration of the column effluent over time for each successive pass of the wastewater through a fresh column. Error bars represent standard deviation from the mean ($n = 2$), and are presented in order to indicate variation between duplicates. 142

Figure 9.4 Chloride concentration of the column effluent after each pass of the wastewater through three fresh columns. Error bars represent standard deviation from the mean ($n = 2$), and are presented to indicate the variation between the duplicate columns.

144

LIST OF TABLES

Table 2.1 Advantages and disadvantages of physico-chemical heavy metal recovery/removal technologies (adapted from Kurniawan <i>et al.</i> , 2006).	12
Table 2.2 A review of recent sorbents used for precious metal biosorption.	14
Table 2.3 Hard, borderline and soft acids (Douglas <i>et al.</i> , 1994).	19
Table 2.4 Base metal ion biosorption by <i>S. cerevisiae</i> in recent literature.	28
Table 4.1 Summarized survey of immobilization techniques.	37
Table 4.2 Matrix for selection of immobilization techniques to be used.	39
Table 4.3 Langmuir equilibrium parameters for precious metal target analysis, PEIGA sorbent component analysis (with platinum target), and alternate production procedure analysis (with platinum target).	52
Table 6.1 Frequently used adsorption isotherm models and their advantages and disadvantages.	80
Table 6.2 Effect of initial platinum concentration on parameters calculated from the pseudo-first order, pseudo second order and intraparticle diffusion models.	84
Table 6.3 Effect of sorbent dose on parameters calculated from the pseudo-first order, pseudo-second order and intraparticle diffusion models.	86
Table 6.4 Effect of temperature on parameters calculated from the pseudo-first order, pseudo-second order and intraparticle diffusion models.	89
Table 6.5 Parameter values calculated from pH isotherms in Figure 6.7 (Temp = 20 °C).	95
Table 6.6 Parameter values calculated from experimental temperature isotherms (pH 1.5).	97
Table 7.1 Analysis of 1 cm column sorption performance at various flow rates.	111
Table 7.2 Parameters predicted by the Thomas, Adams-Bohart, Wolborska and Yoon-Nelson models obtained by linear regression of the column breakthrough curves at different flow rates and column heights.	113
Table 7.3 The effect of retention time on the sorption of platinum within a 1 cm and 5 cm high column (\pm SD, provided as an indication only, because $n = 2$)	115
Table 7.4 Analysis of 5 cm column sorption performance at two flow rates.	117
Table 7.5 Desorption ratios obtained by six desorbents tested at varying concentrations.	124
Table 9.1 Summary of the efficiency of each column with respect to total platinum removal, removal efficiency and specific uptake (\pm SD).	143

LIST OF ABBREVIATIONS

<i>b</i>	Langmuir sorption equilibrium constant (l/mg)	<i>q_i</i>	Metal uptake at $t = i$
BET	Brunauer-Emmet-Teller	<i>Q_{max}</i>	Maximum metal uptake (mg/g)
BIC	Bushveld Igneous Complex	<i>Q_{SA}</i>	Maximum monolayer adsorption (μmol/g)
BSE	Backscattered Electron	<i>R</i>	Gas constant (J/mol/K)
<i>C₀</i>	Metal concentration at $t = 0$	<i>S</i>	Specific surface area (m ² /g)
<i>C_{bp}</i>	Metal concentration at breakthrough point (mg/l)	SE	Simultaneous Electron
<i>C_i</i>	Metal concentration at $t = i$	<i>t</i>	Time (min)
CMC	Carboxymethyl cellulose	<i>T</i>	Solution temperature (K)
<i>C_s</i>	Metal concentration in sorbent phase (mg/g)	<i>t_{bp}</i>	Time at breakthrough point (min)
<i>C_{sp}</i>	Metal concentration at saturation point (mg/l)	<i>t_{sp}</i>	Time at saturation point (min)
<i>C_w</i>	Metal concentration in liquid phase (mg/l)	<i>U₀</i>	Superficial flow velocity (cm/min)
<i>E</i>	Activation energy of sorption (kJ/mol)	UG2	Upper Group 2
<i>FG_{TOTAL}</i>	Total concentration of functional group (mmol/g)	<i>V</i>	Volume of solution (l)
GA	Glutaraldehyde	<i>V_{eff}</i>	Column effluent volume (l)
HRT	Hydraulic retention time	<i>V_{IP}</i>	Volume of NaOH added to reach inflection point (l)
HSAB	Hard and Soft Acids and Bases	<i>Z</i>	Height of column (cm)
<i>K</i>	Freundlich relative sorption capacity (mg/g)	<i>β_a</i>	Wolborska kinetic constant (l/min)
<i>k₀</i>	Temperature-independent factor (g/mg/min)	<i>ΔG^o</i>	Gibbs free energy change
<i>k₁</i>	Rate constant for first order sorption (l/min)	<i>ΔH^o</i>	Enthalpy change
<i>k₂</i>	Rate constant for second order sorption (g/mg/min)	<i>ΔS^o</i>	Entropy change
<i>k_{AB}</i>	Adams-Bohart model kinetic constant (l/mg/min)	<i>σ</i>	Area of a methylene blue molecule (m ²)
<i>K_D</i>	Distribution coefficient (l/g)	<i>τ</i>	Yoon-Nelson model time to reach 50 % breakthrough
<i>k_i</i>	Intraparticle diffusion rate constant (mg/g/min ^{0.5})		
<i>k_{TH}</i>	Thomas model kinetic constant (ml/(mg.min))		
<i>k_{YN}</i>	Yoon-Nelson model kinetic constant (l/min)		
<i>M</i>	Mass of sorbent (g)		
<i>n</i>	Freundlich sorption intensity constant		
<i>N₀</i>	Adams-Bohart saturation concentration (mg/l)		
<i>N_A</i>	Avogadro's number (1/mol)		
PEI	Polyethyleneimine		
PEIGA	PEI-modified and GA crosslinked sorbent		
PGE	Platinum Group Element		
PGM	Platinum Group Metal		
PMR	Precious Metals Refinery		
<i>q</i>	Metal uptake (mg/g)		
<i>Q</i>	volumetric flow rate (ml/min)		
<i>q_{0TH}</i>	Thomas model metal uptake (mg/g)		
<i>q_{0YN}</i>	Yoon-Nelson model metal uptake (mg/g)		
<i>q_e</i>	Metal uptake at equilibrium (mg/g)		

ACKNOWLEDGEMENTS

There are a number of people to whom thanks alone does not seem enough in light of their contribution to my life over the past three years. Nonetheless, I would like to thank them from the bottom of my heart for their constant support and unwavering faith in me.

To my supervisor, Dr Jo Burgess, the biggest THANK YOU goes to you... for giving me the space and opportunity to make this project my own, for being there with good advice when I wasn't sure of myself and for being a supportive friend when I needed one.

To my parents, for giving me so many opportunities to grow, for your support and understanding and for providing a wonderful place to escape to when I felt overwhelmed.

To my best friend, Hylton, your motivation and support gave me inspiration and the necessary will to press on when things were not going well and for providing me with much-needed distraction and escape.

To the members of my lab, Bron, James, Vera, Aruna, and all of the others who have passed through over the years. You have all meant something to me and I am grateful for the shared good times. Special thanks to Doug Sanyahumbi for always believing that I could do this, even when I wasn't so sure of myself – Thank you for your support and encouragement!

To Lauritz, Gerda and Lesley, from Anglo Research, many thanks for the SEM and ICP analyses, and to Bathabile at UKZN for the FTIR analysis.

Thanks to my sponsors, the Atlantic Philanthropies, for making it possible for me to complete my research without financial strain. Similarly, to the National Research Foundation of South Africa, I express my appreciation for your support.

And lastly, but very importantly, to Kerry Slatter, Dr Dave Robinson and Dr Neville Plint from Anglo Platinum, many thanks for the opportunity to complete this research and for the support, interest and guidance provided throughout my association with the company.

CHAPTER 1

Introduction and synopsis

1.1 INTRODUCTION

The extraction and refining of precious metals such as platinum and gold from ores results in the production of large quantities of wastewater every year. For example, the Anglo Platinum operations in South Africa used 5.77 m³ of water per ounce¹ of refined metal (almost 4.5 million ounces produced), almost all of which became wastewater, but released only 137 l of effluent to surrounding surface waters in 2005. The rest was retained in numerous tailings and holding dams or recycled for secondary use within the operation (Anglo Platinum PLC, 2005). These large volumes of retained water contain many of the chemicals and reagents used in the production of the pure metal and it is these contaminants that make the water unsuitable for release into the environment without extensive prior treatment. In fact, some may contain appreciable amounts of valuable metal. Recovery of metals from such large volumes is often hampered by the dilute metal concentration created by the combination of many waste streams before storage. Effective point-source recovery processes would be a far more efficient alternative to the bulk treatment of wastewaters, which ultimately results in a need for further processing or costly disposal. Point-source treatment of the waste streams produced at the Anglo Platinum precious metals refinery (PMR) is made easier by the current setup of the refining process, where each metal is refined separately, and thus, a separate stream is produced containing a pure and high concentration of one metal relative to other metals that are present. It is these waste streams that must be targeted in order to maximize metal recovery from PMR wastewaters.

Conventional methods for the removal of dissolved metal ions from wastewaters, such as cementation, electrolysis, solvent extraction, evaporation, chemical precipitation and ion exchange (discussed in Chapter 2), have significant disadvantages, which include incomplete metal removal, high capital costs, high reagent and/or energy requirements, and generation of toxic sludge or other waste products that require disposal (Göksungur *et al.*, 2005; Cho and Kim, 2003). Their efficiency also depends on the concentration of the metal in solution. At concentrations greater than 500 mg/l, electrolysis would be most efficient, whereas at concentrations lower than 5 mg/l ion exchange or adsorption would be best. At intermediate concentrations (500 – 5 mg/l), chemical precipitation is the most common metal removal technique (Diels *et al.*, 1993). These disadvantages, together with

¹ Metals are sold in Troy ounces. One ounce = 31.103 g.

the need for more economical and effective methods for the recovery of metals from wastewaters, have resulted in the development of alternative separation technologies. One such alternative is biosorption, where certain types of biomass are able to bind and concentrate metals from even very dilute aqueous solutions.

A biosorption-based process offers a number of advantages when compared to the conventional methods used. These include low operating costs, minimization of the volume of chemical and/or biological sludge to be handled and high efficiency in detoxifying effluents (Cho and Kim, 2003; Marques *et al.*, 1999). Biosorption is currently considered one of the most promising technologies that can be used for the recovery of precious metals and for the removal of toxic or pollutant metals (Volesky, 2001).

Currently, PMR wastewaters originating from extraction and refining processes still contain a small but significant (e.g. 20 mgPt/l in the current study) amount of the precious metal targeted. A process such as biosorption could act as a polishing step, recovering metal ions down to the < 1 ppm (mg/l) range, thus speeding up both the downstream water treatment and the metal reclamation processes.

A suitable biological component for a successful biosorbent is one that is either found in abundance in nature, or is a waste product from an existing biological exploitation process, such as spent yeast from a brewery or bacterial waste from a pharmaceutical production process. If neither is available, it is necessary to rely on purpose-made biomass, produced at the lowest possible cost, and with the highest biomass yield. A vast number of organisms have been investigated as potential biosorbents. Bacteria, fungi, yeasts, moulds, algae, seaweeds and higher plants have all been scoured for biomass with outstanding metal sorption potential. Add to this the numerous ways in which the biomass can be enhanced; immobilization, pretreatments, DNA-level surface modifications. All of this greatly increases the possibility of finding (or producing) a biosorbent that suits the needs of a specific metal recovery/removal objective.

The yeast, *Saccharomyces cerevisiae*, is a well-researched biosorbent (review published by Wang and Chen in 2006), with proven sorption capacity for base and precious metals. It is still regarded by some as capable of only average uptake when compared to other biosorbents (Wang and Chen,

2006; Salinas *et al.*, 2000), but there are several advantages associated with its use as a biosorbent, the most important of which is the ease of cultivation. This means that if there is insufficient yeast available as a waste product, it can be easily and inexpensively cultivated with high biomass yields (Kapoor and Viraraghavan, 1995). Once suitably immobilized, *S. cerevisiae* biomass may represent an efficient, low cost and simple solution for the recovery of precious metals from refinery wastewaters.

1.2 SYNOPSIS

In the current research, yeast biomass (*Saccharomyces cerevisiae*) will be used as the basis for a sorption system aimed at recovering precious metal ions from point-source waste streams. The biomass will need to be suitably immobilized in order to produce a sorbent with the characteristics necessary to not only exhibit high uptake efficiency, but also to withstand any mechanical and chemical stresses that may be applied *via* the wastewater or the design of the process. Once immobilized, the uptake efficiency of the sorbent with regard to three economically and strategically important precious metals produced at the Anglo Platinum PMR will be compared. A single target metal will be chosen from the three in order to optimize only the most readily sorbable metal. This choice will be based not only on the affinity of the sorbent for the particular metal, but also on the prevailing metal price and the current worldwide demand.

Initially the sorption system will be optimized for a synthetic metal solution at concentrations equivalent to those found in the PMR wastewater. Environmental parameters such as solution pH and temperature, and operational parameters such as contact time, initial metal concentration and sorbent concentration will all be adjusted to achieve an optimal metal uptake capacity. The system will be modelled using equilibrium and kinetic data. The results of the modelling along with thermodynamics data and inferences drawn from a variety of ancillary experiments will be used to determine the mechanism involved in the sorption of the target metal to the sorbent.

Stirred-batch treatment, however, is not the most suitable design for a biosorption system. A packed-bed column allowing maximal contact between the sorbate liquid and the biosorbent promotes far more efficient utilization of the sorbent material. The system will be applied to synthetic metal-containing solutions in a packed-bed configuration. By varying the metal solution flow rate through the column, the optimal liquid retention time will be determined. The effect of

column height will be explored, as this will also affect the efficiency of the packed-bed sorption system. At this stage, the efficient desorption of precious metals from the sorbent will be investigated, initially in a stirred-batch reactor, and then as a function of a packed-bed contactor.

The complex nature of industrial wastewaters, with their myriad of co-ions and other impurities, implies that extrapolations from single metal sorption experiments are not valid. For most effective application of the sorption process, further investigation is required in order to identify issues of metal competition, synergism and non-interaction. It is thus important to understand the behaviour of the mixture in the wastewater and further explore the effect of the concentration of one wastewater ion on the uptake of other metal ions, in particular, the targeted metal. The effect of negatively charged counter ions, light metal ions, heavy base metal ions, and precious metal anions on the selective sorption of the target ion onto the sorbent surface will be determined.

Finally, the wastewater itself will be characterized in order to determine the actual impurities that may impede selective sorption of the target metal. The system will be re-optimized to fit the constraints of the wastewater and then the metal sorption efficiency of the sorbent for the target metal within a wastewater will be examined in a packed-bed contactor arrangement.

1.3 MATERIALS AND METHODS OVERVIEW

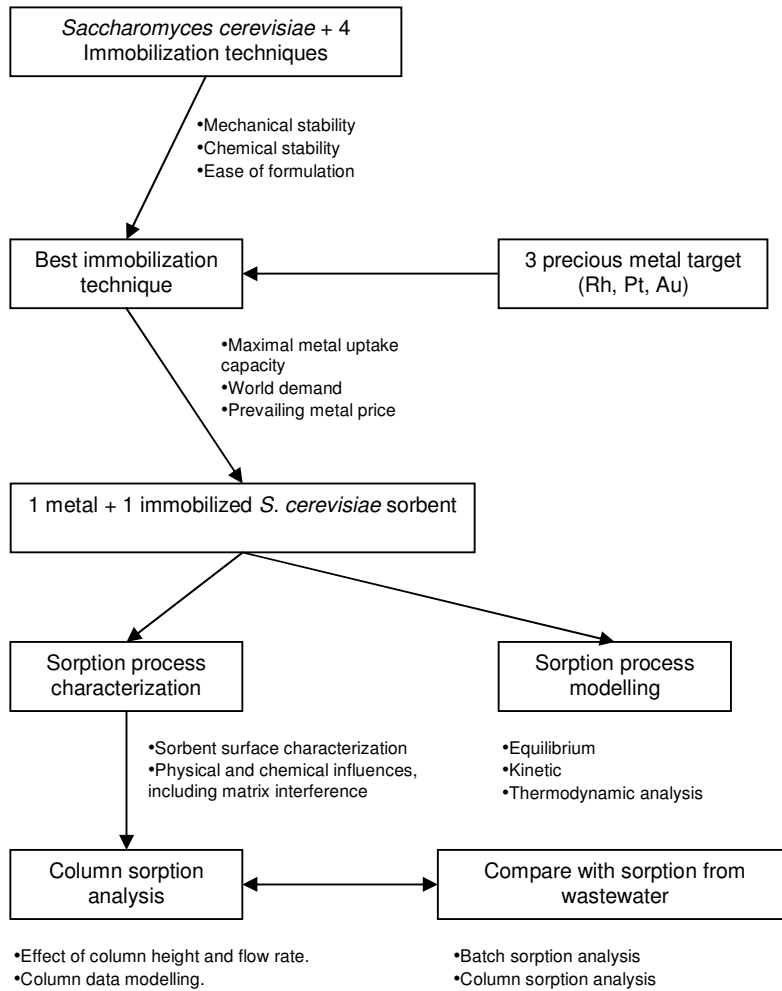


Figure 1.1 Flow diagram outlining the methodology to be used in the project.

CHAPTER 2

Literature review

2.1 PLATINUM GROUP METALS

Platinum group metals (PGMs) or elements (PGEs) are collective names used when referring to the six precious metal elements – platinum (Pt), palladium (Pd), rhodium (Rh), iridium (Ir), ruthenium (Ru) and osmium (Os). In the Earth's crust, the average concentration of these metals is estimated to range from 0.0001 g/t for rhodium to 0.015 g/t for palladium, with platinum, ruthenium, osmium and iridium present in equally small concentrations (Ravindra *et al.*, 2004). The PGMs have unique properties of corrosion resistance, heat resistance, high melting point, high mechanical strength, good ductility and catalytic activity (Ravindra *et al.*, 2004). These properties have led to their use in jewellery manufacture, automotive catalyst manufacture, and in the electronics, glass, electrical, petroleum and medical industries (Johnson-Matthey, 2002; Ravindra *et al.*, 2004).

All the PGMs are generally associated with each other in the Earth's crust. However, the relative proportions of the individual metals are not constant for all PGM deposits. Platinum group metals occur naturally in nickel, copper and iron sulphide seams (Ravindra *et al.*, 2004). The world's largest source of PGMs is the South African Bushveld Igneous Complex (BIC), formed around 2000 million years ago. It consists of a series of distinct layers, three of which are of economic importance as sources of PGMs. These are the Merensky Reef, the Upper Group 2 (UG2) Reef, and the Platreef. The Merensky Reef has been the principal source of PGMs since it was first worked in 1925 and now produces 50 % of all the platinum-bearing ore processed in South Africa. In 1999, the UG2 Reef increased production to yield 42 % of the country's platinum, and the Platreef only began to be exploited on a large scale in 1993 (Johnson-Matthey, 2003). Mill head grades of BIC ore (a measure of the PGM content of the ore on entering the first processing stage) are typically between 4 and 7 g/ton. This translates to between 7 and 12 tons of ore being processed to produce a single ounce of platinum (Johnson-Matthey, 2003). An overview of the entire process involved in producing PGM product is shown in Figure 2.1.

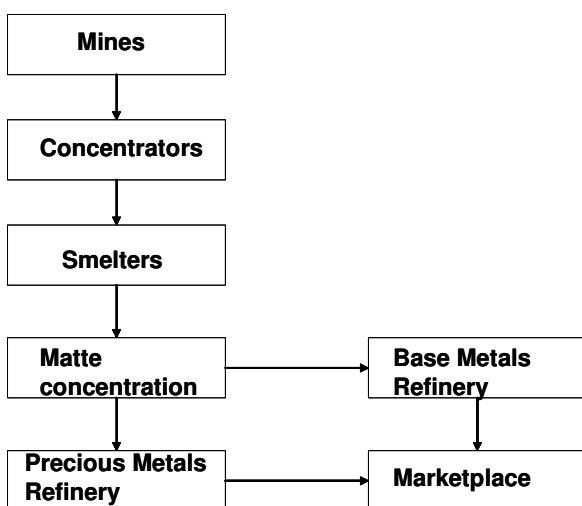


Figure 2.1. Simple overview of the PGM production process (Robinson, 2002, pers. comm).

In the concentrators, the ore is crushed and milled to reduce rock sizes and expose the minerals containing the PGMs. The rock is mixed with water and other reagents and air is pumped through this to create bubbles to which the PGM-containing particles adhere. These float to the surface and are removed as a soapy froth called concentrate. This process is known as flotation. The PGM concentration of this concentrate varies between 100 and 1000 g/ton (Johnson-Matthey, 2003). The concentrate is dried and smelted in furnaces reaching temperatures of 1500 °C and higher. During this process a matte containing the PGMs is separated from the unwanted minerals, which form a slag and are discarded. The matte is transferred to converters, where air is blown through it in order to remove iron and sulphur. The PGM content of converter matte is in excess of 1400 g/ton (Johnson-Matthey, 2003). The next step is to separate base metals from the PGMs. The base metals are transferred to a base metal refinery, where sulphate and metals such as cobalt, nickel and copper are refined for the marketplace. The final stage is the separation and purification of the six PGMs, plus gold, which is a by-product of the ore body. This is performed using hydrometallurgical methods such as solvent extraction and ion exchange. Figure 2.2 illustrates the order in which the precious metals are extracted from the matte. The soluble metals, gold, palladium and platinum are generally removed first. The insoluble metals are then removed; with rhodium usually last to be extracted from the concentrate (Robinson, 2002, pers. comm.).

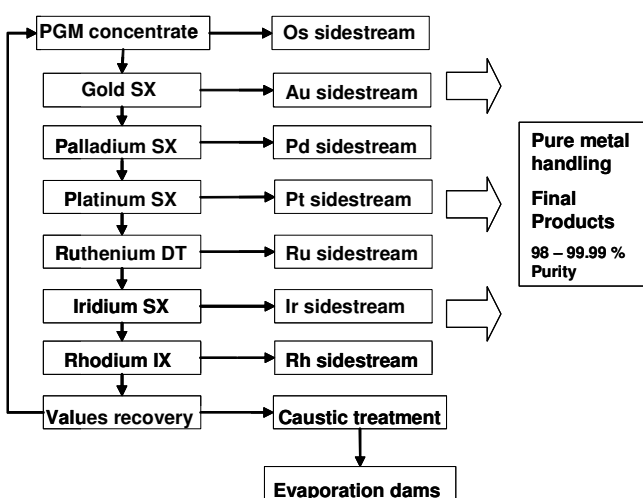


Figure 2.2. Overview of Anglo Platinum Precious Metal Refinery (PMR) flow sheet. SX: Solvent extraction, DT: Distillation, IX: Liquid ion exchange (Robinson, 2002, pers. comm.).

The complex nature of the solution chemistry of PGMs contributes to the difficulty in developing methods for the separation of these metals from one another (Kramer *et al.*, 2004). There are a number of physico-chemical strategies available for the refining of precious metals, but current general trends in metal extraction of PGMs from heterogeneous solutions are ion exchange and solvent extraction. These are often used in combination, as the advantages of ion exchange (high concentrating efficiency and ease of phase separation) offset the inherent disadvantages of solvent extraction (phase separation difficulties during multiple and back-extraction and eventual flooding of the solvent with entrained contaminants) (Corvalan *et al.*, 2004).

Solvent extraction involves extracting the metal of interest by contacting the concentrate with an organic reagent that will react with a particular metal in the concentrate and result in its conversion to a form soluble in the solvent. Usually, solvent extraction follows three steps: (1) the extraction step, where the metal ions are solubilized in the organic phase, (2) the scrubbing step, where any co-extracted metals are removed from the organic phase, and (3), the stripping step, where the isolated metal ions are removed from the organic phase (Bernardis *et al.*, 2005). The extraction of metals in this way is widely employed for selective recovery. It is one of the most common methods used for the separation of PGMs from aqueous solutions due to the simplicity of the process (Gholivand and Nozari, 2000). However, these methods are relatively expensive with elaborate equipment, high operation costs and energy requirements. At the Anglo Platinum refinery, these organic solvents include methyl-*iso*-butylketone (for gold extraction), a *beta*-hydroxyoxime (for palladium extraction), an amine (for platinum extraction) and an amide extractant (for iridium extraction)

(Cole *et al.*, 2006). A major cost is the regeneration and/or disposal of the solvent liquid and the spent solvent itself, where these organic solvents, strip and scrub liquors all represent a large environmental burden in terms of disposal (Wong *et al.*, 2003). The scrub liquors are of particular interest for the current study, as they often require reprocessing due to the significant amounts of PGMs that they contain (Bernardis *et al.*, 2005).

The refined PGMs usually have a purity of over 99.95 % and are produced in a number of forms, including ingots, grains or fine powders known as sponges. However, a percentage of the mined PGMs are not recovered by these techniques and remain in the wastewaters stored by the refineries in evaporation dams.

The refining of PGMs using hydrometallurgical processes such as solvent extraction and ion exchange results in large volumes of liquid waste that requires suitable treatment before any disposal can be contemplated. The wastewater streams are characterized by extremes of pH, high inorganic ion content (such as chloride), significant residual metal loads and small amounts of entrained organic compounds such as those mentioned previously. The composition of these wastewaters precludes any direct discharge to surrounding surface waters, and renders them untreatable by conventional domestic wastewater treatment plants. Thus, they must be managed within the refinery.

2.2 RECOVERY OF METALS FROM REFINING WASTEWATERS

The recovery of metals from wastewater has a twofold advantage. Firstly, it minimizes contamination of aquatic environments and secondly, recovering metals of value such as gold and PGMs holds significant commercial value (Volesky, 2001). A third, and less obvious advantage is that the removal of metal ion contaminants may generate a stream that is more amenable to further treatment, or reuse within the industry (as a substitute for potable water where only low quality water is required). Currently, the majority of metal removal and recovery technologies are physical or chemical in nature. These technologies include chemical precipitation and evaporation as cheapest alternatives. Other technologies applied to metal-laden wastewaters include coagulation-flocculation, flotation, ion exchange, membrane filtration, and electrochemical techniques

(Kurniawan *et al.*, 2006) (Table 2.1). Each of these techniques and a number of examples of their application were reviewed by Kurniawan *et al.* in 2006.

Alkaline chemical precipitation is the most common method used for the removal of heavy metals from wastewaters (Liu *et al.*, 2003) as it is considered the simplest and cheapest means of removing most heavy metals from solution. For these and other reasons, chemical precipitation is employed at the Anglo Platinum precious metals refinery as a means of removing metals from wastewaters. This removal is mostly achieved by increasing the pH of the wastewater to basic conditions (pH 11), thereby precipitating the metal in an insoluble form, usually its hydroxide (Kurniawan *et al.*, 2006). Traditionally, hydroxide precipitants such as lime and caustic soda have been favoured, but sodium hydroxide is the best-favoured alkali as it introduces the smallest amount of inert material to the sludge. A problem often experienced with industrial precipitation of metal hydroxides however, is that the large volumes of wastewater to be treated often hamper the precise management of the pH levels, leading to lower effective removal rates. Other problems encountered with the treatment of large volumes in this way include slow precipitation, poor settling and the aggregation of metal precipitates (Kurniawan *et al.*, 2006). Following chemical precipitation of metal ions from wastewaters, atmospheric evaporation, using wastewater reservoirs known as “dams”, is used to produce a concentrated metal-bearing sludge.

The efficient recovery of precious metal ions from a wastewater using chemical precipitation and subsequent evaporation is hampered by a number of disadvantages inherent in each process. In the long term this treatment becomes expensive, as large volumes of wastewater must be treated daily and a significant volume of metal-laden sludge is produced (Goyal *et al.*, 2003). For example, the hydroxide precipitation of 100 mg copper(II) produces as much as 1000 mg sludge (Peña-Castro *et al.*, 2004). This leaves a vast quantity of sludge to be treated in order to recover a relatively small quantity of metal. The sludge produced is also heterogeneous in terms of metal content, as chemical precipitation of this nature is non-specific. This increases the cost of processing the sludge in the case of a precious metal refinery, as each metal must be extracted from the sludge into a pure stream in order to produce a product of at least 99 % purity. The evaporation process also creates difficulties in that recovery of the metal sludge can only occur after a significant amount of water has evaporated, often for only low metal recovery yields (Salinas *et al.*, 2000). The dams (reservoirs) required for this method can occupy vast areas of land, making it a viable option only

for processes where this land is available in close proximity to the point of origin. It must be noted, however, that many of the disadvantages of alkaline chemical precipitation can be overcome if precipitation with sulphide is considered. One is the production of lower sludge volumes compared to hydroxide precipitation (Kaksonen *et al.*, 2003). This has huge financial impacts on waste management strategies for all metal producers, as smaller volumes result in lower disposal or reclamation costs. Sulphide also readily forms metal sulphides, the solubilities of which are very low in comparison to the corresponding hydroxides (Kaksonen *et al.*, 2003; Hao, 2000) and carbonates (El Bayoumy *et al.*, 1999), hence even moderate sulphide outputs can effectively precipitate metals, reducing levels to well below those permitted for environmental discharge (White *et al.*, 1997). Additionally, valuable metals can be recovered from the sulphide sludges (Kaksonen *et al.*, 2003).

There is, however, a global trend moving towards more stringent environmental standards and legislation regarding industrial wastewater and the treatment thereof, and in light of this the current economic climate encourages the introduction of relatively low-cost pollution treatment systems such as those offered by biologically-mediated processes (Aksu and Dönmez, 2001). The recalcitrance of refinery wastewaters in terms of their inorganic composition represents a challenge when biological remediation is attempted; in combination, it is almost impossible for an organism to flourish in such harsh conditions. Biological systems however, are gaining in popularity, often as complementary technologies after a physical or chemical process has removed some of the more toxic pollutants. These systems have often proved to be as effective as the physical methods while operating at substantially lower cost (Kuroda and Ueda, 2003). Two such treatment alternatives for the removal of metal ions from wastewater are biosorption and bioaccumulation. Both are important phenomena implicated in all biological systems capable of reducing the metal content of aqueous environments.

Table 2.1 Advantages and disadvantages of physico-chemical heavy metal recovery/removal technologies (adapted from Kurniawan *et al.*, 2006).

Process	Principle	Recovery range	Advantages	Disadvantages
Alkaline chemical precipitation	pH is adjusted to basic conditions, causing dissolved metals to be converted to insoluble solids	> 1000 mg/l	Simple Inexpensive Safe Convenient	Not 100 % efficient Large chemical requirements High sludge production and disposal problems Slow metal precipitation Poor settling
Coagulation-Flocculation	Destabilization of colloids by the addition of a coagulant results in sedimentation of particles. Flocculant is applied in order to increase the particle size of the resultant floccules	> 1000 mg/l or < 100 mg/l	Improved sludge settling and dewatering characteristics Sludge stability Bacterial inactivation	High operating costs due to chemical consumption High sludge volumes
Flotation	Separation of solids or dispersed liquids from a liquid phase <i>via</i> bubble attachment. The target floated substance is then separated in a foaming step.	< 50 mg/l or > 150 mg/l	Good removal of small particles Short retention times Low cost	May require pretreatment such as chemical precipitation
Membrane electrolysis		> 2000 mg/l or < 20 mg/l		High energy consumption
Ion exchange	Interchange of ions with like charge between insoluble phase (resin) and liquid phase without structural change to resin	10 – 100 mg/l or greater	No sludge Selectivity Simple and rapid	Pretreatment required, e.g. suspended solids removal Limited availability of highly selective resins
Electrodialysis	Membrane separation, where ionized metals in solution are passed through an ion exchange membrane by applying an electrical potential	< 1000 mg/l, best at < 20 mg/l	Highly concentrated metal stream for recovery	May require pretreatment to slow fouling High maintenance cost
Electro-chemical precipitation	Modification of conventional chemical precipitation <i>via</i> addition of electrical potential	> 2000 mg/l	Acidic or basic conditions Small footprint Short retention times Low energy requirement	

2.3 BIOSORPTION OF METAL IONS

Biosorption is the term given to the passive sorption and/or complexation of metal ions by biomass. It describes metabolism-independent sorption that occurs between metals and cellular components of the biomass cell wall. As it is a passive process, the biomass need not be living, and in fact, a number of highly efficient commercial biosorbents are dead; AlgaSorb consists of dead *Chlorella vulgaris* immobilized on silica, AMT-Bioclaim uses non-living *Bacillus* species as a sorbent, and Bio-fix employs a combination of dead cyanobacteria, yeast, algal and plant materials (Gupta *et al.*, 2000). These biosorption commercializations have unfortunately not lived up to their potential, and are still only used in small specialized operations as it seems that metal-laden wastewater generating industries either have no interest or lack the capacity to treat their effluents, with most opting for a basic treatment in order to comply with prevailing legal requirements (Gupta *et al.*, 2000).

The mechanisms of biosorption are generally based on physico-chemical interactions between metal ions and the functional groups present on the cell surface, such as electrostatic interactions, ion exchange and metal ion chelation or complexation (Özer *et al.*, 2004). Functional groups most commonly implicated in such interactions include carboxylate, hydroxyl, amine and phosphoryl groups present within cell wall components such as polysaccharides, lipids and proteins (Dziwulska *et al.*, 2004). The binding process is independent of metabolism and hence, of a physical nature. It is also usually rapid and reversible and requires minimal energy for activation; in the region of 21 kJ/mol, as opposed to the activation energy required for bioaccumulation (63 kJ/mol) (Kaduková and Virčíková, 2005). This allows for metal ion desorption followed by regeneration and reuse of the biosorbent in successive sorption/desorption cycles. Despite these advantageous process characteristics, few industrial processes make use of biosorption technology for the purpose of recovering metal ions from wastewaters. This is usually due to the complex nature of the wastewater interfering with the sorption of target metal ions.

The type of biomass used for biosorption of precious metal ions is varied. However, Table 2.2 indicates a trend in the biomass types chosen for the sorption of precious metals, with various forms of chitosan preferred. Chitosan is a deacetylated derivative of chitin, the second most abundant biopolymer on earth after cellulose. The major advantage of using chitosan for precious metal sorption is that the amino sites of chitosan are easily protonated in acid media, accentuating the electrostatic forces often implicated in the initial stages of sorption. Chitosan can be easily modified

by grafting new functional groups onto the polymer backbone. In this way, it is comparable to cellulose, which can also be modified to increase its range of properties and functionalities (Guibal *et al.*, 2002). Tannins are also potent precious metal sorbents, but are more commonly used for their redox capabilities than for functional group composition (Ogata and Nakano, 2005; Ma *et al.*, 2006).

Table 2.2 A review of recent sorbents used for precious metal biosorption.

Sorbent	Metal	Maximum metal uptake (mg/g)	Reference
Chitosan (glutaraldehyde-crosslinked)	Au(III)	565.5	Arrascue <i>et al.</i> , 2003
Chitosan (sulphur-grafted)		624.0	
Condensed tannin gel particles	Au(III)	8 000.0	Ogata and Nakano, 2005
<i>Cladosporium cladosporioides</i> strain 1	Au(III)	81.1	Pethkar <i>et al.</i> , 2001
<i>Cladosporium cladosporioides</i> strain 2		101.0	
<i>Cladosporium cladosporioides</i>	Au, synthetic solution	100.0	Pethkar and Paknikar, 1998
	Au, wastewater	36.0	
Calcium alginate beads	Au(III)	290.0	Torres <i>et al.</i> , 2005
Egg shell membrane	Au(I)	147.0	Ishikawa <i>et al.</i> , 2002
	Au(III)	618.0	
<i>Fomitopsis carnea</i> (immobilized in polyvinyl alcohol)	Au(III)	94.3	Khoo and Ting, 2001
<i>Ucides cordatus</i> (waste crab shells)	Au(CN) ₂ ⁻	33.2	Niu and Volesky, 2003
Dealginated seaweed waste	Au(III)	78.0	Romero-González <i>et al.</i> , 2003
Chitosan (glutaraldehyde crosslinked)	Pd(II)	180.0	Ruiz <i>et al.</i> , 2000
Chitosan (glutaraldehyde crosslinked)	Pt(IV), Pd(II)	NC	Chassary <i>et al.</i> , 2005b
Chitosan (polyethyleneimine grafted)	Pt(IV), Pd(II)	NC	
Chitosan (thiourea grafted)	Pt(IV), Pd(II)	NC	
Alfalfa	Au(III)	38.0	Gamez <i>et al.</i> , 2003
Chitosan (rubeanic acid derivative)	Pt(IV)	400 - 600	Guibal <i>et al.</i> , 2001
	Pd(II)	200 - 300	
Bayberry tannin immobilized collagen fibre membranes	Pt(IV)	41.7	Ma <i>et al.</i> , 2006
	Pd(II)	27.5	
Chitosan (L-lysine modified)	Pt(IV)	129.3	Fujiwara <i>et al.</i> , 2007
	Pd(II)	109.5	
	Au(III)	70.3	
Alfalfa (esterified)		Removal from a 100 ng/l solution	Parsons <i>et al.</i> , 2003
	Pt(IV)	90 %	
Alfalfa (native)	Pd(II)	25 %	
	Pt(IV)	65 %	
	Pd(II)	80 %	

NC: Not calculated (experiments with bicomponent solutions)

2.4 METAL BINDING MECHANISMS

The model first described by Dzombak and Morel in 1990 attempted to illustrate the relative contributions made by each stage in the metal sequestration process, using physical adsorption and cell-surface precipitation as examples. The model suggested an initial rapid sorption stage followed by a slower surface precipitation stage, resulting in an adsorbed layer on the surface covered by a precipitated layer (Schneider *et al.*, 2001). This was further explained by Aksu and Dönmez in 2001, where the metal ions, once diffused to the cell surface, bind to sites exhibiting a chemical affinity for the metal ion. This binding would occur through any of a number of processes, such as physical adsorption, ion exchange, coordination, complexation, chelation or microprecipitation. This stage of adsorption is generally fast, reversible and a non-limiting factor in terms of metal uptake kinetics. This phase is often followed by a slower binding process in which appreciable amounts of additional metal ions are bound, often irreversibly, *via* a number of mechanisms such as covalent bonding, surface precipitation, redox reactions, and cell surface crystallization or, in the case of living cells, diffusion into the cell interior.

However simple or complex the processes involved may seem, the actual mechanisms used are thought to vary depending on the biosorbent used and/or the metal to be sorbed. Two examples of this were discovered early on in the development of the knowledge of biosorption mechanisms. Tsezos and Volesky (1982a; 1982b) proposed two different processes to describe the sorption of uranium and thorium by non-living *Rhizopus arrhizus* cells based on experimental results. In the case of uranium, they suggested an initial complex formation step, a metal nucleation step and a final complex hydrolysis and surface precipitation step. With thorium however, the results suggested the initial coordination/complexation step followed by hydrolysis and finally, adsorption to the cell wall.

Due to the complex nature of the cell wall surface, there are many possible explanations for the sequestration of metal ions by the cell. As stated previously, for non-viable biosorbents these are generally of a physico-chemical nature, i.e. ion exchange, chelation, physical adsorption or microprecipitation (Pagnanelli *et al.*, 2000). Chassary *et al.* (2005a) suggested that certain mechanisms are more prominent under certain conditions, such as chelation of metal cations in near-neutral solutions or ion exchange of metal anions in acidic solutions. These interactions are thought to occur between structures on the cell walls such as carboxylate, phosphate, sulphhydryl,

amino, amide and hydroxyl groups (Esposito *et al.*, 2002; Vasudevan *et al.*, 2002), with the acceptance that amine sites are often the main reactive sites for precious metal ions, with hydroxyl and carboxyl groups contributing to a lesser extent (Guibal, 2004).

2.4.1 Environmental factors affecting the biosorption mechanism

Factors that influence the interactions of these major groups with metal ions include the metal species, the pH and the solution matrix (i.e. at weak acidity, the free electron doublet on the nitrogen ion may bind metal cations, while in acidic solutions, protonation of the amine groups infers a cationic behaviour and thus the potential to attract anionic metals) (Guibal, 2004). According to Aksu and Dönmez (2001), pH is the single most important parameter in the biosorption process. It affects both the biomass and the metal ions in solution by influencing the surface metal binding sites and the metal solution chemistry. In fact, a change of less than 1 pH unit has been known to increase adsorption from 0 to 100 % (Muter *et al.*, 2002). Other factors that affect some, but not all biosorption interactions include temperature, biosorbent concentration, initial metal concentration and type of competing ions in solution (Cho and Kim, 2003).

Solution pH

The pH of the sorbate solution is considered one of the most important environmental factors affecting the biosorption process. This factor is capable of influencing not only the binding site dissociation state, but also the solution chemistry of the target metal in terms of hydrolysis, complexation by organic and/or inorganic ligands and redox potentials (Fiol *et al.*, 2006). This accounts for the specific sorption of some metal species rather than others at various conditions of pH (Godlewska-Żyłkiewicz and Kosłowska, 2005). Other metal-specific pH influences include precipitation, speciation and the availability of the metal for biosorption (Esposito *et al.*, 2002). Successful biosorption of base metal cations usually takes place in the range of pH 3–7, and is extremely pH dependent. Özer and Özer (2003) reported an optimal pH value for lead and nickel uptake of 5.0, while Vianna *et al.* (2000) found that copper, cadmium and zinc uptake was maximal at pH 4.5, and decreased significantly when the pH was dropped to 3.5 or 2.5. This led them to suggest that an initial electrostatic attraction between the negatively charged functional groups and the metal cations was involved in the biosorption reaction.

The response of metal ions to a biosorption process has allowed for the classification of metal ions into three classes, dependent on their behaviour at a specific pH (Madrid and Cámara, 1997). Class

I metals (Al^{3+} , Cu^{2+} , Cr^{3+} , Co^{2+} , Fe^{3+} , Ni^{2+} , Pb^{2+} , UO_2^{2+} and Zn^{2+}) are strongly bound at near-neutral pH, but are not bound or are easily stripped from the biosorbent at $\text{pH} < 2$. This is thought to be due to electrostatic interactions between the metal ions after the ionization of chemical functional groups such as carboxylates at these near-neutral pH values. Class II metals (PtCl_4^{2-} , CrO_4^{2-} and SeO_4^{2-}) exhibit the opposite behaviour to class I metals. They are bound strongly at low pH and only very weakly at $\text{pH} > 5$. Class III metals are the most strongly bound of all metals, as their binding is pH-independent (Ag^+ , Hg^{2+} and AuCl_4^-) (Madrid and Cámara, 1997). Most metal ions present as anions in solution fall into classes II and III. Precious metals (gold and PGMs) are routinely present in solution in anionic form. This implies that along with other metals present in anionic form, e.g. CrO_4^{2-} , SeO_4^{2-} , VO_4^{3-} , they are bound most strongly at low pH or exhibit pH independent binding and thus fall into Class II/III. This classification has been confirmed by numerous authors: Niu and Volesky (2003) determined the optimal pH for adsorption of anionic gold-cyanide, selenate, chromate and vanadate to waste crab shells. All pH optima were found to be below 5 (gold at pH 3.4, selenium at pH 3.0, chromium at pH 2.0 and vanadium at pH 2.5). Gamez *et al.* (2003) showed the pH-independent binding pattern of AuCl_4^- on to alfalfa, confirming the classification of this anion as class III. Both Uzun *et al.* (2003) and Bai and Abraham (2001) showed that the chromate anion binds optimally at $\text{pH} < 2$ on two different biosorbents, pine cone biomass (*Pinus sylvestris*) and the fungus *Rhizopus nigricans*, respectively. Guibal (2004), using glutaraldehyde cross-linked chitosan as an adsorbent, showed that palladium chloride adsorbs optimally at pH 2, similar to the results of Torres *et al.* (2005), who found that the binding of gold to calcium alginate beads was highly pH-dependent, with maximal adsorption occurring at pH 2.

At low pH values cell wall ligands undergo a high degree of protonation, resulting in an overall positive surface charge. This is likely to assist in the attraction of negatively charged ions to the cell wall functional groups through similar electrostatic forces (Parsons *et al.*, 2003). Metal anions such as those formed by Cr(VI) (Özer and Özer, 2003), Au, V and Se (Niu and Volesky, 2003) are all maximally sorbed at pH 3 or less. Dziwulska *et al.* (2004) investigated the ability of the alga *Chlorella vulgaris*, immobilized on Cellex-T, a resin made from highly purified cellulose powder, for selective binding of platinum and palladium from acidic solution (pH 0.5 - 4.5). It was found that retention of platinum by the sorbent was most efficient in the pH range of 1.5 - 2.0. The same was found for the yeast *Saccharomyces cerevisiae* immobilized in calcium alginate (Godlewska-Żyłkiewicz and Kosłowska, 2005), where palladium sorption was most efficient at pH in the range

1.6 - 2.2, and decreased with a decrease in solution acidity. Parsons *et al.* (2003), investigating at a higher pH range (2.0 - 6.0) found that platinum bound optimally to alfalfa biomass at pH 3.0.

The biosorption process is not necessarily limited by this apparent dependence on the small pH range within which optimal sorption occurs. Arrascue *et al.* (2003) made an interesting discovery when screening four variants of immobilized chitosan for gold binding capabilities. They found that by grafting sulphur compounds onto the biosorbent they could decrease the influence of pH *via* modification of the uptake mechanism from pure ion exchange to a combination with sulphur chelation. This would not only increase the uptake capacity, but also allow a much broader operating range if similar modifications are made to other already successful biosorbents. Parsons *et al.* (2003) also found that chemical modification (esterification) of the alfalfa biomass resulted in an increase in the pH at which maximal platinum binding occurred, to pH 6. This, they suggested was due to the conversion of carboxyl groups on the biomass surface to methyl esters, thus removing a large proportion of the negative electrostatic charge at higher pH and thus allowing the platinum ions to approach the biomass and bind in greater amounts at higher pH.

Solution temperature

The temperature at which a sorption reaction takes place is seldom of importance (Panda *et al.*, 2006), with most reactions being temperature-independent (Bhainsa and D'Souza, 1999) or exothermic reactions (Sağ and Kutsal, 2000). There are exceptions however, where temperature does affect the interaction between the biosorbent and the metal ions, usually by influencing the stability of the metal ions in solution (Sağ and Kutsal, 2000), the stability of the metal-sorbent complex, and the ionization of the cell wall chemical moieties (Özer *et al.*, 2004).

Wang *et al.* (2005a) studied the effect of temperature (30 - 50 °C) on the sorption of platinum by immobilized bayberry tannin and found that unlike base metals (iron, copper, nickel and zinc), where an increase in temperature decreased the adsorption capacity, platinum and palladium adsorption was enhanced by increasing the incubation temperature. This was based on the fact that the maximum specific uptake (Q_{max}) increased with an increase in temperature to a plateau at 50 °C of 0.599 mmol platinum(II)/g and 1.29 mmol palladium(II)/g, thereby implying a need for energy in the form of heat for the maximal adsorption of metal ions.

Godlewska-Żyłkiewicz (2003) found only a minor influence of temperature with respect to the sorption of platinum and palladium on *C. vulgaris* and *S. cerevisiae*. In the range 20 - 50 °C, maximal retention was observed on both the alga and the yeast at 20 - 25 °C with only a slight decrease at higher temperatures.

Competing ions

A major complication in the application of biosorption to industrial conditions is the presence of other metal ions in the wastewater to be treated. These will often either compete with the metal of interest for binding sites, or lower the specificity of the biosorbent by binding to sites to which the metal ions of interest do not bind. Tsezos *et al.* (1996) related this to the Pearson classification of metal ions according to the theory of hard and soft acids and bases (HSAB) (Pearson, 1968). The HSAB theory can be condensed into a simple statement, “Hard acids prefer to associate with hard bases and soft acids prefer to associate with soft bases”. Table 2.3 illustrates the acid (metal) categorization according to Pearson’s theory. The precious metals (boldface) all fall into the classification of soft or borderline acids.

Table 2.3 Hard, borderline and soft acids (Douglas *et al.*, 1994).

Hard	Borderline	Soft
H ⁺ , Li ⁺ , Na ⁺ , K ⁺ , Be ²⁺ , Mg ²⁺ , Ca ²⁺ , Sr ²⁺	B(CH ₃) ₃	B(CH ₃) ₂ ,
BF ₃ , Al ³⁺ , AlCl ₃ , Al(CH ₃) ₃	Fe ²⁺ , Co ²⁺ , Ni ²⁺ , Cu ²⁺ , Zn ²⁺	GaCl ₃ , GaI ₃ , GaBr ₃
Mn ²⁺ , Cr ³⁺ , Cr(VI), Mn(VII),	Ru²⁺ , Rh²⁺ , Sn ²⁺ , Sb ³⁺	Cu ⁺ , Co(CN) ₅ ³⁻ , Ag ⁺ , Cd ²⁺ ,
Mo(VI), W(VI) Sc ³⁺ , La ³⁺ , Ce ³⁺ ,	Rh³⁺ , Ir³⁺ , Pb ²⁺ , Bi ³⁺	Pd²⁺ , Pt²⁺ , Pt⁴⁺ , Au ⁺ , Hg ₂ ²⁺ , Hg ²⁺ ,
Lu ³⁺ , Ti ⁴⁺ , Zr ⁴⁺ , Hf ⁴⁺ , VO ₂ ⁺ ,		Tl ⁺
Th ⁴⁺ , Pu ⁴⁺		M ⁰ (metal atoms)
CO ₂ , SO ₃		

The implication within the context of metal biosorption is that the metals present in a wastewater that are similarly classified, i.e. both soft or both hard, will exhibit similar binding site preferences. Tsezos *et al.* (1996) tested this theory, and in the case of precious metals (soft/borderline acids), they showed that the presence of a hard acid (yttrium) had no effect on the biosorption of a soft acid (silver). The presence of a borderline acid (nickel) also had no effect on silver (soft acid) adsorption. However, when testing the effects of a second soft acid (gold) on the biosorption of a target soft acid (palladium) there was a significant negative effect on the sorption of palladium. Both metal ions are classified as soft acids and have similar preferences for biomass binding site ligands.

A factor that further emphasizes this competition is that in high chloride environments, neither of the metals are present as simple ionic forms, but as chloride complexes. Therefore, the complex ionic species must be considered because the observed effects cannot be directly related to the chemical coordination characteristics of the simple metal ions. For example, the chloride species (PdCl_4^{2-} and AuCl_4^-) when compared, both have the same (d^8) electronic configuration and both exhibit square planar stereochemistry (Tsezos *et al.*, 1996). These similar characteristics further explain the competitive nature of soft acids (particularly precious metals in high chloride environments) for biomass binding sites. A further complication arising from the presence of a large excess of chloride ions is the strong competition between the anions of the acid (chloride) and the metal species. This may result in the restriction of metal sorption (Godlewska-Żyłkiewicz, 2003), which is particularly important when considering any laboratory results with an idea to apply a similar system to a high chloride, industrial wastewater environment.

This chloride competition was echoed by Dziwulska *et al.* (2004), who used immobilized *C. vulgaris* as a platinum and palladium biosorbent. They pointed out that at very low pH, strong competition between anions of the acid (chlorides) and platinum species inhibits biosorption of the metal. They also showed that of all of the base metals tested for their impact on palladium and platinum sorption (zinc(II), nickel(II), cobalt(II), copper(II), manganese(II), iron(III) and sodium(I)), only iron and zinc ions interfered with the binding of platinum and palladium, probably due to their ability to form chloride complexes in excess chloride ions at acidic pH.

2.4.2 Precious metal biosorption mechanisms

In wastewaters with high chloride concentrations, and typically low pH, such as platinum group metal (PGM) refinery wastewaters, PGMs are present in the form of anionic chlorocomplexes with complicated solution chemistry. The species composition is dependent on factors such as chloride concentration, pH, ionic strength, temperature, and the age of the solution. The formation of metal complexes (especially chlorocomplexes) by PGMs is related to the solution composition. This in turn may affect the adsorption mechanism involved, i.e. chelation rather than ion exchange, and the affinity of the metal species for sorption sites on the biomass (Chassary *et al.*, 2005a). To further complicate the recovery, the different species present react differently to the extraction process. This is further compounded by the fact that the solution chemistry of precious metals is generally very different to that of base metals. For example, in biosorption processes, anions are typically

adsorbed at low pH (1.0–3.0) such as pH 1.6–1.8 for platinum and palladium (Godlewska-Zyłkiewicz, 2003), whereas cations adsorb at higher pH (3.0–7.0) e.g. pH 5.0 for lead and copper, and pH 5.5 for cadmium, zinc, and nickel (Sheng *et al.*, 2004).

Large volumes of published data exist regarding the recovery or removal of base metals from aqueous solutions, but the same cannot be said for precious metal recovery, where the industrial value of such information requires that it be closely guarded. Historically, published precious metal biosorption data has focused on gold recovery, but over the last fifteen to twenty years, interest in the recovery of strategically valuable metals such as platinum and palladium has increased.

Gold

In 1986, with biosorption studies using *C. vulgaris*, Darnall *et al.* (1986) showed that the alga was capable of removing more than 90 % of the gold present from even very dilute solutions. The brown marine alga *Sargassum natans* was also found to be highly selective for gold (Kuyucak and Volesky, 1990). Further experimentation showed that *S. natans* was capable of reducing ionic gold and storing it in elemental form on the cell wall. The gold uptake capacity was found to be higher than that of commercial ion exchange resins available at the time.

More recently, studies have begun to focus significantly on the mechanisms involved in the binding of gold ions to biomass. Initially this took the form of conjecture, but now the use of spectroscopic methods such as variants of x-ray and Fourier-transform infra red (FTIR) spectroscopy for the elucidation of binding mechanisms is widely used. X-ray photoelectron (XPS) and FTIR spectroscopy were used by Pethkar *et al.* (2001) to determine the mechanism involved in the adsorption of gold ions to two strains of the fungus, *Cladosporium cladosporioides*. These methods confirmed that that no chemical change to the biosorbent took place after metal loading, suggesting that the acidic conditions merely favoured electrostatic interaction between gold anions (AuCl_4^-) and protonated biomass. Similarly, x-ray diffraction (XRD) and FTIR spectroscopy were used by Ogata and Nakano (2005) to explain the binding mechanism taking place between gold ions and tannin gel particles capable of extremely high gold uptake relative to other systems (Table 2.4). The results suggested that a redox reaction between the tannin gel and the AuCl_4^- species was occurring, resulting in the reduction of trivalent Au(III) ions to Au(0) and the oxidation of the hydroxyl groups

of the tannin gel to carbonyl groups. The complete reaction is shown in Equation 2.1. This mechanism is similar to that suggested by Kuyucak and Volesky (1990).



Fourier-transform infra-red analysis suggested the involvement of carboxyl and hydroxyl groups in binding and later reduction of Au(III) to Au(0) and Ag(I) to Ag(0) in the case of metal binding to calcium alginate beads (Torres *et al.*, 2005). Lin *et al.* (2005) characterized the biosorption of Au(III) to brewery waste *S. cerevisiae* using numerous spectroscopic techniques. X-ray diffraction patterns suggested that Au(III) ions bound to the cell wall were reduced to elemental Au(0). Fourier-transform infra-red spectroscopy indicated that functional groups, such as hydroxyl and carboxylate anions may be gold binding sites, with the hemiacetalic hydroxyl groups present on reducing sugars responsible for electron donation in the reduction of Au(III) to Au(0).

There is now significant evidence that the metal binding mechanism occurring in one system bears little or no similarity to mechanisms involving the same metal and a different biomass (form or type). However, the chemical characteristics of certain metals ensure a common mechanistic thread. For example, the literature reviewed here regarding gold biosorption often cite the reduction of Au(III) to Au(0) as the final stage in the immobilization of the metal onto a sorbent.

Platinum and palladium

In the case of PGM biosorption (especially platinum and palladium), there is more consensus regarding the binding mechanism debate, with most authors in agreement with an initial electrostatic interaction. Guibal *et al.* (1999) studied the recovery of platinum ions from dilute solutions by chitosan cross-linked with glutaraldehyde. The maximum specific metal uptake (Q_{max}) reached 300 mg/g at an optimum adsorption pH of 2. The glutaraldehyde cross-linking was necessary for stabilization of the chitosan in acidic pH, and interestingly, chloride and nitrate anions significantly decreased the uptake of the platinum chloride anions. This suggests competition for protonated binding sites, implying a simple electrostatic binding mechanism. Godlewska-Żyłkiewicz (2003) further explained this when considering the binding of palladium and platinum by *C. vulgaris* and *S. cerevisiae*. Both indicated pH-dependent binding, with the highest metal

retention at pH 1.6 - 2.2. Usually, such pH-dependent binding signifies interactions *via* an ion exchange mechanism, but in acidic solutions platinum and palladium occur mostly in anionic form while functional groups of the cell wall are protonated. Again, this suggests that binding is also consistent with electrostatic forces, where at low pH, surface charge is positive and aids in negatively charged ion binding. Functional groups contributing to the binding mechanism were suggested to be protonated amine, imidazole or thiol groups capable of interacting with the precious metal anions *via* the N or S atoms. The differing pH profiles obtained from the *C. vulgaris* and *S. cerevisiae* were attributed to dissimilar binding mechanisms for alga and yeast with respect to functional group content and involvement.

Similar to Arrascue *et al.* (2003), who grafted sulphur moieties onto chitosan and found a mechanism shift, Parsons *et al.* (2003) found that esterification of alfalfa biomass allowed not only comparable platinum(IV) recovery at pH 2 (untreated optimum) and pH 6 (esterified optimum), but also 10 – 15 percent more platinum was bound by the esterified biomass. This increase may have been a result of the esterification process converting the biomass carboxylic groups to methyl esters, allowing platinum to approach the esterified biomass and to bind in greater amounts at higher pH.

Immobilized *C. vulgaris* has also been studied as a platinum and palladium biosorbent (Dziwulska *et al.*, 2004). The pH optima were 1.5–2.0 for both metals. Again, this was suggested to be an electrostatic mechanism, where at low pH the overall surface charge on the biomass is positive, assisting in the approach of negatively charged platinum and palladium ions through electrostatic forces. They also suggested that functional groups containing nitrogen and/or sulphur atoms from protonated amine or imidazole as well as thiol groups might be responsible for biosorption.

Although the electrostatic mechanism seems to be generally accepted, evidence against such a simple mechanism exists. Reversal of the electrostatic interaction should be easily achieved by pH adjustment, which would result in the reversal of the forces governing the reaction and the subsequent repulsion of the metal ions by the biomass surface charges. This is not the case in most reported desorption studies involving platinum and palladium. In most cases, in fact, a strong metal chelating agent such as acidified thiourea is needed in order to recover quantities of any

significance from the sorbent surface (Godlewska-Żyłkiewicz and Kosłowska, 2005; Ma *et al.*, 2006).

A different scenario is presented by workers using tannins to sorb platinum and palladium, where chemical mechanisms and redox reactions are implicated. The selectivity of collagen fibre-immobilized bayberry tannins for biosorption of platinum(II) and palladium(II) discussed by Wang *et al.* (2005a) was attributed to a chemical adsorption mechanism. This assumption was based on the observation that the Q_{max} increased with an increase in temperature to a plateau at 50 °C of 0.599 mmol platinum(II)/g and 1.29 mmol palladium(II)/g, thereby implying a need for energy in the form of heat for the maximal adsorption of metal ions. Kim and Nakano (2005) applied tannin gel particles to palladium recovery, and results published were similar to that of the gold reduction mechanism, where a redox reaction resulted in the reduction of palladium(II) to palladium(0).

Again, it seems that the mechanism responsible for metal (platinum or palladium) binding depends largely on the type or form of the sorbent used. This emphasizes the need for mechanism elucidation on a case-by-case basis, and the use of published literature only as a comparison point as it would seem that unless identical systems are compared, the comparison may not be valid.

2.5 YEAST BIOSORPTION

Yeast biomass (such as *Saccharomyces cerevisiae*), while not particularly high in chitin content, is cheap and readily available as a waste product from various sources. It is also simple and inexpensive to produce on a large scale. This has resulted in it being one of the most commonly screened biomass types for biosorption ability, and has been shown to sorb both precious and base metals from solution. This sorption capacity has been improved in numerous studies by pretreatment and/or immobilization.

Many species of yeast biomass, in diverse forms, have been investigated for the ability to adsorb metals. Studies have shown that a number of yeast species are capable of adsorbing heavy metals such as copper, cadmium, zinc, lead, chromium and many others (Lozovaya *et al.*, 2005; Mapolelo *et al.*, 2005; Cho and Kim, 2003; Muter *et al.*, 2002). The ability of yeast biomass to accumulate

precious metals such as palladium and platinum has also been investigated (Godlewska-Żyłkiewicz and Kosłowska, 2005; Godlewska-Żyłkiewicz, 2003). Yeast species are of particular interest as biosorbents due to their abundance as waste from fermentation processes and their relative ease of cultivation and as such, they are a ready source of cheap biomass (Aksu and Dönmez, 2001).

The pigmentation, or lack thereof, of yeast cells seems to play a role in metal biosorption. Of the eight yeast species studied by Lozovaya *et al.* (2005), three were non-pigmented (*S. cerevisiae* 1968, *Candida krusei* 61t and *Williopsis californica* 248), four carried a pink/red pigment (*Rhodoturula mucilaginosa* 1776, *Rhodoturula aurantiaca* 1198 and 1195, *Rhodoturula sp.* 4) and one was black-pigmented (*Cryptococcus sp.* WT). In general, they found that for the biosorption of Cr(VI) by living cells, the non-pigmented yeasts (*C. krusei* 61t and *W. californica* 248) performed better than their pigmented counterparts. But when non-living yeasts were used, the pink- or red-pigmented *Rhodoturula* yeasts were the best (*Rhodoturula sp.* 4 $Q_{max} = 1100$ mol/g and *Rhodoturula mucilaginosa* 1776 $Q_{max} = 1000$ mol/g). This was thought to be due to the chelation abilities of melanin and carotenoids present on the cell wall of the pigmented species. Salinas *et al.* (2000) investigated a similarly pigmented species, *Rhodoturula rubra*, for biosorption of Cd(II) and Pb(II). They concluded that when compared to *S. cerevisiae*, red-pigmented yeasts are better than non-pigmented for Cd bioaccumulation due to the difference in composition of the cell walls. *Saccharomyces cerevisiae* is an ascomycete with a cell wall composed of glucan and mannan with only traces of chitin, whereas *R. rubra* is a basidiomycete, the cell wall of which is characteristically high in mannan, in particular, highly branched polymer called fucogalactomannan, which is not present in *S. cerevisiae*. There is also a high chitin content with traces of glucan and the production of capsular exopolysaccharides which further increase adsorption. Chitin is a well-documented biosorptive agent (Guibal, 2004) and may further aid the uptake capacity of the *Rhodoturula rubra* yeast in the same way as suggested for *R. arrhizus*, i.e. metal coordination to the amine N of the cell wall chitin (Salinas *et al.*, 2000). The ability of *Rhodoturula glutinis* to biosorb lead, investigated by Cho and Kim (2003), was similarly enhanced by the production of an extracellular polysaccharide.

Both *Rhodoturula* species studied (Cho and Kim, 2003; Salinas *et al.*, 2000) showed similar metal binding affinities. The pH optimum for lead biosorption was 4.0 – 4.5 for both species, and the Q_{max} values were higher than those reported for *S. cerevisiae* and numerous fungal biomass types

(*R. glutinis* $Q_{max} = 74.5$ mg Pb(II)/g biosorbent). Both studies also focussed on the effects of temperature on metal binding. Salinas *et al.* (2000) found that an increase in temperature from 25 °C to 37 °C inhibited lead uptake but increased cadmium uptake by *R. rubra*, while for *R. glutinis*, an increase in temperature from 15 °C to 45 °C had no effect on lead uptake (Cho and Kim, 2003). This suggests different interactions between the cell wall ligands and the metal ions. For cadmium uptake, the enhancement by temperature increase suggests a chemical adsorption process, whereas the inhibition by temperature increase suggests a physical adsorption process for lead (Salinas *et al.*, 2000). Cho and Kim (2003) suggested that ion-exchange followed by microprecipitation by phosphate ions released by *R. glutinis* biomass was responsible for lead adsorption.

Further evidence for the enhancement of metal biosorption by extracellular polysaccharides was reported by Breierová *et al.* (2002). Eight yeast species were investigated for use as Cd(II) bioaccumulators. They found that the ability to adapt to the toxicity of the metal ions was largely dependent on the ability to produce an extracellular glycoprotein. The highest tolerance to cadmium toxicity was exhibited by *Hansenula anomala*, with the glycoprotein responsible for almost 90 % of the accumulated metal. The lowest tolerance was exhibited by *S. cerevisiae*, with only 6 % of the accumulated metal being sequestered to the glycoprotein fraction. The authors suggested that the difference was caused by the variable saccharide composition of the glycoprotein, which resulted in insufficient production of the correct extracellular glycoprotein to protect *S. cerevisiae* from internalising cadmium ions to toxic levels.

Mapolelo *et al.* (2005) surveyed a number of yeast species for the ability to preconcentrate trace metals from aqueous solutions for subsequent analysis. The results showed that the yeast species (including *S. cerevisiae* and *Candida tropicalis*) were viable trace metal scavenging agents and could be used, freely suspended, to recover metals from aqueous solutions at relatively low metal concentrations. Muter *et al.* (2002) studied the effects of cationic base metals (Cu(II), Zn(II), Cd(II) and Pb(II)) in solution on the uptake of anionic Cr(VI) by live and dried *Candida utilis*. They found that all of the metals tested influenced the chromium biosorption; copper and lead enhanced, while zinc and cadmium inhibited chromium uptake. With regard to uptake by the other metals, the presence of chromium in solution influenced only the uptake of cadmium, causing slight inhibition. Aksu and Dönmez (2001) used a further *Candida* species in various forms for copper biosorption.

Dried, autoclaved, perchloric acid-washed and ethanol-washed *Candida* all performed better than the live culture; in the case of dried yeast, by up to 90 %. Suggested reasons for this uptake enhancement rest on the assumption that the treatments are removing cations or organic compounds from the cell surface, thereby creating new binding sites (either by creating new electrostatic bonds, changing the overall surface charge or modifying existing binding sites). Conversely, it was suggested that the formaldehyde might mask reactive sites initially available on the biomass.

2.5.1 *Saccharomyces cerevisiae* biosorption

Historically, *S. cerevisiae* has been the most widely studied yeast species in the field of heavy metal biosorption (Cho and Kim, 2003), and this is despite several references to its biosorptive potential by some as 'mediocre at best' (Wang and Chen, 2006; Salinas *et al.*, 2000). Table 2.5 illustrates the wide range of metals used for sorption experiments involving *S. cerevisiae*. The highest specific uptake recorded was for whole, non-viable biomass (270.3 mg/g) by Özer and Özer for lead in 2003.

Precious metal biosorption is not well documented, for reasons explained earlier. A few examples of biosorption of platinum, palladium, gold and rhodium by *S. cerevisiae* can be found in literature and are reviewed here.

In previous research, *Saccharomyces cerevisiae*, pretreated with polyethyleneimine and immobilized with glutaraldehyde was investigated as a biosorbent for the recovery of rhodium chloride anions from synthetic solutions and wastewater from a precious metals refinery. The maximum specific uptake was calculated in both the synthetic and the true wastewater (7.96 mg/g and 0.36 mg/g, respectively) (Mack, 2005). These results indicate that optimization of a biosorption system within the actual environment it is intended is extremely important, as synthetic solutions almost never completely mimic those found in a real industrial wastewater.

Increasingly, PGMs are detected in environmental samples such as grass and dust near highways. This is due to the increasing prevalence of catalytic converters in motor vehicles (Ravindra *et al.*, 2004). Immobilized *S. cerevisiae* (within calcium alginate beads) was used by Godlewska-Żyłkiewicz and Kosłowska (2005) to extract palladium from road dust. The calculated efficiency of

biosorption of palladium from samples was approximately 80 %, and elution with 0.3 M thiourea in 0.25 M HCl resulted in approximately 100 % elution of the metal ions from the biosorbent beads.

Table 2.4 Base metal ion biosorption by *S. cerevisiae* in recent literature.

Metal	Biosorbent form	pH optimum	Maximum metal uptake (mg/g)	Reference
Ag	Whole ^a	4	42.7	Chen and Wang, 2007
As(V)	Methylated ^a	7		Seki <i>et al.</i> , 2005
Ca	Protonated ^a	6.75	1.00 meq/g*	Vasudevan <i>et al.</i> , 2002
Cd	Protonated ^a	6.5	91.7	Vasudevan <i>et al.</i> , 2003
	Ethanol ^a	6.0	31.75	Göksungur <i>et al.</i> , 2005
Cr(VI)	Whole ^b	2	6.08 l/mg	Goyal <i>et al.</i> , 2003
	Whole ^a	1	32.6	Özer and Özer, 2003
	Methylated ^a	6	N.C.	Seki <i>et al.</i> , 2005
	Whole ^a	2	N.C.	Park <i>et al.</i> , 2005
	Cationic, surfactant-modified ^a	4.5-5.5	94.34	Bingol <i>et al.</i> , 2004
Cs	Whole ^a	4	12.09	Chen and Wang, 2007
Cu(II)	Caustic ^a		181.8	Göksungur <i>et al.</i> , 2003
	Formaldehyde ^a		0.75 l/mg	Jianlong, 2002
	Glutaraldehyde ^a		2.4 l/mg	Jianlong, 2002
	Methanol ^a		0.99 l/mg	Jianlong, 2002
	Whole ^a		1.25 l/mg	Jianlong, 2002
Hg	Magnetically modified ^a	7	133.3	Yavuz <i>et al.</i> , 2006
K	Protonated ^a		0.100 meq/g*	Vasudevan <i>et al.</i> , 2002
Mg	Protonated ^a		0.360 meq/g*	Vasudevan <i>et al.</i> , 2002
Ni(II)	Whole ^a	5	46.3	Özer and Özer, 2003
	Protonated ^a	6.75	16.9	Padmavathy, <i>et al.</i> , 2003
Pb(II)	Immobilized ^a	5	30.0	Çabuk <i>et al.</i> , 2007
	Whole ^a	4	85.6	Chen and Wang, 2007
	Whole ^a	5	270.3	Özer and Özer, 2003
Sr	Whole ^a	4	6.66	Chen and Wang, 2007

^a: non-viable biosorbent, ^b: viable biosorbent, *: Calculated by titration method, N.C.: not calculated

Lin *et al.* (2005) characterized the biosorption of gold(III) to brewery waste *S. cerevisiae* using numerous spectroscopic techniques. X-ray diffraction (XRD) patterns suggested that gold(III) ions bound to the cell walls was reduced to elemental gold(0). Fourier-transform infra-red (FTIR) spectroscopy indicated that functional groups, such as hydroxyl and carboxylate anions may be gold

binding sites, with the hemiacetalic hydroxyl groups present on reducing sugars responsible for electron donation in the reduction of Au(III) to Au(0).

Godlewska-Żyłkiewicz (2003) used whole viable *S. cerevisiae* as a biosorbent for the preconcentration and separation of platinum and palladium before analysis. The highest retention for each metal by the yeast was 65 % of a 75 ng/ml platinum concentration and 95 % of a 25 ng/ml palladium concentration. Both were obtained at acidic pH (1.6 – 2.2). The maximum uptake capacity of whole, viable *S. cerevisiae* was calculated as 12.0 µgPd/g and 0.8 µgPt/g.

Overall, *S. cerevisiae* has been studied as a potential sorbent for recovery or removal of trace amounts of metal ions, and only rarely as a recovery option for PGMs from refinery waste streams. As a cheap and readily available resource (either as an existing waste product or as an easily producible biomass), *S. cerevisiae* may represent a simple and cost-efficient means for the recovery of PGMs. The optimization of such a process, encompassing the use of cheap and readily available resources would be of great benefit both as a means of increasing the efficiency of the recovery of PGMs and also for simplifying the downstream treatment of the wastewaters.

2.6 PRELIMINARY SUMMARY AND CONCLUSIONS

Platinum group metals are of extreme strategic and economic value, especially to developing economies such as South Africa. South Africa is fortunate enough to hold the world's largest source of PGMs, in the Bushveld Igneous Complex, from which more than 50 % of the world platinum demand is supplied. The biggest PGM refiner in the country is the Anglo Platinum precious metals refinery in Rustenburg, in the Northwest Province. Here PGMs are refined using hydrometallurgical methods such as solvent extraction and liquid ion exchange. These processes produce large volumes of liquid wastes with high inorganic loads, extremes of pH, residual metal loads, and organic compounds. Such wastewaters require extensive treatment in order to meet legislation regarding their output to the surrounding environment. Currently, the refinery stores its liquid wastes onsite indefinitely after basic treatment.

The recovery of precious metals from such wastewaters has numerous advantages; it minimizes environmental contamination and the recovered metal can be reprocessed for sale. Currently physico-chemical methods such as chemical precipitation are used to remove the bulk of the metals entrained within the wastewater. This technique in particular has high operating costs, produces a secondary waste which is difficult to treat, and can be inefficient if the operating parameters are not closely monitored. At the Anglo Platinum PMR, chemical precipitation with sodium hydroxide is used to remove metals from the wastewaters. This is followed by atmospheric evaporation in dams (reservoirs) in order to concentrate the resulting sludge. Interest has been shown in a biological alternative, not necessarily to chemical precipitation itself, but for something that would make the recovery of valuable metals easier. This alternative must be impervious to the harsh conditions presented by the wastewaters. Literature suggests that one such alternative technology is biosorption.

Biosorption is a term used to describe the passive sorption of metals by charged functional groups present on a cell surface. It has proved to be efficient even at very low metal concentrations (< 10 mg/l). The type of biomass used is an important consideration; not only must it be widely and cheaply available, but certain types are more suited to precious metal sorption than others. Generally, organisms that possess a higher percentage of amine, thiol, and sulphhydryl groups, such as those with a cell wall containing chitin, are more successful as precious metal sorbents. This includes some fungi and seaweeds, and crustacean wastes. The mechanisms governing the sorption of metal ions by biomass vary depending on the biomass, the state in which said biomass is used, the metal, the species of the metal within a solution, solution pH, solution temperature, and the general composition of the metal-containing solution. With so many factors affecting both the mechanism of sorption and the efficiency of sorption, it is apparent that much work is required in order to optimize a sorption system.

From the literature reviewed, it is evident that there is a pressing requirement for an effective metal recovery technology at the Anglo Platinum PMR that would both decrease the potential cost to the environment and increase the effective metal production from the site. Biosorption is an alternative that could be used successfully as a point-source metal recovery step, and a suitably immobilized *S. cerevisiae*-based sorbent could be produced and a sorption system designed with a specific waste

stream in mind, taking into account the wide variety of wastewater components that may interfere with the metal sorption.

CHAPTER 3

Hypothesis, Aims and Objectives

3.1 HYPOTHESIS

A biosorbent comprising suitably immobilized baker's yeast (*Saccharomyces cerevisiae*) is capable of quantitative (complete) recovery of precious metal ions from a precious metal refinery (PMR) wastewater *via* the process of biosorption.

3.2 AIM AND OBJECTIVES

3.2.1 Aim

To develop a cost-effective biosorption system for the recovery of one or more metal ions from wastewater streams generated at the precious metals refinery.

3.2.2 Objectives

1. To produce a *S. cerevisiae*-based sorbent suitable for use in the recovery of precious metals from PMR wastewaters.
2. To determine the target metal for which the sorbent has the greatest affinity.
3. To optimize the physical and chemical parameters affecting the sorption process in order to maximize metal recovery.
4. To investigate the sorption mechanisms/processes underlying the biosorption phenomenon in this particular system.
5. To compare the sorption process in a stirred batch system with a fixed-bed column system.
6. To quantify the competitor or inhibitor cations and anions present in the PMR wastewater and further optimize the sorption system in order to overcome this inhibition.

CHAPTER 4

Immobilization of *Saccharomyces cerevisiae* biomass

4.1 INTRODUCTION

The most important physical characteristics of a successful biosorbent are mechanical stability, porosity, particle size and density. These characteristics help to ensure that the biosorbent is capable of withstanding high liquid pressures that may be experienced in the biosorption environment and still maintaining superior removal efficiency. A broad tolerance to a number of factors including temperature, pH and solvent content are also highly beneficial, especially in cases where the effluent to be treated is highly acidic in nature or contains organic compounds that could possibly render the biosorbent useless. A commonly overlooked aspect of biosorbent design is settleability, which is necessary to ensure effective downstream separation of the used biosorbent from the wastewater (Liu *et al.*, 2003).

Availability is a major factor in the selection of biomass to be used as a biosorbent. An enormous pool of possible biosorbent material exists in nature and many of these natural biosorbents are cheaply available as they can often be acquired as waste biomass from existing processes, such as spent yeast from breweries or bacterial biomass from pharmaceutical industries. The use of waste biomass is currently in favour as it not only provides a sustainable disposal and reuse cycle, the cycle is also an environmentally positive one. A rapidly growing number of waste products have been screened for biosorptive abilities, as they have been recognized as being the most cost effective solutions to commercialization of biosorption processes. Agricultural wastes such as carrot residues (Nasernejad *et al.*, 2004), crab shells (Vijayaraghavan *et al.*, 2004), olive mill residues (Vegliò *et al.*, 2003), rice milling by-products (Tarley and Arruda, 2004), rice bran (Wang and Qin, 2004) and wheat husks (Basci *et al.*, 2004) have been screened for biosorptive activity. Metals such as copper, zinc, chromium, cadmium, nickel, aluminium and lead have been shown to adsorb to some or all of these. In all cases, encouraging potential for efficient removal of metal ions from aqueous solutions was shown.

The metabolic status of the biomass, i.e. viable (living) or non-viable (dead) also impacts on the efficiency of the biosorption process. The use of non-viable biomass has a number of advantages over viable biomass, the greatest being the complete lack of toxicity limitation. Others include

reductions in cost, as growth medium or nutrient addition is not necessary, ease of handling, cheap industrial waste biomass can be used, and disposal problems usually associated with living cells are not encountered (Padmavathy *et al.*, 2003). Process design is also much simpler using a non-viable biosorbent, as less stringent process control is required, e.g. continual temperature or pH adjustment is not necessary. Efficient pretreatment of the biosorbent is also far easier, as the potential harshness of the treatment process is no longer a factor, as the biomass does not need to be maintained as a viable culture. The biosorbent can also be stored with ease for a much longer period of time than can viable biosorbents.

Desorption of sorbed metals and subsequent reuse of the biomass is also much easier to accomplish when using non-viable biomass, as regeneration usually entails elution with mineral acids or (more often in the case of precious metals) complexing or chelating agents such as thiourea (Godlewska-Zytkiewicz, 2003) or thiocyanates.

The cell wall composition of the biomass chosen also plays an important role in the efficiency of the process. Biomass cell walls consist principally of polysaccharides, proteins and lipids and offer many functional groups that can bind metal ions such as hydroxyl, carboxylate, phosphate, amino and sulphate groups. The quantity and type of the active sites on the cell surface may be a major factor in the binding behaviour of the metal ion of interest, and Pethkar *et al.* (2001) suggested that it may be possible to create highly selective biosorbents (based on their cell wall composition) by manipulating factors such as growth conditions or physico-chemical pretreatment. For example, cell wall soluble proteins that cause problems in metal extraction, by forming complexes with metal ions, can be fixed by some denaturation processes such as heat or ethanol treatment. The caustic treatment of *S. cerevisiae* cells enabled higher uptake of copper ions by eliminating protein groups on the cell wall that were producing non-adsorbable complexes with the copper ions (Göksungur *et al.*, 2003). Biomass dehydration is considered as a promising way to enhance adsorption capacity. Additionally, it can improve the ease of biomass storage and transportation.

4.1.1 The *Saccharomyces cerevisiae* cell wall

The average size of a yeast cell is 3.5 microns (Szabo *et al.*, 2006). The cell walls of yeast and other fungi have been found to consist of three major groups of polysaccharides (Figure 4.1).

These are mannoproteins (mannose covalently linked to peptides), β -glucans (glucose polymers) and chitin (*N*-acetylglucosamine polymers) (Magnelli *et al.*, 2002).

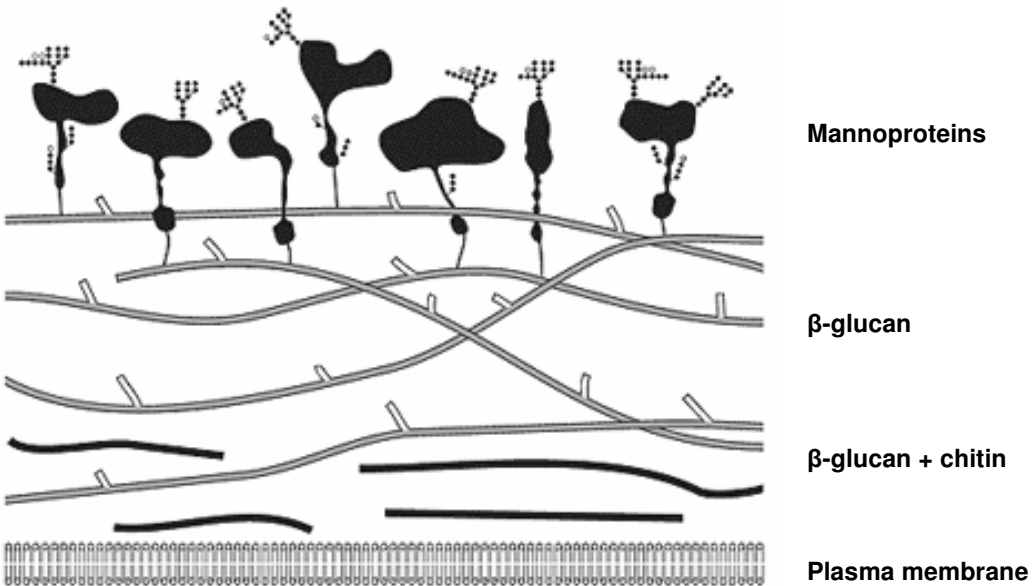


Figure 4.1 Structure of the yeast cell wall (Adapted from Kapteyn *et al.*, 1996 and Grun, 2003).

Analysis of the cell wall using negative staining under an electron microscope showed a layered structure, with an electron-transparent inner layer and an electron-dense outer layer (Klis *et al.*, 2002). The inner layer (50-60 % dry weight of wall) is responsible for the mechanical strength of the wall and is composed of β 1,3-glucan and chitin. The outer layer (30 % dry weight of wall) regulates cell-cell recognition, protects the plasma membranes from foreign enzymes and may be involved in water retention. This layer is composed of heavily glycosylated mannoproteins (Klis *et al.*, 2002). Most cell wall proteins are *O*- and *N*-glycosylated. The *O*-chains are attached to serine or threonine residues and are short, linear chains. The *N*-chains are linked to aspartic acid and are highly branched (Breierová *et al.*, 2002). The metal binding capabilities of *S. cerevisiae* and other fungi have largely been attributed to the charge resulting from the dissociation of weakly acidic carboxyl and the amino acid functional groups reported to be present on the cell wall (Skountzou *et al.*, 2003; Breierová *et al.*, 2002). Phosphomannans have also often been identified as sites for metal binding (Cho and Kim, 2003).

The cell wall adsorptive capacity is determined largely by the structural organization of the protein-carbohydrate complex, by the degree to which the negatively charged functional groups are dissociated and their accessibility to the target metals (Cho and Kim, 2003; Palmieri *et al.*, 2000).

In recent years, cell-surface engineering of yeast has attracted a great deal of interest. The ability to endow intact cells with new functional groups has implications for a wide variety of applications (Kuroda and Ueda, 2003). Such modifications make it possible to construct yeast species for use in specific bioremediation scenarios. For example, a cell-surface engineered yeast displaying a hexa-His protein enhanced both the adsorption of and tolerance to high levels of Cu(II) (Kuroda *et al.*, 2002).

4.2 CHOICE OF IMMOBILIZATION TECHNIQUE

Physical or chemical pretreatment of the biomass in several ways has been found to increase the biosorption capacity of the biosorbent (Aksu and Dönmez, 2001). For example, Yu *et al.* (2007) increased the lead uptake capacity of *S. cerevisiae* fifteen fold by polyamic acid grafting. Pretreatment techniques designed to kill the biomass are advantageous for several reasons other than increased capacity. The cells may be stored or used for extended periods at room temperature, they are not subject to metal toxicity and nutrient supply is not necessary (Aksu and Dönmez, 2001). In fact, many studies comparing the adsorption capacities of viable and non-viable biomass have shown that the non-viable biomass can adsorb far greater amounts of metal. Widely used methods for the simple and efficient killing of biomass include heat treatment, air-drying and freeze drying (lyophilization) (Pagnanelli *et al.*, 2003; Aksu and Dönmez, 2001).

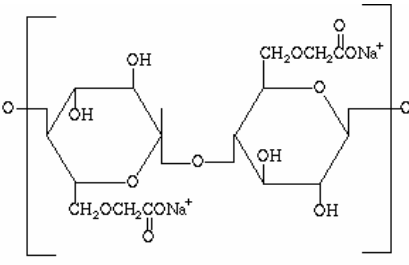
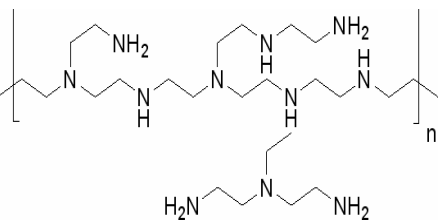
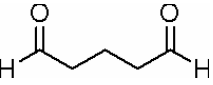
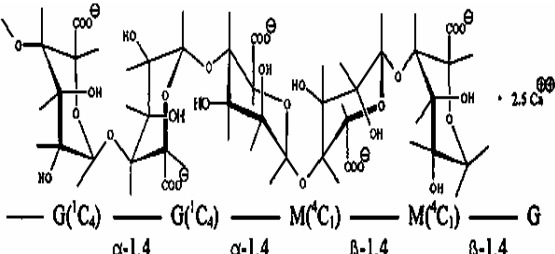
Immobilization of the biomass to be used as a biosorbent is favoured over native, free forms. This has advantages that greatly affect the efficiency of the biosorption process as a whole. It has been found that the small particle size and low mechanical strength of fungal cells can cause difficulties in biosorption processes, so fungal biosorption applications are preferred only if the biomass is immobilized or pelletized before use (Khoo and Ting, 2001). The advantages inherent in the use of immobilized biomass include ease of separation of the biosorbent from a metal-laden wastewater (Valdman *et al.*, 2001), improved hydraulic resistance of the biosorbent for use in fixed or fluidized columns (Al-Rub *et al.*, 2004; Rangsayatorn *et al.*, 2004), enhancement of the physical and chemical stability of the biosorbent (Beolchini *et al.*, 2003; Alhakawati and Banks, 2004) and enhancement of the adsorption and desorption characteristics of the biosorbent (e.g. increasing porosity by cross-linking with a polymer) and extension of the metal selectivity range of the biosorbent (e.g. by addition of metal-specific ligands) (Deng and Ting, 2005).

Literature describes four main techniques used in the immobilisation of biomass to produce effective biosorbents. These are entrapment in polymeric matrices, adsorption on inert supports, cross-linking and covalent bonding onto support media.

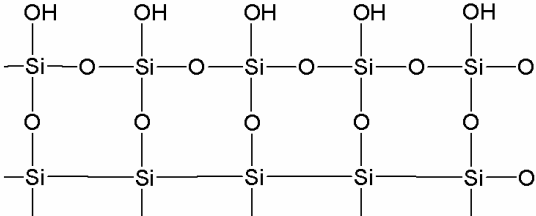
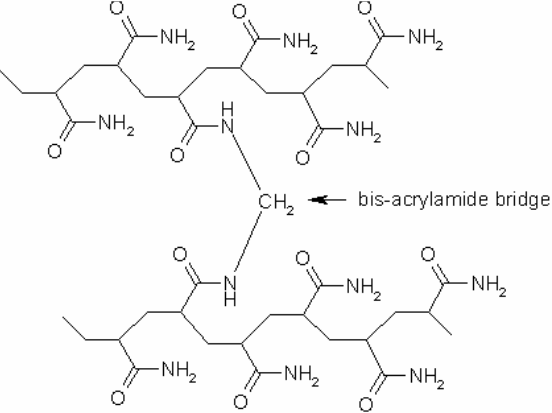
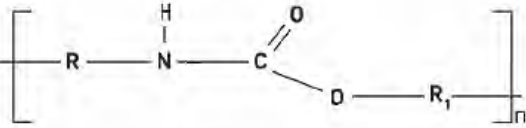
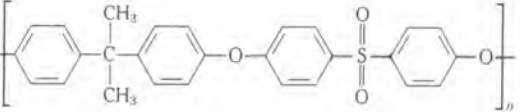
4.2.1 Common immobilization techniques

A summary of immobilization techniques applied in recent years is shown in Table 4.1. Each technique was rated on a scale of 1 – 3 (3 being best) for characteristics necessary for an immobilization procedure suitable for the current study.

Table 4.1 Summarized survey of immobilization techniques.

Immobilization	Biomass	Viable/Non-viable	Reference
<p>Carboxymethyl cellulose (CMC)</p> 	Fungi Fungi Fungi	Viable Viable Viable	Bayramoğlu <i>et al.</i> , 2003 Saglam <i>et al.</i> , 2002 Arica and Bayramoğlu, 2005
<p>Polyethyleneimine</p>  <p>and glutaraldehyde</p> 	Yeast Seaweed Chitosan Fungi	Non-viable Non-viable Non-viable Non-viable	Stoll and Duncan, 1997 Valdman and Leite, 2000 Guibal, 2004 Deng and Ting, 2005
<p>Calcium alginate</p> 	Fungi Cyanobacteria Algae Algae	Non-viable Non-viable Non-viable Non-viable	Khoo and Ting, 2001 Rangsayatorn <i>et al.</i> , 2004 Al-Rub <i>et al.</i> , 2004 Aksu <i>et al.</i> , 1998

Chapter 4 Immobilization of *S. cerevisiae* biomass

Silica	Algae Cyanobacteria	Non-viable Non-viable	Carrilho <i>et al.</i> , 2003 Rangsayatorn <i>et al.</i> , 2004
			
Polyacrylamide	Yeast	Non-viable	Wilhelmi and Duncan, 1995
			
Polyurethane	Fungi	Non-viable	Alhakawati and Banks, 2004
			
Polysulfone	Cyanobacteria Bacteria	Non-viable Non-viable	Blanco <i>et al.</i> , 1999 Beolchini <i>et al.</i> , 2003
			

The following characteristics: toxicity of immobilization agents, mechanical and chemical stability, cost to fabricate, reusability and ease of production, were weighted according to the importance of each characteristic relative to the others. The weighting is shown beneath Table 4.2. The initial scores of those characteristics with a high weighting were multiplied by three, those with a medium rating by two, and those with a low weighting retained their original score. Where no information was available regarding the characteristics of a particular technique, a score of 0 was given. This score did not contribute to the overall technique score. Table 4.2 rates the characteristics of seven common immobilization techniques in order of best score to worst score. It was decided that the top four techniques would be used to immobilize *Saccharomyces cerevisiae* biomass and then the

form which exhibited the highest uptake capacity while maintaining the characteristics of a good biosorbent (as discussed previously) determined.

Table 4.2 Matrix for selection of immobilization techniques to be used.

Method	Immobilization characteristics						Score
	Toxicity (/9)	Mechanical stability (/6)	Chemical stability (low pH) (/9)	Cost (/3)	Reusability (/3)	Production ease (/9)	
Carboxymethyl cellulose (CMC)	9	0	6	3	3	6	27/33 (82%)
Silica	9	0	6	2	3	6	26/33 (79%)
Polyethyleneimine/ glutaraldehyde	6	2	9	2	0	9	28/36 (78%)
Calcium Alginate	9	4	3	2	2	9	29/39 (74%)
Polyacrylamide	6	0	0	2	3	6	17/24 (71%)
Polyurethane	9	0	0	1	2	3	15/24 (63%)
Polysulfone	3	0	6	2	3	6	20/33 (61%)

0: no information available.

Weighting

High

Chemical stability

Toxicity

Production ease

Medium

Mechanical stability

Low

Cost

Reusability

From the results of the literature survey and analysis (Table 4.2), four immobilization techniques were compared experimentally. These were: carboxymethyl cellulose entrapment, silica gel surface immobilization, polyethyleneimine modification with glutaraldehyde crosslinking, and calcium alginate encapsulation.

4.3 MATERIALS AND METHODS

Compressed yeast biomass (*S. cerevisiae*, Anchor Yeast, Inc., South Africa) was purchased at a local supermarket and used in all biosorbent formulations requiring dried yeast biomass. A 2 kg

yeast cake was crumbled and oven-dried at 60 °C for 48 hours, with further crumbling throughout the drying period. The resultant yeast grains were ground to a fine powder.

When required, live yeast (*S. cerevisiae* INVScI, (Invitrogen, Germany)) was sterilely cultured in YPD broth (30 g yeast extract (Biolab, Merck, South Africa), 10 g peptone (Biolab, Merck, South Africa), and 200 ml 1 % D(+)glucose solution (uniLAB, Merck, South Africa) in 1 L). After 24 hours the broth was centrifuged (4000 g for 10 min) in order to pellet the yeast cells. The pellet was then washed in sterile deionized water and resuspended in 30 ml sterile deionized water.

4.3.1 Immobilization procedures

Carboxymethyl cellulose (CMC) beads

Carboxymethyl cellulose sodium salt (Sigma Aldrich, Germany) was dissolved in distilled water (2 % w/v 50 ml). This was then mixed with the biomass previously resuspended in 30 ml sterile deionized water. This solution was dripped through a Pasteur pipette into a 0.2 M ferric chloride (uniLAB, Merck, South Africa) solution to produce beads. The solution was constantly stirred to prevent aggregation of the beads. The beads were cured for 30 minutes in the ferric chloride solution before being washed twice in sterile distilled water. The beads were then incubated for 5 days in YPD broth. After the incubation, the beads were removed and washed in distilled water and then stored at 4 °C until use (Saglam *et al.*, 2002; Bayramoğlu *et al.*, 2003; Arica and Bayramoğlu, 2005).

Silica granules

Approximately 4 g of dried, powdered biomass and 10 g of dried silica gel (Particle size 1 -3 mm, Merck, South Africa) were mixed to form a paste by adding a few drops of deionized water and blending the mixture. The paste was then dried at 80 °C for 20 minutes. This procedure of wetting and drying the biomass-silica material was repeated 3-5 times in order to maximize the immobilization efficiency. The dried matrix was sieved to discard free biomass and uncoated silica gel (Carrilho *et al.*, 2003).

Polyethyleneimine modification and glutaraldehyde crosslinking

Yeast biomass was immobilized using polyethyleneimine (PEI) and glutaraldehyde (GA) as embedding and crosslinking agents, respectively, and subsequently treated with hot alkali (3 % potassium hydroxide) solution (Stoll and Duncan, 1997).

An initial ratio of PEI: GA: yeast (v/v/w) of 1.2: 1: 40 was found to be optimal in the process designed by Stoll (1996). As such, 40 g (wet weight) of yeast was hand-mixed with 4 ml distilled water to form a smooth paste. A 25 % (v/v) solution of GA (50 % aqueous glutaraldehyde, Sigma-Aldrich, Germany) was added to the yeast-paste and blended until smooth. A 33 % (v/v) PEI (50 % aqueous polyethyleneimine, Sigma-Aldrich, Germany) solution was added and the mixture was blended until moist dough was obtained. This dough was then crumbled to form granules and the granules were oven-dried overnight at 80 °C.

The immobilized yeast pellets were suspended in 3 % (w/v) KOH (univAR, Merck, South Africa) solution and heated to 70 °C in a water bath. The granules were then settled and separated from the caustic solution. The caustic solution was retained and the biomass was washed twice with distilled water (the wash water being added to the caustic solution each time). The alkali-soluble components of the biomass were reconstituted by acidification of the caustic solution with 32 % HCl (uniLAB, Merck, South Africa). The HCl was added with stirring until a pH of 6.0 was reached. Subsequent centrifugation (4000 g for 10 min) pelleted out the reconstituted biomass. The washed and reconstituted biomass was then added to the alkali-insoluble fraction and both were oven-dried overnight at 80 °C.

Calcium alginate entrapment

One gram of powdered yeast biomass was mixed with 3 ml of deionized water and 7 ml of a 2 % (w/v) solution of alginic acid disodium salt (Sigma-Aldrich, Germany) to form a slurry. The slurry was then dripped through a Pasteur pipette into a 0.1 M CaCl₂ (uniLAB, Merck, South Africa) solution, which was constantly stirred on a magnetic stirrer to avoid bead aggregation. The beads were stored overnight at 4 °C in 0.1 M CaCl₂ in order to harden. After hardening, the beads were rinsed in sterile deionized water and stored at 4 °C until used (Khoo and Ting, 2001).

Metal sorption analysis

The silica granules and the PEIGA granules showed characteristics necessary for a good biosorbent. Further studies were undertaken in order to evaluate their ability to sorb precious metals from aqueous solutions. Three metals were chosen based on their value, both monetary and strategic. These were gold, platinum and rhodium. A final decision regarding the target metal to be used in all subsequent experiments was made based on the following experimental data.

Metal solutions

All metal solutions were made up by suitable dilution of 1000 mg/l atomic absorption spectrometry standard solutions (EC Labs, South Africa). All glassware was soaked in 5 % HNO₃ (55 %, univAR, Merck, South Africa) overnight and then rinsed for 4 – 6 hours in distilled water before use.

All batch comparison experiments were performed in 10 ml volumes of 200 µM metal concentrations. A sorbent concentration equivalent to 1 g/l of yeast was used in order to accurately compare uptake efficiencies. The pH of the metal solutions was set at an initial pH of < 2 using 1.0 M HCl. This was measured again upon termination of the experiment and was found not to have changed significantly. MacCartney bottles containing the metal solutions and the sorbents (in triplicate) were agitated at room temperature on a bench top shaker at 170 rpm for the required incubation time (3 hours or 24 hours). Protonation of the sorbent surface was achieved by incubation of 1 g of sorbent in 100 ml of 0.1 M HCl (uniVar, Merck) for 24 hours. Samples were centrifuged at 2000 g for five minutes in order to remove particulates, and then assayed for residual metal concentration *via* atomic absorption spectrometry (909AA GBC, Australia). Both the silica granules and the PEIGA granules were assessed using scanning electron microscopy (SEM), but only the SEM results of the silica granule assessment are reported in this section. The SEM results of the PEIGA assessment and further method information regarding SEM analysis can be found in Chapter 5.

The PEIGA sorbent was found to be most suitable for the recovery of precious metals from low pH aqueous solutions. In this section, the metal for which the sorbent has the highest affinity was determined. Also, the contribution of the separate components of the sorbent (the PEIGA polymer and *S. cerevisiae* biomass) to the sorption of metal was examined. An alternate procedure for the production of PEIGA sorbent was compared to the original method described previously. These studies were performed by comparison of sorption isotherms and subsequent calculation of the parameters of the Langmuir isotherm model, which is discussed in more detail in Chapter 6.

For the determination of the highest metal affinity, 1 g/l of PEIGA sorbent was incubated in 50 ml of metal solution of increasing concentration (50 – 1000 µmol/l) for 24 hours with agitation at room temperature (bench top shaker at 170 rpm). In order to compare the relative contributions of the PEIGA polymer and the yeast biomass to sorption, 1 g/l of each were placed in 50 ml of metal

solution of increasing concentration for 24 hours with agitation at 170 rpm at room temperature. The alternate production method was used to produce 5 g of PEIGA sorbent B (as detailed below). Again, each was placed in 50 ml of metal solution of increasing concentration for 24 hours with agitation at 170 rpm.

Samples were removed after 24 hours, centrifuged to remove any particulate matter and the residual metal concentration of the supernatant analyzed by atomic absorption spectrometry.

Alternate PEIGA sorbent production method

According to a method modified from Deng and Ting (2005), 5 grams of dried *S. cerevisiae* biomass was incubated in a 10 % (v/v) solution of PEI (50 % aqueous polyethyleneimine, Sigma-Aldrich) in methanol for 24 hours at room temperature. The biomass was then transferred to a 500 ml solution of 1 % GA (v/v) (25 % aqueous glutaraldehyde, Sigma-Aldrich) for 20 minutes at room temperature. The modified biomass was then thoroughly rinsed with deionized water, oven-dried at 60 °C overnight and then stored in an airtight container before use. This method is simpler, and thus more easily converted to large-scale production than the original procedure.

4.4 RESULTS

4.4.1 Immobilization procedure comparison

Carboxymethyl cellulose beads

The beads formulated using carboxymethyl cellulose formed homogeneously sized, tear-drop shaped beads. However, these beads were very fragile, and even under the gentle agitation called for in the production method, they tended to break apart. Figure 4.2 shows the beads, some of them broken, that resulted from the formulation process. The concentration of carboxymethyl cellulose used was increased in an attempt to strengthen the beads, but at 8 % (w/v), there was still no significant improvement, and it became increasingly difficult to dissolve the carboxymethyl cellulose, even with heating. No further experimental work could be completed with these beads.

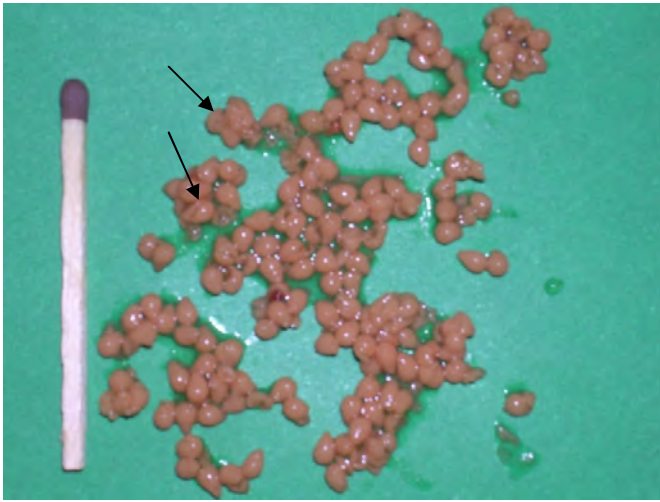


Figure 4.2 Yeast cells immobilized within carboxymethyl cellulose. Arrows indicate ruptured and broken beads. The match provides a size scale (1.2× magnification).

Silica granules

The silica granules exhibited good mechanical stability and density, which resulted in good settling characteristics, and hence easy solid/liquid separation. Particles of less than 1 mm diameter were discarded along with any non-immobilized yeast powder. This did not result in homogenous particle sizes, as the particles larger than 1 mm varied in size from approximately 1 to 3 mm (Figure 4.3).



Figure 4.3 Yeast cells immobilized on the surface of silica gel particles. The match provides a size scale (1.2× magnification).

This can be seen in the series of scanning electron micrographs of the silica granules shown in Figures 4.4A-D. Figure 4.4A shows the smooth and angular surface of free silica gel granules before the immobilization of the yeast cells, while Figure 4.4B shows the changes to the surface

morphology of the silica granules after layered immobilization of the yeast cells. It also highlights the differences in both the size and shape of individual granules. Figures 4.4C and D show the surface magnified in order to indicate the heterogeneity of the granule surface, with numerous layers of yeast cells not forming a smooth surface, thus increasing the surface area available for sorption of metal ions.

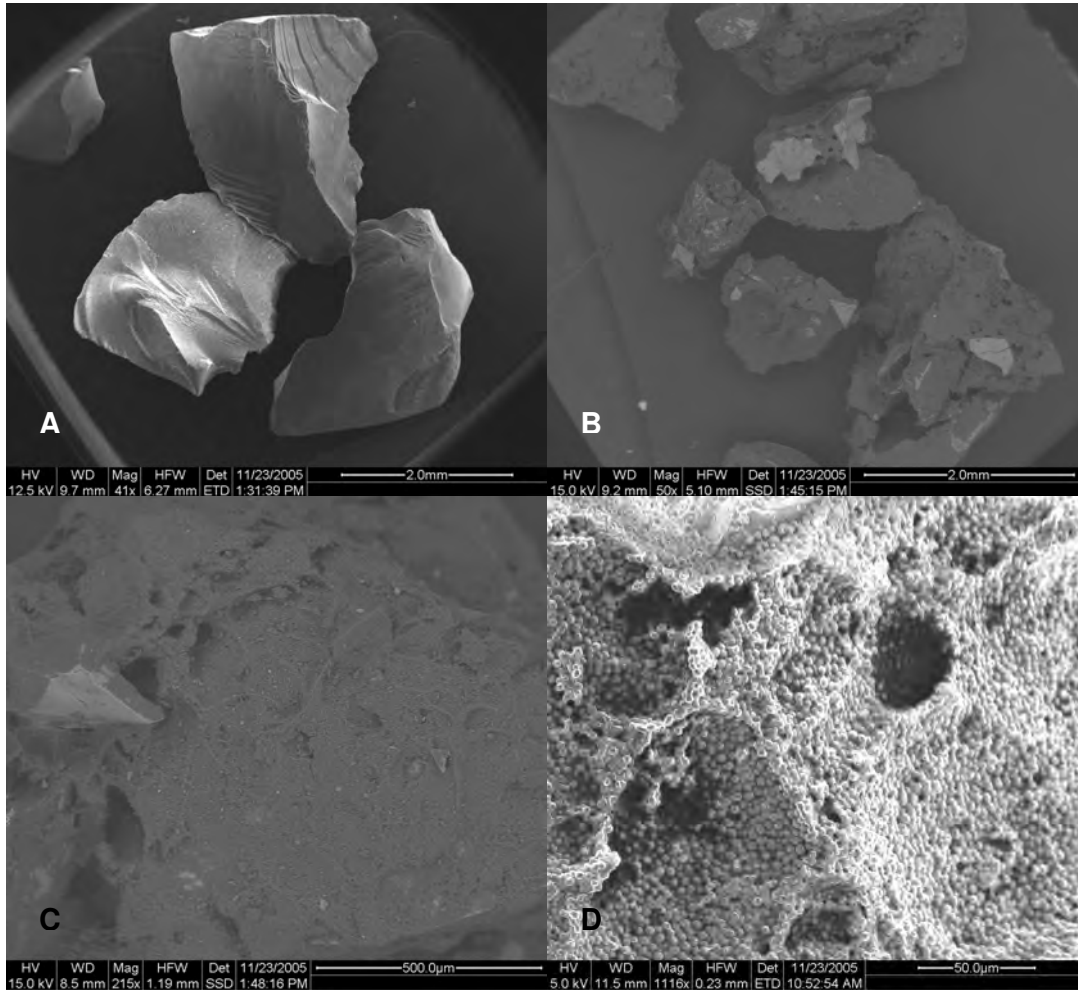


Figure 4.4 Scanning electron micrographs of silica-immobilized yeast granules. **A:** free silica gel granules. **B:** Yeast immobilized on silica gel granules. **C:** View of the layering of yeast cells on the silica surface. **D:** Indication of the dense layers of yeast immobilized on a silica granule.

PEIGA granules

The granules produced *via* surface modification with polyethyleneimine and crosslinking with glutaraldehyde were both mechanically and chemically stable. The granules were not equally sized or similarly shaped (Figure 4.5). The shape and size seemed to be determined by the degree of crumbling during the drying stages, with more crumbling resulting in smaller granules and a higher

proportion of almost powdered sorbent. However, even in the more powdered form, the immobilized sorbent was superior to native yeast in terms of solid/liquid separation.



Figure 4.5 Yeast cells modified with polyethyleneimine and crosslinked with glutaraldehyde. The match provides a size scale (1.2× magnification).

Calcium alginate beads

The beads produced *via* entrapment of powdered yeast within a calcium alginate matrix were mechanically stable, and of even size and shape. However, chemically they were deemed unsuitable for use in the current sorption system. In acidic solutions the beads dehydrated, shrinking by up to 20 % (Figure 4.6).

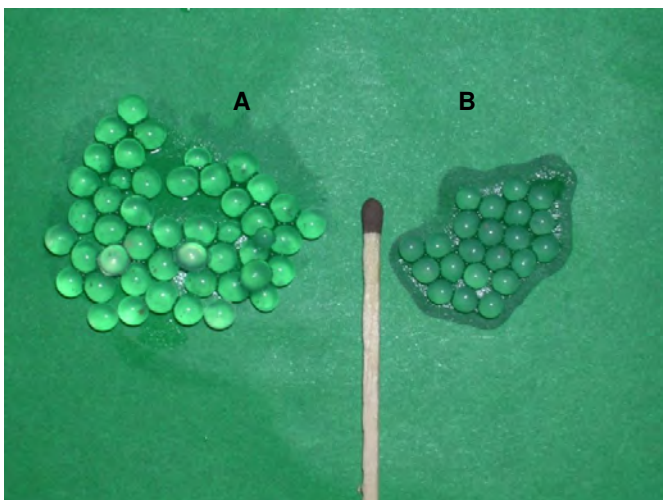


Figure 4.6 Yeast cells immobilized within calcium alginate matrix (A) beads maintained in 0.1 M CaCl_2 , (B) beads maintained in 0.1 M HCl . The match provides a size scale (1.2× magnification).

A simple batch sorption study was performed at low pH in order to determine whether the dehydration had an effect on metal uptake efficiency. Figure 4.7 shows the metal removal efficiency of the calcium alginate beads at a more neutral pH (4) and at the low pH and high acidity expected within a wastewater (pH 1). The uptake capacity of the beads was completely abolished at low pH, rendering them useless for metal uptake within the constraints of the current study as the PMR wastewater is highly acidic, making the application of these beads impossible.

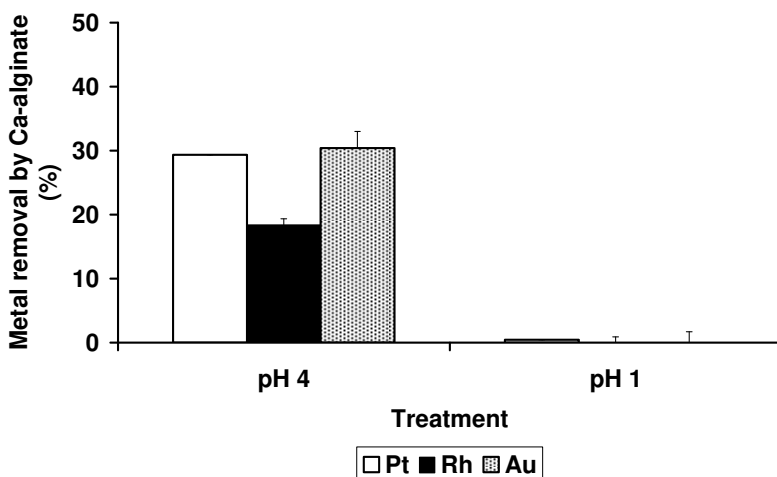


Figure 4.7 Precious metal removal efficiency of calcium alginate-immobilized yeast at low (pH 1) and more neutral pH (4). (200 μ M metal solution, 3 hour incubation, 1 g/l sorbent dose, room temperature). Error bars represent standard deviation from the mean ($n = 3$).

4.4.2 Metal sorption analysis

Figure 4.8 compares the equilibrium uptake of precious metals by the PEIGA and silica sorbents after a three hour incubation period. The PEIGA granules showed the highest uptake capacity for platinum and gold, but both the PEIGA and silica granules exhibited similarly low rhodium uptake capacity.

The incubation time was increased in order to improve the metal uptake. For the silica granules this had no effect on the uptake calculated after three hours. For the PEIGA granules, however, after 24 hours the uptake of platinum and gold had both increased by 15 – 20 % (Figure 4.9). This seemed to suggest that a slower and more complex mechanism was involved in the sorption of platinum and gold onto PEIGA than that of their sorption onto the silica sorbent.

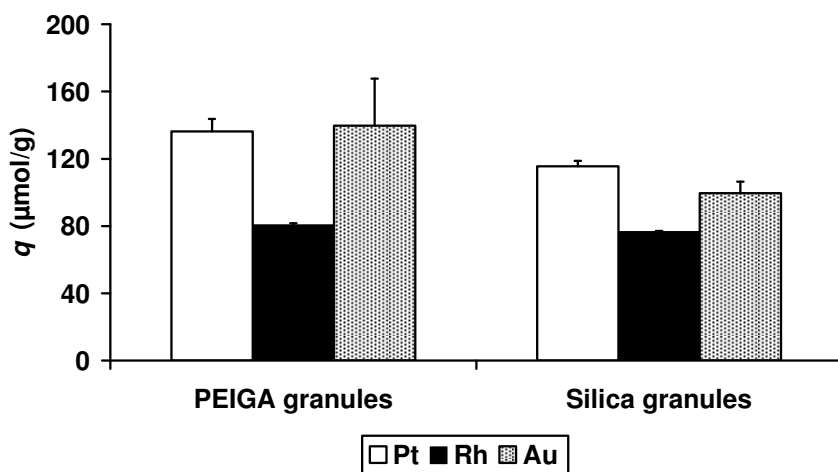


Figure 4.8 Metal uptake (q) of precious metals by PEIGA granules and silica granules. The error bars represent the standard deviation from the mean ($n = 3$).

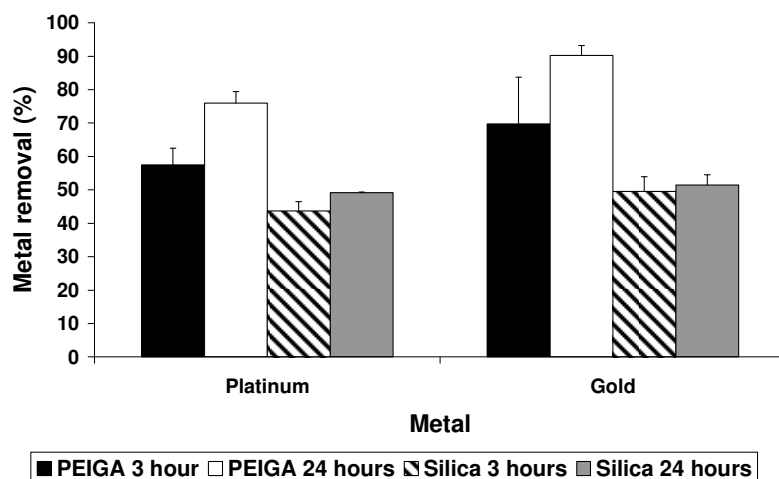


Figure 4.9 Removal efficiency (%) of PEIGA and silica granules after three hours and twenty four hours of incubation with platinum and gold solutions ($200 \mu\text{M}$). Error bars represent standard deviation from the mean ($n = 3$).

Protonation of the sorbent will increase the overall positive charge of the sorbent surface, thereby enhancing the electrostatic attraction between the metal anions and the sorbent surface. Both sorbents were protonated in order to increase the metal uptake capacity. This had no obvious positive effect on the uptake of any metal by either of the sorbents (Figure 4.10). In fact, in a number of cases it seemed to have decreased metal uptake capacity, most noticeably that of gold by both sorbents.

During the course of the experiments with the silica granules, it was noticed that the yeast sloughed off the silica gel surface during agitation. This was investigated by SEM analysis of the sorbent surface. Figure 4.11 shows various magnifications of the silica sorbent after attrition. Each, when compared to the images in Figures 4.4B to D clearly shows the decrease in coverage of the silica gel surface by the immobilized yeast. In particular, Figures 4.11C and D show the exposed surface of the silica gel, where before incubation with metal and subsequent agitation, a thick multiple layer coating of yeast cells was present.

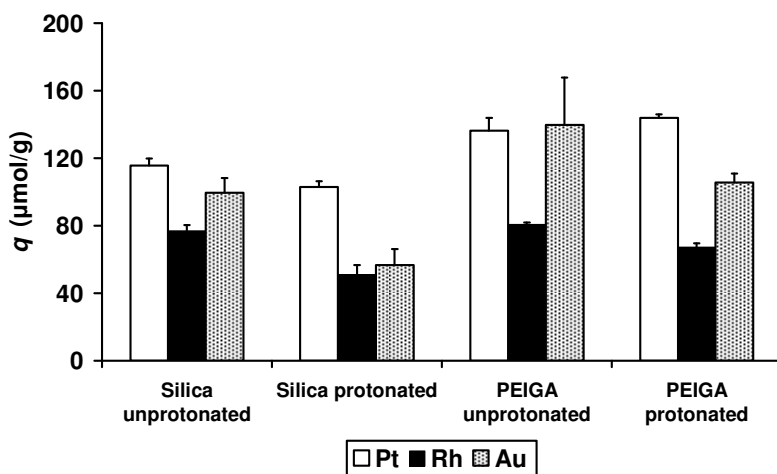


Figure 4.10 Metal uptake (q) by both protonated and unprotonated sorbents. Error bars represent standard deviation from the mean ($n = 3$).

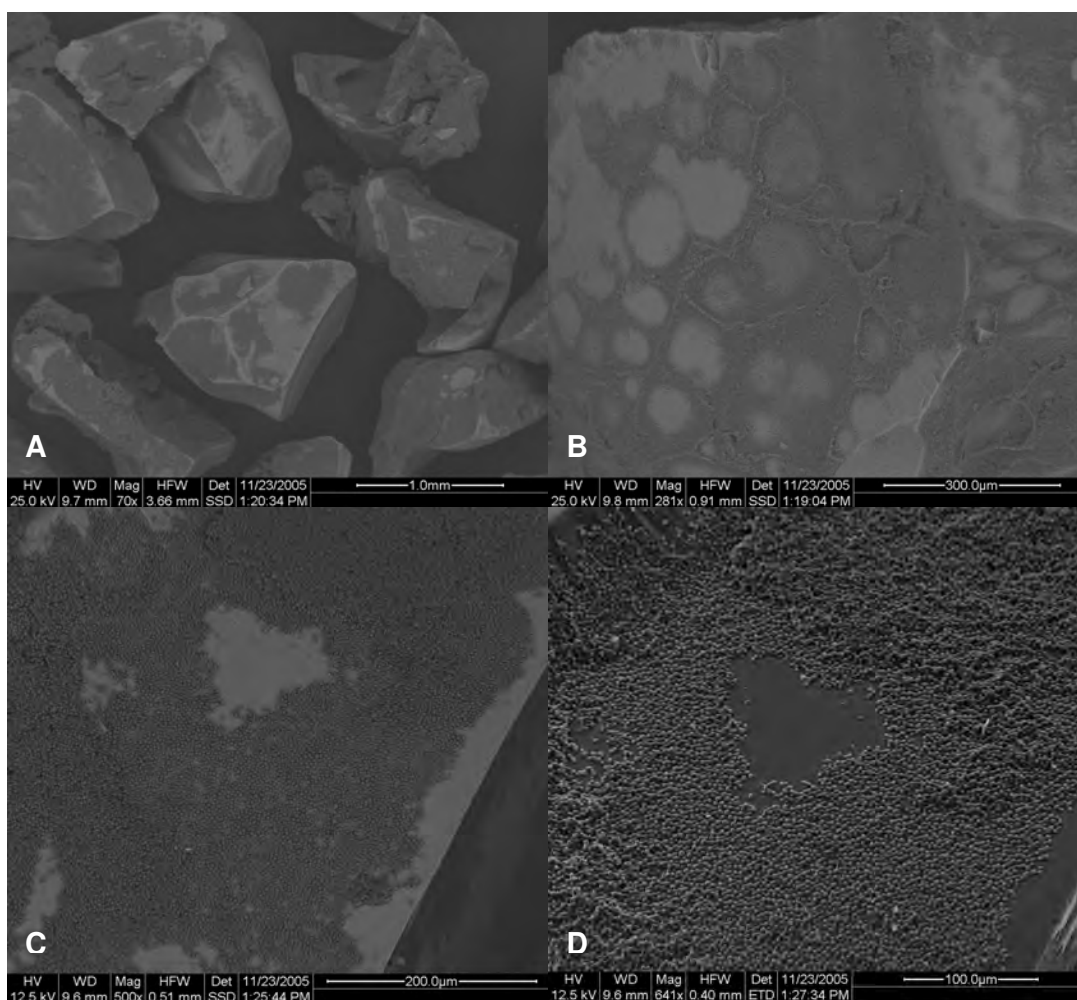


Figure 4.11 Scanning electron micrographs of the silica sorbent surface showing, at increasing magnification, the damage inflicted on the immobilized yeast layers by mechanical shear caused by agitation.

4.4.3 PEIGA sorbent

Figure 4.12 shows the sorption isotherm curves of the three metals, platinum, rhodium and gold, on the PEIGA sorbent. The initial slopes of the curves indicated that an affinity series in the order platinum > gold > rhodium existed. The Langmuir parameters (Table 4.3) supported this trend, where the calculated affinity ($1/b$) was lowest for rhodium, increased for gold, and was highest for platinum. The sorption curves also showed an initial indication of a maximum uptake capacity (Q_{max}) for each metal (Figure 4.12). The platinum curve appeared to have reached a plateau at approximately 600 $\mu\text{mol/g}$, but both the gold and rhodium curves seemed to still be increasing. Q_{max} values calculated according to the Langmuir isotherm model are indicated in Table 4.3.

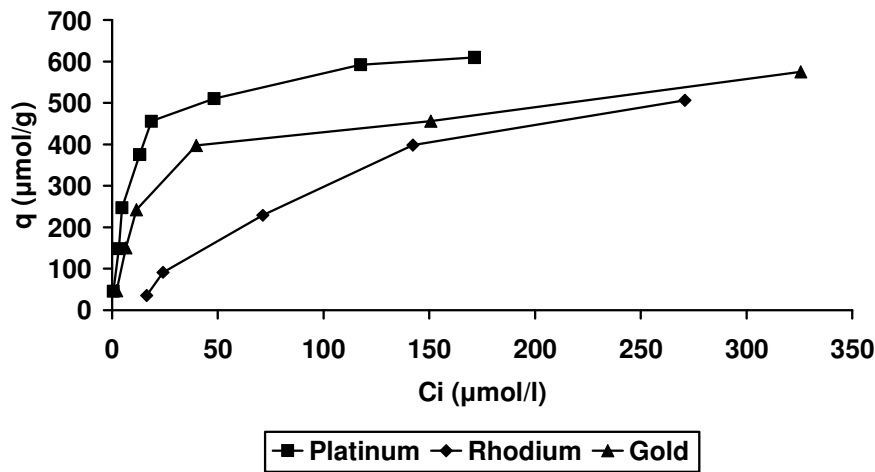


Figure 4.12 Sorption isotherm curves of platinum, rhodium and gold on PEIGA sorbent.

As suggested by the isotherm curves, the maximum metal uptake value of rhodium had not yet been attained. The value calculated ($909 \mu\text{mol/g}$) is significantly higher than that calculated for the platinum curve ($625 \mu\text{mol/g}$). However, in this case, the affinity ($1/b$) was the determining factor with respect to deciding on a specific precious metal target for all subsequent studies. The affinity of the sorbent for platinum was twice as high as that for gold, and twenty times higher than that for rhodium.

Figure 4.13 shows the curves describing the sorption of platinum by three separate components of the PEIGA sorbent; PEIGA without yeast, yeast alone, and the combined PEIGA/yeast sorbent. The curve for the PEIGA without yeast seems almost linear. This means that the uptake capacity will continue to increase with an increase in initial metal concentration to a much greater extent than either the yeast biomass alone or the PEIGA sorbent could sustain. The use of PEIGA as an immobilizing strategy does improve the performance of the yeast biomass. When compared to the yeast biomass curve, the PEIGA sorbent curve indicates a higher affinity for platinum (introduced to the sorbent surface *via* immobilization), and a greater uptake capacity. Both of these are confirmed by the Langmuir equilibrium parameters shown in Table 4.3.

Table 4.3 Langmuir equilibrium parameters for precious metal target analysis, PEIGA sorbent component analysis (with platinum target), and alternate production procedure analysis (with platinum target).

Linearized Langmuir equilibrium parameters			
	Q_{max} (mg/g)	$1/b$	R^2
Precious metal target			
Platinum	121 (625 μ mol/g)	0.113	0.999
Rhodium	93 (909 μ mol/g)	0.005	0.991
Gold	104 (526 μ mol/g)	0.047	0.996
Component analysis			
PEIGA - yeast	D.N.C.	D.N.C	D.N.C
PEIGA + yeast	152	0.107	0.993
Yeast	114	0.056	0.801
Alternative production			
A (original)	130	0.448	0.987
B (alternate)	106	0.288	0.979

D.N.C.: did not calculate

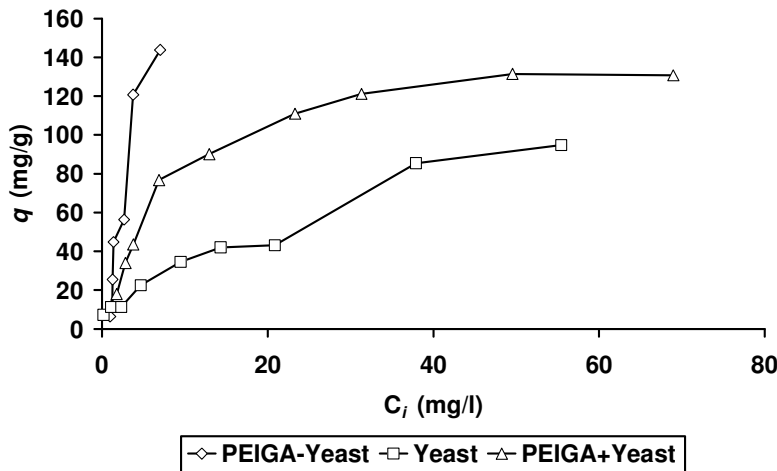


Figure 4.13 Sorption isotherm curves describing the sorption of platinum by the three components that make up the PEIGA sorbent.

In Figure 4.14 a comparison was made between two procedures for the production of PEIGA sorbent granules. The alternate procedure (B) exhibited a much lower metal affinity and a plateau at a lower level than the original process (A). This was confirmed by calculation of the Langmuir equilibrium parameters shown in Table 4.3.

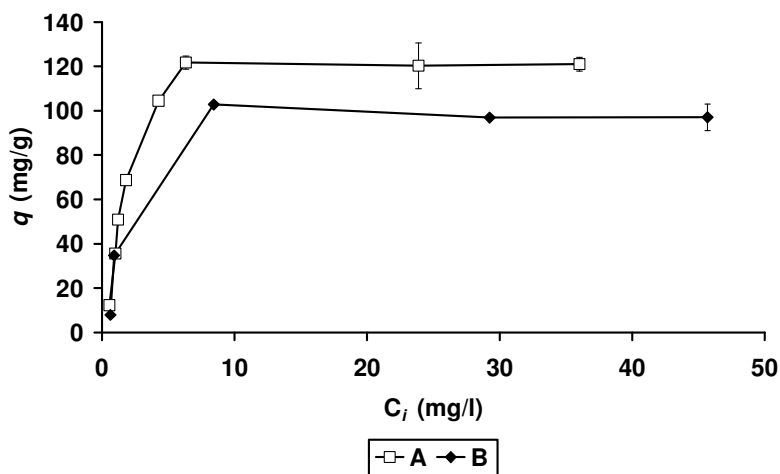


Figure 4.14 A comparison between two methods for the production of PEIGA sorbent granules. A: initial process (described in section 4.2.2), B: alternate process (described in section 4.4.1).

4.5 DISCUSSION

4.5.1 Immobilization procedure analysis

Overall, only two immobilization techniques produced sorbents with the characteristics suited to a system to be designed for biosorption of metal ions from wastewaters with extreme conditions. The CMC-immobilized beads showed very low mechanical stability, immediately eliminating their use in a packed or fluidized bed sorption process and thus eliminating the technique from the screening procedure. These beads have been used successfully in other studies, though. Saglam *et al.* (2002) immobilized a white-rot fungus, *Phanerochaete chrysosporium*, in CMC and were able to sorb up to 100 mg of mercury per gram of beads. The same group also immobilized *Lentinus sajor-caju* for chromium(VI) removal (Arica and Bayramoğlu, 2005) and *Trametes versicolor* for copper, lead and zinc sorption. In all cases the beads were found to be stable under experimental conditions.

The calcium alginate-entrapped beads showed good mechanical stability, but did not respond favourably to extremes of pH. At low pH, the uptake capacity of the beads was completely abolished due to the dehydration of the beads, which would have caused any porosity on the bead surface to have diminished, thus hindering access to possible metal sorption sites. In stark contrast, Godlewska-Żyłkiewicz and Kosłowska (2005) used similarly immobilized *S. cerevisiae* to successfully sorb palladium from solution at low pH (1.0 - 1.2). They did report shrinkage (by up to 10 %) of the beads, but only after numerous sorption/desorption cycles. A mitigating factor may

be that the metal concentrations used in the study by Godlewska-Żyłkiewicz and Kosłowska were far lower than those used in the present study (50 ng/ml vs. 50 µg/ml). This may have resulted in successful uptake of the low concentrations, whereas at high concentrations, the surface area is insufficient for significant uptake. Numerous calcium alginate-immobilized fungal sorbents have successfully sorbed base metals from more neutral-pH solutions. For example, Arica *et al.* (2004) used a wood-rotting fungus (*Funalia trogii*) to remove cadmium, zinc and mercury from solution. They found that the sorption of all three metals was optimal at pH 6, where the beads would not be affected by acid dehydration such as that seen in the current study.

Both the silica surface-immobilized yeast sorbent and the PEIGA immobilized yeast sorbent exhibited good mechanical and chemical stability, and good solid/liquid separation characteristics. Both were used for further experimentation, described in the following sections.

4.5.2 Metal sorption analysis

The silica sorbent showed a lower affinity for the metals used in the experiments than the PEIGA sorbent, and neither extended incubation nor protonation improved this. The apparent simplicity of the immobilization procedure was the major reason for the sorbent's failure to meet the requirements for a suitable sorbent. The immobilization of the yeast biomass to the silica surface was not permanent. A small number of studies support this finding. Godlewska-Żyłkiewicz (2003) used free and immobilized *S. cerevisiae* and *Chlorella vulgaris* to sorb platinum and palladium from aqueous solutions. The author found that free yeast sorbed 62 – 65 % of the platinum from a 75 ng/ml solution at pH 1.6 – 2.2. However, when sorption was attempted with the silica-immobilized yeast, the experiment was abandoned due to time-consuming solid/liquid separation and an inability to regenerate the sorbent. These reasons may imply a problem of poor yeast adhesion to the silica. The silica-immobilized algal sorbent was used in further studies, with no problems reported. However, the subsequent experiments took place in a column, where the sorbent was not exposed to agitation. Ghoul *et al.* (2003) reported similar detachment from a silica surface. In this case, the authors modified the surface of silica gel granules with polyethyleneimine. This sorbent exhibited a high uptake capacity for lead, cadmium, zinc and nickel. However, desorption of the polymer from the sorbent was reported during metal sorption at low pH. In an attempt to remedy this, the silica-PEI sorbent was crosslinked with glutaraldehyde. This successfully stopped the polymer desorption, but the metal uptake capacity was decreased by 20 – 40 %. Overall, this seems to suggest that a combination of mechanical shear caused by agitation

and the low pH at which precious metal sorption occurs makes the silica-immobilized sorbent unsuitable for use in the present study.

The PEIGA sorbent exhibited a higher metal uptake with respect to gold and platinum than the silica sorbent. An increase in the incubation time from 3 to 24 hours had a significant and positive effect on metal uptake. Protonation did not further increase metal uptake. After the analysis discussed in this section, the PEIGA sorbent was deemed to be the most suitable of those produced from *S. cerevisiae* in the current study.

4.5.3 PEIGA sorbent

Chemical modification of *S. cerevisiae* biomass with polyethyleneimine followed by crosslinking with glutaraldehyde produced granules of variable size, but with excellent mechanical and chemical stability. The sorbent also exhibited a good affinity for precious metals, platinum in particular, (120 – 150 mg/g). This high affinity was due to the presence of a large number of amine groups introduced *via* modification with PEI. Polyethyleneimine is known for its metal chelation properties and is often used for sorbent surface modification in order to increase sorption capacity (Ghoul *et al.*, 2003). The alkaline treatment of the sorbent also played a role in increasing the sorption capacity. For example, it is the alkaline deacetylation of chitin which increases the number of amine groups on the surface that results in the far more potent sorbent, chitosan (Tan and Cheng, 2003). The crosslinking agent, glutaraldehyde, is necessary to prevent desorption of PEI from the biomass surface. This has also been previously noted by Ghoul *et al.* (2003) and Deng and Ting (2005).

The PEIGA sorbent exhibited the highest affinity for platinum ions, followed by gold and then rhodium. The maximum uptake capacity was different, with rhodium, platinum and then gold ($\mu\text{mol/g}$ values). This reversal is not uncommon, and has been described by Mohapatra and Gupta (2005). In their investigations, the authors found that in single metal solutions of copper, zinc and cobalt, the metal uptake capacity decreased in the order zinc > cobalt > copper but the affinity decreased in the order copper > cobalt > zinc. No explanation has yet been offered for this phenomenon. Numerous arguments have been presented in order to explain affinity series and differences in metal uptake. Metal-specific (and even metal species-specific) characteristics such as electronegativity, ionic radius, paramagnetic nature, coordination number and covalent index have all been used to explain the higher affinity for one metal over another (Mohapatra and Gupta, 2005;

Yokel *et al.*, 2006). For precious metals, and anionic chloro-species in particular, it has been suggested that the order in which the metal species will react with donor ligands is directly related to periodicity, with PGMs in the second row (e.g. rhodium) being more reactive than third row PGMs (e.g. platinum and gold) (Bernardis *et al.*, 2005). This would explain the decrease in uptake capacity from rhodium to platinum and gold seen in the current study (Table 4.3). The affinity of the metal chloro-complexes for the sorbent may also be due to differences in charge density. According to Bernardis *et al.* (2005), such complexes form ion pairs with anion-exchangers in the order: $[\text{MCl}_6]^{2-} > [\text{MCl}_4]^{2-} \gg [\text{MCl}_6]^{3-} >$ aquo species. Species with low charge densities pair more readily than those with a higher charge density. The species of the metals used in the current study are unknown; it has been assumed that all are present as chloro-complexes as the metals are supplied in 1 M HCl solution. Thus it is impossible to determine whether the charge density theory applies here. As the sorbent exhibited the highest affinity for platinum, this metal was used in all subsequent experiments.

Polyethyleneimine is known for its potency as a PGM sorbent due to the high amine functionality content (Chassary *et al.*, 2005b), and in combination with *S. cerevisiae*, an efficient platinum sorbent was produced. The polyethyleneimine polymer has characteristically high nitrogen content, present in the form of amine groups. It is these amine groups that are responsible for metal ion binding through chelation mechanisms. Due to its pK_a range 6.5 - 8.8, it is protonated in acidic solutions and is also capable of metal sorption through anion exchange mechanisms. Crosslinking of the amine groups of both the yeast cells and the PEI with glutaraldehyde served to stabilize the sorbent in acidic solutions (Guibal *et al.*, 1999), and prevent desorption of PEI from the yeast surface (Ghoul *et al.*, 2003). Modification of the yeast surface with PEI has been used to increase sorption efficiency, improve sorption selectivity, and decrease the sensitivity of the sorption process to environmental conditions (Arrascue *et al.*, 2003).

The alternative method for PEIGA granule formulation was simpler than the original and resulted in granules of more uniform size, but exhibited no other advantages over the original method. Both the uptake capacity and the affinity for platinum were lower than the original method, thus it was discarded.

4.6 SUMMARY

A literature survey was undertaken in order to identify immobilization techniques that could be applied to *S. cerevisiae* biomass with the resultant sorbent exhibiting characteristics suitable for sorption of PGMs from refinery wastewaters. The sorbent must have mechanical and chemical stability; simple solid/liquid separation characteristics, have a simple formulation, low toxicity, low cost and the possibility of reusability. Based on information regarding these characteristics, four techniques were chosen for experimentation; carboxymethyl cellulose entrapment, silica gel surface immobilization, polyethyleneimine modification with glutaraldehyde crosslinking and calcium alginate encapsulation.

After formulation of the sorbents, each was evaluated according to the most important process characteristics: chemical and mechanical stability, and solid/liquid separation. The CMC beads were extremely fragile and were thus deemed unsuitable for further use. The calcium-alginate beads were mechanically stable and were easy to separate, but at low pH the beads dehydrated, losing the ability to sorb metal ions. Both the silica granules and the PEIGA granules seemed chemically and mechanically stable and exhibited good settleability. These were subjected to further experimentation in order to determine which of the two exhibited superior metal uptake capacity.

The PEIGA sorbent exhibited slightly higher metal uptake capacity than the silica granules after three hours of incubation with metal ions. An increase in the incubation time from three to twenty four hours resulted in an increase in the uptake capacity of the PEIGA sorbent, but did not significantly alter that of the silica granules. The sorbents were then protonated in order to increase the level of electrostatic attraction between the sorbent surface and the PGM chloro-anions. This produced no significantly positive effect on either sorbent. It was observed, however, that during incubation the yeast cells detached from the silica gel surface as a result of attrition. This made separation of solid from liquid far more difficult than was experienced with the PEIGA sorbent. The silica sorbent was therefore deemed unsuitable.

Three metals of superior strategic and economic value (rhodium, platinum and gold) were chosen as possible target metals for sorption. The metal to be used in all further studies was determined *via* equilibrium modelling using the Langmuir isotherm. The PEIGA sorbent exhibited the highest affinity for platinum, but the highest uptake capacity for rhodium. Through consultation with

industrial partners in the research, it was decided that platinum was the most valuable target for recovery. Thus platinum became the target metal used in all further research.

The relative contributions to platinum uptake made by the separate components of the PEIGA sorbent, namely the PEIGA polymer and the *S. cerevisiae* biomass, were determined. Polyethyleneimine is known as a potent PGM scrubber and the results demonstrated that, but crosslinked with GA only, it was mechanically weak and difficult to handle. *S. cerevisiae* biomass was an acceptable platinum sorbent, but suffered from a serious disadvantage with respect to solid/liquid separation. Together, the PEIGA/yeast sorbent was chemically and mechanically stable, was easily separated from solution, and showed a high uptake capacity for platinum. An alternative, simpler formulation method was compared to the original, but showed a much lower uptake capacity and a lower affinity for platinum.

4.7 CONCLUSIONS

- Of the four techniques investigated, PEIGA immobilization of yeast cells resulted in the best sorbent. It was both chemically and mechanically stable, exhibited good solid/liquid separation characteristics, and good PGM uptake.
- It was decided that platinum would be the target metal for all further experimentation. Of the three metals discussed, platinum was determined to be the most valuable product for recovery. The PEIGA sorbent also exhibited the highest affinity for platinum.

CHAPTER 5

Sorption of platinum by PEIGA-immobilized *S. cerevisiae* sorbent

5.1 INTRODUCTION

The process of biosorption involves a solid (sorbent) and a liquid phase containing a dissolved species to be sorbed (sorbate). Depending on the affinity of the sorbent for the sorbate, the sorbate is attracted to the solid phase and bound by a number of mechanisms until equilibrium is established between the dissolved and solid-bound sorbate. The quality of a biosorbent is determined by how much sorbate it can sorb and maintain in an immobilized form (Volesky, 2003). A large number of factors, both physical and chemical can affect the efficiency of a sorbent. These include the solid/liquid ratio, degree of contact between sorbent and sorbate, solution pH, solution temperature, solution ionic strength, target metal concentration and surface characteristics of the sorbent (Çeribasi and Yetis, 2001; Chen and Wang, 2007). If a sorption system is to be applied in an industrial setting, the parameters optimized must complement those defined by the wastewater and the process from which it originates.

5.2 MATERIALS AND METHODS

5.2.1 Surface characterization

Scanning electron microscopy

Scanning electron microscope images were taken using a Quanta 600 SEM (FEI, USA) equipped with x-ray microanalysis capabilities (Genesis, EDAX, USA). Samples were carbon-coated to minimize the effect of electron charging of the surface, which would have distorted the images.

Fourier Transform Infrared-Attenuated Total Reflectance (FTIR-ATR)

Fourier Transform Infrared analysis is used to gather information regarding the molecular structure and/or chemical bonding of organic and inorganic materials. It can also be used to identify unknown materials present in a sample, and in this way is complementary to EDAX analysis. The technique exposes a spot on a sample to an infrared beam, and based on the transmittance and reflectance of the infrared rays at different frequencies, different bonds and groups of bonds can be identified based on their characteristic vibration frequencies (SiliconFarEast, 2001).

No sample preparation was required for FTIR-ATR analysis of the non-immobilized and PEIGA-immobilized yeast samples. The analysis was performed using a Spectrum 100 Series ATR (Perkin Elmer, USA). Intact samples were placed on the instrument crystal with the instrument arm being used to ensure sufficient contact between the sample and the crystal.

Calculation of surface area

The method described by He and Tebo (1998) and Kaewprasit *et al.* (1998) was used to determine the specific surface area of the immobilized yeast biosorbent. The method is based on the sorption of the methylene blue monomer. Concentrations less than 7 $\mu\text{mol/l}$ were used, as the molecule dimerizes at higher concentrations. The structure of a monomer of methylene blue is regarded as an approximately rectangular box with dimensions of $1.7 \times 0.76 \times 0.325$ nm, with projected molecule surface areas of 1.30, 0.55 and 0.25 nm^2 (Kaewprasit *et al.*, 1998). The monolayer adsorption value can be calculated by construction of an adsorption isotherm and application of the Langmuir isotherm model. This value can be related to the specific surface area using Equation 5.1.

$$S = Q_{\max} N_A \sigma \quad (\text{Eq. 5.1})$$

Where S is the specific surface area (m^2/g),

Q_{\max} is the maximum monolayer adsorption ($\mu\text{mol/g}$),

N_A is Avogadro's number ($6.02 \times 10^{23} \text{ 1/mol}$),

σ is the area of a methylene blue molecule, ($0.55 \times 10^{-18} \text{ m}^2$ when maximum monolayer adsorption occurs (Kaewprasit *et al.*, 1998).

The experiment was performed in 100 ml conical flasks containing increasing concentrations of methylene blue (50 ml). A sorbent dose of 1 g/l was added to the flasks, which were then incubated on a bench top shaker (170 rpm) for 24 hours. After incubation, the sorbent was separated from the solution and

Potentiometric titration

An autotitrator (Titroline *Easy*, Schott Instruments, Germany) was used to determine the surface charges on the immobilized biomass. The method used was modified from Deng and Ting (2005). Dry biosorbent (0.1 g in triplicate) was protonated by shaking (150 rpm) on an orbital bench top

shaker (Labcon, South Africa) at room temperature in 100 ml 0.1 M HCl (uniVar, Merck Chemicals Ltd, South Africa) for 24 hours. The biosorbent was then filtered and rinsed with deionized water to reach a constant pH and then dried at 50 °C overnight. Before titration, samples were left to stand for 12 hours in 50 ml 0.01 M NaCl (Saarchem, Merck) in order to equilibrate. The solution was then titrated with standardized 0.1 M NaOH (Saarchem, Merck) to a pH of 12. All glassware used was soaked in 5 % HNO₃ (uniVar, Merck) for 24 hours and then rinsed repeatedly with deionized water prior to use.

5.2.2 Sorption optimization

Metal uptake (q) can be defined as the amount of sorbate bound by the unit of solid phase, i.e. mg metal/g biomass (dry weight), and is calculated according to the mass balance described in Equation 5.3.

$$q = \frac{V(C_0 - C_i)}{M} \quad (\text{Eq. 5.3})$$

Where V is the bulk solution volume (l),

C_0 and C_i are the initial and final metal concentrations, respectively (mg/l),

M is the mass of sorbent (g).

Batch sorption analysis

Batch sorption experiments were conducted to examine the time-dependent sorption behaviour, the effect of solution pH and optimal sorbent concentration on the sorption performance. For the kinetic experiments, a sorbent concentration of 1 g/l was applied to 100 ml aliquots of platinum solution (pH < 2) at concentrations ranging from 10 to 200 mg/l. Thirteen samples were removed at intervals over a period of six hours. For the sorbent concentration experiments the sorbent dose was varied from 0.1 g/l to 10 g/l in 50 ml aliquots of both a 20 and a 50 mg/l platinum solution (pH < 2). Samples were analyzed after a three hour incubation period. For the solution pH experiments, the initial pH of a 50 mg/l platinum solution was adjusted to the desired value, ranging from 1 to 4, using 1 M HCl or 1 M NaOH. A mass of 0.05 g (1 g/l) of sorbent per flask was used. An initial platinum concentration of 50 mg/l was used and samples were removed after three hours. The

platinum solutions were prepared by dilution of a 1000 mg/l atomic absorption spectrometry standard solution (EC Labs, South Africa). All experiments were conducted with agitation on an orbital bench top shaker (Labcon, South Africa) at 170 rpm for 24 hours at room temperature unless otherwise stated. In all experiments, sorbent-free controls were analyzed alongside the experimental flasks. All samples were adjusted to $\text{pH} < 2$ and centrifuged at 2000 g (Labofuge, Heraus, Germany) for five minutes to separate particulate matter. The residual platinum concentration in solution was measured by atomic absorption spectrophotometry (GBC 909AA, GBC Instruments, Australia). All experiments were conducted in triplicate and the arithmetic means are reported. Error bars indicate the standard deviation from the calculated means, and in some cases are not visible on the graphs.

5.3 RESULTS

5.3.1 Surface characterization

Scanning electron microscopy

Micrographs of the sorbent surface were obtained in two viewing modes. Simultaneous secondary electron (SE) mode allows for the observation of biological microstructures. Backscattered electron (BSE) mode highlights areas of non-biological composition, i.e. bound metal. A selection of micrographs taken of the carbon-coated sorbent are shown in Figure 5.1. Both Figure 5.1A (SE) and Figure 5.1B (BSE) show the macrostructure of the granules at approximately 100 \times magnification. It is important to note that no non-biological component was identified in Figure 5.1B. In Figures 5.1C and D (both SE), the surface structure is shown at magnifications approximately 2500 \times and 3500 \times . Figure 5.1C shows the tight arrangement of the yeast cells; whereas the closer view of Figure 5.1D shows the pits on the surface. The existence of these pits and folds greatly increased the surface area available for metal sorption.

Figures 5.2A-D show sorbent that has been incubated with platinum ions. Figure 5.2A (SE) indicates that no changes were apparent in the macrostructure of the sorbent, while Figure 5.2B, a BSE mode picture, provides an initial indication of the presence of platinum ions on the surface of the sorbent (white patches). It was noted that the platinum ions did not sorb in a mono-layer across the entire surface of the granule, but instead appeared to nucleate only in certain areas, leaving other areas free of platinum. This may have been due to the small amount of platinum bound not being sufficient to display a monolayer sorption pattern. Figures 5.2C and D depict a portion of the

sorbent surface to which platinum ions have bound and formed aggregates. Figure 5.2C (SE) shows the change to the sorbent surface at the point of sorption. The cells were seen to have deformed as a result of the sorption. The cells adjacent to the circled area appeared normal. Figure 5.2D is a BSE mode micrograph of the same area, and confirms the presence of non-biological residues at the circled position.

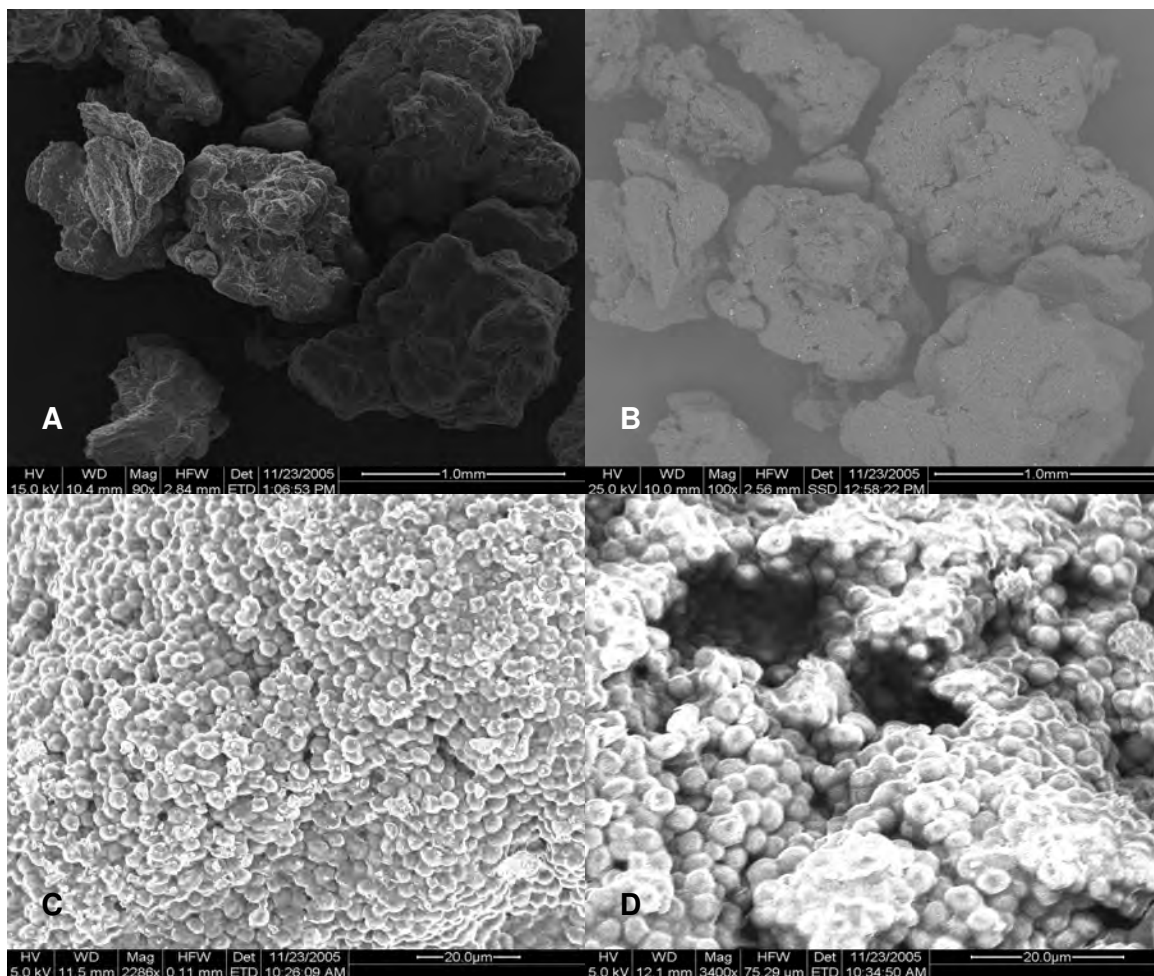


Figure 5.1 Scanning electron micrographs of the sorbent showing granule macrostructure (A and B) and surface structure (C and D).

The area indicated in Figure 5.2C and D was scanned using x-ray microanalysis in order to determine the composition of the non-biological residue. Figure 5.3A (overleaf) is an energy dispersive spectroscopic (EDS) representation of the surface composition at this point, and should be compared to Figure 5.3B, an analysis of an area not exhibiting the white residue. Both the platinum (2.00 and 8.00 keV) and chloride peaks in Figure 5.3A are far higher than in Figure 5.3B, confirming the presence of platinum (possibly bound to the sorbent surface as a platinum chloride

anion). Both peaks are also significantly higher than the C and O peaks present at the lower energy range of the scan.

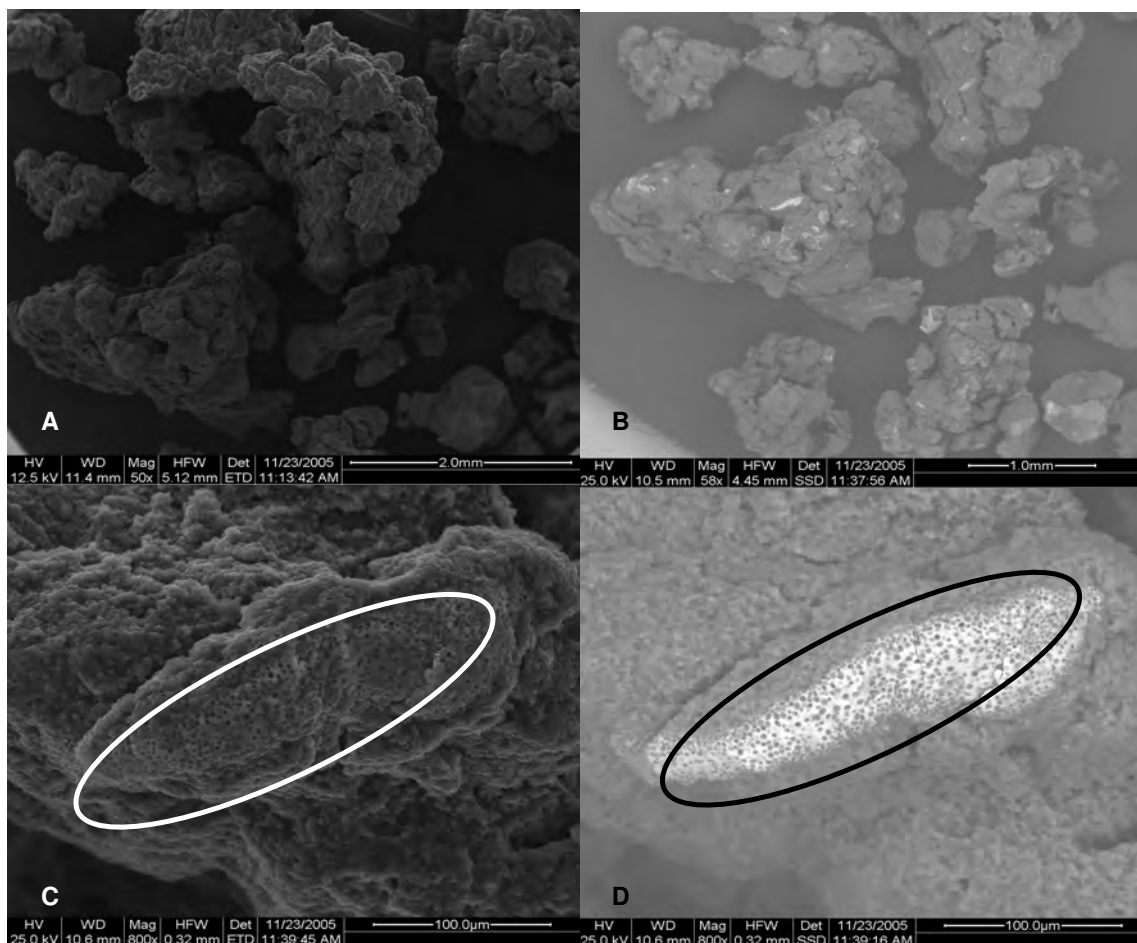


Figure 5.2 Scanning electron micrographs of the sorbent, showing the sorbent macrostructure (A and B) and the sorbent surface (C and D) after incubation with platinum.

Fourier Transform Infrared-Attenuated Total Reflectance analysis

Figure 5.4 shows the FTIR spectra of the native dried yeast, the PEI-modified and GA-crosslinked sorbent, and sorbent with sorbed platinum ions. There was little difference between the native (A) and the immobilized (B) yeast. However, immobilization seemed to have a general effect by decreasing the intensity of the peaks. The changes on Figure 5.4 that should be noted include: (1) the peak at 3274.99 broadened slightly and moved to 3280.05, (2) the peak at 1639.54 decreased in intensity and moved to 1629.73, (3) the peak at 1535.64 shifted to 1522.12, and (4) the peaks at 1452.85 and 1395.16 decreased in intensity but only shifted slightly. Sorption of platinum to immobilized yeast (C) had only the slightest effect on the surface structure suggested by FTIR

analysis. Two new peaks emerged at 2854.10 and 1155.90 cm^{-1} . The peaks at 1629.73 and 1522.12 cm^{-1} increased in intensity and shifted to 1634.46 and 1517.1 cm^{-1} , respectively.

Surface area calculation

The isotherm describing the adsorption of methylene blue onto the immobilized yeast biomass is shown in Figure 5.5. The initial slope of the curve does not lie close to the y-axis, which indicates a low affinity for methylene blue. The isotherm also shows that the amount of methylene blue adsorbed increased with an increase in concentration. This should reach a saturation point (not reached in this experiment), beyond which a concentration increase would not cause an adsorption increase.

The maximum methylene blue uptake capacity was calculated from a half-reciprocal plot of C_i/q vs. C_i (Figure 5.6, $R^2 = 0.93$). A value of 9.1×10^{-6} mol/g of sorbent was obtained which, when substituted into Equation 5.1 resulted in a specific surface area of 3.01 m^2/g .

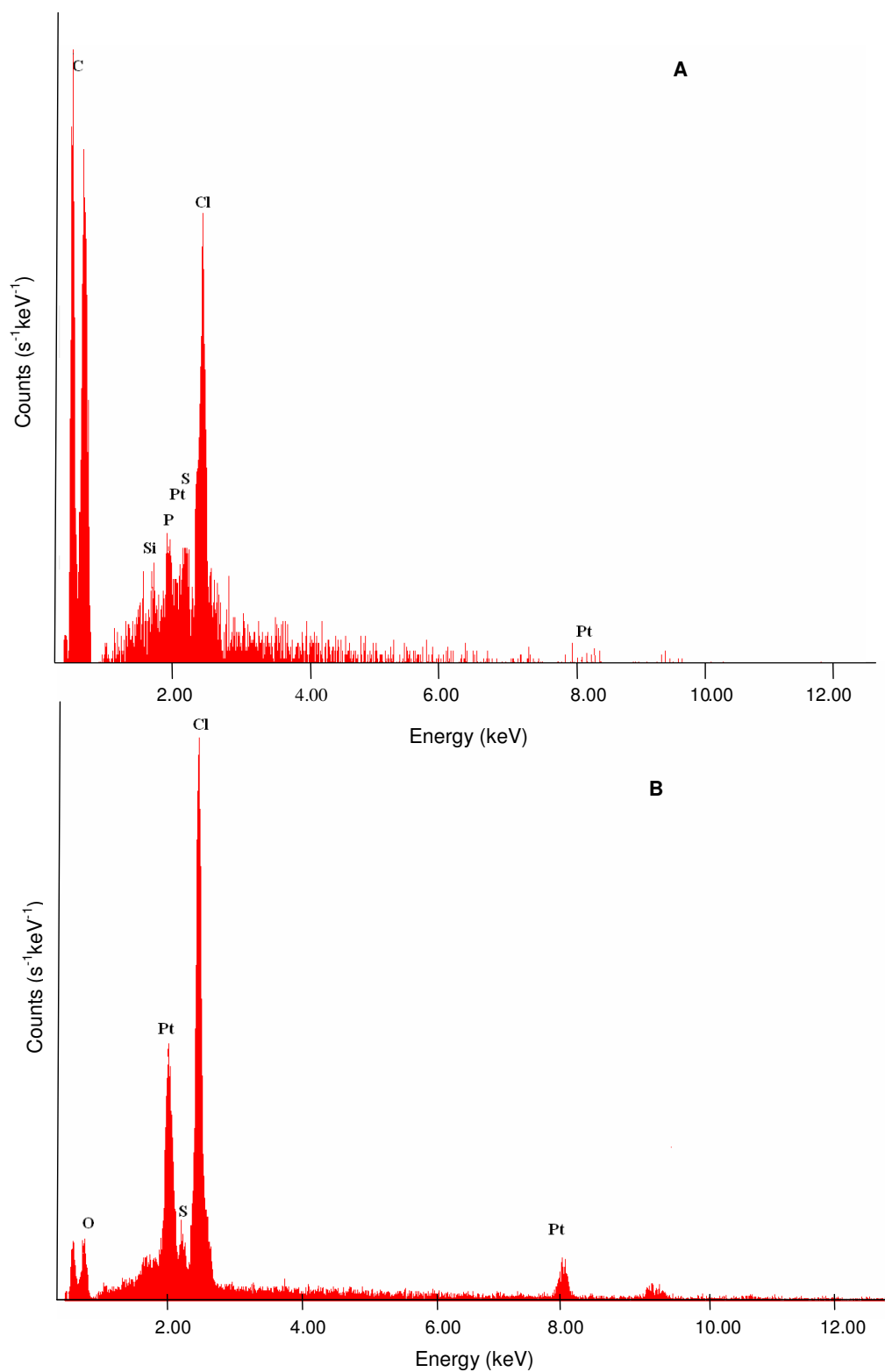


Figure 5.3 Energy dispersive x-ray (EDX) analysis of white (A) and dark (B) areas of Figure 5.2D, confirming the adsorption of platinum chloride ions to the white area of the sorbent.

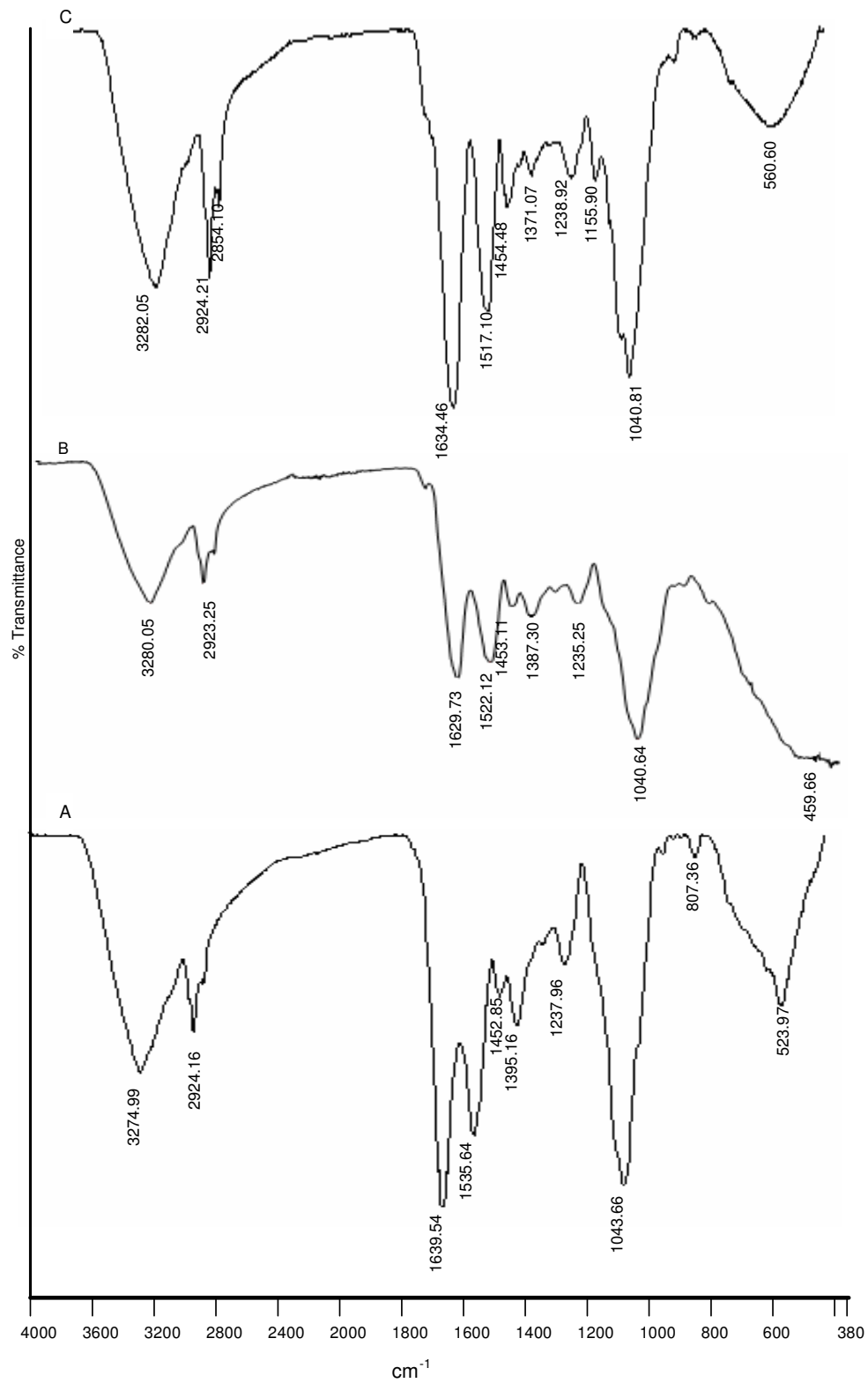


Figure 5.4 FTIR-ATR analyses of (A) native dried yeast, (B) immobilized dried yeast, and (C) platinum-bound immobilized dried yeast.

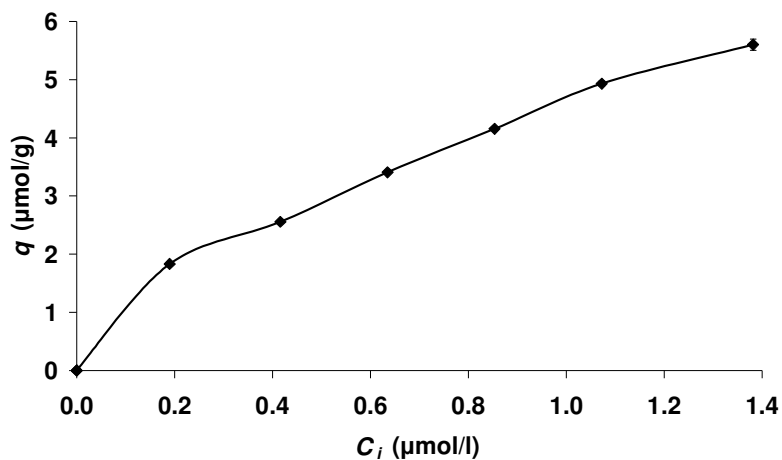


Figure 5.5 Sorption isotherm showing the sorption of methylene blue onto the *S. cerevisiae* sorbent. Error bars represent the standard deviation from the mean, and in most cases are too small to be visible ($n = 3$).

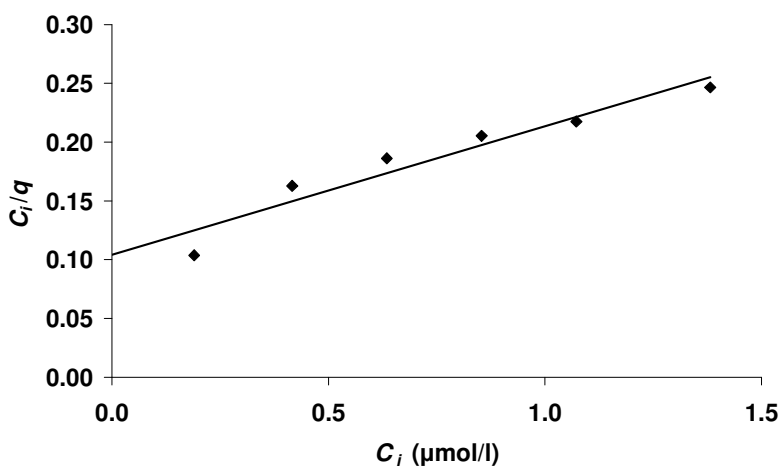


Figure 5.6 A half-reciprocal plot used to calculate the sorbent maximum specific uptake of methylene blue.

Potentiometric titration

The potentiometric titration curve of the immobilized *S. cerevisiae* sorbent is presented in Figure 5.7. From the data it is possible to determine both qualitative and semi-quantitative information regarding the type and number of active sites present on the sorbent surface. The curve shows at least two inflection points, one at approximately pH 7.3 (A) and the other at pH 9.7 (B), which correspond to the pK_a values of two types of functional groups.

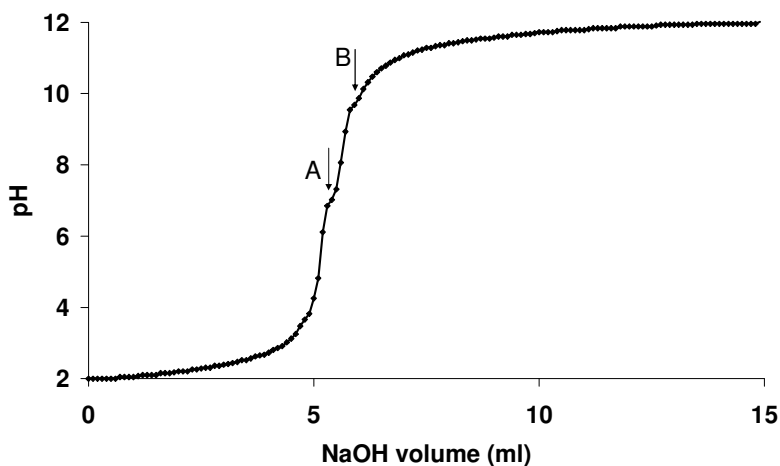


Figure 5.7 Potentiometric titration curve of *S. cerevisiae* sorbent. Arrows indicate inflection points at pH 7.3 (A) and 9.7 (B).

The concentration of functional groups A and B per gram of sorbent can be calculated by the estimation of the inflection points in the titration curve, according to Equation 5.2 (Senthilkumar *et al.*, 2007; Lodeiro *et al.*, 2004).

$$[FG_{TOTAL}] = \frac{V_{IP} \times [NaOH]}{M} \quad (\text{Eq. 5.2})$$

Where $[FG_{TOTAL}]$ is the concentration of functional group (mmol/g),

V_{IP} is the volume of NaOH added to reach the inflection point (l),

M is the mass of the sorbent (g).

The concentration of A sites was calculated as 5.5 mmol/g and the concentration of the B sites was calculated as 5.9 mmol/g.

5.3.2 Sorption optimization

Batch sorption analysis

The sorption of platinum ions to the sorbent showed an initial, rapid phase and then a much slower phase moving towards equilibrium (Figure 5.8). At a low initial platinum concentration (10 mg/l), the initial phase was complete before the first sample was removed. At a higher concentration (200 mg/l), the rapid initial sorption phase was visible for up to 30 minutes. In all cases, the slow phase was reached within 60 minutes.

The results shown in Figure 5.9 indicated that pH 1 – 2 seemed to favour platinum sorption, with greater than 90 % platinum removal from an initial concentration of 50 mg/l at both pH 1 and 2. At the higher pH levels, the uptake capacity (q) decreased by almost 50 %, from 19 mg/g to 9 mg/g (an increase from pH 1 to pH 4).

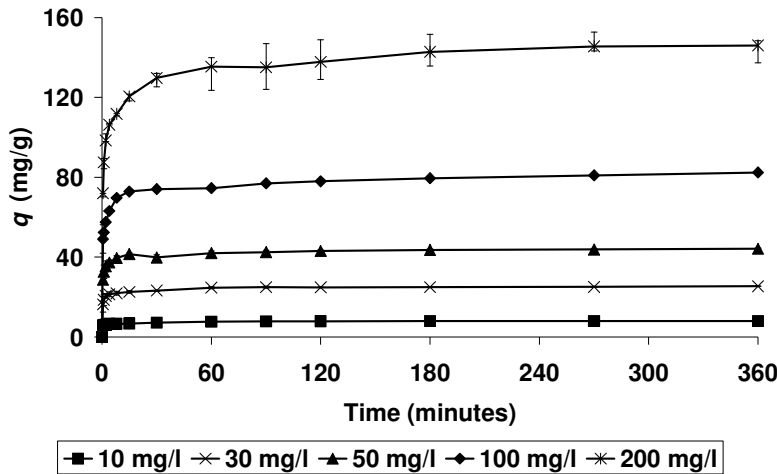


Figure 5.8 Metal uptake (q) values at intervals throughout a six hour platinum biosorption reaction using initial platinum concentrations of 10 – 200 mg/l, a sorbent dose of 1 g/l, and at pH 1.5. Error bars represent standard deviation from the mean ($n = 3$).

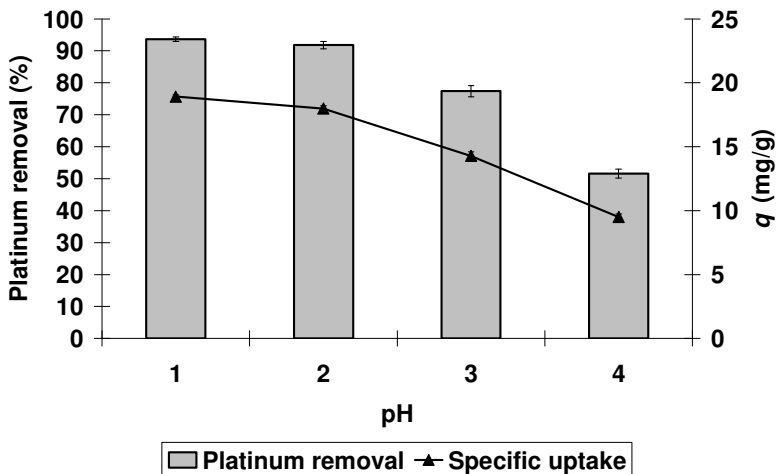


Figure 5.9 Effect of pH on the platinum sorption capacity of the *S. cerevisiae* sorbent. Error bars represent the standard deviation from the arithmetic mean, and in some cases are too small to be visible ($n = 3$).

The effect of sorbent concentration was studied by varying the sorbent dose between 0.1 and 10 g/l at platinum concentrations of 20 and 50 mg/l. The data at both concentrations (Figure 5.10) showed that an increase in the sorbent dose increased the removal efficiency of platinum by increasing the

number of available active sites, but this reached a plateau at 0.5 g/l for the 20 mg/l solution and 1.0 g/l for the 50 mg/l solution. The metal uptake of platinum by the sorbent decreased as the sorbent dose increased (± 140 mg/g to less than 10 mg/g for the 50 mg/l platinum concentration).

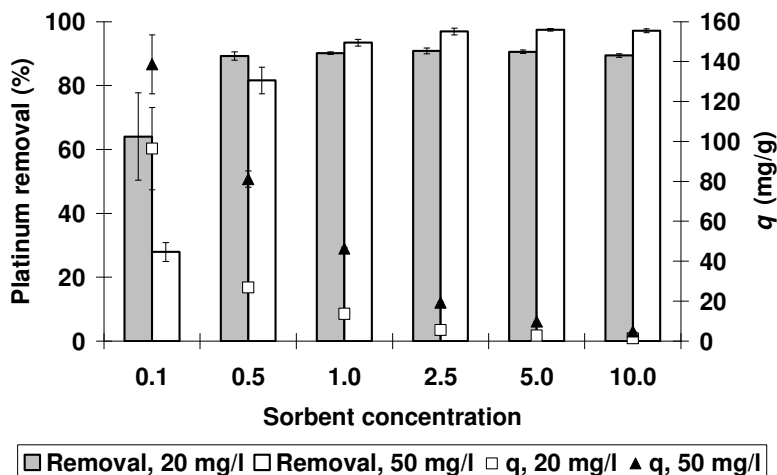


Figure 5.10 The effect of sorbent concentration on platinum removal (%) and metal uptake (q) in 20 mg/l and 50 mg/l platinum solutions. Error bars represent the standard deviation from the arithmetic mean ($n = 3$).

The distribution coefficient, K_D , can be used to describe the binding ability of the sorbent surface with respect to a specific metal. The value of K_D is calculated as shown in Equation 5.5 (Oguz, 2007; Bhainsa and D'Souza, 1999; Sujana *et al.*, 1998).

$$K_D = \frac{C_s}{C_w} \quad (\text{Eq. 5.4})$$

Where C_s is the concentration of metal adsorbed to sorbent (mg/g),
 C_w is the concentration of metal remaining in solution (mg/l).

Figure 5.11 shows that the distribution coefficient decreased with an increase in sorbent dose from 0.5 g/l at an initial platinum concentration of 20 mg/l. At 50 mg/l platinum, the decrease was less rapid, with the sorbent doses of 0.5 g/l and 1 g/l remaining similar, with a larger decrease taking place at higher doses.

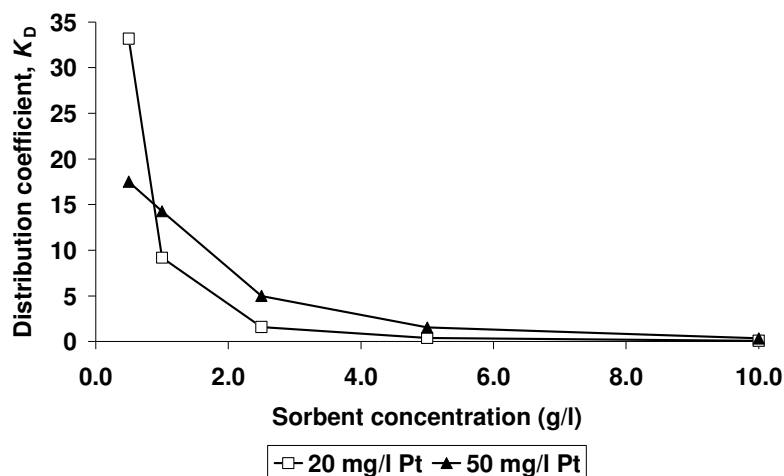


Figure 5.11 Distribution coefficient as a function of sorbent concentration.

5.4 DISCUSSION

5.4.1 Surface characterization

Analysis of the sorbent surface using scanning electron microscopy (SEM) showed that the surface was rough and uneven, with a high apparent surface area per granule. The SE micrographs also highlighted the changes to the surface structure made by sorption of platinum ions. There is no evidence of similar surface modification by the sorption of metal ions reported in available literature.

The spectrum of the native yeast (Figure 5.4A) indicated a number of functional groups present on the surface of the biomass. The broad peak spanning the range 3200 to 3600 cm^{-1} may have been due to overlapping of OH and NH stretching vibration. This is consistent with the peaks at 1043 and 1237 cm^{-1} , which can be assigned to alcoholic C-O and C-N stretching vibration (Coates, 2000). These two sets of peaks indicated the presence of hydroxyl and amine groups on the biomass surface (Deng and Ting, 2005). The strong peak at 1639 cm^{-1} can be assigned to a C=O stretching in either carboxyl or amide groups (Yu *et al.*, 2007). The peak at 2924 cm^{-1} can be attributed to CH stretching vibrations of CH, CH₂ and CH₃ groups (Yu *et al.*, 2007). The peak at 1535 cm^{-1} can be attributed to N-H bending (Coates, 2000). The two small peaks at 1452 and 1395 cm^{-1} can be attributed to C=O asymmetric and symmetric stretching in carboxylate groups, respectively (Yu *et al.*, 2000; Coates, 2000). The groups identified are commonly found on all biomass surfaces to varying degrees.

Modification of the surface with polyethyleneimine (PEI) resulted in changes to the spectrum exhibited by the native yeast (Figure 5.4B). The overlapping peak at 3274.99 cm^{-1} broadened due to the number of amine groups introduced onto the surface *via* the modification. A number of hydroxyl groups was also formed during the modification, and these further added to the broadening of the peak. This is similar to the findings of Deng and Ting (2005), who also used PEI surface modification. Imine groups were also formed during the immobilization. These have a characteristic peak at around 1650 cm^{-1} (Ghoul *et al.*, 2003), and contributed to the changes seen in the peak of C=O stretching at 1639.54 cm^{-1} , which moved to 1629.73 cm^{-1} . The changes to the peaks in the range $1350\text{ to }1550\text{ cm}^{-1}$ are a further result of the addition of amine functionalities by immobilization using PEI (Deng and Ting, 2005).

Figure 5.4C shows the changes to the spectrum caused by sorption of platinum to the sorbent surface. The peak at 1522.12 cm^{-1} , which can be attributed to NH bending, shifted to a lower peak at 1517.10 cm^{-1} . This is similar to results published by Deng and Ting (2005), who found that sorption of copper, lead and nickel to PEI-immobilized biomass resulted in a shift in the peak in the region of 1550 cm^{-1} to a peak at a lower wavenumber. However, the shift reported by Deng and Ting (2005) was accompanied by a shift of the C-N stretching peak ($1040\text{-}1080\text{ cm}^{-1}$), which was absent in the current study. A further contradiction of the results of the study by Deng and Ting (2005) is evident when comparing the behaviour of the peak at 1629.73 cm^{-1} on the immobilized sorbent. Deng and Ting reported that no change was noted for a peak at a similar wavenumber. This, they concluded, meant that no interactions were taking place that could be attributed to chemical sorption mechanisms. In the current study, the peak at 1629.73 cm^{-1} shifted significantly, to 1634.46 cm^{-1} , indicating that the C=O and C=N groups are involved in chemical interactions with the platinum anions.

The adsorption of methylene blue in liquid phase for the determination of the specific surface area of a sorbent has been used for various natural solids such as activated carbon, charcoal, graphite and silica (Kaewprasit *et al.*, 1998) as well as for the spores of some marine bacteria (He and Tebo, 1998). The trends highlighted in the isotherm (Figure 5.5) indicated two characteristics of the sorbent's sorption of methylene blue. The shallow slope of the curve may have indicated that either the affinity of the methylene blue for the sorbent was low to moderate, or that the affinity was driven by weak Van der Waals forces (He and Tebo, 1998). The existence of an apparent sorbent saturation point is typical of a sorbent with a limited number of sorption sites.

He and Tebo (1998) tested the reliability of this method by comparison with the Brunauer-Emmet-Teller (BET) surface area analysis method, which utilizes the adsorption of nitrogen gas. The comparison was not favourable as the BET method measures the surface area of a dry sample, this drying may significantly alter the structure and surface characteristics of the sorbent. The area of freeze-dried marine *Bacillus* sp. spores measured with a BET surface area analyzer ($6.86 \text{ m}^2/\text{g}$) was very similar to the geometric surface area calculated from theory ($6.27 \text{ m}^2/\text{g}$). He and Tebo postulated that a surface area of the size measured ($6.27 \text{ m}^2/\text{g}$) may indicate that the surface was smooth and contained no pores. However, the surface area of one gram of *Bacillus* sp. spores calculated by the methylene blue method was $74.7 \text{ m}^2/\text{g}$. The immobilized yeast sorbent has a much smaller surface area available per gram ($3.01 \text{ m}^2/\text{g}$) of sorbent than the *Bacillus* spores. This is to be expected though, as the small size and the large number of particles required to make up one gram of spores is far more than that necessary with the yeast sorbent where each granule is 0.1 – 2.0 mm in diameter. The surface areas of other yeast-based sorbents have not been measured in this way, but it would be expected that the smaller the granules are, the higher the specific surface area would be. As the results shown by He and Tebo (1998) indicate, analysis of surface area size *via* BET analysis seems to greatly underestimate the actual surface area as measured by the methylene blue method. In the current study, the surface area calculated by the methylene blue method is small, and will thus have a similarly small surface area *via* BET analysis when compared to the results of the *Bacillus* spore surface area analysis.

Literature suggests that the sites identified by potentiometric titration of the sorbents could be amine (or thiol) and hydroxyl groups (Volesky, 2003). This was expected as the immobilization procedure would result in the sorbent surface becoming coated in amine-type and hydroxyl functional groups (as discussed in Chapter 4). As the sorption experiments were all carried out at pH values lower than the pK_a values of either of these active groups, both groups would have been completely protonated. The protonated hydroxyl sites will have had neutral charge, and did not impact on the sorption process in any way. The protonated amine/thiol sites will have been positively charged, providing an initial electrostatic attraction between the sorbent and the platinum ions. The amine/thiol groups may play a larger role, not only in initial electrostatic binding *via* their positive charges, but also *via* their S and N donor atoms. This follows the hard and soft acids and bases theory (HSAB), according to which functional groups containing S and N donor atoms are expected to interact strongly with soft acids such as platinum (Iglesias *et al.*, 1999).

5.4.2 Sorption optimization

The sorption of metal ions onto a sorbent surface is affected by several factors related to both the surface properties of the sorbent and the physicochemical properties of the medium within which the sorption occurs, such as metal ion concentration, temperature, pH and sorbent concentration.

The time-dependent sorption pattern indicated in Figure 5.8 mirrors those in published literature. Sorption has often been shown to consist of two phases, a rapid initial phase lasting 5 - 30 minutes, and a slower phase that may only equilibrate after 24 - 48 hours (Sheng *et al.*, 2004; Uzun *et al.*, 2002). Sheng *et al.* (2004) put forward a number of cases in which this pattern has been found in non-viable biomass biosorption experiments, and Mungasavalli *et al.* (2007) suggested that the slowing of the sorption may be in response to a decrease in available sorption sites. In the current study at low platinum concentration, the initial phase appeared to be absent. This was in fact due to the very low ratio of metal ions to biomass, which masked the initial phase by inducing the reaction to take place almost instantaneously and thus was not measurable at the chosen time intervals.

In applying a process to 'real world' conditions, this rapid adsorption phase would be considered advantageous, since the shorter contact time allows for smaller, rapid flow-through contactor equipment, resulting in positive benefits for both capacity and operation costs (Sheng *et al.*, 2004).

It has been well established that sorption is often pH dependent, as the solution pH affects the solubility of the metal ions, the speciation of the metal ions (in the case of anion complexes) and the ionization state of the functional groups on the sorbent surface (Volesky, 2003). It has been proposed that negatively charged metal ions will compete for binding to positively charged sorbent surface functional groups, and that the uptake mechanism may indeed depend on the charges involved in the sorption system. The results in Figure 5.9 show that low pH (1 to 2) resulted in the greatest platinum uptake. At such low pH the sorbent was fully protonated, allowing for strong attraction of the negatively charged platinum ions to the sorbent surface. At higher pH (3 and 4), uptake decreased by up to 20 %. The potentiometric data presented showed that even at pH 4 the active sites would be fully protonated. This indicated that the decrease in platinum uptake may have been caused by changes in the platinum solution chemistry (i.e. changes in speciation) more than by a change in the sorbent surface chemistry. This is supported by previous authors, who reported that the speciation of platinum also influenced its sorption by bayberry tannin-immobilized collagen fibres (Ma *et al.*, 2006), which achieved maximal uptake at pH 3 with a steady decrease to minimal uptake at pH 7. In media containing chloride ions (such as those used in the present

study), platinum forms chloro-complexes, the states of which depend on pH, chloride concentration and platinum concentration (Chassary *et al.*, 2005a). Thus, as the pH is changed, the charge of the species may change from anionic to neutral and even to cationic, with complete precipitation taking place at higher pH (Ruiz *et al.*, 2000). The impact of pH change on sorption may provide information regarding the mechanism of uptake. Arica and Bayramoğlu (2005) evaluated the effect of pH on Cr(VI), also an anion at low pH, and found that maximum sorption was obtained at pH 2. The protonation of the amine sites was highlighted as positively influencing sorption at low pH. The authors also hypothesized that sorption at such low pH may suggest binding through electrostatic attraction. This may be similar to the mechanism by which the immobilized yeast sorbent initially binds the platinum anions. This was supported by the results of the potentiometric titration, where only the positively charged amine/thiol functional groups are present to initiate the sorption reaction.

Figure 5.10 indicates that as sorbent dose increased, the specific uptake (q) of platinum decreased. This was due to the increase in sorbent dose decreasing the amount of platinum sorbed per unit mass of sorbent, causing the decrease in specific uptake. At higher sorbent concentrations, there was a more rapid sorption of platinum onto the sorbent surface, due to the steeper concentration gradient, that resulted in a lower solute concentration in solution than that produced by a lower sorbent dosage. This appears to be a general trend in batch biosorption experiments, as similar effects have been reported by authors working with different sorbent types such as tree leaves (Han *et al.*, 2007b), rice husks (Vadivelan and Vasanth Kumar, 2005) and activated carbon (Wang *et al.*, 2005b), all of whom noted that an increase in sorbent dosage decreased the uptake capacity of the sorbent material used. The difference in optimal sorbent dose at different initial metal concentrations highlights the necessity for optimization of this parameter in order to closely match the conditions of a wastewater to be treated, thereby minimizing sorbent wastage and maximizing metal recovery.

Figure 5.11 demonstrated that the distribution coefficient decreased with an increase in sorbent dose. According to Oguz (2007), this confirmed that the sorbent surface was heterogeneous, as a homogeneous surface would have displayed constant K_D values at all sorbent doses. Naseem and Tahir (2001) reported an initial increase in K_D with an increase in sorbent dose (bentonite) up to 5 g/l, the removal efficiency of lead remaining constant beyond this point but the K_D values decreased drastically. From those data, the authors determined 5 g/l to be the optimal sorbent dose.

Thus, for all further experiments in the following chapters, a sorbent dose of 0.5 g/l was used at lower concentrations (20 mg/l) and at concentrations of 50 mg/l or higher, 1 g of sorbent per litre was used.

5.5 SUMMARY

A thorough analysis of the sorbent surface and factors that may affect sorption is necessary for the formulation of an efficient and effective sorbent. The effect of such factors and the characteristics of the sorbent surface have been elucidated here in order to better understand the sorption of platinum ions onto the sorbent surface.

Scanning electron microscopy indicated that the granules were not homogenous in terms of size and surface structure. The sorbent surface was similarly rugged and uneven. More detailed analysis showed that the sorption of platinum induced modification of the sorbent at the point of sorption. This was confirmed by EDAX analysis of sites exhibiting the modification and sites not modified. Analysis of the FTIR spectra indicated that a chemical interaction between the cell surface and the platinum ions may have been occurring. Calculation of the surface area of the sorbent was performed using the methylene blue method. A surface area of 3.01 m²/g was calculated, which is very small when compared to other sorbents measured this way. This method is also quite uncommon, so few cases are available for comparison. Potentiometric titration of the sorbent indicated two major functional groups present on the sorbent surface. These were amine and hydroxyl groups. The hydroxyl groups would carry neutral charge at low pH (< 2), while the amine groups would be fully protonated and carry positive charge. This implies that at these low pH conditions, the amine groups would play a major role in the electrostatic attraction of platinum anions.

External factors that may affect the sorption of metal ions include the concentration of the metal ions in solution, the pH of the solution and the concentration of the sorbent in the solution. The initial concentration of platinum ions affected the apparent kinetics of the sorption process. Typically, kinetic data exhibit a two-stage uptake, where stage one is rapid, and lasts for less than thirty minutes, and stage two is slower and may require as much as forty eight hours to achieve equilibrium. In the current study, at low platinum concentration (10 - 30 mg/l), the first stage was so rapid that it did not register at the time intervals measured, whereas at higher concentrations (50 -

200 mg/l) both stages were observed. Solution pH had a profound effect on the uptake capacity of the sorbent. At low pH (pH 1 and 2), uptake was much higher than at higher pH (pH 3 and 4). When this result was considered in combination with the potentiometric titration data, it was apparent that this decrease was not due to changes in the cell wall ionization (which would remain protonated until a much higher pH was obtained) but may in fact have been due to an increase in the aquation of the platinum chloride anion. This change in the metal speciation may be sufficient to reduce the concentration of readily extractable anions and cause the decrease in uptake at lower concentration. An increase in sorbent dose increased the uptake efficiency but decreased the specific uptake capacity. The calculated K_D values decreased with an increase in sorbent dose. The K_D values indicated that the optimal dose for low concentrations (20 mg/l) was 0.5 g/l, while at higher concentrations (50 mg/l) a sorbent dose of 1 g/l was optimal.

5.6 CONCLUSIONS

- Amine functionalities are the groups most likely to act as major attractors of anionic platinum ions, and may bind these ions *via* an initial electrostatic attraction.
 - FTIR analysis indicated the formation of chemical bonds between the sorbent surface and the platinum ions, although this was only slight.
- SEM and EDAX analysis confirmed the presence of platinum on the surface of the sorbent after incubation.
- Initial platinum concentration in solution, sorbent concentration and pH all impact on the efficiency of recovery of platinum ions from solution. These factors must be optimized to suit a particular sorption system.

CHAPTER 6

Equilibrium and kinetic modelling of platinum sorption

6.1 INTRODUCTION

The ability to accurately predict the rate at which a sorption process will proceed is seen as possibly the most important factor in biosorption system design, as both the adsorbate residence time (Nacèra and Aicha, 2006) and the reactor dimensions are controlled by the kinetics of the system (Ho, 2006). Many biosorption processes have been studied in order to adequately explain both the mechanisms involved and their effect on the kinetics of sorption. A variety of kinetics-based models have been suggested in order to describe these processes, including both first and second order models, a review of which was completed by Ho (2006). These models attempt to describe the reaction based on either solution concentration or on adsorbent capacity. In order to distinguish between the two, adsorbent capacity-based models are termed pseudo-first and -second order models (Ho, 2006).

Numerous sorption models have been developed to describe equilibrium sorption process behaviour based on experimental data, the simplest of which is the Langmuir Model (Table 6.1), which expresses the relationship between q and C_i (metal concentration in solution at equilibrium). This model is the most commonly used as it only contains two parameters (Q_{max} and b), is easily understandable and reflects the two most important characteristics of the sorption system, namely maximum metal uptake and sorbent affinity. The Langmuir model is a model for monolayer adsorption, i.e. one must assume a surface with homogenous binding sites, equivalent sorption energies and no interaction between sorbed species (Khoo and Ting, 2001). It is important to realize that the underlying physico-chemical principles of the sorption process are not reflected in the model, the results obtained are only mathematical models capable of describing the relationship as it has been observed (Volesky, 2003).

The Freundlich model (Table 6.1) is often used in conjunction with the Langmuir model. It is, however, strictly empirical and based on the assumption of exponential binding site distribution and energies (Khoo and Ting, 2001), and unlike the Langmuir equation, does not imply saturation of the biomass binding sites, i.e. this model has no equivalent for the Q_{max} value of the Langmuir equation.

In this model, the parameter K is related to the sorbent capacity and $1/n$ is an indication of the sorption efficiency. These and other models used are summarized in Table 6.1.

Table 6.1 Frequently used adsorption isotherm models and their advantages and disadvantages.

Isotherm	Advantages	Disadvantages	Reference
Langmuir	Interpretable parameters	Not structured, monolayer sorption	Volesky, 2003
Freundlich	Simple expression	Not structured, no levelling off	Volesky, 2003
Combination (Langmuir-Freundlich)	Combination of above	Not easily fitted to experimental data	Aquino <i>et al.</i> , 2003
Radke and Prausnitz	Good fit over wide concentration	Empirical, uses three parameters	Aarden, 2001
Reddlich-Peterson	Approaches Freundlich at high concentrations, may reduce to Langmuir	No special advantages	Van Hullebusch <i>et al.</i> , 2005
Brunauer-Emmet-Teller (BET)	Multilayer adsorption; inflection point	No "total capacity" equivalent	Volesky, 2003
Dubinin-Radushkevich	Temperature independent; Polanyi potential theory	Not limited behaviour in the Henry's Law regime	Ho <i>et al.</i> , 2002

6.2 SORPTION KINETICS

6.2.1 Kinetic modelling

The pseudo-first order equation of Lagergren is based on solid capacity and is expressed as:

$$\frac{dq_t}{dt} = k_1(q_e - q_t) \tag{Eq. 6.1}$$

Where

k_1 is the rate constant of first order sorption (l/min),

q_e is the amount of solute sorbed at equilibrium (mg/g),

q_t is the amount of solute sorbed to the sorbent surface at any time, t (mg/g).

After integration by applying boundary conditions ($q_t = 0$ at $t = 0$ and $q_t = q_t$ at $t = t$), Equation 6.1 can be rearranged for linearized data plotting:

$$\log(q_e - q_t) = \log(q_e) - \frac{k_1}{2.303}t \quad (\text{Eq. 6.2})$$

In order to confirm the applicability of the model, a plot of $\log (q_e - q_t)$ against t should yield a straight line. In a true first-order process, experimental $\log q_e$ should be equal to the intercept of the straight line (Arica *et al.*, 2004).

The pseudo-second order kinetic model is expressed as:

$$\frac{dq_t}{dt} = k_2(q_e - q_t)^2 \quad (\text{Eq. 6.3})$$

Where

k_2 is the rate constant of second order sorption (g/mg/min)

After taking into account the boundary conditions, $q_t = 0$ at $t = 0$ and $q_t = q_t$ at $t = t$, the integrated form of Equation 6.3 can be rearranged and expressed as:

$$\frac{t}{q_t} = \frac{1}{k_2 q_e^2} + \frac{1}{q_e}t \quad (\text{Eq. 6.4})$$

The applicability of the pseudo-second order model is confirmed if a plot of t/q_t against t yields a straight line. The values of q_e and k_2 can be determined from the slope and the intercept of the plot, respectively (Nacèra and Aicha, 2006). In a true second-order process, the theoretical q_e values will closely match the experimental values (Arica *et al.*, 2004).

With regard to ease of application, the pseudo-second order equation has an advantage over the pseudo-first order equation: the sorption capacity (q_e) and the rate constant (k_2) can be determined without knowing any of the parameters. Conversely, the pseudo-first order model requires that an effective sorption capacity be assigned prior to determining any subsequent parameters (Ho, 2006).

6.2.2 Intraparticle diffusion model

The intraparticle diffusion model used here was first proposed in 1963 by Weber and Morris (Nacèra and Aicha, 2006), who concluded that sorption is proportional to the square root of contact time:

$$q_t = k_i t^{0.5} \quad (\text{Eq. 6.5})$$

Where

k_i is the intraparticle diffusion rate (mg/g/min^{0.5}).

A basic assumption of this model is that film diffusion is negligible and intraparticle diffusion is the only rate-controlling step (Mukhopadhyay *et al.*, 2007). When intraparticle diffusion controls the sorption process, a graph of q_t against $t^{0.5}$ should yield a straight line passing through the origin. The rate constant can then be calculated from the slope of the line (Venkata Mohan *et al.*, 2007).

6.2.3 Materials and Methods

All experiments were carried out in 250 ml conical flasks. A volume of 100 ml metal solution was used. The pH was adjusted to 1.5 using 1 M HCl, and was monitored throughout the experiment. No significant change was observed. Samples (3 ml) were removed at timed intervals over the course of one hour. These were centrifuged at 2000 g (Labofuge, Heraeus, Germany) for five minutes to remove particulates and then analyzed for residual platinum concentration using atomic absorption spectrometry as described on page 69. All experiments were conducted at a fixed temperature (22 °C), excluding the temperature experiment, where it was varied (4, 20, 37 and 45 °C). The sorbent dose was fixed at 1.0 g/l, excluding the sorbent dose experiment, where it was varied (0.1, 1.0 and 2.0 g/l). The initial platinum concentration was fixed at 100 mg/l for all experiments, excluding the initial concentration experiment, where it was varied (50, 100 and 200 mg/l). All data presented are the arithmetic means of results of experiments conducted in triplicate. Error bars represent standard deviations from the calculated means and in some cases are not visible.

6.2.4 Results

Effect of initial platinum concentration

Figure 6.1 shows the sorption kinetics of platinum removal at 50, 100 and 200 mg/l by plotting the platinum uptake capacity, q_t , against time. Increases in initial platinum concentration lead to an increase in uptake capacity; this indicated that at lower initial platinum concentrations the sorbent was not yet saturated with platinum ions. Platinum removal occurred rapidly during the first five minutes, after which it slowed significantly as it reached equilibrium. This trend was observed at all initial platinum concentrations. The removal efficiency of platinum decreased from 91 to 72 % with the increase in initial concentration from 50 to 200 mg/l.

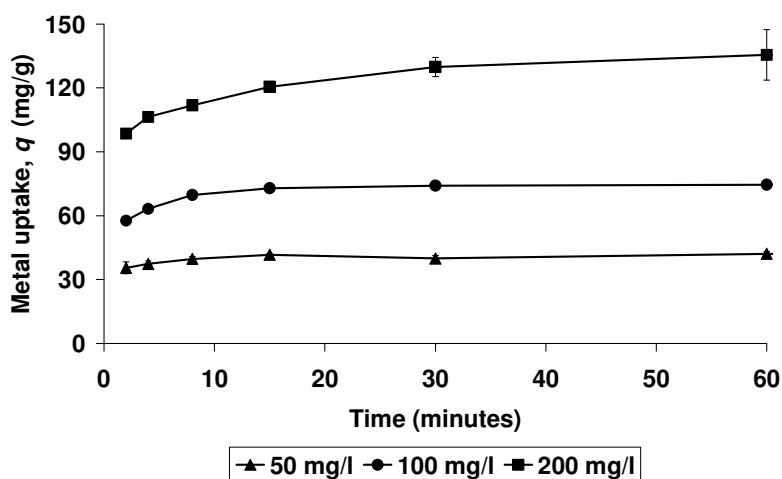


Figure 6.1 Kinetics of platinum uptake by immobilized *S. cerevisiae* at various initial platinum concentrations. Error bars represent standard deviation from the mean ($n = 3$).

The kinetics of platinum sorption were analyzed using pseudo-first order, pseudo-second order and intraparticle diffusion kinetic models. Figure 6.2A-C shows the fit of the initial platinum concentration data to the pseudo-first order, pseudo-second order and the intraparticle diffusion models. The data fitted most closely to the pseudo-second order model (correlation coefficients indicated in Table 6.2). The experimental $\log q_e$ values did not coincide with the values calculated from the pseudo-first order model, whereas the experimental q_e values much more closely matched those calculated from the pseudo-second order model (within 20 %).

The parameters obtained from all three models are compared in Table 6.2. At all initial concentrations of platinum, the correlation coefficients were highest in the pseudo-second order

model. This coupled with the closer agreement between experimental and calculated q_e values, show that the kinetics were best defined by the pseudo-second order model.

Table 6.2 Effect of initial platinum concentration on parameters calculated from the pseudo-first order, pseudo second order and intraparticle diffusion models.

C_0 (mg/l)	Pseudo-first order			Pseudo-second order			Intraparticle diffusion			
	k_1 (min^{-1})	R^2_1	$\log q_e$ (exp.)	$\log q_e$ (calc.)	k_2 (g/mg/min)	q_e (exp.)	q_e (calc.)	R^2_2	k_i ($\text{mg/g/min}^{0.5}$)	R^2_i
50	6.7×10^{-2}	0.41	1.07	1.65	1.1×10^{-2}	44.25	36.10	0.99	1.5	0.65
100	1.3×10^{-1}	0.96	1.42	1.92	3.6×10^{-3}	81.97	75.19	0.99	3.6	0.74
200	7.4×10^{-2}	0.95	1.66	2.16	2.1×10^{-3}	147.06	126.58	0.99	7.9	0.83

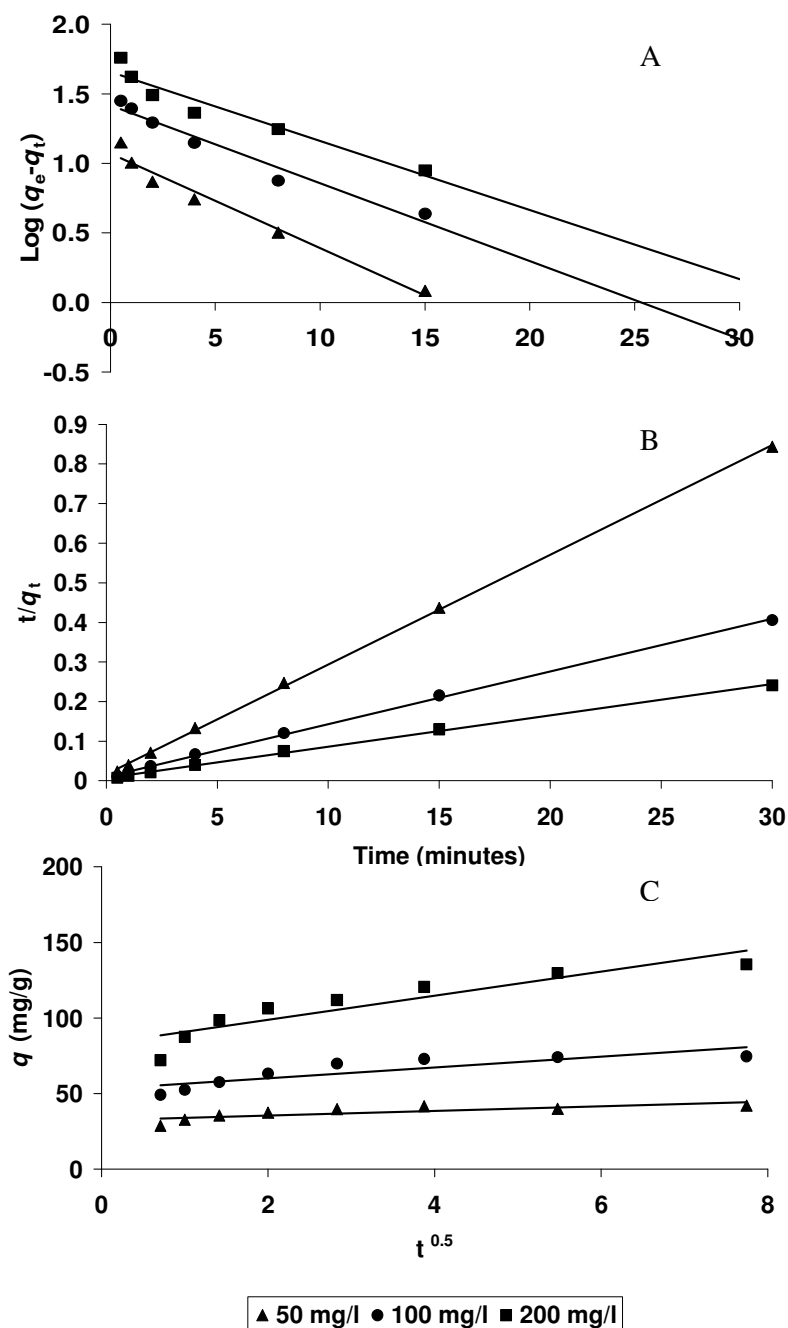


Figure 6.2 Fit of the data describing the effect of initial platinum concentration on sorption kinetics to (A) the pseudo-first order kinetic model, (B) the pseudo-second order kinetic model and (C) the intraparticle diffusion model.

Effect of sorbent dose

Sorbent capacity, shown in Figure 6.3, decreased with an increase in sorbent dose for an initial platinum concentration of 100 mg/l. The equilibrium sorption capacity decreased from 131 to

41 mg/g when the sorbent dose was increased from 0.1 to 2.0 g/l. The removal efficiency increased from 14 to 96 % with an increase in dosage from 0.1 to 2.0 g/l.

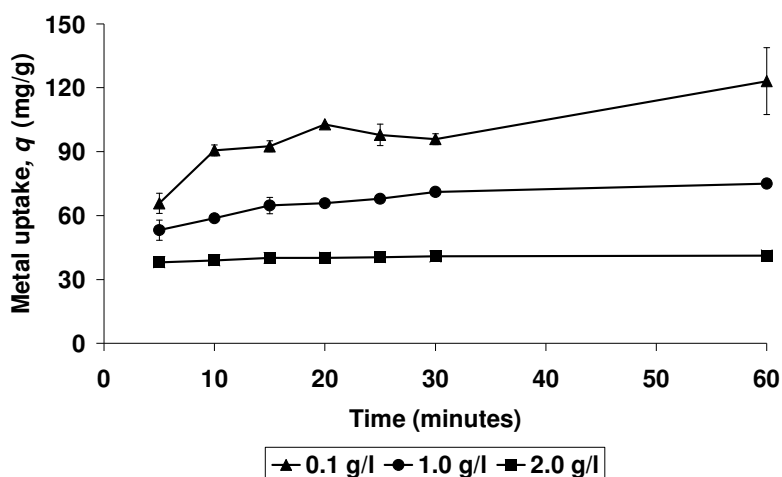


Figure 6.3 Kinetics of platinum uptake by immobilized *S. cerevisiae* at various sorbent doses. Error bars represent standard deviation from the mean ($n = 3$).

Figures 6.4A-C show the fit of the data to the pseudo-first order, pseudo-second order and the intraparticle diffusion model. By plotting t/q_t against t , the parameters of Equation 6.4 can be calculated from the slope and the intercept of the straight line. The parameters are compared in Table 6.3.

Both the pseudo-first and pseudo-second order rate constants (k_1 and k_2) increased with an increase in sorbent dose. The intraparticle diffusion rate constant (k_i), decreased with an increase in sorbent dose from 0.1 to 2.0 g/l. The correlation coefficients (R^2_1 , R^2_2 and R^2_i) compared in Table 6.3 indicated that the pseudo-second order kinetic model described the data most accurately.

Table 6.3 Effect of sorbent dose on parameters calculated from the pseudo-first order, pseudo-second order and intraparticle diffusion models.

Biomass (g/l)	Pseudo-first order		Pseudo-second order				Intraparticle diffusion			
	k_1 (min^{-1})	R^2_1	Log q_e (exp.)	Log q_e (calc.)	k_2 (g/mg/min)	q_e (exp.)	q_e (calc.)	R^2_2	k_i ($\text{mg/g/min}^{0.5}$)	R^2_i
0.1	2.8×10^{-2}	0.55	2.09	1.70	1.2×10^{-3}	123.15	131.58	0.98	8.77	0.84
1.0	6.4×10^{-2}	0.97	1.88	1.48	3.9×10^{-3}	75.03	78.74	0.99	3.95	0.91
2.0	7.9×10^{-2}	0.96	1.62	0.66	3.9×10^{-2}	41.23	41.67	1.00	0.56	0.83

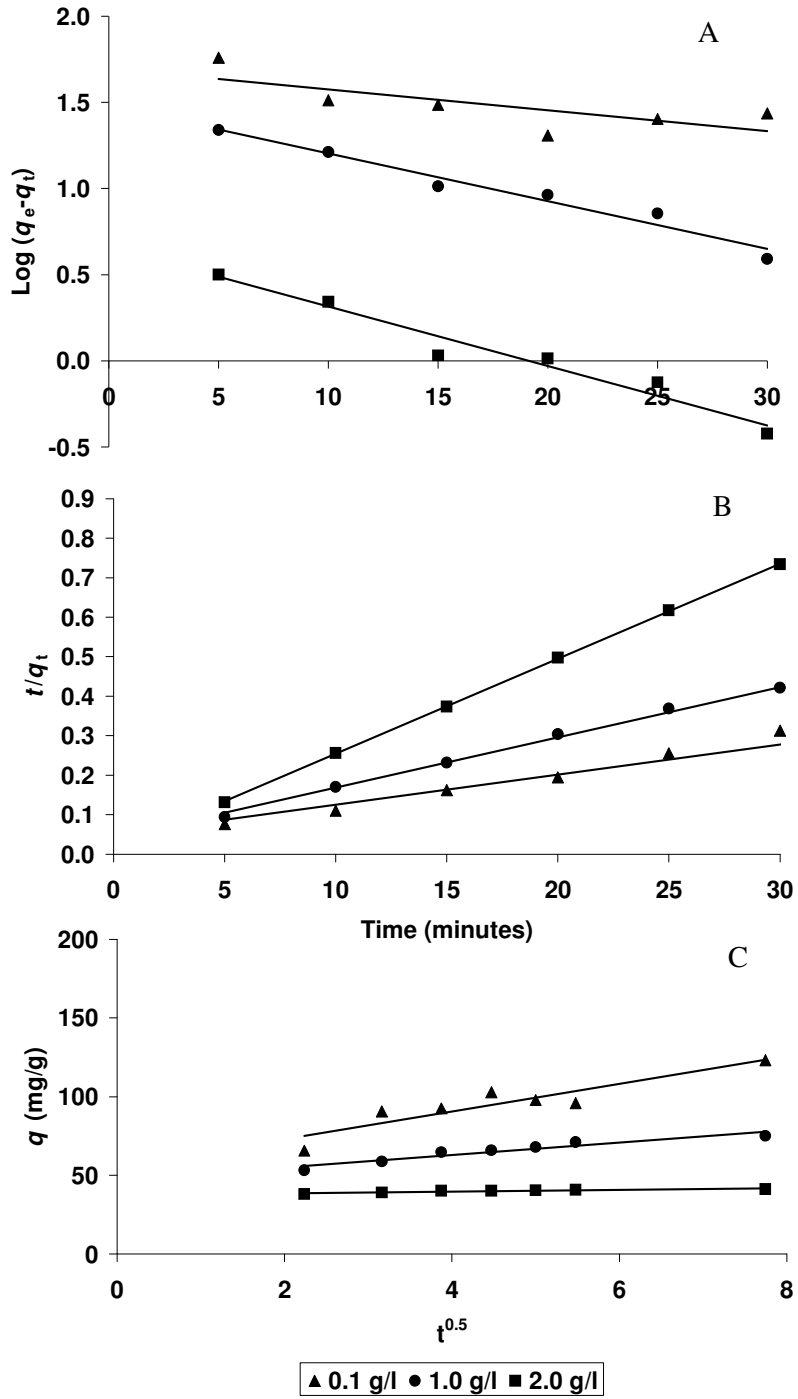


Figure 6.4 Fit of the data describing the effect of sorbent dose on sorption kinetics to (A) the pseudo-first order, (B) the pseudo-second order and (C) the intraparticle diffusion model.

Effect of temperature

Figure 6.5 illustrates the sorption kinetics of platinum uptake by the immobilized yeast biomass at 4, 20, 37 and 45 °C. The apparent kinetics did not change with the increase in temperature. Rapid sorption took place within the first ten minutes, followed by a slower phase as the concentration of platinum ions moved towards equilibrium between sorbed and unsorbed ions. A temperature increase from 4 to 37 °C increased the sorption capacity of the sorbent (63 to 92 mg/g), while a further increase to 45 °C (75 mg/g) decreased it to levels equivalent to those observed at 20 °C (73 mg/g). The removal efficiency of platinum from a 100 mg/l solution increased from 73 % at 4 °C to 92 % at 37 °C with an insignificant drop to 91 % at 45 °C.

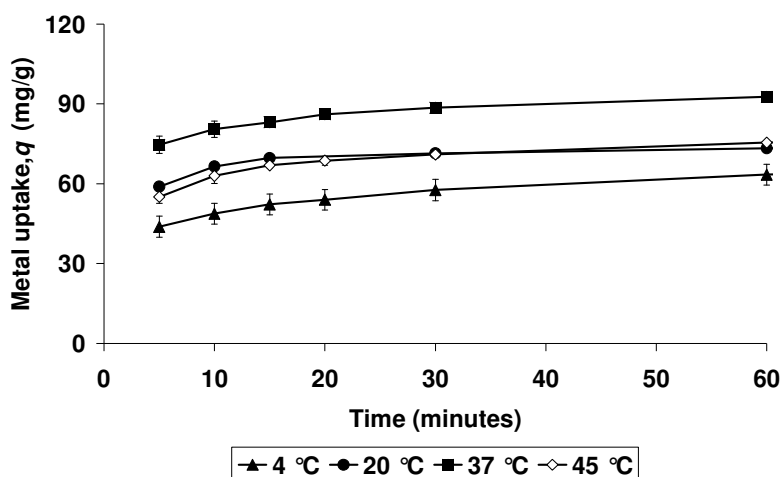


Figure 6.5 Kinetics of platinum uptake by immobilized *S. cerevisiae* at various temperatures. Error bars represent standard deviation from the mean ($n = 3$), and are sometimes too small to be visible.

The parameters for the pseudo-first order, the pseudo-second order and the intraparticle diffusion models calculated from the temperature data are presented in Table 6.4. The overall highest correlation coefficients were again calculated for the pseudo-second order model.

Table 6.4 Effect of temperature on parameters calculated from the pseudo-first order, pseudo-second order and intraparticle diffusion models.

Temp (°C)	Pseudo-first order			Pseudo-second order				Intraparticle diffusion		
	k_1 (min ⁻¹)	R^2_1	Log q_e (exp.)	Log q_e (calc.)	k_2 (g/mg/min)	q_e (exp.)	q_e (calc.)	R^2_2	k_i (mg/g/min ^{0.5})	R^2_i
4	4.8×10 ⁻²	0.99	1.84	1.42	3.9×10 ⁻³	68.43	66.67	0.99	3.48	0.97
20	7.0×10 ⁻²	0.89	1.87	1.11	1.0×10 ⁻²	74.77	74.63	1.00	2.25	0.74
37	5.9×10 ⁻²	0.99	1.97	1.34	5.5×10 ⁻³	94.27	95.24	0.99	3.13	0.92
45	5.9×10 ⁻²	0.96	1.89	1.34	6.9×10 ⁻³	78.35	75.19	1.00	2.51	0.76

The pseudo-second order rate constant (k_2) can be expressed as a function of temperature using the Arrhenius equation:

$$k_2 = k_0 \exp(-E / RT) \quad (\text{Eq. 6.6})$$

Where

k_0 is the temperature independent factor (g/mg/min),

E is the activation energy of sorption (kJ/mol),

R is the gas constant (8.314 J/mol/K)

T is the solution temperature (K).

A linear plot of $\ln k_2$ against reciprocal temperature allows for the calculation of E from the slope of the plot. Figure 6.6 shows the linearization of the data according to Equation 6.6. The plot indicates two temperature-dependent stages; one endothermic (4 to 20 °C) and one exothermic (20 to 45 °C). The activation energy for stage one (low temperature) was calculated as 67.7 kJ/mol, and that of stage two (high temperature) was calculated as -28.7 kJ/mol.

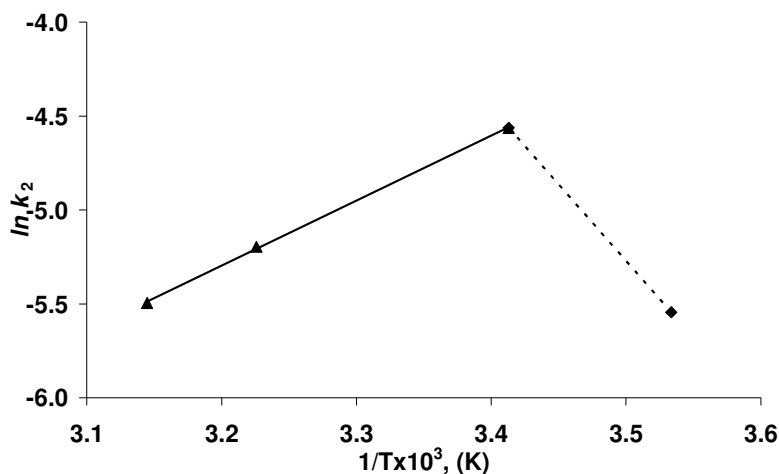


Figure 6.6 Plot of $\ln k_2$ against reciprocal temperature for sorption of platinum onto yeast sorbent. The solid line represents the exothermic stage, and the dotted line is the endothermic stage.

6.2.5 Discussion

The patterns highlighted in the experiment illustrating the sorption kinetics at increasing platinum concentration (Figure 6.1) follow the trends expected in a biosorption process. The increase in uptake capacity with increasing platinum concentration corroborates data reported by Han *et al.* (2007b), who attributed this increase to an increase in the driving force of the concentration gradient. The rapid removal of platinum during the initial stages of the experiment, followed by a slower removal towards equilibrium is supported by other work performed with yeast biomass, e.g. Çabuk *et al.* (2007) showed that *S. cerevisiae* sorption of lead was rapid in the first thirty minutes, with no significant increase in the subsequent two hours. The initial rapid stage may also be attributed to an initial non-specific sorption of platinum ions due to electrostatic attractions between the protonated sorbent and the platinum chloro-complex anions. This rapid stage may be followed by a slower conversion of the electrostatic bonds to chemical bonds. This rapid sorption is considered advantageous at full scale, where small retention times are required for maximal recovery efficiency. The decrease in removal efficiency (percentage removal) with an increase in platinum concentration (Figure 6.1) was as a result of the biomass becoming more highly saturated at each increase in concentration, while leaving an increasingly high residual metal concentration. These trends are similar to those found by Nacèra and Aicha (2006) for the sorption of methylene blue by dead *Streptomyces rimosus* biomass and the sorption of various textile dyes by *S. cerevisiae* (Kumari and Abraham, 2007), indicating that this is a trend shared by many sorption systems. Due to the efficiency of most platinum refining processes however, the initial concentrations of platinum that would be encountered at the outset of an industrial biosorption process such as this would

generally result in extremely low residual metal concentrations after biosorption. The close fit of the data to the pseudo-second order model (Table 6.2) implies that despite the possibility of a contribution to sorption by physical sorption mechanisms (such as electrostatic attraction), the overall sorption may have been controlled by chemical sorption mechanisms such as covalent bonding or microprecipitation.

In the case of the effect of sorbent dose on platinum sorption kinetics (Figure 6.3), an increase in sorbent dose decreased the specific uptake capacity (q) but increased the sorption efficiency. This showed that increasing the sorbent dosage increased the surface area available, hence the number of sites available for sorption increased. At higher sorbent concentrations, there was a more rapid sorption of platinum onto the sorbent surface that resulted in a lower solute concentration in solution than that produced by a lower sorbent dosage. Thus, with increasing sorbent dose, the amount of platinum sorbed per unit mass of sorbent was reduced, causing the decrease in uptake capacity. Similar effects have been reported previously by Han *et al.* (2007b), Vadivelan and Vasanth Kumar (2005) and Wang *et al.* (2005b), all of whom noted that an increase in sorbent dosage decreased the uptake capacity of the sorbent material used. So in order to apply this process to the recovery of platinum from wastewaters at full scale, the sorbent dose must be closely matched to the platinum concentration in order to maximize the efficiency of the sorbent. However, the application of excess sorbent will result in a less financially sound recovery system. An optimized system would be one in which the total mass of metal per mass of sorbent (maximum uptake capacity) results in the minimum residual metal concentration. This has been calculated for this particular system (Chapter 6) as approximately 150 mg platinum per gram of sorbent, which implies that the sorbent can be exposed to 3 l of 50 mg/l platinum concentration solution before the uptake capacity is reached and fresh sorbent is required. Modelling of the data reiterated that the pseudo-second order model best described the sorption kinetics, corroborating the suggestion that the process may be controlled by chemical sorption mechanisms. This may indicate a major drawback to the application of such a process to the recovery of platinum from wastewaters, as chemical sorption is seldom reversible, which precludes the possibility of sorbent regeneration and reuse. This further implies that a destructive method, such as returning the metal-laden sorbent to the smelting operation, will need to be employed to free the sorbed platinum. Both of these issues would negatively impact on the low-cost aspect usually associated with biosorption processes. The desorption of platinum from the sorbent and subsequent sorbent regeneration will be investigated in Chapter 7.

The interesting pattern described by the results of the experiment to determine the effect of temperature on sorption kinetics (Figure 6.5), where an increase in temperature from 4 to 37 °C increased the uptake capacity. A further increase to 45 °C decreased the uptake to levels equivalent to that obtained at 20 °C contradicts observations made by Nacèra and Aicha (2006), who found that increasing the temperature at which *S. rimosus* (20 to 50 °C) adsorbed methylene blue decreased both the sorption capacity and the removal efficiency. They did not suggest a reason for this decrease in capacity and removal efficiency, but perhaps the discrepancy in temperature effect may be due to the physical stability of the sorbent itself. It may have been that the surface of the *S. rimosus* sorbent was more temperature sensitive than the sorbent used in the current investigation. This sensitivity may have led to a breakdown in surface integrity at a lower temperature than experienced by the sorbent used here, resulting in a decrease in sorption capacity with an increase in temperature from 20 to 50 °C. The correlation coefficient was again highest for the pseudo-second order kinetic model, implicating a chemical sorption mechanism as the most significant rate limiter in the sorption process.

The mechanism of sorption of metal ions by biomass is usually characterized as one of three general types; physical sorption, ion exchange and chemical sorption. The weak forces involved in physical sorption result in low activation energies. Sağ and Kutsal (2000) stated that the activation energy of physical sorption is usually no more than 4.2 kJ/mol, but other literature suggests that activation energies of up to 20 kJ/mol are evidence of physical sorption. The sorption of methylene blue to *S. rimosus* was characterized as a physical sorption mechanism with low activation energy (7.18 kJ/mol) (Nacèra and Aicha, 2006). Ion exchange typically exhibits activation energies of between 8 and 16 kJ/mol (Al-Rub *et al.*, 2006; El-Naas *et al.*, 2006). Chemical sorption is indicated by high activation energies (>20 kJ/mol) (Özer *et al.*, 2004). The activation energy calculated for both stages of the platinum sorption in this study was greater than 20 kJ/mol. This implies that for the current sorption process, chemical sorption is the controlling factor. Özer *et al.* (2004), investigating the sorption of copper by *Cladophora crispata* found a similar two-stage process. At 20 to 25 °C sorption was endothermic ($E = 51.5$ kJ/mol) and at higher temperature this converted to an exothermic ($E = -35$ kJ/mol) process. Both stages exhibited activation energies in the range of chemical sorption, similar to that found in this study. The evidence of an exothermic process is advantageous when a low-cost biosorption process is considered at full scale. It implies that minimal energy need be expended in heating the process. If temperatures lower than the threshold

temperature are reached for short periods, the system will recover quickly, and not suffer any long-term loss of efficiency experienced by biologically active bioremediation systems.

6.3 SORPTION ISOTHERMS AND THERMODYNAMICS

The two most commonly applied sorption isotherm models are the Langmuir and Freundlich isotherm models. These two are the simplest (only two unknown parameters per model) and the most easily understood, as the resultant parameters can be easily interpreted; for example the Q_{max} value of the Langmuir model. The Langmuir Model (Equation 6.7) expresses the relationship between q and C_i (metal concentration in solution at equilibrium):

$$q = \frac{Q_{max} b C_i}{1 + b C_i} \quad (\text{Eq. 6.7})$$

Where Q_{max} is the total biosorbent capacity (mg/g),

b is a constant related to the energy of the reaction (l/mg).

A plot of C_i/q vs. C_i allows for the calculation of Q_{max} and b . This model makes three important assumptions firstly that sorption does not exceed a monomolecular layer, secondly that the biosorbent has a finite number of sites and thirdly that all sites exhibit equal affinity for the metal ion of interest.

The Freundlich model is empirical in nature, and assumes that the adsorption energy of a metal ion binding to a site on the sorbent surface depends on the occupancy of the adjacent sites. In Equation 6.8, K and n are the Freundlich parameters and indicate adsorption capacity and adsorption intensity, respectively. Equation 6.8 can be linearized in logarithmic form and the constants determined.

$$q = K(C_i)^{1/n} \quad (\text{Eq. 6.8})$$

Thermodynamic parameters such as enthalpy change (ΔH°), Gibbs free energy (ΔG°) and entropy change (ΔS°) can be estimated by using changes in equilibrium constants due to temperature increase. Gibbs free energy change is an indication of the spontaneity of a reaction, i.e. if ΔG° is

negative, a reaction will occur spontaneously. The value of ΔG° can be determined using Equation 6.9.

$$\Delta G^\circ = -RT \ln b \quad (\text{Eq. 6.9})$$

Where ΔG° is the Gibbs free energy change (kJ/mol).

The Gibbs free energy change of a system can be related to enthalpy and entropy change. The magnitude of the enthalpy change (ΔH°) can be used to define the type of sorption process, i.e. if ΔH° is negative, the sorption is exothermic, and if it is positive, an endothermic sorption process is active. Enthalpy and entropy change can be related to ΔG° by Equation 6.10 (Mungasavalli *et al.*, 2007).

$$\Delta G^\circ = \Delta H^\circ - T\Delta S^\circ \quad (\text{Eq. 6.10})$$

Where ΔH° is enthalpy change (kJ/mol),
 ΔS° is entropy change (kJ/(mol.K)).

6.3.1 Materials and Methods

Sorbent at a concentration of 1 g/l was added separately to 50 ml platinum solutions of varying concentration (10 – 200 mg/l) in 100 ml Erlenmeyer flasks. These were agitated on an orbital bench top shaker (Labcon, South Africa) (150 rpm) at room temperature for 24 h. Samples were removed and centrifuged at 2000 g (Labofuge, Heraeus, Germany) for five minutes to remove particulates. The residual metal concentration was measured by atomic absorption spectrometry. The effect of pH on sorption was studied at pH of 1.0, 1.5 and 2.0, keeping other experimental parameters constant. This experiment was then repeated varying the incubation temperatures (10, 20, 37 and 45 °C) at the optimum pH. All experiments were performed in triplicate. An example of the data analysis performed is shown in Appendix A.

6.3.2 Results

Effect of initial solution pH on sorption

Figure 6.7 shows the isotherm data determined at pH 1.0, 1.5 and 2.0. At low pH (pH 1), the biosorbent had a significantly higher platinum uptake capacity than at higher pH. These data were

modelled well using the Langmuir model; the correlation coefficients, Q_{max} and b values are shown in Table 6.5, along with the Freundlich parameter values.

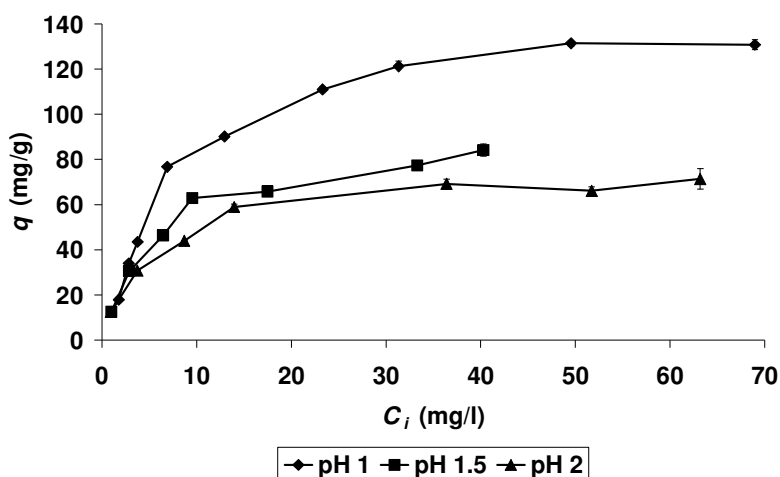


Figure 6.7 Sorption isotherms showing the sorption of platinum onto *S. cerevisiae* sorbent at increasing pH (Temp = 20 °C). Error bars represent the standard deviation from the mean ($n = 3$), and in most cases are too small to be visible.

The pH of the bulk solution impacted significantly on the uptake capacity of the sorbent. Even a small change from pH 1.0 to pH 1.5 decreased the Q_{max} value from 151.52 mg/g to 97.09 mg/g. A similar decrease in the Freundlich K value was observed as the pH increased. In all cases, the experimental data fit the Langmuir model more closely than the Freundlich model.

Table 6.5 Parameter values calculated from pH isotherms in Figure 6.7 (Temp = 20 °C).

pH	Langmuir Parameters			Freundlich Parameters		
	Q_{max} (mg/g)	$1/b$ (binding constant)	R^2	K	$1/n$	R^2
1.0	151.52	0.11	0.99	20.33	0.50	0.89
1.5	97.09	0.13	0.97	15.00	0.49	0.91
2.0	76.92	0.16	0.99	15.55	0.40	0.92

Effect of solution temperature on sorption

Figure 6.8 indicates that the uptake capacity of the sorbent increased with an increase in temperature, i.e. the sorption process was favoured at higher temperatures, although a decrease in uptake occurred above 37 °C.

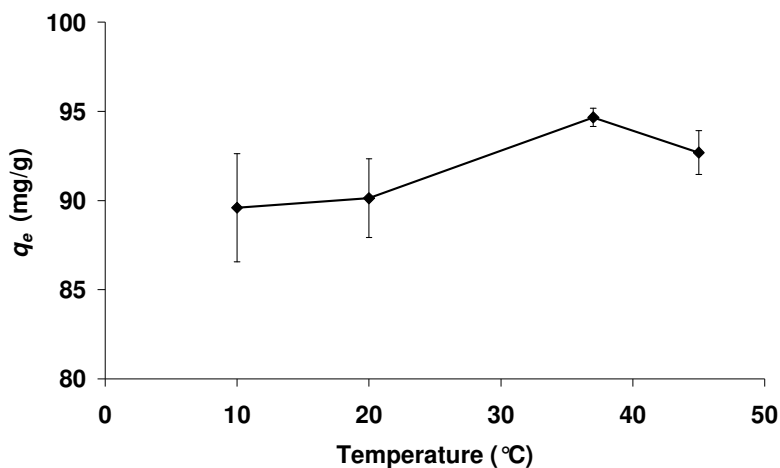


Figure 6.8 Equilibrium metal uptake (q_e) after incubation with sorbent at controlled temperatures (100 mg/l initial platinum concentration, pH 1.5). Error bars represent standard deviation from the mean ($n = 3$).

The initial slopes of the isotherm curves shown in Figure 6.9 indicate that as the temperature increased, the affinity of the sorbent for the metal ions was decreased.

Linearization of the curves shown in Figure 6.9 yields calculated theoretical Q_{max} , b , K and n parameter values (Table 6.6). Similar to the equilibrium uptake values shown in Figure 6.8, the Q_{max} and K values increased with an increase in temperature up to 37 °C. At temperatures higher than this, the maximum uptake was negatively affected. Similar to the experimental isotherm data recorded in the solution pH experiments (Table 6.5), the data fit the Langmuir model more closely than they did the Freundlich model.

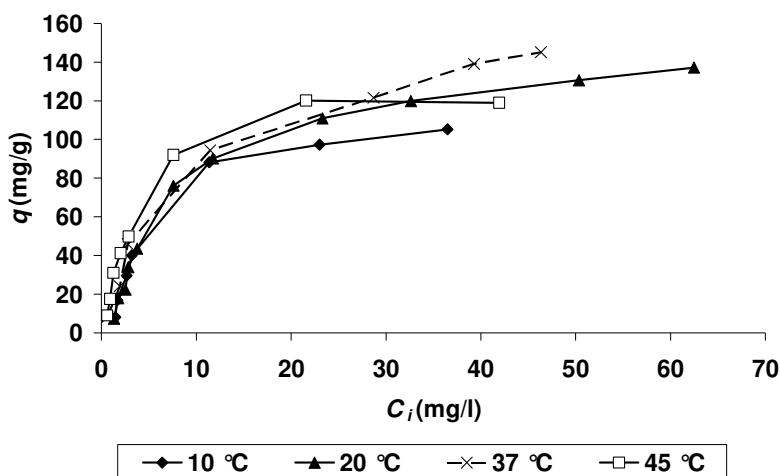


Figure 6.9 Sorption isotherms showing the sorption of platinum onto *S. cerevisiae* sorbent at various temperatures. Error bars represent the standard deviation from the mean, and in all cases are too small to be visible ($n = 3$).

Table 6.6 Parameter values calculated from experimental temperature isotherms (pH 1.5).

Temperature (°C)	Langmuir Parameters			Freundlich Parameters		
	Q_{max} (mg/g)	$1/b$ (binding constant, K)	R^2	K	$1/n$	R^2
10	166.67	0.07	0.94	9.46	0.99	0.86
20	172.41	0.07	0.94	13.10	0.65	0.86
37	178.57	0.09	0.99	20.56	0.58	0.86
45	138.89	0.18	0.99	19.96	0.68	0.89

The temperature isotherm data can also be analyzed in a way that helps to discriminate between a physical and a chemical sorption mechanism. Equation 6.9 relates the biosorbent affinity, b , to the heat of biosorption, ΔH° (absolute value). The positive or negative calculated ΔH° value also identifies the temperature preference of the reaction, i.e. exo- vs. endothermic. Linearization of the equation and plotting of $\ln b$ versus $1/T$ allows for a linear regression of the data (Figure 6.10) (Özer and Özer, 2003). The slope and intercept of the line were then analyzed and ΔH° was calculated to be 26.07 kJ/mol. Gibbs free energy change and ΔS° were determined as -43.12 kJ/mol and 69.19 kJ/(mol.K) respectively, using Equation 6.10.

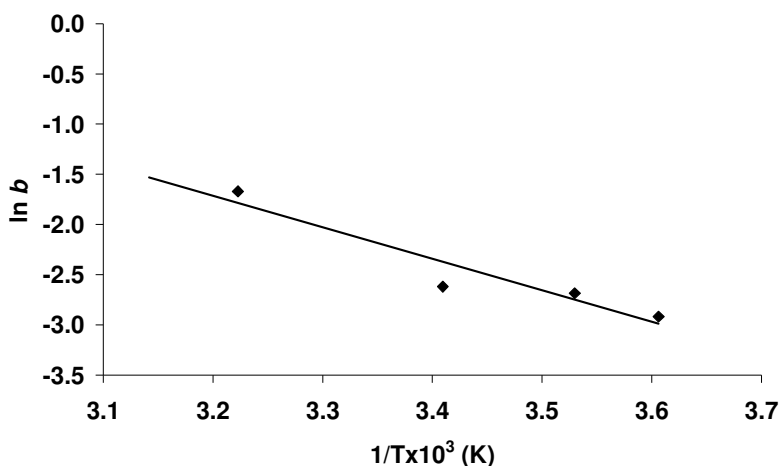


Figure 6.10 Linearization of the temperature affinity data in order to determine thermodynamic characteristics of the sorption reaction.

6.3.3 Discussion

Solution pH is perhaps the most important condition affecting the sorption reaction. It can influence both the ionization of the biosorbent surface sites and the speciation chemistry of the metal and non-metal ions in solution (Fiol *et al.*, 2006). This accounts for the specific sorption of some metal species rather than others at various conditions of pH (Godlewska-Żyłkiewicz and Kosłowska, 2005). The drop in sorption capacity with an increase in pH (Figure 6.7) may have been a result of the increasing instability of the metal ions in solution, thus it could be surmised that any negative effect on sorption capacity by pH change was due to changes in the aqueous metal chemistry, resulting in a decrease in the concentration of easily extractable species. The reaction took place optimally at low pH (1.0 or less). At all experimental pH values, the data fit the Langmuir model more closely than they did the Freundlich model. This is similar to other investigations considering the sorption of PGMs. Guibal *et al.* (2002) found that the Langmuir model better fitted the data for the sorption of palladium onto sulphur derivatives of chitosan, and Ma *et al.* (2006) found a similar best fit to the Langmuir model when modelling the sorption of platinum onto bayberry tannin immobilized collagen fibre membranes. This does not, however, imply that all PGM biosorption can be best modelled using the Langmuir model. Ruiz *et al.* (2000) compared both the Langmuir and the Freundlich model fit to data from the sorption of palladium onto chitosan and found that the Freundlich model fit was superior. It is important to note that the best fitting of experimental data to these mathematical expressions is in no way sufficient evidence to conclude that the assumptions used in the definition of the model may be used to completely describe the sorption mechanism. It may be possible though, to assume that for example, in the

case of a best fit to the Langmuir model, that the sorption mechanism is perfectly homogenous on the sorbent surface (Ruiz *et al.*, 2000). However, in the current study, the SE micrographs in Chapter 5 indicate that sorption to the sorbent occurs in patches rather than homogeneously across the surface. Although, without further confirmation of the reason for the patchy distribution, the possibility still exists that it is an artefact resulting from the preparation of the sample for SEM analysis or the non-saturated state of the sorbent analyzed.

Successful biosorption of base metal cations usually takes place in the range of pH 3 - 6, and is extremely pH dependent. Özer and Özer (2003) reported an optimal pH value for lead and nickel uptake of 5.0 for *Cladophora crispata*, while Vianna *et al.* (2000) found that copper, cadmium and zinc uptake was maximal at pH 4.5 for *S. cerevisiae*, *Bacillus lentus* and *Aspergillus oryzae*, and decreased significantly when the pH was dropped to 3.5 or 2.5. This led them to suggest that an initial electrostatic attraction between the negatively charged functional groups and the metal cations was involved in the biosorption reaction. At low pH values cell wall ligands undergo a high degree of protonation, resulting in an overall positive surface charge. This is likely to assist in the attraction of negatively charged platinum anions to the cell wall functional groups through similar electrostatic forces (Parsons *et al.*, 2003). Metal anions such as those formed by Cr(VI) (Özer and Özer, 2003), Au, V and Se (Niu and Volesky, 2003) are all maximally sorbed at pH 3 or less.

The optimum sorption pH (1 or less) derived here was lower than has been reported previously for platinum sorption. Dziwulska *et al.* (2004) investigated the ability of *Chlorella vulgaris*, immobilized on Cellex-T, for selective binding of platinum and palladium from acidic solution (pH 0.5 - 4.5) and found that retention of platinum by the sorbent was most efficient in the pH range of 1.5 - 2.0. The same was observed for *Saccharomyces cerevisiae* immobilized in calcium alginate (Godlewska-Żyłkiewicz and Kosłowska, 2005), where palladium sorption was most efficient at pH in the range 1.0 - 2.5, and decreased with a decrease in solution acidity (from 3.0 to 11.5). Parsons *et al.* (2003), investigating the pH range 2.0 - 6.0 found that platinum bound optimally to alfalfa biomass at a pH of 3. From the data presented in this study (Table 6.5) and published information, it is evident that PGMs sorb optimally at low pH (3 or less). This may indicate an overall initial mechanism of electrostatic attraction, similar to that suggested by Arica and Bayramoğlu (2005) for the sorption of anionic Cr(VI).

Changes in temperature may influence a number of factors of importance in the sorption of metal ions. These include the interaction between the biosorbent and the metal ions, usually by influencing the stability of the metal ions in solution (Sağ and Kutsal, 2000), the stability of the metal-sorbent complex (Özer *et al.*, 2004), and also the sorbent surface itself, in terms of cell wall configuration and the ionization of the chemical moieties on the cell wall (Özer *et al.*, 2004). The sorption of platinum was favoured at higher temperatures, with a decrease in uptake occurring above 37 °C (Figure 6.8). The parameters calculated from the isotherm models mirror the pattern seen in the uptake capacity curve, Figure 6.9; both the Q_{max} and K values increased up to 37 °C and decreased at higher temperature, possibly due to the onset of damage to the surface structure. This is similar to other studies involving platinum biosorption. Wang *et al.* (2005a) investigated the effect of temperature (30 – 50 °C) on the sorption of platinum by immobilized bayberry tannin and found that unlike base metals (Fe, Cu, Ni and Zn), where an increase in temperature decreased the adsorption capacity, platinum adsorption was enhanced by increasing the incubation temperature from 30 °C to 50 °C. This, Wang *et al.* (2005a) suggested, may be an indication of a chemical sorption reaction. A similar trend was seen in this study, but at lower temperatures. The affinity of the platinum ions for the sorbent also decreased with an increase in temperature above 37 °C. This may have been due to the increasing incompatibility of the sorbent surface with the metal ions due to possible changes in surface structure or ionization state, although this may not be the case, as the temperatures reached during formulation of the sorbent were much higher than 45 °C, which should have rendered the surface capable of resisting any changes at lower temperatures. This suggests that it may be caused by a combination of factors within the sorption system at higher temperatures that are responsible for the decrease in platinum uptake. Further evidence of this increased incompatibility is the apparent plateau reached by the 45 °C isotherm (Figure 6.9), which is reached much more rapidly than at any other temperature, in fact, at most other temperatures the curves have yet to reach a similar plateau, indicating that it will take longer to reach equilibrium at the lower temperatures.

The calculated ΔG° of -43.12 kJ/mol indicates that the sorption process is spontaneous. The positive value of ΔS° indicated that the sorbent had a high affinity for the platinum ions and may indicate that sorption of platinum ions may cause changes to the sorbent surface (Uslu and Tanyol, 2006). The positive value of ΔH° (26.07 kJ/mol, $R^2 = 0.90$) indicated that this reaction was endothermic (Sağ and Kutsal, 2000). Uslu and Tanyol (2006) investigated the sorption of copper and lead by *Pseudomonas putida* in single and binary metal solutions. They calculated an enthalpy

change value of 23.12 kJ/mol for the sorption of copper from a single-metal solution, and -13.13 kJ/mol for a binary lead solution. The authors linked these values with possible temperature sensitivity experienced by the sorption process, where the higher the enthalpy change value, the more temperature sensitive the reaction. If this is the case, the sorption of platinum by the sorbent used in the current study is temperature sensitive. This is similar to results published by Fujiwara *et al.* (2007), investigating the sorption of platinum ions by L-lysine modified crosslinked chitosan. They described the reaction (based on thermodynamic analysis) of platinum sorption as spontaneous and exothermic, both the ΔG° and ΔH° values calculated were negative. The calculated value of ΔH° was -94.181 kJ/mol; this would also indicate a temperature sensitive sorption process.

The sorption reaction taking place between the platinum chloride anions and the sorbent could be preliminarily described as a chemical sorption mechanism, based on the similarity between this study and that of Wang *et al.* (2005a). Relating ΔH° to literature, the value of 26.07 kJ/mol falls within the range generally accepted to indicate a chemical sorption mechanism (physical sorption 2.1 - 20.9 kJ/mol vs. chemical sorption 20.9 - 418.4 kJ/mol) (Sağ and Kutsal, 2000). The calculated ΔH° falls at the lower limit of chemical sorption, making it a tenuous conclusion when compared to other published data such as that of Sağ and Kutsal (2000), who concluded that the exothermic sorption reaction between *Rhizopus arrhizus* and Ni(II) ions ($\Delta H^\circ = 21.4$ kJ/mol) was a physical sorption mechanism. This evidence may indicate that sorption of platinum to immobilized *S. cerevisiae* is a combination of both physical and chemical sorption mechanisms.

6.5 SUMMARY

A thorough and meaningful evaluation of sorption performance is usually based on a combination of both kinetic and equilibrium parameters. Both have been evaluated here in order to better understand the mechanics of the sorption of platinum ions onto the sorbent.

Analysis of the kinetic performance under various operating parameters was undertaken. In all cases, sorption was rapid, and an apparent equilibrium was achieved between sorbed ions and those left in solution within 30 minutes. Where changes were made to the concentration of platinum in solution prior to sorption, it was found that increasing the initial concentration increased the uptake capacity (q) but decreased the uptake efficiency (% removal). This is due to an increase in the

degree of saturation of the sorbent with a concomitant increase in the residual metal concentration after sorption. The data were best defined by the pseudo-second order kinetic model ($R^2 \geq 0.99$). The experimental q_e values fell within 20 % of those calculated from the model, whereas the experimental $\log q_e$ values were different to those calculated from the pseudo-first order model (in some cases, greater than 20 % difference).

An increase in the sorbent dosage had an opposite effect to that seen with an increase in platinum concentration. As the sorbent dose was increased, specific uptake decreased but uptake efficiency increased. This was caused by the increase in available sorption sites allowing for higher uptake efficiency, but also resulting in inefficient sorbent usage due to an excess of sorption sites. Again the data was best defined by the pseudo-second order kinetic model ($R^2 \geq 0.98$). The experimental q_e values were within 10 % of those calculated from the model, whereas the experimental $\log q_e$ values differed from the calculated values by up to 60 %.

Changes in the solution temperature had a profound effect on the sorption of platinum. An increase in temperature from 4 to 37 °C increased both the uptake capacity and the uptake efficiency. However, a further increase to 45 °C decreased both the uptake capacity and the uptake efficiency. This may have been caused by a breakdown in the surface integrity of the sorbent, either mechanically or chemically due to the effect of temperature. The temperature effects data were best defined by the pseudo-second order kinetic model ($R^2 \geq 0.99$). The experimental q_e values were within 5 % of the model calculations, whereas the experimental $\log q_e$ values were different to those calculated by up to 40 %.

Analysis of the activation energy of the system using the kinetic data at increasing temperature revealed two temperature dependent stages. At the lower temperatures (4 – 20 °C) a high positive activation energy was calculated (67.7 kJ/mol), which indicated an endothermic reaction. At the higher temperatures (20 – 45 °C) a lower negative activation energy was calculated (-28.7 kJ/mol), thus an exothermic reaction was evident.

Equilibrium studies were carried out in order to analyze the effect of pH and temperature on the sorption of platinum by the sorbent. The isotherms were modelled using the Langmuir and the Freundlich isotherm models. The prevailing pH had a significant effect on uptake; as the pH was increased from 1.0 to 1.5 and then to 2.0, the slope of the curves flattened and the curves reached a

plateau at much lower uptake capacities. The Q_{max} value calculated from the Langmuir isotherm decreased from approximately 151 mg/g to approximately 97 mg/g with a pH increase from 1.0 to 1.5. The Freundlich K parameter also decreased. The affinity of the sorbent for the metal ions also decreased with an increase in pH (Langmuir b value). The n value calculated from the Freundlich equation showed that in all cases the sorption reaction was favourable ($n > 1$). The data for the pH experiments most closely fit the Langmuir model ($R^2 \geq 0.97$).

The isotherm curve comparing uptake at increasing temperature did not immediately indicate a temperature effect on sorption; however, modelling of the data indicated a trend similar to that shown in the kinetic analysis. As temperature increased to 37 °C, the Q_{max} value increased to a maximum of 178 mg/g. A further increase to 45 °C decreased Q_{max} to 138 mg/g. This pattern was mimicked by the Freundlich K values. The increase to 45 °C also decreased the affinity of the sorbent for the metal ions. The n values showed that at all temperatures sorption was favourable. The data for these experiments were best modelled by the Langmuir model ($R^2 \geq 0.94$).

Analysis of the thermodynamic parameters based on the b values calculated from the Langmuir isotherm model showed that the sorption of platinum ions by the sorbent was spontaneous and feasible ($-\Delta G^\circ$), was endothermic and characterized by strong bonding ($+\Delta H^\circ$), and that the sorbent exhibited a high affinity for the metal ions ($+\Delta S^\circ$). The high ΔH° value is indicative of a temperature sensitive reaction. The magnitude of the heat of biosorption (ΔH°) seemed to indicate the involvement of a chemical sorption mechanism.

6.6 CONCLUSIONS

- Factors such as initial platinum concentration, sorbent concentration and temperature affect the rate of sorption in either of two ways:
 - By changing the metal concentration gradient and hence the driving force of the reaction to reach equilibrium.
 - By affecting the affinity of the sorbent for the metal by changing the surface structure either physically or chemically (or both).
- In all experimental cases the pseudo-second order kinetic model was the closest fit to the data. This implies that the rate of the sorption reaction is limited by a chemical sorption mechanism.

- Calculation of the activation energy of the system revealed a temperature dependent change in the sorption reaction, from endothermic at lower temperatures to exothermic at higher temperatures. The activation energies calculated for each reaction type were higher than usual for a physical sorption process, indicating an overriding chemical sorption process.
- Increasing the pH from 1.0 to 2.0 decreases the metal uptake capacity of the sorbent. This, when viewed in combination with the potentiometric titration data presented in Chapter 5 (Figure 5.7), which shows no change in the overall surface charge of the sorbent below approximately pH 8, may indicate that the decrease in uptake is due to a decrease in the metal ion affinity for the sorbent. In effect, the increase in pH changes the metal speciation chemistry by increasing the degree of aquation of the platinum chloride ions, decreasing their sorbability.
- Increases in temperature to 37 °C increased the metal uptake capacity. This is further evidence of an endothermic reaction, where heat input enhances the sorption performance. Further increase to 45 °C decreases the specific uptake capacity. This is likely to be due to the onset of changes in the surface charge and structure, but could also be due to increasing instability of the metal-sorbent complex.
- All isotherm data were successfully modelled using the Langmuir isotherm model. However, this does not in itself prove that any of the assumptions made by the model are true.
- Thermodynamic data suggest that the sorption of platinum ions by the sorbent is feasible, spontaneous, temperature sensitive and predominantly endothermic. The data also indicate that the platinum ions may be strongly bound and that sorption may cause physical changes to the sorbent surface.

CHAPTER 7

Application considerations

7.1 INTRODUCTION

The successful scale-up of a biosorption process greatly depends on the choice of reactor configuration. There are three basic types of sorption contact systems (Volesky, 2003): the packed bed column, the fluidized bed system and the completely mixed system. The packed bed column is the most effective configuration and holds a number of advantages over the other options. It is simple to operate, can be operated in continuous flow, has no solid/liquid separation step, can be easily scaled up and allows for *in situ* desorption and regeneration (Valdman *et al.*, 2001; Volesky, 2003).

The concept of the breakthrough curve is used to describe the performance of a packed bed reactor. Both the shape of the breakthrough curve and the time until sorbed species are detected in the column effluent (breakthrough point) at a given concentration are equally important characteristics in terms of column operation and process design as they directly affect the economics and feasibility of the process (Lodeiro *et al.*, 2006). Figure 7.1 shows the shape of a typical breakthrough curve. This shape is influenced by the individual sorbate transport processes within the column. For maximally efficient sorption performance, the shape of the curve must be as sharp as possible (Chu, 2004). In Figure 7.1, the sorbate is taken up completely by the column in the early stages, after which it begins to break through and the effluent concentration increases. In a single-column operation, it is common to terminate the flow of fresh sorbate solution once the effluent concentration reaches a specified concentration (c_{bp} , breakthrough point). In multiple-column operations, where several columns are operated in series, flow continues until the column becomes saturated with sorbate (c_{sp} , saturation point). Conditions such as bed depth, flow rate and sorbate concentration and column sorption capacity all influence the breakthrough and saturation points, and are thus of importance when attempting to optimize column operation (Volesky, 2003).

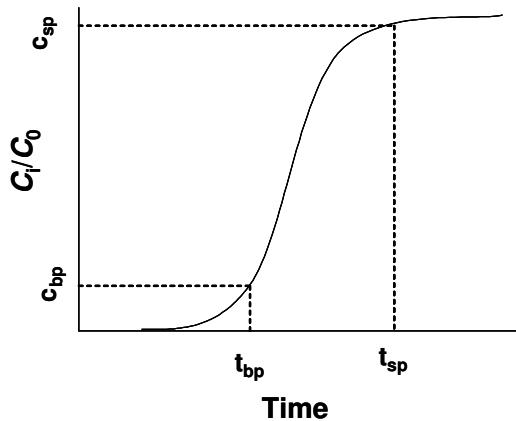


Figure 7.1 A typical sorption breakthrough curve (Adapted from Chu, 2004).

7.2 MATHEMATICAL MODELLING OF BREAKTHROUGH CURVES

The performance of a packed bed column is described using the concept of the breakthrough curve, a plot of time (or effluent volume) *versus* effluent concentration (Preetha and Viruthagiri, 2007). In order to design a successful column sorption process, accurate prediction of the breakthrough curve is necessary. The development of a model to accurately predict the dynamic behaviour of sorption in a fixed bed system is inherently different, as the concentration profiles in both the liquid and solid phase vary significantly (Aksu *et al.*, 2007). Several simple models have been applied to sorption columns. These include the Yoon-Nelson model (Aksu *et al.*, 2007), the Thomas model (Aksu *et al.*, 2007; Preetha and Viruthagiri, 2007; Han *et al.*, 2006; 2007a; Mungasavalli *et al.*, 2007), the Adams-Bohart model (Lodeiro *et al.*, 2006; Preetha and Viruthagiri, 2007), the Yan model (Mungasavalli *et al.*, 2007; Lodeiro *et al.*, 2006) the bed depth service time (BDST) model (Lodeiro *et al.*, 2006), the Belter model (Lodeiro *et al.*, 2006; Chu, 2004), the Chu model (Lodeiro *et al.*, 2006; Chu, 2004) and the Wolborska model (Preetha and Viruthagiri, 2007). Four of these models were compared in this investigation, namely the Thomas, Adams-Bohart, Wolborska and Yoon-Nelson models, selected for their potential suitability for platinum sorption based on literature.

The Thomas model has been widely used to study the performance of heavy metal biosorption in columns. This model assumes Langmuir adsorption kinetics, and that the rate of sorption is governed by second-order reaction kinetics (Aksu *et al.*, 2007; Mungasavalli *et al.*, 2007). The model has the form (Equation 7.1):

$$\frac{C_i}{C_0} = \frac{1}{1 + \exp[(k_{Th} / Q)(q_{0TH} M - C_0 V_{eff})]} \quad (\text{Eq. 7.1})$$

Where

k_{Th} is the kinetic constant (ml/(mg.min)),

Q is the volumetric flow rate (ml/min),

q_{0TH} is the specific uptake of metal (mg/g),

M is the mass of sorbent (g),

C_0 and C_i are initial and final metal concentration, respectively (mg/l),

V_{eff} is the volume treated by the column (l).

This model can be linearized and fitted to breakthrough data to obtain K_{Th} and q_{0TH} . The linearized form is shown in Equation 7.2.

$$\ln\left(\frac{C_0}{C_i} - 1\right) = \frac{k_{Th} q_{0TH} M}{Q} - \frac{k_{Th} C_0 V_{eff}}{Q} \quad (\text{Eq. 7.2})$$

The Adams-Bohart model is used to describe the initial part of the breakthrough curve i.e. up to 50 % sorbate breakthrough (Equation 7.3). This model assumes that the sorption rate is proportional to both the residual capacity of the sorbent and the concentration of the species to be sorbed (Preetha and Viruthagiri, 2007; Lodeiro *et al.*, 2006).

$$\ln \frac{C_i}{C_0} = k_{AB} C_0 t - \frac{k_{AB} N_0 Z}{U_0} \quad (\text{Eq. 7.3})$$

Where

k_{AB} is the kinetic constant (l/mg/min),

N_0 is the saturation concentration (mg/l),

Z is the height of the column (cm),

U_0 is the superficial velocity (cm/min).

From this equation, operational parameter values can be determined using a plot of $\ln C_i/C_0$ against time at a given flow rate and bed height.

The Wolborska model can be used to describe the adsorption dynamics of a sorption system using mass transfer equations to simulate diffusion mechanisms active in the range of the low-concentration breakthrough curve (Preetha and Viruthagiri, 2007). The model is represented in Equation 7.4.

$$\ln \frac{C_i}{C_0} = \frac{\beta_a C_0 t}{N_0} - \frac{\beta_a Z}{U_0} \quad (\text{Eq. 7.4})$$

Where

β_a is the kinetic constant of the external mass transfer (1/min)

The solution expression of the Wolborska model is equivalent to the Adams-Bohart model if the constant k_{AB} is equal to β_a/N_0 . Due to the similarity between the two models, a plot of $\ln(C_i/C_0)$ versus time will provide information on both the Adams-Bohart and Wolborska models.

The model of Yoon and Nelson is relatively simple. It is based on the assumption that “the rate of decrease in the probability of adsorption for each adsorbate molecule is proportional to the probability of adsorbate breakthrough on the adsorbent” (Aksu *et al.*, 2007). The model also requires no detailed information regarding the characteristics of the sorbent, sorbate or physical properties of the sorption bed. The linear form of the Yoon-Nelson model is represented in Equation 7.5.

$$\ln\left(\frac{C_i}{C_0 - C_i}\right) = k_{YN}t - \tau k_{YN} \quad (\text{Eq. 7.5})$$

Where

k_{YN} is the Yoon-Nelson rate constant (1/min)

τ is the time required for 50 % sorbate breakthrough (min)

The parameters k_{YN} and τ can be determined from a plot of $\ln(C_i/(C_0-C_i))$ versus time. In order to determine the sorption capacity of a column using the Yoon-Nelson model, Equation 7.6 is used.

$$q_{0YN} = \frac{C_0 Q \tau}{1000M} \quad (\text{Eq. 7.6})$$

Where

q_{0YN} is the Yoon-Nelson sorption capacity of the column (mg/g).

All four of the models described above will be applied to breakthrough data generated using columns packed with immobilized yeast for platinum sorption in order to assess the applicability of the previous batch studies (Chapters 5 and 6) to a continuous flow system. The breakthrough point (20 % breakthrough) and the 50 % saturation points will be used to compare the efficiency of each column. The goodness of fit of the data to the models will also be assessed.

7.2.1 Materials and Methods

Sorption studies were carried out in a fixed bed glass column reactor with an internal diameter of 2.5 cm (schematic shown in Figure 7.2). The column was packed with varied amounts of dry sorbent (1 g or 5 g). The sorbent was pre-swelled by soaking in deionized water for 30 minutes in order to attain the correct column height (1 cm or 5 cm). The temperature of the column was maintained at room temperature throughout all experiments. Platinum-containing aqueous solutions ($C_0 = 50$ mg/l, pH 1.1-1.8) produced by dilution of 1000 mg/l atomic absorption spectrometry standard solutions (EC Labs, South Africa) were pumped through the column in an upflow mode, and the flow rate was regulated with a variable peristaltic pump (Ismatec, Switzerland). Samples were taken from the effluent at timed intervals by a fraction collector (Pharmacia Biotech, South Africa) and analyzed for residual platinum concentration using atomic absorption spectrometry as described previously. The experiments were continued until column saturation was observed. The data presented represents the mean values from two replicates. Error bars represent standard deviation from the calculated mean, and are shown only to indicate variation between duplicates.

Four flow rates (1.3, 0.98, 0.49 and 0.33 ml/min) were investigated at a column height of 1 cm. This resulted in hydraulic retention times (HRTs) of 3.5, 5, 10 and 15 min. For the longer column (5 cm), flow rates of 1.3 and 0.8 ml/min were investigated (HRT = 18 and 30 minutes).

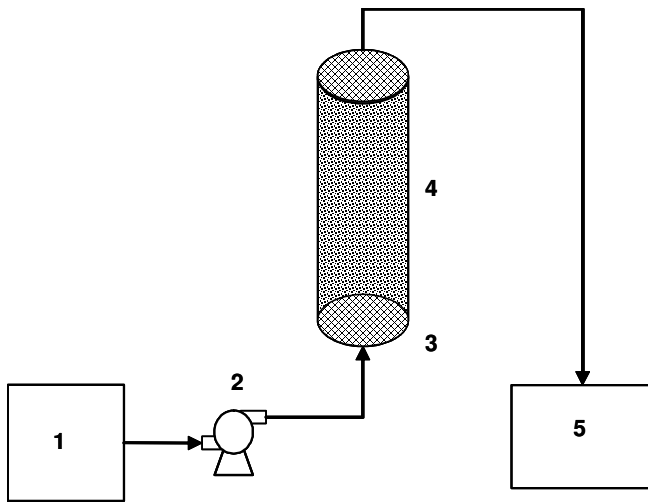


Figure 7.2 Schematic diagram of experimental column setup: (1) Influent reservoir holding platinum solution, (2) peristaltic pump, (3) porous material, (4) packed column, (5) fraction collector and effluent storage.

7.2.2 Results

Figure 7.3 indicates the breakthrough curves for the sorption of platinum at different flow rates in 1 cm columns. The sharp leading edge at each flow rate indicates poor utilization of the column sorption capacity. As the flow rate was decreased, the breakthrough point time ($C_i/C_0 = 0.2$) and the amount of metal sorbed to the column surface both increased.

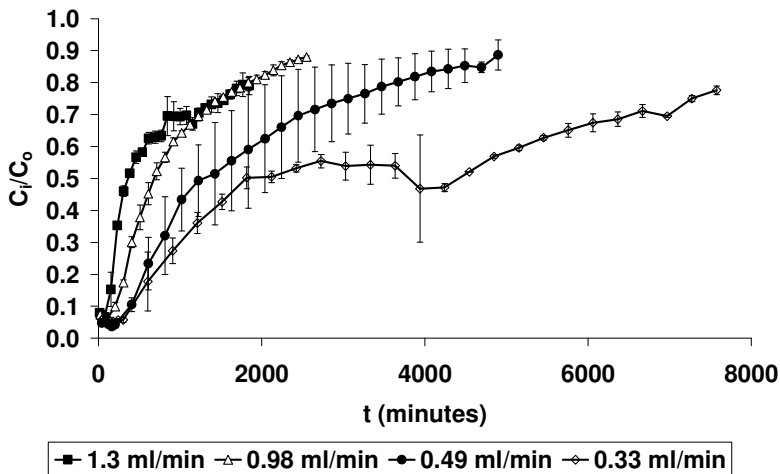


Figure 7.3 Breakthrough curves for the sorption of platinum by a 1 cm column at four flow rates. Error bars represent standard deviation between duplicate samples.

Table 7.1 summarizes the column operation parameters such as the effective column time (i.e. how long the column operated before 20 % platinum breakthrough), the volume treated before 50 %

platinum breakthrough was reached and how many bed volumes were effectively treated before the 20 % breakthrough point was reached.

Table 7.1 Analysis of 1 cm column sorption performance at various flow rates.

Flow rate	20 % breakthrough time (minutes)	Volume treated before 50 % breakthrough (ml)	Bed volumes treated before 20 % breakthrough
1.30	153	400	50
0.98	306	700	75
0.49	612	700	75
0.33	606	700	75

The data obtained in the 1 cm column experiments were fitted to the Thomas model in order to determine the Thomas rate constant (k_{TH}) and the equilibrium specific uptake of platinum (q_{0TH}). These parameters were calculated from the slopes and intercepts, respectively, of the curves plotted in Figure 7.4 and are tabulated in Table 7.2. The linearized Thomas model did not adequately describe the breakthrough sorption data. This is evident in Figure 7.4 and when the experimental and theoretical equilibrium specific uptake values are compared (Table 7.2 and 7.3). The linear regression coefficients are low (all less than 0.90), also indicating a less than perfect fit to the model. There is still some value to the model, as it showed that the kinetic constant (k_{TH}) was influenced by flow rate (Table 7.2). The value of the constant increased with an increase in flow rate (0.003 ml/mg/min at 0.33 ml/min to 0.049 ml/mg/min at 1.30 ml/min), and the equilibrium specific uptake decreased with an increase in flow rate (57.6 mg/g at 0.33 ml/min to 48.6 mg/g at 1.30 ml/min).

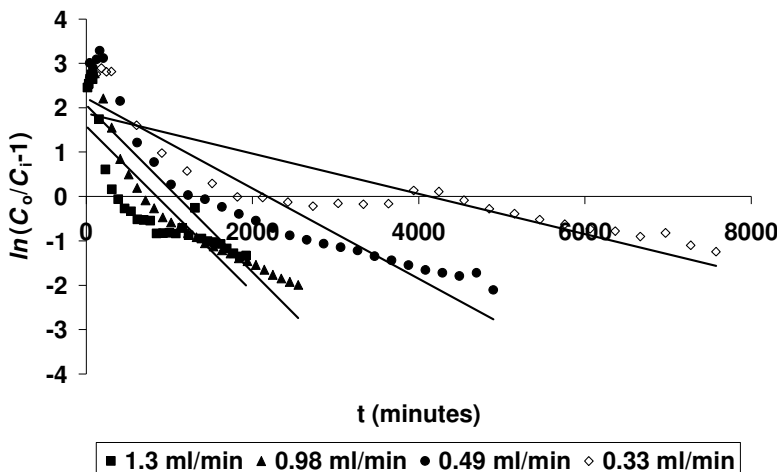


Figure 7.4 The Thomas Model for continuous sorption of platinum by a 1 cm column of immobilized yeast sorbent. The transformed data are not linear, indicating that they do not fit the model.

A linear relationship between $\ln(C_i/C_0)$ and t was obtained for the initial parts of the breakthrough curves in Figure 7.3 (up to 50 % platinum breakthrough) and is shown in Figure 7.5. These curves allow for the calculation of the Adams-Bohart and the Wolborska model parameters. Figure 7.5 illustrates that the data fall along non-linear curves which are not represented closely by the linear trendlines provided by the models. However, the values of N , k_{AB} and β_a are presented in Table 7.2. The values of the kinetic constant (k_{AB}) were influenced by residence time, and increased as residence time decreased from 15 to 3.5 minutes. The saturation concentration (N) did not seem to be affected by residence time. A decrease in residence time increased the Wolborska parameter (β_a) from 0.11 l/min at 15 minutes to 0.46 l/min at 3.5 minutes. The linear regression coefficients were all higher than those calculated from the Thomas model ($R^2 > 0.90$) and indicated a better fit of the data to the Adams-Bohart/Wolborska models despite the appearance of Figure 7.5.

Chapter 7 Application considerations

Table 7.2 Parameters predicted by the Thomas, Adams-Bohart, Wolborska and Yoon-Nelson models obtained by linear regression of the column breakthrough curves at different flow rates and column heights.

Column height (cm)	Flow rate (ml/min)	Thomas Model			Adams-Bohart Model			Wolborska Model		Yoon-Nelson Model			
		k_{TH} (ml/mg/min)	q_{oTH} (mg/g)	R^2	k_{AB} (l/mg/min)	N_o (mg/l)	R^2	β_a (1/min)	R^2	k_{YN} (l/min)	τ (min)	q_{oYN} (mg/g)	R^2
1	1.30	0.049	41.58	0.71	1.3×10^{-4}	3509.64	0.93	0.46	0.93	1.9×10^{-3}	831.53	54.05	0.71
	0.98	0.037	54.29	0.87	7.2×10^{-5}	4636.72	0.95	0.33	0.95	1.9×10^{-3}	1084.63	53.15	0.87
	0.49	0.009	110.73	0.85	4.2×10^{-5}	4313.10	0.92	0.18	0.92	1.0×10^{-3}	2125.90	52.08	0.83
	0.33	0.003	187.56	0.75	3.0×10^{-5}	3781.45	0.93	0.11	0.93	5.0×10^{-4}	3751.20	61.89	0.75
5	1.30	0.023	76.10	0.94	3.2×10^{-5}	9921.60	0.91	0.32	0.91	9×10^{-4}	7478.67	97.23	0.94
	0.80	0.016	90.43	0.98	2.0×10^{-5}	9001.54	0.98	0.18	0.98	1×10^{-3}	8957.52	71.66	0.98

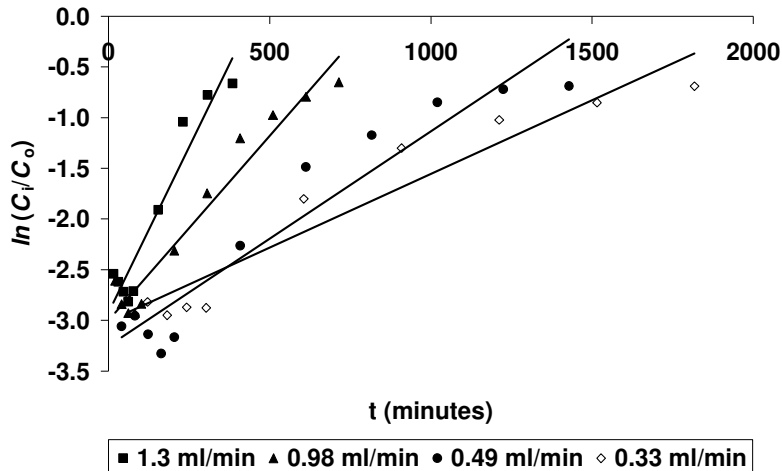


Figure 7.5 The Adams-Bohart model for the continuous sorption of platinum by a 1 cm column of immobilized yeast sorbent. The distance of the data points from the lines indicates poorness of fit.

The values of the Yoon-Nelson parameters k_{YN} (rate constant) and τ (time required for 50 % platinum breakthrough) were calculated from the linearized breakthrough curves shown in Figure 7.6, and the values are shown in Table 7.2. Residence time within the column influenced both parameters; the rate constant decreased with an increase in residence time, while the breakthrough time (τ) increased with an increase in residence time. Column capacity cannot be obtained directly from the Yoon-Nelson model, but it can be calculated as a function of τ using Equation 7.6. The column capacity (q_{0YN}) increased with an increase in residence time, most significantly from 52.08 mg/g at 10 minutes to 61.89 mg/g at 15 minutes residence time. The Yoon-Nelson model did not exhibit high linear regression coefficients ($R^2 < 0.90$), indicating that it may not be the best description of the data. This was confirmed by the fact that the τ values greatly overestimated those seen in the experimental data.

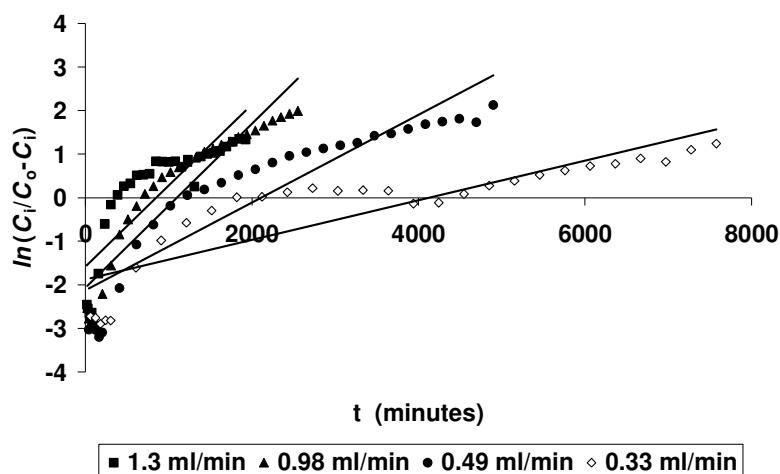


Figure 7.6 The Yoon-Nelson model for the continuous sorption of platinum by a 1 cm column of immobilized yeast sorbent.

Table 7.3 shows the effect of flow rate on the amount of platinum sorbed (mg), the uptake of platinum (mg/g) and the removal efficiency (%) of the 1 cm columns. As the retention time increased (from 3.5 to 15 minutes), both the total and specific platinum uptake of the 1 cm column increased (from 48.6 mg/g to 57.6 mg/g). The retention times used in these column experiments were lower than the total incubation times used in the batch experiments. This was because the batch studies showed that the largest proportion of the sorption took place in the initial stages of sorbent/sorbate contact, making longer incubation times unnecessary. At higher flow rates (1.3 – 0.49 ml/min), the removal efficiency of the column was almost unchanged, but at the lowest flow rate (0.33 ml/min) the removal efficiency increased by almost 10 % (from 38.9 % at 1.3 ml/min to 46.1 % at 0.33 ml/min).

Table 7.3 The effect of retention time on the sorption of platinum within a 1 cm and 5 cm high column (\pm SD, provided as an indication only, because $n = 2$)

Flow rate (ml/min)	Retention time (min)	Total amount of platinum sent to column (mg)	Total amount of platinum sorbed (mg)	Percentage removal of platinum (%)	Metal uptake (mg/g)
1 cm					
1.30	3.5	125	48.6 ± 1.5	38.9 ± 1.2	48.6 ± 1.5
0.98	5	125	45.2 ± 0.2	36.2 ± 0.2	45.2 ± 0.2
0.49	10	125	49.0 ± 5.4	39.2 ± 4.3	49.0 ± 5.4
0.33	15	125	57.6 ± 1.0	46.1 ± 0.8	57.6 ± 1.0
5 cm					
1.30	18	660	464 ± 26.9	70.3 ± 4.1	92.8 ± 5.4
0.80	30	525	335 ± 4.8	63.9 ± 0.9	67.1 ± 0.9

The column height was adjusted from 1 cm to 5 cm in order to further establish the column operating conditions. Figure 7.7 shows the breakthrough curves of two 5 cm columns, one with a retention time of 20 minutes (1.3 ml/min) and one with a retention time of 30 minutes (0.8 ml/min). The column with the higher retention time showed a higher effective column time (time taken to reach breakthrough point of 20 % platinum) and treated a higher volume of platinum solution before reaching the column exhaustion point ($C_i/C_0 = 0.50$).

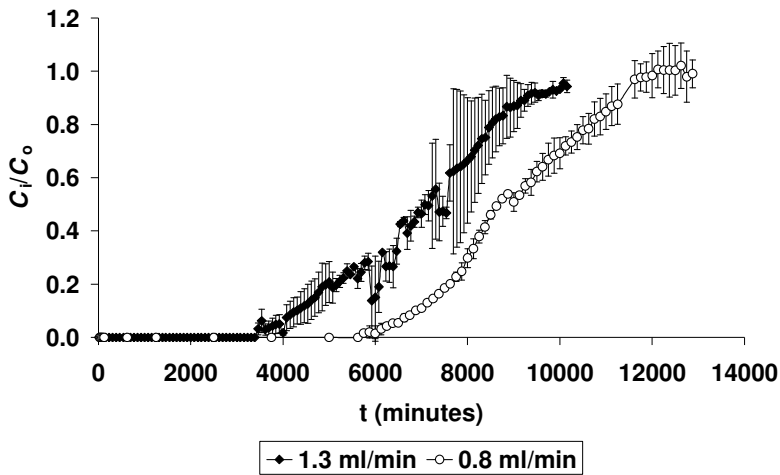


Figure 7.7 Breakthrough curves for the sorption of platinum by a 5 cm column at two flow rates. Error bars represent standard deviation from the mean ($n = 3$) and are presented only to indicate variation between columns.

Table 7.4 summarizes the column operation parameters such as the effective column time (i.e. how long the column operated before 20 % platinum breakthrough), the volume treated before 50 % platinum breakthrough was reached and how many bed volumes were effectively treated before the breakthrough point was reached for the 5 cm columns. When comparing the results at each flow rate, the information is correct at the breakthrough point, where the lower flow rate has a higher effective column time and treated a slightly higher number of bed volumes. However, when comparing the data at 50 % breakthrough, the higher flow rate had treated a higher volume of platinum solution. This was due to repeated column blockage, where the volume within the column at the time of the blockage was in contact with the sorbent for a much longer time than it should have been. This has affected all of the modelling parameters and calculated values for the 1.30 ml/min column were affected in a way that suggests that the higher flow rate results may be better than the 0.8 ml/min data. The results obtained at this flow rate are presented here mainly for comparison with the 0.8 ml/min column up to the breakthrough point (no blockages occurred before this). For all subsequent column experiments, a small amount of porous fabric (cheesecloth) was

placed at either end of the column to prevent migration of the smaller sorbent granules into the column tubing. No further blockages were observed.

Table 7.4 Analysis of 5 cm column sorption performance at two flow rates.

Flow rate (ml/min)	20 % breakthrough time (minutes)	Volume treated before 50 % breakthrough (ml)	Bed volumes treated before 20 % breakthrough
1.30	5307	9000	183
0.80	7625	7200	187

The data obtained in the 5 cm column experiments were also fitted to the Thomas model in order to determine the Thomas rate constant (k_{TH}) and the equilibrium specific uptake of platinum (q_{0TH}). These parameters were calculated from the slopes and intercepts, respectively, of the curves plotted in Figure 7.8 and are tabulated in Table 7.2. The linearized Thomas model did not adequately describe the breakthrough sorption data. This is evident when the experimental and theoretical equilibrium specific uptake values are compared (Table 7.2 and 7.3). However, the high linear regression coefficients ($R^2 > 0.90$) and Figure 7.8 indicated a good fit to the model. The Thomas model showed that the kinetic constant (k_{TH}) was influenced by flow rate. The value of the constant increased with an increase in flow rate (from 0.016 ml/mg/min at a flow rate of 0.80 ml/min to 0.023 ml/mg/min at 1.30 ml/min), and the equilibrium specific uptake decreased with an increase in flow rate (from 90.43 mg/g at 0.80 ml/min to 76.10 mg/g at 1.30 ml/min).

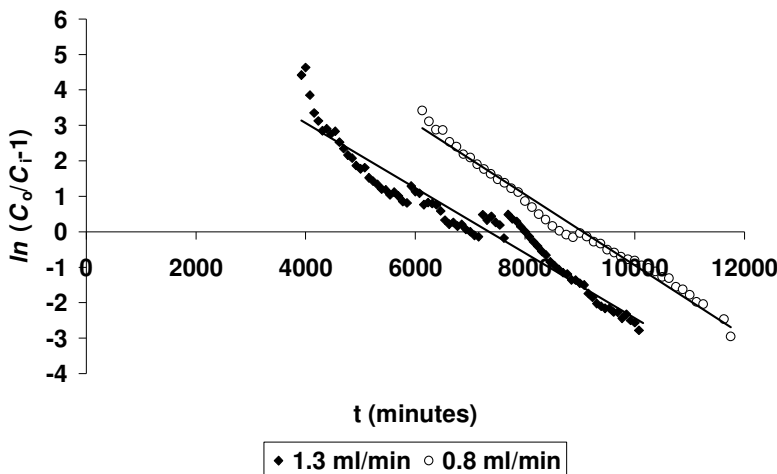


Figure 7.8 The Thomas model for the continuous sorption of platinum by 5 cm columns of immobilized yeast sorbent.

A linear relationship between $\ln(C_i/C_0)$ and t was obtained for the initial parts of the breakthrough curves in Figure 7.7 (up to 50 % platinum breakthrough) and is shown in Figure 7.9. These curves

allow for the calculation of the Adams-Bohart and the Wolborska model parameters. The values of N_0 , k_{AB} and β_a are presented in Table 7.2. The values of the kinetic constant (k_{AB}) were influenced by residence time, and increased as residence time decreased from 30 to 20 minutes. The saturation concentration (N_0) decreased with an increase in residence time. A decrease in residence time increased the Wolborska parameter (β_a) from 0.18 l/min at 30 minutes to 0.32 l/min at 20 minutes. The linear regression coefficients were high ($R^2 > 0.90$) and indicated a good fit of the data to the model.

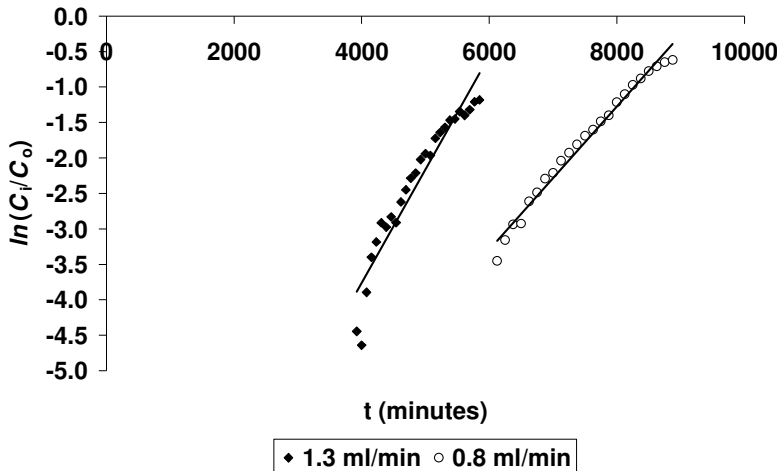


Figure 7.9 The Adams-Bohart model for the continuous sorption of platinum by 5 cm columns of immobilized yeast sorbent.

The values of the Yoon-Nelson parameters k_{YN} (rate constant) and τ (time require for 50 % platinum breakthrough) were calculated from the linearized breakthrough curves shown in Figure 7.10, and the values are shown in Table 7.2. The rate constant did not seem to be influenced significantly by an increase in residence time (9.0×10^{-4} l/min at 20 minutes and 1.0×10^{-3} l/min at 30 minutes). The breakthrough time (τ) increased with an increase in residence time. The column capacity, calculated using Equation 7.6, decreased with an increase in residence time. The Yoon-Nelson model exhibited high linear regression coefficients ($R^2 > 0.90$), indicating that it may be used to describe the data. This was confirmed by the fact that the τ values although overestimated, were still fairly comparable to those seen in the experimental data (e.g. at 0.8 ml/min, the experimental τ was 8750 minutes, and that calculated from the model was 8957 minutes).

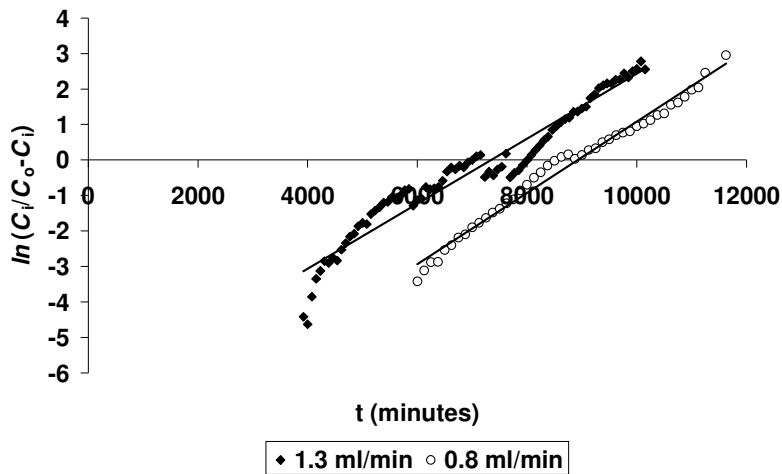


Figure 7.10 The Yoon-Nelson model for the continuous sorption of platinum by 5 cm columns of immobilized yeast sorbent.

7.2.3 Discussion

The 1 cm column information (Table 7.3) showed that the results from the batch studies in the preceding chapters (5, 6) cannot be adapted directly onto a column. These columns, containing 1 g of sorbent, should have been capable of almost quantitative removal of the platinum passed through them (based on the batch Q_{\max} value of between 120 and 150 mg/g). The highest specific uptake attained by a 1 cm column occurred at a residence time of 15 minutes (influent flow rate of 0.33 ml/min) and was approximately one third of the estimated uptake capacity (57 mg/g). However, this is not unusual, such poor performance of columns compared to batch studies has been previously reported in the literature. Mungasavalli *et al.* (2007) found a similar discrepancy between batch data and column data when investigating the sorption of chromium(VI) by pretreated *Aspergillus niger*. The Q_{\max} value calculated *via* modelling of batch data to the Langmuir isotherm was 30.1 mg/g at 30 °C, whereas the column only achieved a metal uptake value of 5.8 mg/g. In direct opposition to this, Preetha and Viruthagiri (2007) investigated the sorption of chromium by *Rhizopus arrhizus* immobilized in calcium alginate. The batch Q_{\max} value (calculated *via* Langmuir) was 23.92 mg/g, but the columns attained more than double that. In contrast to both of these, Guibal *et al.* (2001) found that the specific uptake capacity of modified chitosan for platinum and palladium in a column was very similar to that found in the batch studies. The cases presented here are evidence that it is not possible to simply convert a sorption system from batch to column and expect the same result. Other factors, in particular the aspect column ratio, must be considered, as this would have an effect on the type of contact between the sorbent and the sorbate, i.e. a

column with a smaller diameter allows for more extended contact than one with a large diameter. This is believed to be a major reason for the disparity in data in the current study.

Due to the lack of significant contact between the sorbent and the sorbate in the 1 cm columns, modelling of the data showed a poor fit to all of the models used (Table 7.2). However, the modelled parameters did show some of the trends expected. For example, the Thomas model k_{TH} value increased with an increase in flow rate. This trend has been reported previously by numerous authors, all investigating different sorbents and metals (Han *et al.*, 2007a; Preetha and Viruthagiri, 2007; Naddafi *et al.*, 2007). Aksu *et al.* (2007) stated that this relationship between k_{TH} and flow rate showed that the overall sorption is dominated by external mass transfer. Both the k_{AB} and β_a values followed established trends, with both parameters increasing with an increase in flow rate. These trends are supported by other investigations, such as that of Preetha and Viruthagiri (2007), where the same trends were seen in the column sorption of chromium(VI) by immobilized *Rhizopus arrhizus*. The Yoon-Nelson parameters showed similar trends to those reported by Aksu *et al.* (2007), in which the sorption of three dyes by dried *R. arrhizus* was investigated.

The increase in bed height from 1 cm to 5 cm increased both the breakthrough point time and the amount of platinum sorbed by the sorbent. This was mainly due to an improved aspect ratio, which allows for better and longer contact time between the sorbent and the sorbate. There was also a higher number of binding sites available for the sorption of platinum.

The influence of flow rate on the 5 cm columns was similar to that shown in the 1 cm columns, but the increase in column height allowed for better overall fits of the data to the models used. The linearized Thomas model (Figure 7.8) adequately described the breakthrough sorption data based on the regression coefficients calculated and the trend with respect to the Thomas rate constant increasing with an increase in flow rate was the same as that described by Aksu *et al.* (2007). However, the the calculated specific uptake (q_{0TH}) and that determined experimentally were very different (76.10 vs. 92.80 mg/g at 1.30 ml/min). Aksu *et al.* (2007) suggested that discrepancies such as this may occur as a result of the system failing to conform to one or more of the assumptions of the model. In the case of the Thomas model, which is one of the most widely used theoretical models to describe column sorption, the model assumes that external and internal diffusions are not limiting factors, that Langmuir-type (second-order chemical reaction) kinetics are valid and that there is no influence by axial dispersion (Naddafi *et al.*, 2007). However, most

sorption is not limited by chemical reaction kinetics, and axial dispersion is often important, especially at low flow rates (Aksu *et al.*, 2007). These factors can often lead to errors when using the Thomas model.

The Adams-Bohart and Wolborska sorption models were used to describe the initial part of the breakthrough curve, i.e. up to 50 % breakthrough. This they appeared to do ($R^2 > 0.90$). The kinetic constants (k_{AB} and β_a) were influenced by flow rate, and increased with an increase in flow rate. Similar results were reported by Preetha and Viruthagiri (2007) and by Han *et al.* (2007a). The Wolborska kinetic coefficient is related to external mass transfer, which according to the data in Table 7.2, decreased with a decrease in flow rate.

The calculated parameters of the Yoon-Nelson model were in good agreement with the experimental data (Table 7.2 and Table 7.3). The values of τ closely matched the experimental 50 % breakthrough time, and the q_{0YN} values matched the experimental uptake capacities at each flow rate (despite the experimental data being affected by the column blockages in the 1.3 ml/min column). The regression coefficients were also high, indicating a good fit of the data to the model. The values of k_{YN} were only mildly influenced by flow rate, τ decreased with an increase in flow rate, and q_{0YN} increased with an increase in flow rate (due to column blockages). Generally the Yoon-Nelson model is used to model symmetric breakthrough curves and disregards the effects of axial dispersion, and similar to the Thomas model, deviations from the model are observed when the breakthrough curves are of a more asymmetric shape (Aksu *et al.*, 2007).

Overall, the 5 cm columns were well described by all of the models (all $R^2 > 0.90$), but only the Thomas and Yoon-Nelson models could be tested further by comparing the experimental data with that calculated from the models. The Yoon-Nelson model best fitted the experimental data, even reflecting the result of the column blockages (1.3 ml/min showed a higher specific uptake than 0.8 ml/min). A greater increase in the height of the column may yield better fits to the models tested here, and as such, this should be investigated further.

7.3 DESORPTION OF PLATINUM FROM THE SORBENT

7.3.1 Materials and Methods

Fresh sorbent (50 g) was contacted (5 g per 2 l flask), with agitation (bench top shaker (Labcon, South Africa) at 170 rpm), with a platinum solution (100 mg/l prepared from an atomic absorption standard solution (EC Labs, South Africa)) for 24 hours. The sorbent was then separated by centrifugation (2000 g for five minutes (Labofuge, Heraeus, Germany)) from the liquid phase and oven-dried (60 °C) overnight in order to accurately standardize the dry weight of sorbent used in the subsequent experiments. The resultant metal-laden sorbent was estimated (based on residual metal concentration in platinum solution) to contain 13.10 mgPt/g.

For desorption screening experiments, 0.05 g of metal-laden sorbent was contacted with 12.5 ml platinum solution in triplicate flasks (4-fold concentration) of desorbent (see Table 7.5 for desorbent concentrations) for 24 hours, shaken at 170 rpm on a bench top shaker (Labcon, South Africa). Different strength HCl, HNO₃ and NH₃ solutions were prepared from 32 %, 55 % and 25 % solutions (univAR, Merck). The thiourea (Saarchem, Merck) solutions were made up in HCl concentrations described in Table 7.5, and the NaOH solutions were made up from NaOH pellets (Saarchem, Merck) dissolved in deionized water. Deionized water was used as a control desorbent. Samples were taken after 24 hours and then analyzed for platinum concentration using atomic absorption spectroscopy as described previously.

The three desorbents with the highest desorption ratio were each applied to metal-laden sorbent in a column configuration (duplicate columns per desorbent). Three grams of sorbent (to produce a 3 cm column) were packed into a column set up as described for the sorption of platinum in section 7.2.1. Initially, a flow rate of 5 ml/min was used, and all three desorbents were tested in an upflow conformation. The desorbent that performed best was investigated further, by varying the flow rate (1, 3 and 5 ml/min) and the flow direction (upflow and downflow). Samples were manually collected from the column effluent at 50 ml increments. Again the samples were analyzed for platinum content using atomic absorption spectroscopy as described previously. The desorption ratio was calculated from the amount of metal (in mg) adsorbed onto the sorbent and the final metal ion concentration in the desorption medium, according to Equation 7.7. A desorption ratio of 1.0 would indicate 100 % (total) desorption.

Desorption ratio = amount of metal ions desorbed/amount of metal ions adsorbed (Eq. 7.7)

7.3.2 Results

The results of the initial flask desorbent screening are shown in Table 7.5. The highest acid concentrations (10.5 M HCl and 5.0 M HNO₃) desorbed the highest proportion of platinum of the acid concentrations tested, with the 10.5 M HCl desorbing one third of the bound platinum. However, this was largely due to the partial digestion of the sorbent, which is undesirable if the aim of desorption is reuse of the sorbent. The acidified thiourea desorbents all showed similar desorption ratios (0.12 – 0.13), excluding that with the highest concentration of HCl. Of the thiourea concentrations, again as the concentration increased so did the desorption ratio. But, as the thiourea concentration increased, it became increasingly difficult to dissolve, to the point where the 0.8 M concentration required significant heating before suitable dissolution of the thiourea was attained. Of the bases investigated, 10.0 M NH₃ achieved the highest desorption ratio (0.15), but similar to the 10.5 M HCl, this came at a cost to the integrity of the sorbent. The 5.0 M concentrations of NaOH and NH₃ and the 1.0 M NaOH showed similar desorption ratios (0.10 – 0.12).

The most effective acid (5.0 M HNO₃), alkali (1.0 M NaOH) and acidified thiourea (2.0 M HCl + 0.1 M thiourea) were investigated further, as platinum desorbents in a column conformation. The three desorbents were compared at a flow rate of 5 ml/min in an upflow conformation. Figure 7.11 shows that in this comparison, the acidified thiourea (0.20) desorbed double the amount of platinum that was desorbed by the 1.0 M NaOH (0.10). The 5.0 M HNO₃ desorbed half that of the 1.0 M NaOH. As the desorbent that removed the most platinum from the sorbent in a column, acidified thiourea desorbent was investigated further.

Table 7.5 Desorption ratios obtained by six desorbents tested at varying concentrations.

Desorbent	Desorption ratio (desorbed/adsorbed (mg))
1.0 M HCl	0.03
5.0 M HCl	0.16
10.5 M HCl	0.33
1.0 M HNO ₃	0.06
5.0 M HNO ₃	0.19
1.0 M HCl + 0.1 M Thiourea	0.13
1.0 M HCl + 0.5 M Thiourea	0.12
2.0 M HCl + 0.1 M Thiourea	0.13
3.0 M HCl + 0.8 M Thiourea	0.09
0.1 M Thiourea	0.12
0.5 M Thiourea	0.14
0.8 M Thiourea	0.16
0.5 M NaOH	0.09
1.0 M NaOH	0.12
5.0 M NaOH	0.10
0.1 M NH ₃	0.01
0.5 M NH ₃	0.04
1.0 M NH ₃	0.05
5.0 M NH ₃	0.11
10.0 M NH ₃	0.15

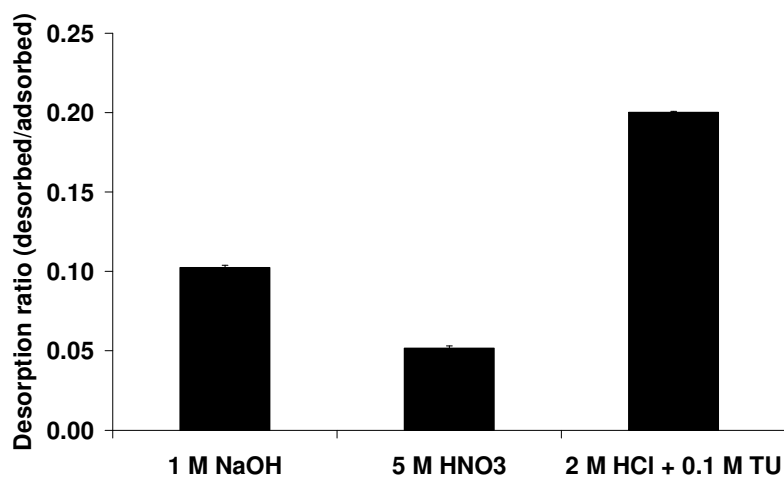


Figure 7.11 Desorption ratio attained by desorption of platinum from metal-laden sorbent by an acid (HNO₃), an alkali (NaOH) and acidified thiourea (TU) in a column setup with a desorbent flow rate of 5 ml/min. Error bars illustrate the standard deviation from the mean (Provided as a visual guideline only, $n = 2$).

The flow rate and the flow direction in which the acidified thiourea was introduced into the column was varied in order to attain maximal platinum desorption (Figure 7.12). As the flow rate was decreased to 3, and then to 1 ml/min, the desorption ratio increased from 0.20 to 0.35 (5 ml/min to 3 ml/min), but decreased to 0.26 with a decrease in flow rate to 1 ml/min. Variation of the flow direction from upflow to downflow (at 3 ml/min) increased the desorption ratio marginally from 0.35 for upflow to 0.37 for downflow.

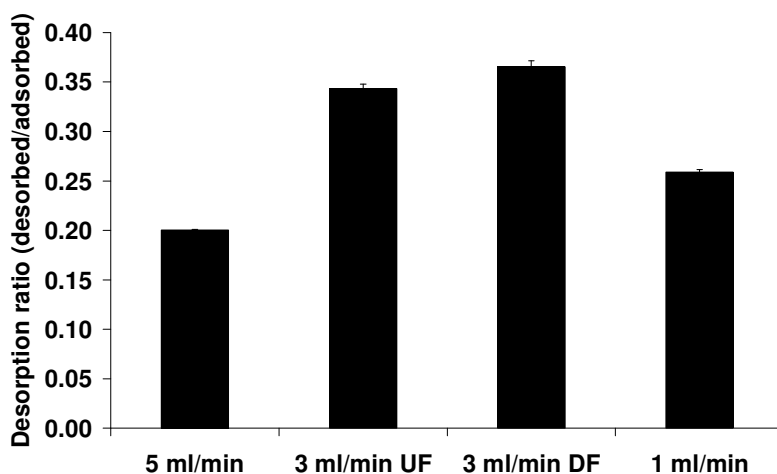


Figure 7.12 Effect of varying flow rate and direction on the desorption ratio attained by acidified thiourea on desorption of platinum from the metal-laden sorbent. UF: upflow, DF: downflow. Error bars illustrate the standard deviation from the mean (Provided as a visual guideline only, as $n = 2$).

7.3.3 Discussion

In order to achieve the most cost-effective sorption process, it must be possible to desorb metal ions from the sorbent, leaving the sorbent in a state suitable for reuse in subsequent sorption cycles is possible (Fujiwara *et al.*, 2007). Acids (HCl and HNO₃), alkalis (NaOH and NH₃) and a potent chelating agent (thiourea) were investigated for their capacity to desorb platinum from the immobilized yeast sorbent.

After 10.5 M HCl (which partially digested the sorbent), a 5.0 M solution of HNO₃ was shown to be the best acid for desorption, recovering approximately 20 % of the bound metal in the batch study (Table 7.5). In the column study, however, the performance of nitric acid as a desorbent was decreased to approximately 5 % recovery of platinum (Figure 7.11). This is contrary to the findings of Uheida *et al.* (2006), who found that nitric acid successfully desorbed platinum, palladium and rhodium from iron oxide granules. This, the authors suggested, indicated that pH had a strong effect on both the adsorption and desorption processes. In the same study, Uheida *et al.* (2006)

found that sodium perchlorate solutions were also capable of desorbing platinum, pointing to the presence of an ion exchange mechanism, where the platinum ions are not strongly bound to the iron oxide particles. They thus implied that a simple change of pH was all that was necessary to desorb these metals from the granules. In the case of desorption from the immobilized yeast sorbent, desorption was more difficult. Generally, mineral acids are used to desorb base metals, where only a change in pH is required to break the bond between the metal ion and the biosorbent. This desorption usually requires a 1.0 M concentration or less. In this case, the far stronger bond between the sorbent and the metal ions that caused the low recovery from the sorbent suggests that sorption was not caused by simple ion exchange but by a stronger attractive force.

A 1.0 M sodium hydroxide solution recovered the highest percentage of bound platinum from the sorbent out of all of the alkali solutions tested. In both the batch (Table 7.5) and column study (Figure 7.11), 10 % of the bound platinum was recovered using 1.0 M NaOH. However, Mungasavalli *et al.* (2007) found that 1.0 M NaOH was an effective desorbent, and was able to recover more than 90 % of the chromium(VI) bound to a pretreated *Aspergillus niger* sorbent. The authors surmised that the dichromate anions were bound, for the most part, by electrostatic attraction only. However, similar to the current study, only low recoveries of platinum, palladium and gold from lysine-modified crosslinked chitosan have been reported by Fujiwara *et al.* (2007). The authors' explanation for such low recovery is similar to that suggested above with respect to acid desorption. The chelating mechanism involved in platinum sorption by the immobilized yeast sorbent cannot be reversed by a simple change in pH.

Thiourea and acidified thiourea all recovered 10 – 20 % of the platinum bound to the sorbent in the batch study (Table 7.5), while acidified thiourea (2.0 M HCl + 0.1 M thiourea) recovered almost 40 % in a column conformation (Figure 7.11). Chassary *et al.* (2005b) also found that acidified thiourea was the most efficient platinum eluant compared to others they tested (HCl, ammonium hydroxide, acidified thiourea and thiourea only). When eluting platinum from a glutaraldehyde-modified chitosan sorbent, the acidified thiourea increased recovery to more than 70 % compared to that of thiourea alone (40 %). However, when the same experiment was performed using polyethyleneimine-modified chitosan, the pattern was reversed, with thiourea alone recovering more (70 %) than the acidified variant (45 %). Ma *et al.* (2006) and Fujiwara *et al.* (2007) also found acidified thiourea to be the best desorbent of those they tested. This reversal may provide an indication of the mechanism governing sorption and desorption. The success of acidified

(protonated) thiourea relative to the non-acidified form may indicate an electrostatic interaction, whereas the non-acidified would act via a chelation mechanism. However, there is a major drawback to the use of thiourea as a desorption agent, that is the difficulties experienced when attempting to separate the metal from the thiourea molecule. This problem usually makes metal recovery from such complex metal solutions almost impossible (Chassary *et al.*, 2005b) and limits the application of thiourea desorption.

When the application of a packed-bed reactor configuration for a continuous biosorption process is considered, the overall efficiency of the system is evaluated using a ratio of eluate metal concentration to feed metal concentration (Jalali *et al.*, 2002). The results of these experiments showed that acids and alkalis were not optimal eluants for the recovery of platinum from the immobilized yeast sorbent, but acidified thiourea may recover a portion of the bound platinum. The 40 % desorption of platinum by acidified thiourea in a column (Figure 7.12) improved the overall desorption efficiency over that seen in the batch studies (20 %). However, 40 % is a very low recovery, and it is not practically feasible as a means for the recovery of platinum from the sorbent. In terms of ideal application, complete desorption of the platinum from the sorbent would have made it possible to divert the concentrated desorbent stream to the head of the PMR refining process, or even to the start of the platinum solvent extraction step (see Figure 2.1 and Figure 2.2). The lack of effective desorption would result in the introduction of the metal-laden sorbent to the smelters, thus re-introducing the metal far closer to the beginning of the overall metal extraction process. In effect, the further back in the process the biosorption product (be it desorbent stream or metal-laden sorbent) is reintroduced, the lower the chances of complete metal recovery. So in order to be maximally efficient, the product should be introduced as close to the end of the process as possible.

7.4 SUMMARY

The performance of 1 cm columns at all flow rates was poor and did not attain the theoretical specific uptake values determined in the batch studies. The specific uptake values at all flow rates were far lower than the calculated maximum uptake capacity of 150 – 170 mg/g. The breakthrough curves did not fit any of the models used ($R^2 < 0.90$), but the influence of flow rate on the calculated model parameters was similar to that reported in literature. The shape (aspect ratio) of the column may have been the overriding factor in the failure of the 1 cm columns. Better results may have

been obtained if a column with a smaller diameter was used for such a small mass of sorbent, rather than the relatively large one (2.5 cm).

An increase of the column height from 1 cm to 5 cm improved both the breakthrough point time and the specific uptake of platinum. However, the repeated blockages experienced by the column run at a flow rate of 1.3 ml/min impacted on the breakthrough curve data obtained for those columns, by overestimating the efficiency of the column at this flow rate. Despite this, the breakthrough data fitted to all of the models used ($R^2 > 0.90$). Further comparison of the experimental data to the calculated parameters indicated that of the models tested, the Yoon-Nelson model best described the breakthrough data. This model even exhibited the overestimation of the higher flow rate efficiency by providing a higher theoretical specific uptake capacity at the higher flow rate rather than at the lower flow rate, which was expected.

Desorption of platinum from the sorbent was initially investigated in a batch setting, where six desorbents were compared in order to find the most effective platinum desorbent. These experiments showed that of those tested, 1.0 M NaOH, 5.0 M HNO₃ and 2.0 M HCl + 0.1 M thiourea were the three most effective platinum desorbents. These desorbents were investigated in a column environment, where the acidified thiourea desorbent showed an improved efficiency, and was further studied in order to determine the optimal flow rate and mode (upflow or downflow) for maximal desorption. Desorption efficiency doubled with a decrease in flow rate from 5 ml/min to 3 ml/min, and the mode of flow made no impact on this. However, at optimized conditions, the acidified thiourea was only able to desorb 40 % of the sorbed platinum ions. This implied that a more destructive method may be required in order to recover the sorbed metal.

7.5 CONCLUSIONS

- Columns of 1 cm height did not corroborate batch information. The aspect ratio of a column must be adapted in order to maximize efficient use of the sorbent.
- The 5 cm columns most closely fitted to the Yoon-Nelson model.
- Acidified thiourea desorbed the largest amount of previously sorbed platinum. However, only 40 % could be desorbed, which is not high enough for this method of recovery to be feasible. The platinum may instead be recovered *via* smelting of the sorbent.

CHAPTER 8

Inhibition of platinum sorption

8.1 INTRODUCTION

Industrial wastewater streams contain various compounds which are considered as impurities that may affect the performance of a sorption process intended to recover one or more specific components from the wastewater. These impurities could include light metal ions, several heavy metal ions, surfactants and chelating agents. For example, gold mine tailings have been found to contain many other metal ions such as copper, lead, iron, zinc, calcium and magnesium (Gamez *et al.*, 2003). The effect of multiple-metal solutions on the sorption of a specific metal depends on the number of metals competing for the same sorption sites, the particular metal combinations, and the concentrations in which the metals are present (Aksu and Dönmez, 2006). The resulting sorption mechanisms are far more complex than that of a single metal solution. One or more of three possible types of behaviour can be expected; synergism, antagonism and non-interaction. Synergism implies that the effect of the mixture is greater than that of the sum of the effects of the individual constituents, i.e. will result in a higher uptake of the target ion. Antagonism refers to the opposite situation, where the effect of the mixture is less than that of the sum of the individual constituents. When no change in effect is brought about by the mixture, it is termed non-interaction (Li *et al.*, 2004). This behaviour cannot be predicted based on single metal studies (Puranik and Paknikar, 1999). For this reason, it is necessary to examine the effects of co-ions on the uptake of the primary ion in order to better represent the sorption ability of the sorbent in the environment for which it is being developed.

8.2 INHIBITION OF PLATINUM SORPTION

Non-metal counter-ions such as chlorides, nitrates and sulphates affect the efficiency of sorption. Changes in the ionic strength (background electrolyte concentration) influence the sorption process by increasing or decreasing the activity of the electrolyte and/or by affecting the competition between the electrolyte ions and the adsorbing anions for available binding sites (Niu and Volesky, 2003). In the current study, the target metal, platinum, is most likely to be present as an anionic species, which would result in direct competition between the platinum anions and the similarly charged counter-ions.

Precious metal-laden wastewaters, due to their origins in mining environments, naturally contain high concentrations of light metals such as calcium and magnesium (Gamez *et al.*, 2003), and while these metal ions cannot directly compete with platinum for sorption sites, it is possible that complexation between the light metals and the platinum ligands within the solution may take place, resulting in soluble species for which the sorbent has a low affinity.

Base metals are normally not considered as possible interferents in the biosorption of anionic metal species as they generally carry the opposite charge and therefore do not compete for the same category of binding sites. But, carrying the opposite charge immediately allows for the possibility of base metals bonding to the negatively charged platinum ions, reducing the ability of these ions to bind to the sorbent.

8.2.1 Materials and Methods

The effect of ionic strength on the sorption process was studied by using various concentrations (0.01, 0.1 and 1.0 M) of NaCl, NaNO₃ and Na₂SO₄ solution (Saarchem, Merck) as a dilution agent for the platinum solutions (EC Labs, South Africa). The effect of light metal ions on sorption was investigated by addition of Ca(II), Mg(II), K(I) and Na(I) from 1000 mg/l atomic absorption standard solutions (EC Labs, South Africa) to achieve concentrations of 20, 100 and 200 mg light metal/l in a 50 mg/l platinum solution. Similarly, the effect of base metals (Ni(II), Co(II), Fe(II), Cu(II)) and precious metals (Rh(III), Au(III) and Pd(II)) were determined by the addition of metal from 1000 mg/l atomic absorption standard solutions (EC Labs, South Africa) to achieve concentrations of 20, 100 and 200 mg base metal/l in a 50 mg/l platinum solution. PEIGA sorbent (0.05 g) prepared according to Section 4.2.2 was added separately to 50 ml platinum solution (50 mg/l) in 100-ml Erlenmeyer flasks and agitated (150 rpm) on a bench top shaker (Labcon, South Africa) at room temperature for 24 h. The pH of all experiments was adjusted to < 1.5 using 1 M HCl (univAR, Merck). Samples were removed and centrifuged (2000 g for 5 minutes (Labofuge, Heraeus, Germany) in order to separate the sorbent from the solution. For the anions, light, and base metal experiments, the platinum ion concentration remaining in solution was measured using atomic absorption spectrometry as described in Section 5.3.1. For the precious metal experiments, inductively coupled plasma-mass spectrometry was used to measure the residual metal concentration as the presence of more than one PGM in solution produced a large amount of interference when using atomic absorption spectrometry.

8.2.2 Results

Figure 8.1 illustrates the effect of the anionic ligands chloride, nitrate and sulphate on the platinum removal efficiency of the sorbent. Nitrate had little effect at low concentration (0.01 M), but reduced the platinum removal efficiency by 20 % at 0.1 M and 60 % at 1.0 M. The presence of both chloride and sulphate (even at low concentration, 0.01 M) decreased the removal efficiency by 10 and 20 %, respectively. At the higher concentrations sulphate seemed to exert a more significant impact on the platinum removal efficiency, reducing it to 46 % at 0.1 M and 36 % at 1.0 M. The suppression of platinum sorption for these anionic ligands appeared to follow the trend sulphate > chloride > nitrate (based on suppression of platinum uptake at 0.01 M). In all cases the effect was inhibitory to platinum uptake.

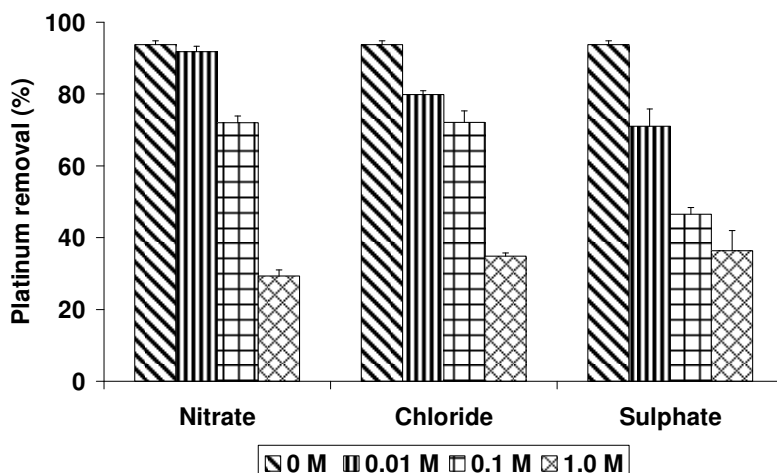


Figure 8.1 The effect of the presence of anionic ligands at 0.01 M, 0.1 M and 1.0 M on the efficiency of platinum sorption by immobilized *S. cerevisiae*. The error bars indicate standard deviation from the mean ($n = 3$).

The effect of light metals on the sorption efficiency of platinum is shown in Figure 8.2. The light metals exerted a much lower influence on platinum sorption than the anionic ligands. At low concentrations (20 mg/l), calcium suppressed platinum uptake by 8 %, whereas magnesium, potassium and sodium showed very low suppression (< 5 %). At higher concentrations (100 and 200 mg/l), calcium and magnesium suppressed platinum uptake by approximately 20 %, while sodium and potassium were only able to decrease platinum uptake by 8 – 10 %. Suppression of platinum sorption by light metals followed the trend: magnesium \approx calcium > potassium > sodium.

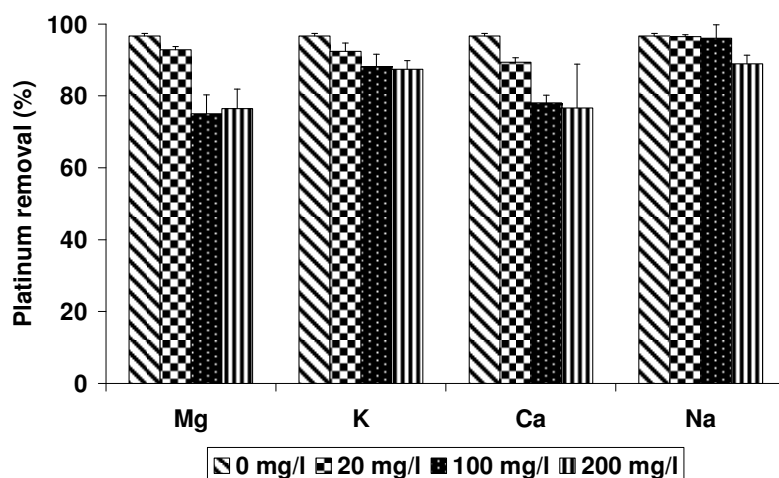


Figure 8.2 The effect of different concentrations of light metal ions on the efficiency of platinum sorption by immobilized *S. cerevisiae*. Error bars represent standard deviation from the mean ($n = 3$).

In Figure 8.3, the suppression of platinum sorption by cobalt, copper, nickel and iron is shown. At low concentration of base metal (20 mg/l), no major effects were noted. Copper reduced platinum uptake by 5 %, and nickel increased uptake by 2 %. At the highest concentration of base metal (200 mg/l), a trend with respect to suppression of platinum uptake was apparent. Nickel and iron decreased uptake by 25 – 30 %, copper reduced it by 40 %, and cobalt achieved the highest suppression, 60 %. The suppression trend was thus: cobalt > copper > nickel > iron.

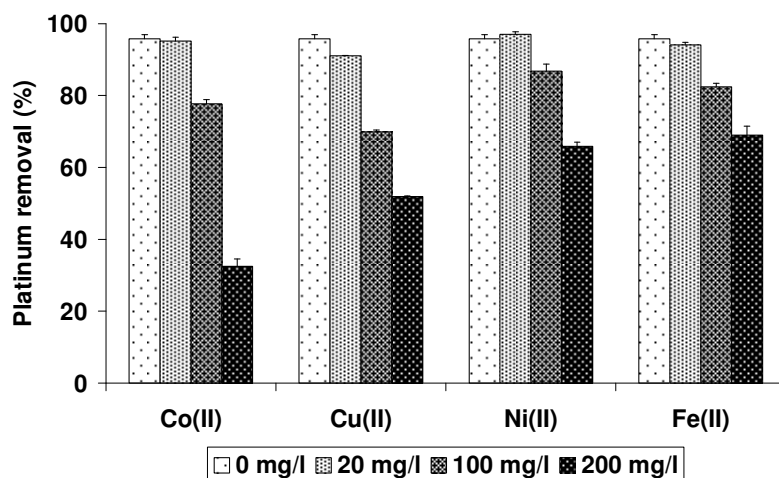


Figure 8.3 The effect of varying concentrations of base metal ions on the efficiency of platinum sorption by immobilized *S. cerevisiae*. Error bars represent the standard deviation from the mean ($n = 3$).

Competing precious metal anions exerted a profound effect on the sorption of platinum by the sorbent (Figure 8.4). Even at low concentration (20 mg/l), where the platinum concentration was higher (50 mg/l), uptake was reduced by > 30 % by all three metals. At the higher concentrations

(100 and 200 mg/l), the suppression trend became apparent. Rhodium reduced uptake by 35 and 40 %, gold decreased platinum uptake by 45 and 55 %, and palladium reduced platinum removal by 65 and 75 %. Hence, the suppression trend followed: palladium > gold > rhodium.

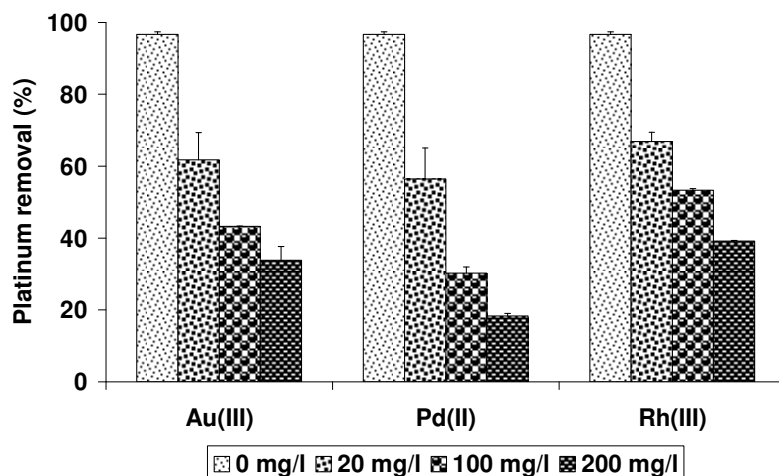


Figure 8.4 The effect of different concentrations of precious metal anions on the efficiency of platinum sorption by immobilized *S. cerevisiae*. Error bars represent standard deviation from the mean ($n = 3$).

8.2.3 Discussion

It was immediately obvious that the ligands (sulphate, chloride and nitrate) carry negative charge, and thus competed directly with the platinum chloride anions for sorption sites. In general when dealing with precious metal sorption, chloride is thought to be of most importance as an inhibitor of biosorption. This is mostly due to the fact that industrial wastewater containing a precious metal is most likely to be extremely high in chloride content due to the extraction and refining procedures. For example, Godlewska-Żyłkiewicz (2003) found that at low pH (1.6 – 1.8) the presence of a large excess of chloride ions resulted in strong competition between the anions of the acid (chloride) and the metal species, thus restricting the biosorption of platinum by *Chlorella vulgaris*. A similar result was reported by Uheida *et al.*, (2006), who reported that chloride exhibited a competitive influence on the sorption of platinum by iron oxide particles (Fe_3O_4).

In a more fundamental study, Sanyahumbi *et al.* (2005) investigated the effect of sulphate, chloride and nitrate on the biosorption capacity of *Desulfovibrio desulfuricans* for platinum and palladium. Nitrate ions, in the form of NaNO_3 , $\text{Ca}(\text{NO}_3)_2$ and NH_4NO_3 were used. They found that NaNO_3 and $\text{Ca}(\text{NO}_3)_2$ had a negligible effect on uptake, while the ammonium-containing compound reduced platinum uptake by approximately 65 %. This they attributed to the amine group rather than to the

nitrate moiety. Chloride ions, in the form of NaCl, were found to completely abolish platinum uptake at 0.2 M, while a 0.1 M concentration reduced the palladium uptake by 50 %. Sulphate, as Na₂SO₄, stimulated palladium uptake, but at 0.1 M, decreased platinum removal by 80 %, and completely abolished it at 0.5 M. These results corroborate the trend found in the present study with regard to platinum sorption (Figure 8.1); sulphate had the highest antagonistic effect, followed by chloride, and lastly nitrate.

The light metals investigated all carry positive charge, ensuring that they are unable to compete with platinum for similar binding sites. In fact, the overall positive charge of the sorbent surface should repel all positively charged ions. Yet, they were still capable of reducing the uptake efficiency of platinum by the sorbent to a small degree in the order: magnesium \approx calcium > potassium > sodium (Figure 8.2). Sodium and potassium have shown similarly low impact on sorption of base metals such as lead and copper at concentrations up to 50 mg/l (Dahiya *et al.*, 2008). At a higher concentration (500 mg/l) the authors found that sodium reduced lead and copper uptake by crab shell biomass by 20 % and potassium by only 10 %. Calcium and magnesium decreased the uptake of lead and copper by 20 – 30 % (Dahiya *et al.*, 2008). Lopez *et al.* (2004) evaluated the effects of calcium and magnesium on gold uptake by hop biomass. It was found that at pH 2, calcium only decreased gold uptake by 10 %, whereas magnesium increased gold sorption by 5 – 10 %. Parsons *et al.* (2003) studied calcium, magnesium and sodium and found that calcium had the greatest effect on the binding of platinum to alfalfa biomass (pH 2). In general, it has been observed that the light metals provide little competition for binding sites (even with similarly charged base metals), and will seldom reduce the heavy metal sorption capacity of the sorbent (Tobin *et al.*, 1993).

The base metals investigated (copper, iron, nickel and cobalt) are often associated with the PGMs in the Earth's crust, and as such persist as contaminant metals throughout the PGM refining process. Cobalt showed the highest inhibition of platinum sorption efficiency (60 % at 200 mg cobalt/l), followed by copper, nickel and then iron (Figure 8.3). With regard to base metal interference with base metal biosorption, it is no surprise that interactions occur; they may be direct competition for binding sites (e.g. Kaewsarn *et al.* (2001) found that silver, manganese, iron, zinc, cobalt, nickel, cadmium and lead all inhibited copper uptake by marine algae by at the least 10 % (silver) and at the most 90 % (lead) (initial copper concentration = 2 mM, inhibitor metals = 4 mM)). The differences in the degree of inhibition of uptake of one base metal due to the presence of another

have been linked to a number of characteristics specific to a particular metal, such as ionic radius (El-Naas *et al.*, 2006), electronegativity (Al-Rub *et al.*, 2006), and far more complex characteristics such as the metal hardness/softness as categorized by Pearson (1968), who crystallized the theory of Hard and Soft Acids and Bases (HSAB) discussed in Chapter 3. The implication within the context of metal biosorption is that metals present in aqueous solution that are similarly classified, e.g. both soft or both hard, will exhibit similar binding site preferences. Tsezos *et al.* (1996) tested this theory, and in the case of precious metals (soft/borderline acids), they showed that the presence of a hard acid (yttrium) had no effect on the biosorption of a soft acid (silver). The presence of a borderline/hard acid (nickel) also had no effect on silver (soft acid) adsorption. However, when testing the effects of a second soft acid (gold) on the biosorption of a target soft acid (palladium) there was a significantly negative effect on the sorption of palladium. Both metal ions are classified as soft acids and have similar preferences for biomass binding site ligands.

All four of these base metals (copper, iron, nickel and cobalt) are classified as borderline acids (Section 2.4.1), but iron and copper tend more towards soft characteristics, whereas nickel and cobalt tend towards hard characteristics. Platinum is a soft acid, which may explain the strong influence of the copper ions on the sorption of platinum. Iron did not exert the same effect, and cobalt decreased platinum uptake the most. It is therefore necessary to consider the hard/soft character of the chloro-platinum anion rather than the platinum(IV) cation alone in order to determine a reason for the cobalt effect based on the HSAB theory. However, this still does not satisfactorily explain the reduction in platinum sorption, as no base metal sorption was observed. The decrease must, therefore, be due to interactions between the positively charged base metal ions and the platinum anions, resulting in complexes with reduced binding affinity for the sorbent, similar to the much lower influence of the light metals.

The presence of precious metal chloro-complexes other than platinum in solution had a significant impact on the sorption of platinum from solution. This indicated that the sorption mechanism was non-specific, and governed by electrostatic interactions at low pH. This is supported by Chassary *et al.* (2005b), and confirmed by the strong competition effect of chloride and sulphate anions on platinum sorption. A minor trend regarding the reduction of platinum sorption by the sorbent occurred, with palladium exhibiting the highest influence, followed by gold, and finally rhodium (Figure 8.4). The competitive effects between platinum and palladium have also been investigated for sorption onto modified chitosan (Chassary *et al.*, 2005b). The authors stated that platinum and

palladium will compete for the same binding sites regardless of the sorbent type, but that platinum sorption is greatly decreased in the presence of excess palladium. The palladium sorption is also faster and more efficient than that of platinum. Chassary *et al.* (2005b) attributed these observations to differences in metal affinity for the sorbent, and to the metal speciation (which is dependent on pH, metal concentration and chloride concentration). In particular, platinum speciation may be affected by the excess palladium *via* the faster formation of chloro-palladate anions, which would reduce the availability of chloride ions for the formation of high affinity chloro-platinate anions. Far less is known about the competition effects regarding gold and rhodium, but it may be assumed that a similar argument would hold.

The reactivity trends of the PGMs, as described by Lee (1991), increase from ruthenium to rhodium to palladium, and from osmium to iridium to platinum, with gold the most reactive. These trends confirm the apparent affinity series exhibited in the results obtained. A further possible explanation of the affinity trend is the shape of the metal chloro-complexes, where the most compact shape would ease the degree of sorption by allowing a higher number of anions to bind than would a larger shape. The chloro-palladate anion and the chloro-aurate anion are both compact, square planar molecules, whereas the chloro-platinate and chloro-rhodate anions are larger octahedral structures, thus allowing fewer ions to bind *via* steric hindrance (Lee, 1991).

8.3 SUMMARY

The anionic ligands investigated (chloride, sulphate and nitrate) exerted a direct and antagonistic effect on the sorption of platinum by the sorbent. This effect was due to direct competition for similarly charged binding sites. The degree of platinum sorption reduction occurred in the order sulphate > chloride > nitrate.

The light metals exhibited only a small ability to reduce platinum sorption. The highest reduction (40 %) was observed at a magnesium concentration four times that of the platinum. The light metals did not compete directly for sorption sites. The influence was possibly due to complex formation between the chloroplatinate anion and the light metal cations, with an ensuing decrease in binding affinity.

The presence of base metals decreased platinum uptake to varying degrees. As no base metal sorption was observed, it is highly plausible that an effect similar to, but stronger than, that exerted by the light metals was responsible for the platinum sorption reduction.

The presence of precious metal co-ions in solution was profound, even at low concentrations. This negative impact on platinum sorption was primarily due to the non-specific nature of the metal sorption, where each ion has the same opportunity to sorb, independent of the type of ion. Secondary to this is the effect of shape, which results in the smaller ions binding more closely, and thus allowing a greater number of ions to bind. The shape order, from smallest to largest, is palladium \approx gold < platinum \approx rhodium.

This evidence of non-specific binding driven primarily by electrostatic attraction contradicts previously reported data from this study implicating chemical sorption mechanisms. This may be a result of different experiments targeting different phases or stages of the sorption process, thus highlighting only the dominant mechanism at that stage. If this is the case, then it can be argued that a combination of electrostatic and chemical sorption mechanisms occur, if not simultaneously, then in a very tight sequential order.

8.4 CONCLUSIONS

- The presence of anionic ligands, especially chloride and sulphate, had an antagonistic effect on the sorption of platinum by competing directly with the platinum anions for similar binding sites.
- The light metals exerted a low impact on platinum sorption, possibly due to the formation of mildly lower-affinity complexes.
- In the presence of excess base metal (in particular, cobalt and copper), platinum sorption significantly decreased. This may also be due to the formation of lower-affinity complexes between the base metal cations and the platinum anions. No evidence of base metal sorption was observed.
- The sorption of platinum in the presence of other precious metals was profoundly affected. This can be explained in a number of ways:
 - Electrostatic attraction *via* non-specific binding.

- Reactivity, where one precious metal forms an extractable species faster than, and at the expense of, another.
- Molecular shape and size.

CHAPTER 9

Sorption of platinum from PMR wastewater

9.1 INTRODUCTION

The ultimate outcome of any biosorption research is the successful application of the knowledge gained from studying a sorption system under laboratory conditions to an industrial problem, in this case the recovery of a valuable resource (platinum) that would otherwise be lost. The wastewater to under investigation originated from the solvent extraction separation of platinum from other PGMs in the matte concentrate received from the smelting operations (see Figure 2.1 and Figure 2.2). The wastewater is low in contaminant metals, but high in inorganic ion content (Appendix B). In particular, the high concentration of chloride ions is cause for concern with regard to negative impacts on platinum sorption, as it has already been shown (Figure 8.1) that chloride, sulphate and nitrate ions will limit the uptake of platinum by the sorbent. The presence of similarly-charged PGMs would also interfere with the selective recovery of platinum, but analysis of the wastewater showed that these metals were present at trace concentrations only, and as such were not expected to play a significant role in the suppression of platinum sorption.

9.2 BATCH SORPTION OF PLATINUM FROM WASTEWATER

In order for a wastewater treatment process to be sufficiently low-cost, pretreatment of the wastewater must be kept to a minimum; the treatment process must, as far as possible, treat a wastewater in the state in which it exists as it exits the primary process. If this premise is to be adhered to in this case there is little need for optimization, as the only readily variable parameter is the dosage of sorbent necessary for maximal platinum sorption.

9.2.1 Materials and Methods

Aqueous wastewater from the Anglo Platinum precious metals refinery (PMR), originating from the solvent extraction separation of platinum from the matte concentrate was used in all experiments in which wastewater was required. A simple comparison was performed in order to gauge the difference in platinum sorption from the wastewater as opposed to the aqueous solutions used thus far. The synthetic solution was made up to a similar platinum concentration to the wastewater (approximately 18 mg/l) by dilution of a 1000 mg/l atomic absorption standard solution (EC Labs,

South Africa) with deionized water. A sorbent dose of 1 g/l was added to flasks containing 50 ml of either wastewater or synthetic solution. These were agitated on an orbital bench top shaker at 170 rpm for 24 hours at room temperature, after which a sample was removed for metal analysis. In all experiments, sorbent-free controls were analyzed alongside the experimental flasks. All samples were then centrifuged (Labofuge, Heraus, Germany) at 2000 g for five minutes to separate particulate matter. The residual platinum concentration in solution was measured by atomic absorption spectrophotometry (GBC 909AA, GBC Instruments, Australia) as described previously. A second experiment determined the effect of increasing the sorbent dosage on the uptake of platinum from the wastewater. This experiment was run in the same way as the previous one, except that increasing concentrations of sorbent (1.0 – 20.0 g/l) were added to flasks containing 50 ml of wastewater. All experiments were conducted in triplicate and the arithmetic means are reported. Error bars indicate the standard deviation from the calculated means, and in some cases are not visible on the graphs.

9.2.2 Results

Figure 9.1 compares the removal efficiency and uptake capacity of the sorbent in wastewater to that in synthetic solution. In both cases the performance of the sorbent was better with the synthetic solution than with the wastewater. At an initial concentration of approximately 18 mg/l, almost 100 % removal of platinum was achieved in the synthetic solution compared to a little over 20 % in the wastewater. Similarly, an equilibrium specific platinum uptake of 19 mg/g was calculated for the synthetic solution, with approximately one fifth of that (4 mg/g) calculated for the wastewater.

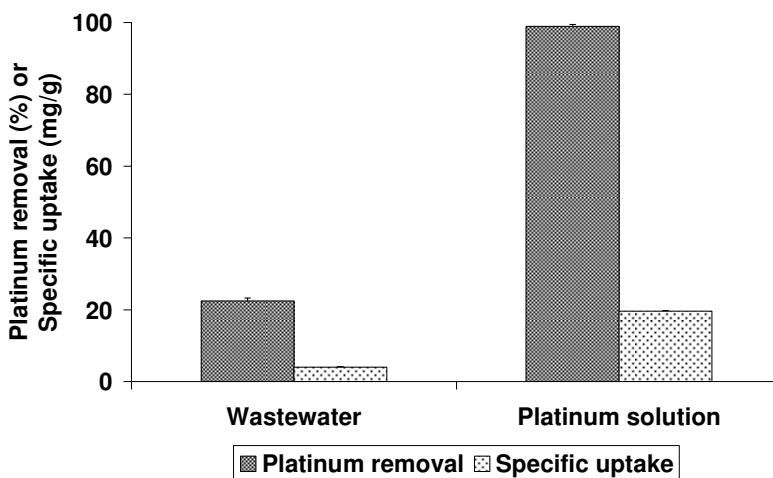


Figure 9.1 A comparison of the platinum removal efficiency and specific uptake capacity of the sorbent in synthetic solution and in wastewater. Error bars represent standard deviation from the mean ($n = 3$).

The sorbent dosage was increased in an attempt to overcome the suppression of platinum sorption by the excess of contaminant ions in the wastewater. Figure 9.2 shows the removal efficiency and specific uptake capacity of the sorbent at increasing sorbent concentration. A five-fold increase in the sorbent dose resulted in a doubling of the removal efficiency (from 22 % at 1 g/l to 39 % at 5 g/l). This did not improve significantly as the sorbent dose was further increased to 20 g/l (45 % removal efficiency). The specific uptake capacity (as expected) decreased as the sorbent concentration increased.

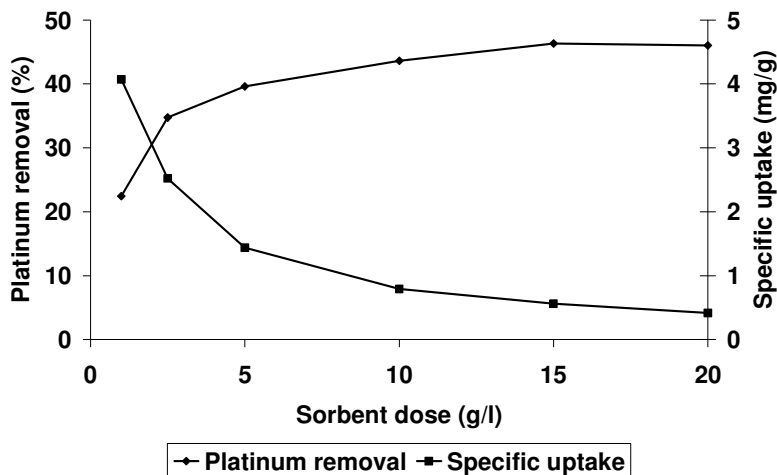


Figure 9.2 The effect of increased sorbent dose on the removal efficiency and specific uptake capacity of the sorbent in wastewater. Error bars represent the standard deviation from the mean (SD < 1%) and are all too small to be visible ($n = 3$).

9.3 COLUMN SORPTION OF PLATINUM FROM WASTEWATER

The batch experiments showed that increasing the sorbent dose in a mixed incubation system such as a flask test did not significantly improve the uptake efficiency of the system. In the column experiments, it was suggested that multiple passes of the same wastewater sample through fresh column material would result in removal of any competing anions in the initial columns, with subsequent platinum sorption in later columns.

9.3.1 Materials and Methods

The 5 cm columns were set up and run as described in Chapter 7. Five litres of wastewater was passed through the column at a flow rate of 0.8 ml/min giving an HRT of 30 minutes. The column effluent was collected and passed through a column of fresh sorbent. This process was repeated

until the original wastewater had been passed through three columns of sorbent, each of which was fresh, mimicking a ‘columns in series’ setup. Samples were removed at timed intervals, from which the platinum and chloride concentrations remaining in solution were determined *via* atomic absorption spectroscopy and spectroquant (see Appendix B) analysis, respectively.

9.3.2 Results

The breakthrough curves plotted from the data obtained from the three sequential treatment columns are shown in Figure 9.3. The curves do not resemble those of an ideal breakthrough curve (Figure 7.1) or those generated from the treatment of a synthetic platinum solution, as shown in Chapter 7 (Figure 7.5). Throughout the first treatment step (first pass), the normalized concentration (C_i (effluent concentration)/ C_o (influent concentration)) did not fall below 0.75. More importantly, it remained high even in the early stages of the treatment, when the sorbent material was most pristine. This changed in the second pass, when the normalized concentration dropped below 0.8 in the initial period (approximately 0.2 at 20 minutes), but it rapidly increased to over 0.8 by 400 minutes. This trend changed in the third pass. Again the normalized concentration was low in the initial period (approximately 0.2 at 20 minutes), but it did not reach as high as 0.8.

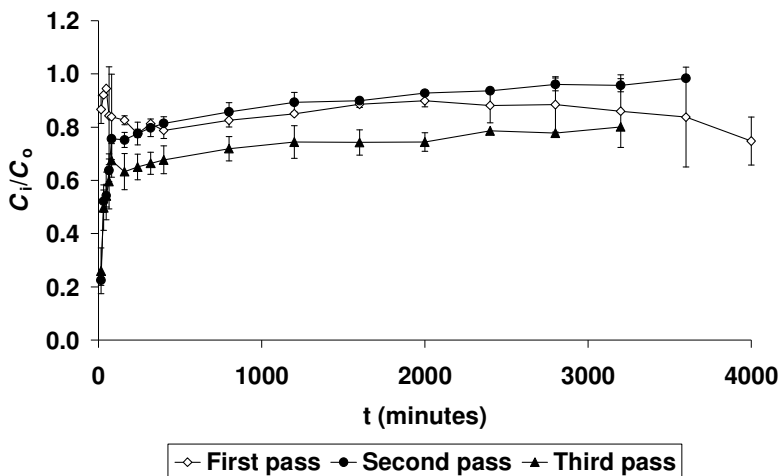


Figure 9.3 Breakthrough curves describing the normalized concentration of the column effluent over time for each successive pass of the wastewater through a fresh column. Error bars represent standard deviation from the mean ($n = 2$), and are presented in order to indicate variation between duplicates.

Table 9.1 compares the efficiency of each column. Each pass was presented with 500 ml less than the previous one due to sampling. The first pass removed approximately 16 % of the platinum in the wastewater, slightly less than was achieved in the batch study. The second pass of the wastewater through a fresh column was not as successful, only removing 4 % of the remaining

platinum in solution after the first pass. This increased to 22 % (of the platinum remaining after the second pass) in the third pass. A similar trend was reflected in the specific uptake of the columns, where the third column removed the most platinum per gram of sorbent, followed by the first, and finally the second.

Table 9.1 Summary of the efficiency of each column with respect to total platinum removal, removal efficiency and specific uptake (\pm SD).

	Wastewater volume (l)	Total platinum sent to column (mg)	Total platinum sorbed by column (mg)	Platinum removal (%)	Specific uptake (mg/g)
First pass	5.0	90.62	14.77 \pm 3.58	16.29 \pm 3.95	2.95 \pm 0.72
Second pass	4.5	75.85	3.05 \pm 0.82	4.03 \pm 1.08	0.61 \pm 0.16
Third pass	4.0	72.80	18.95 \pm 1.89	21.99 \pm 2.6	3.78 \pm 0.38

As the chloride concentration within the wastewater represented the highest contaminating anion concentration, the concentration was monitored throughout each passage of the wastewater through each column. However, as the concentration was so high that it was necessary to dilute each sample significantly in order to obtain values within the working limits of the test method, the concentrations should not be considered as absolute, rather as a means of following trends in removal (Figure 9.4). In each pass, the chloride concentration decreased in the early stages of treatment, indicating that the column did indeed sorb chloride ions. The column rapidly became saturated with sorbate (platinum and other interferents). Within 80 minutes, the chloride concentration of the column effluent from the first pass had reached an average of 24 g/l. This fluctuated over the course of the treatment. The second pass did not significantly decrease the chloride concentration (it had a similarly negligible effect on platinum removal). The effluent concentration rapidly reached an average equivalent to that of the first pass. The third passage was most successful, reducing the average chloride concentration of the wastewater to 21 g/l but, as the error bars on Figure 9.4 show, the uncertainty of measurement of the method makes these data statistically unreliable in spite of the observed decrease in chloride. Nonetheless, chloride was seen to decrease by 6000 mg/l. The use of further columns would inevitably continue to decrease both the platinum and chloride concentrations, but a decision must be made regarding how many columns would be economically feasible. In this study, the column number was held at three.

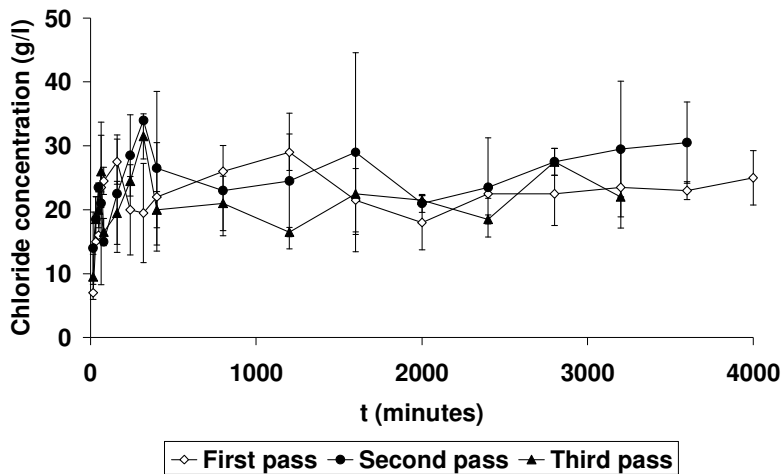


Figure 9.4 Chloride concentration of the column effluent after each pass of the wastewater through three fresh columns. Error bars represent standard deviation from the mean ($n = 2$), and are presented to indicate the variation between the duplicate columns.

9.4 DISCUSSION

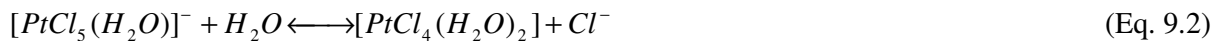
It was apparent, and expected, that the chemical conditions within the wastewater differ vastly from those within the synthetic solution. It was thus not surprising that conclusions drawn from experimentation with a sorbent in a synthetic metal solution could not be easily applied to a wastewater. At equivalent concentrations, the sorbent removed almost 100 % of the platinum in a synthetic solution while only removing 20 % of the platinum from the wastewater (Figure 9.1). This was due, in large part, to the high concentration of inorganic anions such as chloride and nitrate present in the wastewater. As has been previously shown (Figure 8.1), these anions would compete with the platinum chloride anions for similarly-charged binding sites on the sorbent surface.

It had been expected that co-sorption of platinum with other inorganic ions would occur if sufficient sorbent were added. However, an increase in the concentration of sorbent would also lead to increased wastage of sorbent surface area, as more would be sacrificed for the sorption of inorganic anions. It may be that the competitor ions are present in such excess that other than a doubling of the removal efficiency at 1 g/l by a five-fold increase in sorbent dose, no significant improvement in removal efficiency was attained by a twenty-fold increase in the sorbent dose (Figure 9.2). A further and more plausible explanation for the insignificant increase in platinum uptake beyond a sorbent dose of 5 g/l may be that the speciation of the platinum within the wastewater is such that only 40 % is in a form easily sorbed by the sorbent material.

The difference in the platinum sorption capacity of the sorbent for platinum from a synthetic solution compared to that from a wastewater is due to a combination of factors, including platinum and other metal speciation (Figure 9.1), the inorganic components of the wastewater, the organic components of the wastewater, the pH of the wastewater and in some cases the age of the wastewater. The information contained in Appendix B highlights some of the major inorganic components of the wastewater. Of these, it has already been shown (Figure 8.1) that sulphate, nitrate and chloride ions negatively impact on the sorption of platinum by the yeast sorbent by competing directly with the platinum chloride anions for positively charged binding sites.

The high concentration of ammonium ions may also impact on the effective sorption of platinum from the wastewater by affecting the speciation of the platinum anions. It is possible that these ammonium ions have formed complexes with the chloroplatinate ions, forming species with a lowered affinity for the sorbent.

When considering the effect of platinum speciation on its effective extraction from wastewater, factors such as the acidity, chloride and PGM concentration, temperature and age of the wastewater usually determine the extent of hydrolysis and/or aquation (Kramer and Koch, 2006). This hydrolysis will result in the presence of several species in solution, some of which may be much less readily extractable than others. For example, the platinum(IV) species PtCl_6^{2-} undergoes partial aquation in aqueous solution, resulting in monoqua and diaqua species (Equations 9.1 and 9.2)



Hydrolysis will occur with an increase in pH (Equation 9.3).



However, at the low pH of the wastewater, this hydrolysis product is not thought to be present (Kramer and Koch, 2006). Kramer and Koch (2006) studied the speciation and preferential extraction of platinum(IV) halide complexes by a modified silica-based anion exchanger, and

demonstrated that the PtCl_6^{2-} species was extracted preferentially over the aquated species. In the current study, it may be suggested that only 40 % of the total platinum in the wastewater is in a similarly easily extractable form. However, given the high concentration of chloride in the wastewater (25.7 g/l), the common ion effect suggests that equations 9.1 and 9.2 will be driven strongly to the left, resulting in low concentrations of aquated species.

After passing through three columns of fresh sorbent, a total of 40 % of the total platinum present in the wastewater had been recovered onto the sorbent. This was similar to the removal efficiency obtained by the increased sorbent dose in the batch studies (Figure 9.2). This again indicates that only 40 % of the platinum in the wastewater is in a form that is readily sorbed. This is difficult to confirm, as the speciation chemistry of platinum within the wastewater is unknown and the other components of the wastewater were not disclosed.

Three passes, representing a series of three columns, were chosen to be the maximum number of columns to use as more would further increase operational costs and increase sorbent wastage. The low recovery of platinum onto the sorbent after three columns-worth of treatment suggests that pretreatment of the wastewater will be necessary before successful sorption can be achieved.

Other studies have produced better results upon transfer of information from a synthetic solution sorption to one from wastewater. Bahadir *et al.* (2007) removed up to 95 % of lead contained in a storage battery industry wastewater (approximately 3 mgPb/l) using *Rhizopus arrhizus*. Deng *et al.* (2007) were also able to remove lead, copper, chromium and cadmium from an industrial wastewater to levels below the Chinese wastewater discharge standard using *Cladophora fascicularis*. Some have required pretreatment of the wastewater before successful metal recovery was possible. For example, the removal of copper from the spent- lees from a whiskey distilling process by spent grains was enhanced by adjustment of the wastewater pH from 3.8 to 4.5 (Lu and Gibb, 2007). When compared to results from a synthetic wastewater solution, the specific uptake results from the adjusted wastewater were comparable to the solution (2.68 mg/g for unadjusted, 6.59 mg/g for adjusted and 8.48 mg/g for synthetic solution). The decreased uptake efficiency seen in the unadjusted wastewater was attributed to the presence of organic materials such as short-chain fatty acids that may have the capacity to either chelate metal ions or occupy possible copper binding sites. Sankararamkrishnan *et al.* (2007) attempted to minimize the interference of cyanide in the sorption of cadmium from electroplating wastewater by chemically modified chitosan by dilution

and by increasing the sorbent dose. The authors found that at a ten-fold dilution of the wastewater, 76 % removal of cadmium could be achieved at a high sorbent dose, compared to no removal from undiluted wastewater. In the current case, dilution was not considered as an option as it would only serve to increase the amount of wastewater to be treated, thus increasing the cost. It must be noted however, that these cases all address sorption of metals which do not share the PGMs' reputation for being difficult to process chemically.

Wang *et al.* (2003) investigated *Pseudomonas putida* 5-x biomass for the recovery of nickel from electroplating wastewaters. They found that the copper present in the wastewater significantly impeded the selective recovery of nickel, and suggested a two-stage process, in which the sorbent would first be optimized for the removal of copper, allowing for the complete and selective recovery of nickel in the second stage. This type of setup may be useful in improving the efficiency of the current system. An initial stage, in which contaminant anions such as chloride and sulphate were removed, followed by a second stage in which platinum could be recovered may be a feasible alternative to the current process. For example, Pierce *et al.* (2007) have reported some success in the removal of chloride from wastewaters using NO₂ sparging, a process which removes chloride by stripping it from solution in a gaseous form and converting the solution to a nitrate-base one.

9.5 SUMMARY

The platinum removal efficiency of the yeast sorbent from wastewater was 20 %, compared to almost 100 % from a synthetic solution. An increase in sorbent dose (up to 20 g/l) did not improve this efficiency beyond 40 % (at 5 g/l). This may be attributed to the speciation of platinum within the wastewater, as up to 60 % of the platinum in solution may be present in a species that is not readily extracted by the sorbent.

The treatment of 5 l of wastewater by three consecutive columns of fresh sorbent (5 g of sorbent per column) also resulted in a total removal efficiency of approximately 40 %. The concentration of chloride in the column effluent was monitored, as chloride was the contaminant present in the highest concentration. Some chloride was removed by the columns but, especially in the second treatment, chloride did not seem to be the major hindrance to platinum sorption. It may be that the combination of contaminating ions and a large proportion of sparingly extractable platinum species are the cause of the limited sorption of platinum from the refinery wastewater.

The interference of the chloride ions again suggests an electrostatic sorption mechanism. As argued in Chapter 8, the conflicting data produced from various experiments may be used to suggest a combination of mechanisms, of which the electrostatic attraction comprises the initial sorption, followed by the formation of more permanent chemical bonding between the sorbent and the metal ions.

9.6 CONCLUSIONS

- There are two major factors influencing the sorption of platinum from the refinery wastewater.
 - The contaminant ions, and possibly even organic compounds, occupying binding sites.
 - The complex speciation chemistry of the wastewater: the batch and column results suggested that only approximately 40 % of the available platinum is present in the wastewater in a form that can be extracted *via* sorption onto the immobilized yeast surface.
- The low removal efficiency indicated that the sorption process under investigation was not technically feasible in its current form. It may be that the wastewater requires a pretreatment step in order to convert the platinum to a more extractable species, but this must be a low-cost and simple treatment in order to maintain the overall financial attraction of the sorption process.

CHAPTER 10

Conclusions

10.1 CONCLUSIONS

The refining of PGMs results in wastewater streams that are difficult to treat to a point where they can be disposed of to the surrounding environment. The wastewaters also contain appreciable amounts of valuable metal. The loss of metal value to wastewaters represents a step in the metal processing chain that requires investigation in order to minimize these losses and thus improve the metal production efficiency. The aim of this research was to develop a cheap and effective technique, such as biosorption, capable of recovering precious metals from PMR wastewaters. Biosorption can be defined as the ability of certain types of biomass to attract and retain charged metal ions *via* their interactions with cell surface functionalities. As such, a biosorption process should be capable of recovering precious metals from PMR wastewaters. Two major advantages of biosorption are that the biomass used need not be living, and that often cheap and readily available waste biomass can be adapted to this purpose. *Saccharomyces cerevisiae* biomass is obtainable from the brewing and baking industries, and may also be used to some extent in the pharmaceutical industry. The metabolism of *S. cerevisiae* is also very well understood, making it both low-cost and simple to cultivate if necessary. The guiding hypothesis for this research states that:

“A biosorbent comprising suitably immobilized baker’s yeast (*Saccharomyces cerevisiae*) is capable of quantitative recovery of precious metal ions from a precious metal refinery (PMR) wastewater *via* the process of biosorption.”

Thus, the overall aim of the research was to develop a biosorption process using *S. cerevisiae* biomass that was capable of successfully recovering a precious metal from a waste stream generated at the Anglo Platinum precious metals refinery. In order to achieve this aim, a number of objectives were laid out.

10.1.1 Objective 1: Production of an *S. cerevisiae*-based sorbent suitable for use in the recovery of precious metals from PMR wastewaters.

A review of biomass immobilization techniques in published literature was performed (Section 2.5.1 and Section 4.2.1), and four techniques were chosen based on their theoretical suitability (such as estimated chemical and mechanical stability). These were (A) entrapment of live *S. cerevisiae* within carboxymethyl cellulose (CMC) beads, (B) surface immobilization of dried *S. cerevisiae* to silica gel particles, (C) modification of wet (non-viable) *S. cerevisiae* with polyethyleneimine and crosslinking with glutaraldehyde and (D) encapsulation of dried *S. cerevisiae* within a calcium alginate matrix (Table 4.2).

Upon production, the CMC beads showed very low mechanical stability, disintegrating under even very mild agitation. Mechanical strength is vital for a successful sorbent in light of the possible use of a fixed-bed column sorption process. It was concluded that the CMC beads were unsuitable as sorbent material. The calcium alginate beads showed good mechanical stability but low chemical stability, shrinking by up to 20 % under conditions of low pH. Along with the reduction in size, all metal uptake capacity was abolished at low pH. As the PMR wastewater environment is extremely acidic, it was concluded that the calcium alginate beads were unsuitable as sorbents of metals in these conditions.

The PEIGA and silica granules showed excellent mechanical and chemical stability in the preliminary investigation, but the silica granules exhibited a lower affinity for precious metals than that exhibited by the PEIGA granules. Also, more extensive investigation showed that the immobilization of the *S. cerevisiae* cells to the silica surface was reversed by attrition during agitation and possibly also by the low pH conditions. This made the silica granules unsuitable for further use, as the sloughing of the cells into the surrounding solution would complicate downstream solid/liquid separation and thereby decrease the overall efficiency of the sorption process.

Thus, by a process of elimination, the PEIGA immobilization was found to be the most suitable technique for the production of an *S. cerevisiae* sorbent. This sorbent exhibited a high affinity for PGMs and the highest metal uptake capacity, due to the high concentration of amine groups introduced to the sorbent surface *via* the PEI modification, which is known for its metal chelating properties and is a potent PGM scrubber (Chassary *et al.*, 2005a). The pK_a of PEI (6.5 – 8.8) shows

that at low pH, the amines will be protonated and carry a positive charge. The GA functions as a stabilizer of both the biomass/PEI mixture (Ghoul *et al.*, 2003) and of the sorbent as a whole under acidic conditions.

The PEIGA sorbent was capable of sorption of the negatively charged platinum chloride anions in a number of ways. The positive charge carried by the amine functionalities at low pH exerts an electrostatic attraction over the negatively charged platinum ions. The nitrogen atoms of the amine groups are also capable of forming chelates with the platinum ions. Other groups may be involved to a lesser extent, but the results of the potentiometric titration (Figure 5.7) indicated that the most likely functional groups to be involved in sorption were the amine groups.

10.1.2 Objective 2: Determination of the precious metal for which the sorbent has the highest affinity.

Based on current world demand and market price, three precious metals were considered for recovery by the sorbent. These were gold, rhodium and platinum. The PEIGA sorbent exhibited the highest affinity for platinum out of the three metals (Figure 4.9 and Table 4.3). The maximum theoretical specific uptake values (calculated *via* the Langmuir isotherm model) indicated that rhodium would be bound in the highest concentration, followed by platinum and finally gold (refer to Table 4.3 – compared in $\mu\text{mol/g}$).

In making the decision regarding the choice of metal to be targeted, the affinity of the sorbent for a particular metal was of paramount importance, especially with respect to process design, since the metal/sorbent affinity would impact on the contact time required for maximal metal uptake (the higher the affinity, the more rapid the sorption). This higher affinity for platinum may be due to the different charge densities of the metal chlorocomplexes. Al-Bazi and Chow (1984) stated that the interaction between ion-exchanger and metal ion depends on the charge of the complex. Doubly charged complexes such as PdCl_4^{2-} , PtCl_4^{2-} , PtCl_6^{2-} , IrCl_6^{2-} , RuCl_6^{2-} and OsCl_6^{2-} are strongly sorbed, whereas triple-charged complexes such as IrCl_6^{3-} and RhCl_6^{3-} are less strongly bound, and singly charged complexes such as AuCl_4^- are more strongly sorbed than the doubly charged examples. With this in mind, it was decided that platinum would be targeted for recovery from PMR wastewaters using the PEIGA sorbent.

Initial investigation of the platinum/PEIGA system sorption system yielded a maximum specific uptake capacity (Q_{\max}) of between 120 and 150 mg/g (Table 4.3). This value was dependent on the size composition of the sorbent granules used (all were < 2 mm in diameter and smaller), with the smaller granules possessing a much higher surface area for sorption. In all subsequent experiments, attempts were made to maintain a constant size distribution by adding equal amounts of smaller granules (< 0.5 mm) and larger granules (0.5 - 2.0 mm). Experiments were also performed in triplicate in order to minimize possible errors generated by possibly inconsistent size distributions.

10.1.3 Objective 3: Optimization of the physical and chemical parameters affecting metal sorption in order to maximize metal recovery.

The sorption of metal ions onto a sorbent surface is affected by several factors related to both the surface properties of the sorbent and the physicochemical properties of the medium within which the sorption occurs, such as metal ion concentration, temperature, pH and sorbent concentration. An analysis of these factors and how they affect the sorption of platinum onto the PEIGA sorbent was undertaken in order to better optimize this sorption process (Chapter 5).

The uptake of platinum by the sorbent was rapid at all initial concentrations with up to 80 % of sorption occurring within the first 30 minutes and an apparent solid/liquid metal concentration equilibrium reached within 60 minutes. An increase in sorbent dose increased the uptake efficiency but decreased the specific uptake capacity. The sorbent dose required optimization in order to achieve maximal metal uptake while using minimal sorbent (to prevent sorbent wastage by providing excess sorption sites). For an initial platinum concentration of 50 mg/l a sorbent dose of 1 g/l was found to be optimal, and resulted in almost 100 % removal of the metal from solution (Figure 5.10).

Solution pH had a profound effect on the uptake capacity of the sorbent. At low pH (pH 1 and 2), uptake was much higher than at higher pH (pH 3 and 4). When this result (Figure 5.9) was considered in combination with the potentiometric titration data (Figure 5.7), it was apparent that this decrease was not due to changes in the sorbent surface ionization (which would remain protonated until a much higher pH was obtained) but was probably due to an increase in the aquation of the platinum chloride anion. This change in the metal speciation may be sufficient to decrease the concentration of readily extractable anions and cause the decrease in uptake at higher pH.

This initial information regarding the influence of pH was further investigated by modelling the isotherm data (Chapter 6). The Langmuir isotherm model best fitted the data, and showed (*via* calculated Q_{\max} values (Table 6.5)) that platinum uptake was maximal at low pH (pH 1), confirming the preliminary information.

The temperature of the metal-laden solution may influence a number of factors of importance in the sorption of metal ions. These include the interaction between the biosorbent and the metal ions, usually by influencing the stability of the metal ions in solution (Sağ and Kutsal, 2000), the stability of the metal-sorbent complex (Özer *et al.*, 2004), and also the sorbent surface itself, in terms of cell wall configuration and the ionization of the chemical moieties on the cell wall (Özer *et al.*, 2004). The sorption of platinum was favoured at temperatures greater than 20 °C, with a decrease in uptake occurring above 37 °C. Again, the Langmuir model was better suited to describing the data, and the parameters calculated from the isotherm model show that the Q_{\max} value increased up to 37 °C and decreased at higher temperature (Table 6.6). This is due to the increasing incompatibility of the sorbent surface with the metal ions due to possible changes in surface structure or ionization state.

From the information gathered, an optimized sorption reaction involving the sorption of platinum onto the PEIGA sorbent would be one where for an initial concentration of greater than 20 mg/l of platinum, a sorbent dose of 1 g/l would be used. The reaction would be performed at a low pH (pH 1) and at a temperature lower than 45 °C. This reaction should result in rapid platinum sorption, with a maximum uptake capacity of at least 150 – 170 mg/g.

10.1.4 Objective 4: Investigation of the mechanisms or processes governing metal sorption in this system.

Sağ and Kutsal (2000) stated that the mechanism controlling the sorption of metal ions can be one (or more) of three general types: physical sorption, chemical sorption or ion exchange. The information gathered regarding the sorption of platinum onto the PEIGA sorbent will be discussed here with reference to these general mechanisms.

Potentiometric titration of the sorbent (Figure 5.7) indicated the presence of two major functional groups on the surface capable of interaction with metal ions: hydroxyl and amine groups. At low pH though, the hydroxyl groups would be protonated and carry a neutral charge (Volesky, 2003), thus reducing their influence on metal sorption. The amine groups would also be protonated at low

pH, and carry a positive charge. There are two ways in which the amine groups could participate in metal sorption; (1) *via* electrostatic attraction of negatively charged metal ions, and (2) *via* chelation of soft acids (e.g. platinum) by the N atoms of the amine groups. This implies two processes by which the platinum anions could interact with the sorbent surface; (1) electrostatic interaction between the positively charged amine groups, and (2) chelation of the platinum atom with the nitrogen atom of the amine, where process 1 would occur almost instantaneously with process 2 occurring over a longer period of time. However, the second process cannot be confirmed as there is no evidence to either confirm or deny that the platinum chloride species will behave as a soft acid, enabling its interaction with the nitrogen atom of the amine. This information supplied an initial hypothesis regarding the mechanisms involved in the sorption of platinum onto the PEIGA surface.

The kinetics information gathered in Chapter 6 supports this theory by indicating that the reaction kinetics are pseudo-second order, i.e. limited by a chemical sorption mechanism. The involvement of the chemical mechanism is further indicated by information from the FTIR analysis in Chapter 5 and the calculated activation energy in Chapter 6. The FTIR analysis showed a shift of the NH bending peak and of the C=O and C=N peaks. The latter, in particular, points to chemical interactions between the sorbent surface and the platinum ions. The calculated activation energy (51.5 kJ/mol at 20 – 25 °C and 35 kJ/mol at higher temperatures) is higher than that attributed to physical sorption (≤ 20 kJ/mol (Sağ and Kutsal, 2000)), and outside the range of suggested for ion exchange (8 -16 kJ/mol (Al-Rub *et al.*, 2006)). This is thus further evidence of the involvement of a chemical sorption mechanism. Along with this, the inability to effectively desorb the platinum ions from the sorbent (Section 7.3.2) further cements the involvement of chemical sorption mechanisms.

There is also some evidence regarding the possible involvement of ion exchange in the sorption of platinum onto the PEIGA sorbent. The fit of the isotherm data to the Langmuir model has been accepted as an indication of ion exchange based on the model assumption that metal binding occurs within a monolayer only (Schneider *et al.*, 2001), although this has been challenged by some authors (Schiewer, 1999). And in this case, is again challenged by the SEM images obtained (Figure 5.2) that show the patchy sorption of platinum onto the sorbent surface (Barrera *et al.*, 2006), which would not have occurred if ion exchange (and homogenous monolayer sorption) were occurring.

Thus, a simple hypothesis can be provided for the mechanisms involved in the sorption of platinum onto the PEIGA sorbent. The platinum anions are initially attracted to the sorbent surface *via* electrostatic interactions (this would be extremely rapid). Subsequently, a chemical interaction would result in the formation of a metal/sorbent complex through which the platinum ion is bound (almost) irreversibly to the sorbent.

10.1.5 Objective 5: Comparison of the sorption process efficiency in a stirred batch system to that in a fixed-bed column system.

The vast majority of biosorption research in published literature seems to focus mainly on batch-type sorption analysis, with fewer authors publishing information regarding comparisons of the information obtained in batch investigations to that obtained in packed bed columns, the most popular reactor conformation used for scale-up investigations of biosorption.

The most important information to be gleaned from batch experiments and transferred to packed bed column design is the minimum contact time required for maximal sorption, the theoretical uptake capacity of the sorbent and the sorbent dose required to obtain that uptake capacity.

Columns consisting of 1 g of sorbent were prepared and contacted with a total of 125 mg of platinum (2.5 l of 50 mg/l concentration). The results in Table 7.3 show that at none of the flow rates used did the specific uptake reach that calculated in the batch studies. Had it done so, the 1 cm column should have been capable of complete removal of the platinum from solution. Further optimization is obviously required in order to achieve the theoretical maximum uptake capacity. In particular, the column aspect ratio should be adjusted in order to find the appropriate size/shape of the column. In this case, it is likely that changing the column from one with a relatively large diameter (2.5 cm) containing 1 g of sorbent to one with a smaller diameter containing the same amount of sorbent would improve the quality of the contact between the metal ions and the sorbent.

An increase in the height of the column from 1 cm to 5 cm increased the apparent uptake capacity of the sorbent as the change in the aspect ratio affected the actual plug flow compared to the idealized plug flow. This implies that a change in the height of the column would affect the contact time in more ways than could be measured here. Thus the measured uptake capacity increased with an increase in bed height, but the theoretical capacity remained constant. Two flow rates were used, but the results cannot be precisely compared, as the columns with the faster flow rate (1.3 ml/min)

experienced periodic blockages that resulted in the sorbate being in contact with the sorbent for longer periods than expected. The column data fitted well to both the Thomas and Yoon-Nelson models, but more closely matched the Yoon-Nelson, which was able to reflect the discrepancy in the specific capacity trend brought about by the column blockages experienced at a flow rate of 1.3 ml/min.

In general, the conversion of a batch sorption process to one taking place within a packed bed column is complex. The information obtained in batch investigations needs to be combined with column design optimizations with respect to column aspect ratio (in particular) and flow rate. The results obtained in this study are not exhaustive enough to draw firm conclusions regarding the suitability of the packed bed column conformation to the sorption of platinum onto the PEIGA sorbent.

10.1.6 Objective 6: Determination of the effect of wastewater composition on the sorption of the metal from wastewater.

The results of the inorganic analysis of the wastewater (Appendix B) indicated a high ionic concentration, the bulk of which was composed of chloride, sulphate, ammonium and sodium ions. There was generally a very low metal content, even of platinum with only approximately 18 mg per litre of wastewater. In Chapter 8, the effect of increasing concentrations of most of these ions on the sorption of platinum from a synthetic solution was determined. Of those tested and found to be present in high concentration in the wastewater, chloride and sulphate were of particular concern. Both of these were found to significantly inhibit platinum sorption (Figure 8.1), in all likelihood by successfully competing for similarly charged binding sites. Sodium ions, up to a concentration of 200 mg/l were shown to have only a very minor (if at all) inhibitory effect on platinum sorption (Figure 8.2). But at a concentration ten times higher, this interference may increase. The sodium ions will not compete with the platinum anions for binding sites, but may form complexes with the anions in the solution that may display a lowered ease of extractability.

Repeated treatment of a volume of wastewater may remove the inorganic contaminants and subsequently the platinum anions. However, in Chapter 9, a 5 l volume of wastewater was passed through three successive packed bed columns, each containing 5 g of sorbent. The chloride and platinum concentrations were monitored throughout the treatment. The chloride concentration showed an appreciable reduction, decreasing from 27.5 g/l to 21 g/l after the third column (Figure

9.4), but this still left an overall chloride concentration far in excess of the platinum concentration, thus not allowing for full recovery of the platinum.

It is likely that there may be a further explanation for the low recovery of platinum from the wastewater compared to that from a synthetic solution. Evidence suggesting this explanation comes from the batch studies performed with the wastewater and reported in Chapter 9. At a sorbent dose of 1 g/l, 20 % of the platinum in the wastewater was recovered, a five-fold increase in the sorbent dose resulted in a doubling of the platinum recovery to a little over 40 %. All subsequent increases in the sorbent dose, even up to 20 g/l showed little improvement on the 40 % recovery (Figure 9. 2). A similar 40 % was all that was recovered from the wastewater after contact with three columns of sorbent. This suggests the influence of metal speciation within the wastewater. Up to the point where the wastewater was used, the synthetic solutions were assumed to be homogenous in terms of platinum species, most of which was considered to be in the form PtCl_6^{2-} or PtCl_4^{2-} , with a small percentage of monoaquated species. These species are known to be more easily extracted than some other platinum species (Kramer and Koch, 2006). In the wastewater, the speciation chemistry of platinum was far more complex, and dependent on factors such as the age of the solution, the temperature of the solution, the concentration of platinum and chloride and the pH of the solution. All of these unknown effects may have combined to render up to 60 % of the platinum in the wastewater un-extractable by way of the formation of species with low affinity for the sorbent. Those effects could not be predicted and so must be assessed empirically for each wastewater to be treated, even though the biosorption principle has been demonstrated in Chapters 4 to 8.

10.2 FINAL REMARKS

The overall aim of the research was to develop a sorbent from suitably immobilized *Saccharomyces cerevisiae* that was capable of recovering a precious metal from an Anglo Platinum PMR wastewater. The PEIGA immobilization of *S. cerevisiae* proved to be the best sorbent produced, and exhibited a high affinity for platinum. A number of conclusions can be drawn from the results:

- The sorbent that was developed was capable of recovering platinum from aqueous solutions.
- The uptake capacity of the sorbent was comparable to, and in some cases higher than, other sorbents used for the recovery of precious metals from synthetic solutions (150 – 170 mg/g, *cf.* Table 2.2).

- The mechanism of sorption was most likely to be a combination of electrostatic attraction and metal ion chelation by the amine functional groups present in excess on the sorbent surface due to modification with polyethyleneimine.
- The sorption was not easily reversible, which may preclude the regeneration and reuse of the sorbent. It may be most effective to smelt the metal-laden sorbent, thereby transferring the recovered metal back into the refining cycle.
- The sorbent was not capable of efficient recovery of platinum from PMR wastewaters in the packed column conformation tested. The most likely reason for this was the complex speciation of the metal within the wastewater environment.

CHAPTER 11

Further Recommendations

Although the principle of PEIGA-yeast biosorption of platinum from acidic, aqueous solutions has been proven, the PEIGA sorbent was not capable of quantitative recovery of platinum from the PMR wastewater. This failure has been caused not by any fundamental inefficiency of the sorbent, but by the conditions prevailing within the wastewater. A combination of the complex inorganic content (present in very high concentrations) and the largely unknown speciation chemistry of the platinum ions limited the potential of the sorption process in terms of industrial application, despite proof that the process worked extremely well in a synthetic environment. Based on the conclusions drawn from this investigation, the following recommendations regarding application of the sorption process are offered.

- A lack of knowledge regarding the speciation of the platinum in the wastewater solution continues to hamper the optimization of a suitable sorption process for the recovery of precious metals from PMR wastewaters. It has been suggested that the elucidation of this speciation would involve enough work for a PhD research project (Plint, 2007 pers. comm.) But if this lack of knowledge continues to be a stumbling block with regard to the implementation of an efficient platinum recovery process, then it represents knowledge that is necessary and must be acquired.
- The selective recovery of platinum, without the presence of co-sorbed inorganic ions such as chloride or sulphate, is the ultimate goal of a recovery process of this nature. It may therefore be necessary to investigate methods for the pretreatment of the wastewater in order to remove these contaminants. This would have a twofold advantage, as the resultant effluent may be of a quality suitable for reuse within the refinery or even for discharge to the environment or municipal sewer system.
- Alternatives to the biosorption technique must be considered. Johnson-Matthey, a world leader in PGM-related technology, have developed a range of products, jointly called Smopex® scavengers, which are polyolefin-based fibres with metal binding properties. These fibres can achieve excellent recovery efficiencies (> 95 %), are robust, easy to handle, and do not require any adjustments to pre-existing process design. However, the

product is extremely expensive (approximately £100/kg (Plint, 2007, pers. comm.)) requiring that the financial and technical advantages and disadvantages be carefully weighed before implementation of this technology.

Overall, it can be recommended that biosorption technology, due to persisting problems with application to complex industrial wastewaters, may not be the current best available alternative to the existing recovery strategies for the reclamation of PGMs from PMR wastewaters. However, this could change when more information is obtained regarding the composition and speciation of the wastewater. This information would make it possible to prime the wastewater, thus optimizing it for successful metal sorption.

REFERENCES

- Aarden, F.B. (2001) Adsorption onto heterogenous porous materials: Equilibria and kinetics. PHD thesis. Technical University of Eindhoven, Germany.
- Aksu, Z. and Dönmez, G. (2001) Comparison of copper(II) biosorptive properties of live and treated *Candida* sp. *Journal of Environmental Science and Health A* **36(3)**, 367-381.
- Aksu, Z. and Dönmez, G. (2006) Binary biosorption of cadmium(II) and nickel(II) onto dried *Chlorella vulgaris*: Co-ion effect on mono-component isotherm parameters. *Process Biochemistry* **41**, 860-868.
- Aksu, Z., Çağatay, S.S. and Gönen, F. (2007) Continuous fixed bed biosorption of reactive dyes by dried *Rhizopus arrhizus*: Determination of column capacity. *Journal of Hazardous Materials* **143**, 362-371.
- Aksu, Z., Eğretli, G. and Kutsal, T. (1998) A comparative study of copper(II) biosorption on Ca-alginate, agarose and immobilized *C. vulgaris* in a packed-bed column. *Process Biochemistry* **33(4)**, 393-400.
- Al-Bazi, S.J. and Chow, A. (1984) Platinum metals – solution chemistry and separation methods (ion exchange and solvent extraction). *Talanta* **31(10A)**, 815-836.
- Alhakawati, M.S. and Banks, C.J. (2004) Removal of copper from aqueous solution by *Ascophyllum nodosum* immobilized in hydrophilic polyurethane foam. *Journal of Environmental Management* **72(4)**, 195-204.
- Al-Rub, F.A., El-Naas, M.H., Ashour, I., Al-Marzouqi, M. (2006) Biosorption of copper on *Chlorella vulgaris* from single, binary and ternary metal aqueous solutions. *Process Biochemistry* **41**, 457-464.
- Al-Rub, F.A.A., El-Naas, M.H., Benyahia, F. and Ashour, I. (2004) Biosorption of nickel on blank alginate beads, free and immobilized algal cells. *Process Biochemistry* **39(11)**, 1767-1773.
- Anglo Platinum PLC. (2005) www.angloplatinum.com (accessed 15/07/07).
- APHA, AWWA and WEF (1998) Standard methods for the examination of water and wastewater (20th Edition). APHA, Washington DC.
- Aquino, L.C.L., Miranda, E.A., Duarte, I.S., Rosa, P.T.V. and Bueno, S.M.A. (2003) Adsorption of human immunoglobulin G onto methacrylate and histidine-linked methacrylate. *Brazilian Journal of Chemical Engineering* **20(3)**, 251-262.
- Arica, M.Y. and Bayramoğlu, G. (2005) Cr(VI) biosorption from aqueous solutions using free and immobilized biomass of *Lentinus sajor-caju*: preparation and kinetic characterization. *Colloids and Surfaces A: Physicochemical and Engineering Aspects* **253 (1-3)**, 203-211.
- Arica, M.Y., Bayramoğlu, G., Yilmaz, M., Bektaş, S., Genç, O. (2004) Biosorption of Hg²⁺, Cd²⁺, and Zn²⁺ by Ca-alginate and immobilized wood-rotting fungus *Funalia trogii*. *Journal of Hazardous Materials* **B109**, 191-199.
- Arrascue, M.L., Garcia, H.M., Horna, O. and Guibal, E. (2003) Gold sorption on chitosan derivatives. *Hydrometallurgy* **71**, 191-200.
- Bahadir, T., Bakan, G., Altas, L. and Buyukgungor, H. (2007) The investigation of lead removal by biosorption: An application at storage battery industry wastewaters. *Enzyme and Microbial Technology* **41**, 98-102.

- Bai RS and Abraham TE. (2001) Biosorption of Cr(VI) from aqueous solution by *Rhizopus nigrificans*. *Bioresource Technology* **79**, 73–81.
- Barrera, H., Ureña-Núñez, F., Bilyeu, B. and Barrera-Díaz, C. (2006) Removal of chromium and toxic ions present in mine drainage by *Ectodermis of Opuntia*. *Journal of Hazardous Materials* **B136**, 846-853.
- Basci, N., Kocadagistan, E. and Kocadagistan, B. (2004) Biosorption of copper(II) from aqueous solutions by wheat shells. *Desalination* **164**, 135-140.
- Bayramoğlu, G., Bektaş, S. and Arıca, M.Y. (2003) Biosorption of heavy metal ions on immobilized white-rot fungus *Trametes versicolor*. *Journal of Hazardous Materials* **101(3)**, 285-300.
- Beolchini, F., Pagnanelli, F., Toro, L. and Vegliò, F. (2003) Biosorption of copper by *Sphaerotilus natans* immobilised in polysulfone matrix: equilibrium and kinetic analysis. *Hydrometallurgy* **70 (1-3)**, 101-112.
- Bernardis, F.L., Grant, R.A. and Sherrington, D.C. (2005) A review of methods of separation of platinum-group metals through their chloro-complexes. *Reactive and Functional Polymers* **65**, 205-217.
- Bhainsa KC, and D'Souza SF. (1999) Biosorption of uranium(VI) by *Aspergillus fumigatus*. *Biotechnology Techniques* **13**, 695-99.
- Bingol, A., Uzun, H., Bayhan, Y.K., Karagunduz, A., Cakici, A. and Keskinler, B. (2004) Removal of chromate anions from aqueous streams by a cationic surfactant-modified yeast. *Bioresource Technology* **94**, 245-249.
- Blanco, A., Sanz, B., Llama, M.J. and Serra, J.L. (1999) Biosorption of heavy metals to immobilized *Phormidium laminosum* biomass. *Journal of Biotechnology* **69(2-3)**, 227-240.
- Breierová, E., Vajcziková, I., Sasinková, V., Stratilová, E., Fišera, M., Gregor, T. and Šajbidor, J. (2002) Biosorption of cadmium ions by different yeast species. Biohydrometallurgy Conference, Cape Town, South Africa.
- Çabuk, A., Akar, T., Tunali, S., Gedikli, S. (2007) Biosorption of Pb(II) by industrial strain of *Saccharomyces cerevisiae* immobilized on the biomatrix of cone biomass of *Pinus nigra*: equilibrium and mechanism analysis. *Chemical Engineering Journal* **131 (1–3)**, 293–300.
- Carrilho, E.N.V.M., Nóbrega, J.A. and Gilbert, T.R. (2003) The use of silica-immobilized brown alga (*Pilayella littoralis*) for metal preconcentration and determination by inductively coupled plasma optical emission spectrometry. *Talanta* **60 (6)**, 1131-1140.
- Çeribasi, I.H. and Yetis, Ü., 2001. Biosorption of Ni(II) and Pb(II) by *Phanerochaete chrysosporium* from a binary metal system – Kinetics. *Water SA* **27(1)**, 15-20.
- Chassary, P., de Vargas Parody, I., Ruiz, M., Macaskie, L., Sastre, A. and Guibal, E. (2005a) Platinum and palladium recovery from dilute acidic solutions using sulfate reducing bacteria and chitosan derivative materials. Biohydrometallurgy Conference, Cape Town, South Africa.
- Chassary, P., Vincent, T., Marcano, J.S. and Macaskie, L.E. (2005b) Palladium and platinum recovery from bicomponent mixtures using chitosan derivatives. *Hydrometallurgy* **76**, 131-147.
- Chen, C. and Wang, J. (2007) Removal of Pb²⁺, Ag²⁺ and Sr²⁺ from aqueous solution by brewery's waste biomass. doi:10.1016/j.jhazmat.2007.05.046.

- Cho, D.H. and Kim, E.Y. (2003) Characterization of Pb²⁺ biosorption from aqueous solution by *Rhodoturula glutinis*. *Bioprocess and Biosystems Engineering* **25**, 271-277.
- Chu, K.H. (2004) Improved fixed bed models for metal biosorption. *Chemical Engineering Journal* **97**, 233-239.
- Coates, J. (2000) Interpretation of infrared spectra, a practical approach. In: Meyers, R.A. (Ed) *Encyclopedia of Analytical Chemistry*. John Wiley and Sons Ltd, Chichester, 10815-10837.
- Cole, P.M., Sole, K.C. and Feather, A.M. (2006) Solvent extraction developments in Southern Africa. *Tsinghua Science and Technology* **11(2)**, 153-159.
- Corvalan, S.M., Ortiz, I. and Eliceche, A.M. (2004) Optimal design for membrane processes for wastewater treatment and metal recovery. *Computers and Chemical Engineering* **28**, 103-109.
- Dahiya, S., Tripathi, R.M. and Hegde, A.G. (2008) Biosorption of lead and copper from aqueous solutions by pre-treated crab and arca shell biomass. *Bioresource Technology* **99**, 179-187.
- Darnall, D.W., Greene, B., Hosea, M., McPherson, R.A., Henzl, M. and Alexander, M.D. (1986) Trace metal removal from aqueous solutions, In: *The Industrial Division of the Royal Society of Chemistry, Vol.IV. Series*. Thompson, R. (Ed.), Whitstable Litho, Whitstable, Kent, England.
- Deng, L., Su, Y., Su, H., Wang, X. and Zhu, X. (2007) Sorption and desorption of lead(II) from wastewater by green algae *Cladophora fascicularis*. *Journal of Hazardous Materials* **143**, 220-225.
- Deng, S. and Ting, Y-P. (2005) Characterization of PEI-modified biomass and biosorption of Cu(II), Pb(II) and Ni(II). *Water Research* **39**, 2167-2177.
- Diels, L., van Roy, S., Mergeay, M., Doyen, W., Taghavi, S. and Leyson, R. (1993) Immobilization of bacteria in composite membranes and development of tubular membrane reactors for heavy metal recuperation. *3rd International Conference on Effective Membrane Processes – New Perspectives*. Mechanical Engineering Publications Limited. UK.
- Douglas, B., McDaniel, D. and Alexander, J. (1994) *Concepts and models of inorganic chemistry (3rd Edition)*. John Wiley and Sons, Inc. New York, USA.
- Dziwulska, U., Bajguz, A. and Godlewska-Żyłkiewicz, B. (2004) The use of algae *Chlorella vulgaris* immobilized on Cellex-T support for separation/preconcentration of trace amounts of platinum and palladium before GFAAS determination. *Analytical Letters* **37(10)**, 2189-2203.
- Dzombak, D.A. and Morel, F.M.M. (1990) *Surface complexation modelling: hydrous ferric oxide*. Wiley, New York.
- El Bayoumy, M.E., Bewtra, J.K., Ali, H.I. and Biswas, N. (1999) Removal of heavy metals and COD by SRB in UAFF reactor. *Journal of Environmental Engineering* **June**, pp. 532-539.
- El-Naas, M.H., Abu Al-Rub, F., Ashour, I., Al-Marzouqi, M. (2006) Effect of competitive interference on the biosorption of lead(II) by *Chlorella vulgaris*. *Chemical Engineering and Processing* **46(12)**, 1391-1399.
- Esposito, A., Pagnanelli, F. and Vegliò, F. (2002) pH-related equilibria models for biosorption in single metal systems. *Chemical Engineering Sciences* **57**, 307-313.
- Fiol N, Villaescusa I, Martínez M, Miralles N, Poch J and Serarols J. (2006) Sorption of Pb(II), Ni(II), Cu(II) and Cd(II) from aqueous solution by olive stone waste. *Separation and Purification Technology* **50**, 132-40.

- Fujiwara, K., Ramesh, A., Maki, T. Hasegawa, H. and Ueda, K. (2007) Adsorption of platinum (IV), palladium (II) and gold (III) from aqueous solutions onto l-lysine modified crosslinked chitosan resin. *Journal of Hazardous Materials* **146**, 39-50.
- Gamez, G., Gardea-Torresdey, J.L., Tiemann, K.J., Parsons, J., Dokken, K. and Yacaman, M.J. (2003) Recovery of gold(III) from multi-elemental solutions by alfalfa biomass. *Advances in Environmental Research* **7**, 563-71.
- Gholivand, M.B. and Nozari, N. (2000) Extraction and spectrophotometric determination of trace amounts of Pd(II) with 2,2'-dithiodianiline. *Talanta* **52(6)**, 1055-1060.
- Ghoul, M., Bacquet, M. and Morcellet, M. (2003) Uptake of heavy metals from synthetic aqueous solutions using modified PEI-silica gels. *Water Research* **37**, 729-734.
- Godlewska-Żyłkiewicz, B. (2003). Biosorption of platinum and palladium for their separation/preconcentration prior to graphite furnace atomic absorption spectrometric determination. *Spectrochimica Acta Part B: Atomic Spectroscopy* **58(8)**, 1531-1540.
- Godlewska-Żyłkiewicz, B. and Kowłowska, M. (2005) Solid phase extraction using immobilized yeast *Saccharomyces cerevisiae* for determination of palladium in road dust. *Analytica Chimica Acta* **539**, 61-67.
- Göksungur, Y., Üren, S. and Güvenç, U. (2003) Biosorption of copper ions by caustic treated waste baker's yeast biomass. *Tr. J. Biology* **27**, 23-29.
- Göksungur, Y., Üren, S. and Güvenç, U. (2005) Biosorption of cadmium and lead ions by ethanol treated waste baker's yeast biomass. *Bioresource Technology* **96(1)**, 103-109.
- Goyal, N., Jain, S.C. and Banerjee, U.C. (2003) Comparative studies on the microbial adsorption of heavy metals. *Advances in Environmental Research* **7**, 311-319.
- Grün, C.H. (2003) Structure and Biosynthesis of Fungal α -Glucans. Ph.D. dissertation, University of Utrecht, Netherlands.
- Guibal, E. (2004) Interactions of metal ions with chitosan-based sorbents: a review. *Separation and Purification Technology* **38**, pp. 43-74.
- Guibal, E., Larkin, A., Vicent, T. and Tobin, J.M. (1999) Platinum recovery on chitosan-base sorbents. *Process Metallurgy* **9(2)**, 265-275.
- Guibal, E., Von Offenber Sweeney, N., Vincent, T. and Tobin, J.M. (2002) Sulphur derivatives of chitosan for palladium sorption. *Reactive and Functional Polymers* **50**, 149-63.
- Guibal, E., Von Offenber Sweeney, N., Zikan, M.C., Vincent, T. and Tobin, J.M. (2001) Competitive sorption of platinum and palladium on chitosan derivatives. *International Journal of Biological Macromolecules* **28**, 401-408.
- Gupta, R., Ahuja, P., Khan, S., Saxena, R.K. and Mohapatra, H. (2000) Microbial biosorbents: Meeting challenges of heavy metal pollution in aqueous solutions. *Current Science* **78(8)**, 967-973.
- Han, R., Ding, D., Xu, Y., Zou, W., Wang, Y., Li, Y. and Zou, L. (2007a) Use of rice husk for the adsorption of congo red from aqueous solutions in column mode. *Bioresource Technology*, doi:10.1016/j.biortech.2007.06.027
- Han, R., Zhang, J., Zou, W., Xiao, H., Shi, J. and Liu, H. (2006) Biosorption of copper(II) and lead(II) from aqueous solution by chaff in a fixed-bed column. *Journal of Hazardous Materials* **B133**, 262-268.

- Han, R., Zou, W., Yu, W., Cheng, S., Wang, Y. and Shi, J. (2007b) Biosorption of methylene blue from aqueous solution by fallen phoenix tree's leaves. *Journal of Hazardous Materials* **141**, 156-162.
- Hao, O.J. (2000) Metal effects on sulfur cycle bacteria and metal removal by sulfate reducing bacteria. In: *Environmental technologies to treat sulfur pollution*. Lens, P.N.L. and Hulshoff Pol, L. (Eds). IWA Publishing, London. pp. 393-414.
- He, L.M. and Tebo, B.M. (1998) Surface charge properties of and Cu(II) adsorption by spores of the marine *Bacillus* sp. strain SG-1. *Applied and Environmental Microbiology* **64** (3), 1123-1129.
- Ho, Y.-S. (2006) Review of second-order models for adsorption systems. *Journal of Hazardous Materials* **B136**, 681-689.
- Ho, Y.S., Porter, J.F. and McKay, G. (2002) Equilibrium isotherm studies for the sorption of divalent metal ions onto peat: copper, nickel and lead single component systems. *Water, Air and Soil Pollution* **141**, 1-33.
- Iglesias, M., Anticó, E. and Salvadó, V. (1999) Recovery of palladium(II) and gold(III) from diluted liquors using the resin duolite GT-73. *Analytica Chimica Acta* **381**, 61-67.
- Ishikawa S-I, Suyama K, Arihara K and Itoh M. (2002) Uptake and recovery of gold ions from electroplating wastes using eggshell membrane. *Bioresource Technology* **81**, 201-206.
- Jalali, R., Ghafourian, H., Asef, Y., Davarpanah, S.J. and Sepehr, S. (2002) Removal and recovery of lead using nonliving biomass of marine algae. *Journal of Hazardous Materials* **B29**, 253-262.
- Jianlong, W. (2002) Biosorption of copper(II) by chemically modified biomass of *Saccharomyces cerevisiae*. *Process Biochemistry* **37**, 847-850.
- Johnson-Matthey (2003). Platinum Today. www.platinum.matthey.com (accessed 03/02/2003)
- Johnson-Matthey. Platinum 2002 Interim Review. www.platinum.matthey.com (accessed 03/02/2003)
- Kaduková, J. and Virčiková, E. (2005) Comparison of differences between copper bioaccumulation and biosorption. *Environment International* **31**, 227-232.
- Kaewpravit, C., Hequet, E., Abidi, N. and Gurlot, J.P. (1998) Quality Measurements: Application of methylene blue adsorption to cotton fibre specific surface area measurement: Part 1. Methodology. *The Journal of Cotton Science* **2**, 164-173.
- Kaewsarn, P., Yu, Q. and Ma, W. (2001) Interference of co-ions in biosorption of Cu²⁺ by biosorbent from marine alga *Durvillaea potatorum*. *Environmental Engineering Science* **18**(2), 99-104.
- Kaksonen, A.H., Riekkola-Vanhanen, M-L. and Puhakka, J.A. (2003) Optimization of metal sulphide precipitation in fluidized-bed treatment of acidic wastewater. *Water Research* **37**, pp. 255-266.
- Kapoor, A. and Viraraghavan, T. (1995) Fungal biosorption – an alternative treatment option for heavy metal bearing wastewaters: a review. *Bioresource Technology* **53**, 195-206.
- Kapteyn, J.C., Montijn, R.C., Vink, E., de la Cruz, J., Llobell, A., Douwes, J.E., Shimoi, H., Lipke, P.N. and Klis, F.M. (1996) Retention of *Saccharomyces cerevisiae* cell wall proteins through a phosphodiester-linked β -1,3- β -1,6-glucan heteropolymer. *Glycobiology* **6**, 337-345.

- Khoo, K.-M. and Ting, Y.-P. (2001) Biosorption of gold by immobilized fungal biomass. *Biochemical Engineering Journal* **8**, 51-59.
- Kim, Y.H. and Nakano, Y. (2005) Adsorption mechanism of palladium by redox within condensed-tannin gel. *Water Research* **39**, 1324-1330.
- Klis, F.M., Mol, P., Hellingwerf, K. and Brul, S. (2002) Dynamics of cell wall structure in *Saccharomyces cerevisiae*. *FEMS Microbiology Reviews* **26**, 239-256.
- Kramer, J., Driessen, W.L., Koch, K.R. and Reedijk, J. (2004) Highly selective and efficient recovery of Pd, Pt and Rh from precious metal-containing industrial effluents with silica-based (poly)amine ion exchangers. *Separation Science and Technology* **39(1)**, 63-75.
- Kramer, J. and Koch, K.R. (2006) ^{195}Pt NMR study of the speciation and preferential extraction of Pt(IV)-mixed halide complexes by diethylenetriamine-modified silica-based anion exchangers. *Inorganic Chemistry* **45**, 7843-7855.
- Kumari, K., Abraham, T.E., 2007. Biosorption of anionic textile dyes by nonviable biomass of fungi and yeast. *Bioresource Technology* **98**, 1704–1710.
- Kurniawan, T.A., Chan, G.Y.S., Lo, W.H. and Babel, S. (2006) Physico-chemical treatment techniques for wastewater laden with heavy metals. *Chemical Engineering Journal* **118**, 83-98.
- Kuroda, K. and Ueda, M. (2003) Bioadsorption of cadmium ion by cell surface-engineered yeasts displaying metallothionein and hexa-His. *Applied Microbiology and Biotechnology* **63**, 182-186.
- Kuroda, K., Ueda, M., Shibasaki, S. and Tanaka, A. (2002) Cell surface-engineered yeast with ability to bind, and self-aggregate in response to copper ion. *Applied Microbiology and Biotechnology* **59**, 259-264.
- Kuyucak, N. and Volesky, B. (1990) Biosorption by algal biomass. In: Biosorption of heavy metals. Volesky, B. (Ed). CRC Press, Boca Raton, Florida, USA, 174-198.
- Lee, J.D. (1991) Concise inorganic chemistry. 4th Edition. Chapman and Hall, London.
- Li, Q., Wu, S., Liu, G., Liao, X., Deng, X., Sun, D., Hu, Y. and Huang, Y. (2004) Simultaneous biosorption of cadmium(II) and lead(II) ions by pretreated biomass of *Phanerochaete chrysosporium*. *Separation and Purification Technology* **34**, 135-142.
- Lin, Z., Wu, J., Xue, R. and Yang, M.Y. (2005) Spectroscopic characterization of Au^{3+} biosorption by waste biomass of *Saccharomyces cerevisiae*. *Spectrochimica Acta Part A* **61**, 761-765.
- Liu, Y., Xu, H., Yang, S-F. and Tay, J-H. (2003) A general model for biosorption of Cd^{2+} , Cu^{2+} and Zn^{2+} by aerobic granules. *Journal of Biotechnology* **102**, 233-239.
- Lodeiro, P., Cordero, B., Grille, Z., Herrero, R. and de Vincente, M.E.S. (2004) Physicochemical studies of cadmium(II) biosorption by the invasive alga in Europe, *Sargassum muticum*. *Biotechnology and Bioengineering* **88**, 237-247.
- Lodeiro, P., Herrero, R. and Sastre de Vincente, M.E. (2006) The use of protonated *Sargassum muticum* as biosorbent for cadmium removal in a fixed-bed column. *Journal of Hazardous Materials* **B137**, 244-253.
- López, M.L., Gardea-Torresdey, J.L. and Peralta-Videa, J.R. (2004) Study of calcium(II), copper(II), magnesium(II), and iron(III) interference on Au(III) binding to native hop biomass using ICP-OES. *Spectroscopy Letters* **37(2)**, 201-215.

- Lozovaya, O.G., Kasatkina, T.P., Podgorsky, V.S. and Fomina, M.A. (2005) Hexavalent chromium removal by yeasts biomass. Biohydrometallurgy Conference, Cape Town, South Africa.
- Lu, S. and Gibb, S.W. (2007) Copper removal from wastewater using spent-grain as biosorbent. *Bioresource Technology*, doi:10.1016/j.biortech.2007.04.024
- Ma, H., Liao, X., Liu, X. and Shi, B. (2006) Recovery of platinum(IV) and palladium(II) by bayberry tannin immobilized collagen fibre membrane from water solution. *Journal of Membrane Science* **278**, 373-380.
- Mack, C.L. (2005) Screening of technologies for the recovery of rhodium(III) metal ions from a precious metal refinery wastewater. MSc Thesis, Rhodes University, South Africa.
- Madrid Y and Cámara C. (1997) Biological substrates for metal preconcentration and speciation. *Trends in Analytical Chemistry* **16**, 36-44.
- Magnelli, P., Cipollo, J.F. and Abeijon, C. (2002) A refined method for the determination of *Saccharomyces cerevisiae* cell wall composition and β -1,6-glucan fine structure. *Analytical Biochemistry* **301**, 136-150.
- Mapolelo, M., Torto, N. and Prior, B. (2005) Evaluation of yeast strains as possible agents for trace enrichment of metal ions in aquatic environments. *Talanta* **65**, 930-937.
- Marques, P.A., Pinheiro, H.M., Teixeira, J.A., Rosa, M.F. (1999) Removal efficiency of Cu^{2+} , Cd^{2+} and Pb^{2+} by waste brewery biomass: pH and cation association effects. *Desalination* **124**, 137-144.
- Mohapatra, H. and Gupta, R. (2005) Concurrent sorption of Zn(II), Cu(II) and Co(II) by *Oscillatoria angustissima* as a function of pH in binary and ternary metal solutions. *Bioresource Technology* **96(12)**, 1387-1398.
- Mukhopadhyay, M., Noronha, S.B., Suraishkumar, G.K. (2007) Kinetic modelling for the biosorption of copper by pretreated *Aspergillus niger* biomass. *Bioresource Technology* **98**, 1781-1787.
- Mungasavalli, D.P., Viraraghavan, T. and Jin, Y-C. (2007) Biosorption of chromium from aqueous solutions by pretreated *Aspergillus niger*: Batch and column studies. *Colloids and Surfaces A: Physicochemical Engineering Aspects* **301**, 214-223.
- Muter, O., Lubinya, I., Millers, D., Grigorjeva, L., Ventinya, E. and Rapoport, A. (2002) Cr(VI) sorption by intact and dehydrated *Candida utilis* cells in the presence of other metals. *Process Biochemistry* **38**, 123-131.
- Nacèra, Y., Aicha, B. (2006) Equilibrium and kinetics modelling of methylene blue biosorption by pretreated dead *Streptomyces rimosus*: effect of temperature. *Chemical Engineering Journal* **119**, 121-125.
- Naddafi, K., Nabizadeh, R., Saeedi, R., Mahvi, A.H., Vaezi, F., Yaghmaeian, K., Ghasri, A. and Nazmara, S. (2007) Biosorption of lead(II) and cadmium(II) by protonated *Sargassum glaucescens* biomass in a continuous packed bed column. *Journal of Hazardous Materials*, **147**, 785-791.
- Naseem, R. and Tahir, S.S. (2001) Removal of Pb(II) from aqueous/acidic solutions by using bentonite as an adsorbent. *Water Research* **35**, 3982-3986.
- Nasernejad, B., Zadeh, T.E., Pour, B.B., Bygi, M.E. and Zamani, A. (2004) Comparison for biosorption modelling of heavy metals (Cr(III), Cu(II), Zn(II)) adsorption from wastewater by carrot residues. *Process Biochemistry* **40(3-4)**, 1319-1322.

- Niu, H. and Volesky, B. (2003) Characteristics of anionic metal species biosorption with waste crab shells. *Hydrometallurgy* **71**, 209-215.
- Ogata, T. and Nakano, Y. (2005) Mechanisms of gold recovery from aqueous solutions using a novel tannin gel adsorbent synthesized from natural condensed tannin. *Water Research* **39**, 4281-4286.
- Oguz, E., 2007. Equilibrium isotherms and kinetics studies for the sorption of fluoride on light weight concrete materials. *Colloids and Surfaces A: Physicochemical Engineering Aspects* **295**, 258-263.
- Özer A, Özer D and Ekíz HÍ. (2004) The equilibrium and kinetic modelling of the biosorption of copper(II) ions on *Cladophora crispata*. *Adsorption* **10**, 317-326.
- Özer, A. and Özer, D. (2003) Comparative study of the biosorption of Pb(II), Ni(II) and Cr(VI) ions onto *S. cerevisiae*: determination of biosorption heats. *Journal of Hazardous Materials* **B100**, 219-229.
- Padmavathy, V., Vasudevan, P. and Dhingra, S.C. (2003) Thermal and spectroscopic studies on sorption of nickel(II) ion on protonated baker's yeast. *Chemosphere* **52(10)**, 1807-1817.
- Pagnanelli, F., Petrangeli Papini, M., Toro, L. Trifoni, M. and Veglio, P. (2000) Biosorption of metal ions on *Arthrobacter* sp.: Biomass characterisation and biosorption modelling. *Environmental Science and Technology* **34**, 2773-2778.
- Pagnanelli, F., Esposito, A., Toro, L. and Vegliò, F. (2003) Metal speciation and pH effect on Pb, Cu and Cd biosorption onto *Sphaerotilus natans*: Langmuir-type empirical model. *Water Research* **37**, 627-633.
- Palmieri, M.C., Garcia Jr, O. and Melnikov, P. (2000) Neodymium biosorption from acidic solutions in batch systems. *Process Biochemistry* **36**, 441-444.
- Panda GC, Dasa SK, Chatterjee S, Maity PB, Bandopadhyay TS and Guha AK. (2006) Adsorption of cadmium on husk of *Lathyrus sativus*: Physico-chemical study. *Colloids and Surfaces* **B50**, 49-54.
- Park, D., Yun, Y-S. and Park, J.M. (2005) Use of dead fungal biomass for the detoxification of hexavalent chromium: screening and kinetics. *Process Biochemistry* **40**, 2559-2565.
- Parsons, J.G., Gardea-Torresdey, J.L., Tiemann, K.J. and Gamez, G. (2003) Investigation of trace level binding of PtCl₆ and PtCl₄ to alfalfa biomass (*Medicago sativa*) using Zeeman graphite furnace atomic absorption spectrometry. *Analytica Chimica Acta* **478**, 139-145.
- Pearson, R.G. (1968) Hard and soft acids and bases, HSAB, Part I Fundamental principles. *Journal of Chemical Education* **45**, 581-587.
- Peña-Castro, J.M., Martínez-Jeronimo, F., Esparza-García, F. and Cañizares-Villanueva, R.O. (2004) Heavy metals removal by the microalga *Scenedesmus incrassutulus* in continuous cultures. *Bioresource Technology* **94**, 219-222.
- Pethkar, A.V. and Paknikar, KM. (1998) Recovery of gold from solutions using *Cladosporium cladosporioides* biomass beads. *Journal of Biotechnology* **63**, 121-36.
- Pethkar, A.V., Kulkarni, S.K. and Paknikar, K.M. (2001) Comparative studies on metal biosorption by two strains of *Cladosporium cladosporioides*. *Bioresource Technology* **80**, 211-215.
- Pierce, R.A., Campbell-Kelly, R.P., Visser, A.E. and Laurinat, J.E. (2007) Removal of chloride from acidic solutions using NO₂. *Industrial and Engineering Chemistry Research* **46**, 2372-2376.

- Plint, N. (2007) Personal Communication.
- Preetha, B. and Viruthagiri, T. (2007) Batch and continuous biosorption of chromium(IV) by *Rhizopus arrhizus*. *Separation and Purification Technology* **57**, 126-133.
- Puranik, P.R. and Paknikar, K.M. (1999) Influence of co-cations of biosorption of lead and zinc – a comparative evaluation in binary and multimetal systems. *Bioresource Technology* **70**, 269-276.
- Rangsayatorn, N., Pokethitiyook, P., Upatham, E.S. and Lanza, G.R. (2004) Cadmium biosorption by cells of *Spirulina platensis* TISTR 8217 immobilized in alginate and silica gels. *Environment International* **30**, 57-63.
- Ravindra, K., Bencs, L. and van Grieken, R. (2004) Platinum group elements in the environment and their health risk. *The Science of the Total Environment* **318**, 1-43.
- Robinson, D. (2002) Personal Communication.
- Romero-González ME, Williams CJ, Gardiner PE, Gurman SJ and Habesh S. (2003) Spectroscopic studies of the biosorption of gold(III) by dealginated seaweed waste. *Environmental Science and Technology* **37**, 4163-4169.
- Ruiz, M., Sastre, A.M. and Guibal, E. (2000) Palladium sorption on glutaraldehyde crosslinked chitosan. *Reactive and Functional Polymers* **45**, 155-173.
- Sağ, Y. and Kutsal, T. (2000) Determination of the biosorption heats of heavy metal ions on *Zoogloea ramigera* and *Rhizopus arrhizus*. *Biochemical Engineering Journal* **6**, 145-51.
- Saglam A., Yalcinkaya Y., Denizli A., Arica M.Y., Genc O. and Bektas S. (2002) Biosorption of mercury by carboxylcellulose and immobilized *Phanerochaete chrysosporium*. *Microchemical Journal* **71**, 73–81.
- Salinas, E., de Orellano, M.E., Rezza, I., Martinez, L., Marchesvky, E. and de Tosetti, M.S. (2000) Removal of cadmium and lead from dilute aqueous solutions by *Rhodoturulula rubra*. *Bioresource Technology* **72**, 107-112.
- Sankararamkrishnan, N., Sharma, A.K. and Sanghi, R. (2007) Novel chitosan derivative for the removal of cadmium in the presence of cyanide from electroplating wastewater. *Journal of Hazardous Materials* **148**, 353-359.
- Sanyahumbi, D., de Vargas, I., Climo, M., Mabbett, A.N., Yong, P. and Macaskie, L.E. (2005) Selective biosorption of palladium and platinum from bi- and multi-metallic solutions. In: Harrison, S.T.L., Rawlings, D.E., Peterson, J. (Eds) *Proceedings of the 16th International Biohydrometallurgy Symposium*, Cape Town, South Africa, 571-579.
- Schiewer, S. (1999) Modelling complexation and electrostatic attraction in heavy metal biosorption by *Sargassum* biomass. *Journal of Applied Phycology* **11**, 79-87.
- Schneider, I.A.H., Rubio, J. and Smith, R.W. (2001) Biosorption of metals onto plant biomass: exchange adsorption or surface precipitation? *International Journal of Mineral Processing* **62**, 111-120.
- Seki, H., Suzuki, A. and Maruyama, H. (2005) Biosorption of chromium(VI) and arsenic(V) onto methylated yeast biomass. *Journal of Colloid and Interface Science* **281**, 261-266.
- Senthilkumar, R., Vijayaraghavan, K., Thilakavathi, M., Iyer, P.V.R. and Velan, M. (2007) Application of seaweeds for the removal of lead from aqueous solution. *Biochemical Engineering Journal* **33**, 211-216.

- Sheng, P.X., Ting, Y-P., Chen, J.P. and Hong, L. (2004) Sorption of lead, copper, cadmium, zinc and nickel by marine algal biomass: characterization of biosorptive capacity and investigation of mechanisms. *Journal of Colloid and Interface Science* **275**, 131-141.
- SiliconFarEast.com. (2001) FTIR Spectroscopy. www.siliconfareast.com/FTIR.htm
- Skountzou, P., Soupioni, M., Bekatorou, A., Kanellaki, M., Koutinas, A.A., Marchant, R. and Banat, I.M. (2003) Lead(II) uptake during baker's yeast production by aerobic fermentation of molasses. *Process Biochemistry* **38**, 1479-1482.
- Stoll, A. (1996) Bioaccumulation of heavy metals by the yeast *S.cerevisiae* and the bioremediation of industrial waste water. PhD Thesis, Rhodes University, South Africa.
- Stoll, A. and Duncan, J.R. (1997) Comparison of the heavy metal sorptive properties of three types of immobilized, non-viable *Saccharomyces cerevisiae* biomass. *Process Biochemistry* **32(6)**, 467-472.
- Sujana, M.G., Thakur, R.S. and Rao, S.B. (1998) Removal of fluoride from aqueous solution by using alum sludge. *Journal of Colloid and Interface Science* **206**, 94-101.
- Szabo, S., Lindo, K. and Yee, B. (2006) Enumeration and size distribution of yeast cells in the brewing industry. www.beckmancoulter.com/literature/Bioresearch/A-2046A.pdf.
- Tan, T.W. and Cheng, P. (2003) Biosorption of metal ions with *Penicillium chrysogenum*. *Applied Biochemistry and Biotechnology* **104(2)**, 119-128.
- Tarley, C.R.T. and Arruda, M.A.Z. (2004) Biosorption of heavy metals using rice-milling by-products. Characterisation and application for removal of metals from aqueous effluents. *Chemosphere* **54**, 987-995.
- Tobin, J.M., L'homme, B. and Roux, J.C. (1993) Immobilization protocols and effects on cadmium uptake by *Rhizopus arrhizus*. *Biotechnology Techniques* **7(10)**, 739-744.
- Torres, E., Mata, Y.N., Blázquez, M.L., Muñoz, J.A., González, F. and Ballester, A. (2005) Gold and silver uptake and nanoprecipitation on calcium alginate beads. *Langmuir* **21**, 7951-7958.
- Tsezos, M. and Volesky, B. (1982a) The mechanism of uranium biosorption by *Rhizopus arrhizus*. *Biotechnology and Bioengineering* **24**, 385-401.
- Tsezos, M. and Volesky, B. (1982b) The mechanism of thorium biosorption by *Rhizopus arrhizus*. *Biotechnology and Bioengineering* **24**, 955-969.
- Tsezos, M., Remoudaki, E. and Angelatou, V. (1996) A study of the effects of competing ions on biosorption of metals. *International Biodeterioration and Biodegradation* **38(1)**, 19-29.
- Ucun, H., Bayhan, Y.K., Kaya, Y., Cakici, A. and Algur, O.F. (2002) Biosorption of chromium(VI) from aqueous solution by cone biomass of *Pinus sylvestris*. *Bioresource Technology* **85**, 155-158.
- Ucun, H., Bayhan, Y.K., Kaya, Y., Cakici, A. and Algur, O.F. (2003) Biosorption of lead(II) from aqueous solution by cone biomass of *Pinus sylvestris*. *Desalination* **154**, 233-238.
- Uheida, A., Iglesias, M., Fontàs, C., Hidalgo, M., Salvadó, V., Zhang, Y. and Muhammed, M. (2006) Sorption of palladium(II), rhodium(III) and platinum(IV) on Fe₃O₄ nanoparticles. *Journal of Colloid and Interface Science* **301**, 402-408.
- Uslu, G. and Tanyol, M. (2006) Equilibrium and thermodynamic parameters of single and binary mixture biosorption of lead (II) and copper (II) ions onto *Pseudomonas putida*: Effect of temperature. *Journal of Hazardous Materials* **B135**, 87-93.

- Vadivelan, V. and Vasanth Kumar, K., 2005. Equilibrium, kinetics, mechanism, and process design for the sorption of methylene blue onto rice husk. *Journal of Colloid and Interface Science* **286**, 90-100.
- Valdman, E., Erijman, L., Pessoa, F.L.P. and Leite, S.G.F. (2001) Continuous biosorption of Cu and Zn by immobilized waste biomass *Sargassum* sp. *Process Biochemistry* **36**, 869-873.
- Valdman, E. and Leite, S.G.F. (2000) Biosorption of Cd, Zn and Cu by *Sargassum* sp. waste biomass. *Bioprocess Engineering* **22(2)**, 171-173.
- van Hullebusch, E.D., Gieteling, J., Zhang, M., Zandvoort, M.H., Van Daele, W., Defrancq, J. and Lens, P.N.L. (2005) Cobalt sorption onto anaerobic granular sludge: Isotherm and spatial localization analysis. *Journal of Biotechnology* **121(2)**, 227-240.
- Vasudevan, P. Padmavathy, V. and Dhingra, S.C. (2002) Biosorption of monovalent and divalent ions on baker's yeast. *Bioresource Technology* **82**, 25-289.
- Vasudevan, P., Padmavathy, V. and Dhingra, S.C. (2003) Kinetics of biosorption of cadmium on Baker's yeast. *Bioresource Technology* **89**, 281-287.
- Vegliò, F., Beolchini, F. and Prisciandoro, M. (2003) Sorption of copper by olive mill residues. *Water Research* **37**, 4895-4903.
- Venkata Mohan, S., Ramanaiah, S.V., Rajkumar, B., Sarma, P.N., 2007. Removal of fluoride from aqueous phase by biosorption onto algal biosorbent *Spirogyra* sp.-I02: sorption mechanism elucidation. *Journal of Hazardous Materials* **141**, 465-474.
- Vianna, L.N.L., Andrade, M.C. and Nicoli, J.R. (2000) Screening of waste biomass from *Saccharomyces cerevisiae*, *Aspergillus oryzae* and *Bacillus lentus* fermentations for removal of Cu, Zn and Cd by biosorption. *World Journal of Microbiology and Biotechnology* **16**, 437-440.
- Vijayaraghavan, K., Jegan, J., Palanivelu, K. and Velan, M. (2004) Removal of nickel(II) ions from aqueous solution using crab shell particles in a packed bed up-flow column. *Journal of Hazardous Materials* **B113**, 223-230.
- Volesky, B., 2001. Detoxification of metal-bearing effluents: biosorption for the next century. *Hydrometallurgy* **59**, 203-216.
- Volesky, B., 2003. Sorption and Biosorption. BV Sorbex, Inc. Canada
- Wang, L., Chua, H., Wong, P.K., Lo, W.L. and Yu, P.H.F. (2003) Ni²⁺ removal and recovery from electroplating effluent by *Pseudomonas putida* 5-x cell biomass. *Journal of Environmental Science and Health* **A38(3)**, 521-531.
- Wang, R., Liao, X. and Shi, B. (2005a) Adsorption behaviours of Pt(II) and Pd(II) on collagen fibre immobilized bayberry tannin. *Industrial Engineering and Chemical Research* **44**, 4221-4226.
- Wang, S., Zhu, Z.H., Coomes, A., Haghseresht, F. and Lu, G.Q. (2005b) The physical and surface chemical characteristics of activated carbons and the adsorption of methylene blue from wastewater. *Journal of Colloid and Interface Science* **284**, 440-446.
- Wang, J. and Chen, C. (2006) Biosorption of heavy metals by *Saccharomyces cerevisiae*: A review. *Biotechnology Advances* **24(5)**, 427-451.
- Wang, X-S. and Qin, Y. (2004) Equilibrium sorption isotherms for of Cu²⁺ on rice bran. *Process Biochemistry* **40(2)**, 677-680.

- White, C., Sayer, J.A. and Gadd, G.M. (1997) Microbial solubilisation and immobilisation of toxic metals: key biogeochemical processes for treatment of contamination. *FEMS Microbiology Reviews* **20**, pp. 503-516.
- Wilhelmi, B.S. and Duncan, J.R. (1995) Metal recovery from *Saccharomyces cerevisiae* biosorption columns. *Biotechnology Letters* **17(9)**, 1007-1012.
- Wong, K.K., Lee, C.K., Low, K.S. and Haron, M.J. (2003) Removal of Cu and Pb from electroplating wastewater using tartaric acid modified rice husk. *Process Biochemistry* **39(4)**, 437-445
- Yavuz, H., Denizli, A., Güngüneş, H., Safarikova, M. and Safarik, I. (2006) Biosorption of mercury on magnetically modified yeast cells. *Separation and Purification Technology* **52**, 253-260.
- Yokel, R.A., Lasley, S.M. and Dorman, D.C. (2006) The speciation of metals in mammals influences their toxicokinetics and toxicodynamics and therefore human health risk assessment. *Journal of Toxicology and Environmental Health, Part B* **9(1)**, 63 – 85.
- Yu, J., Tong, M., Sun, X. and Li, B. (2007) Biomass grafted with polyamic acid for enhancement of cadmium(II) and lead(II) biosorption. *Reactive and Functional Polymers* **67**, 564-572.

APPENDICES

APPENDIX A CALCULATION OF ISOTHERM MODEL PARAMETERS FROM RAW DATA

The data in Table A1 was obtained from an experiment performed as described in Section 6.3.1, and transformed as shown in the table headings. The transformed data was then used to plot the graphs shown in Figures A1 (Langmuir model, Eq. 6.7) and A2 (Freundlich model, Eq. 6.8).

Table A1 Raw data from an isotherm experiment at pH 1 and 20 °C.

	C_i	C_o	average C_i	q	C_i/q	average q	average C_i/q	$\log q$	$\log C_i$
pH 1	1.788	19.709	1.761	17.921	0.099	17.948	0.098	1.254	0.246
	1.647			18.062	0.091				
	1.849			17.86	0.104				
	2.836	36.85	2.829	34.014	0.083	34.021	0.083	1.532	0.452
	2.835			34.015	0.083				
	2.815			34.035	0.083				
	3.964	47.305	3.765	43.341	0.091	43.539	0.087	1.639	0.576
	3.467			43.838	0.079				
	3.865			43.44	0.089				
	7.523	83.686	6.884	76.163	0.099	76.802	0.089	1.885	0.838
	7.659			76.027	0.101				
	5.471			78.215	0.069				
	15.342	103.072	12.943	87.73	0.175	90.129	0.144	1.955	1.112
	12.509			90.563	0.138				
	10.978			92.094	0.119				
	23.717	134.28	23.302	110.563	0.215	110.978	0.210	2.045	1.367
	23.554			110.726	0.213				
	22.636			111.644	0.203				
	32.642	152.55	31.329	119.908	0.272	121.221	0.259	2.084	1.496
	28.726			123.824	0.232				
	32.618			119.932	0.272				
	47.909	180.991	49.544	133.082	0.359	131.447	0.377	2.119	1.695
	51.176			129.815	0.394				
	49.547			131.444	0.377				
	63.098	199.731	68.972	136.633	0.462	130.759	0.535	2.116	1.839
	81.977			117.754	0.696				
	61.841			137.89	0.448				

The equations of the linear regression lines in Figures A1 and A2 were then used to calculate the model parameters.

The linearized Langmuir isotherm is:

$$\frac{C_i}{q} = \frac{C_i}{Q_{\max}} + \frac{1}{Q_{\max} b} \quad (\text{Eq. A1})$$

The linearized Freundlich isotherm is:

$$\log q = \log K + \frac{1}{n} \log C_i \quad (\text{Eq. A2})$$

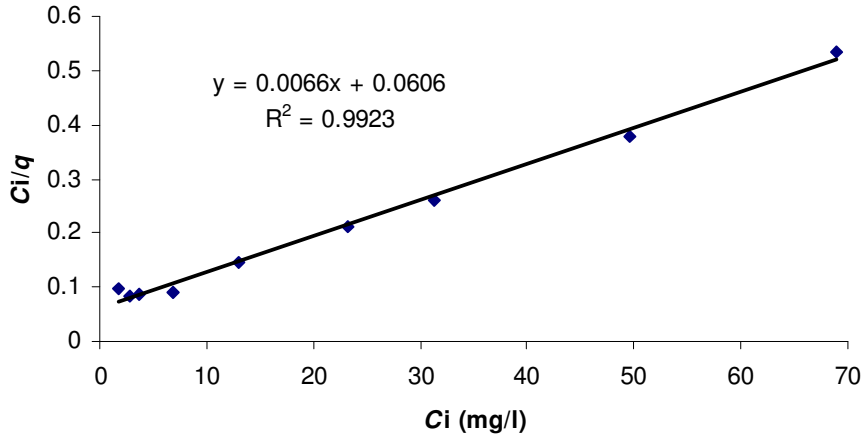


Figure A1 Transformed data fitted to the Langmuir isotherm model.

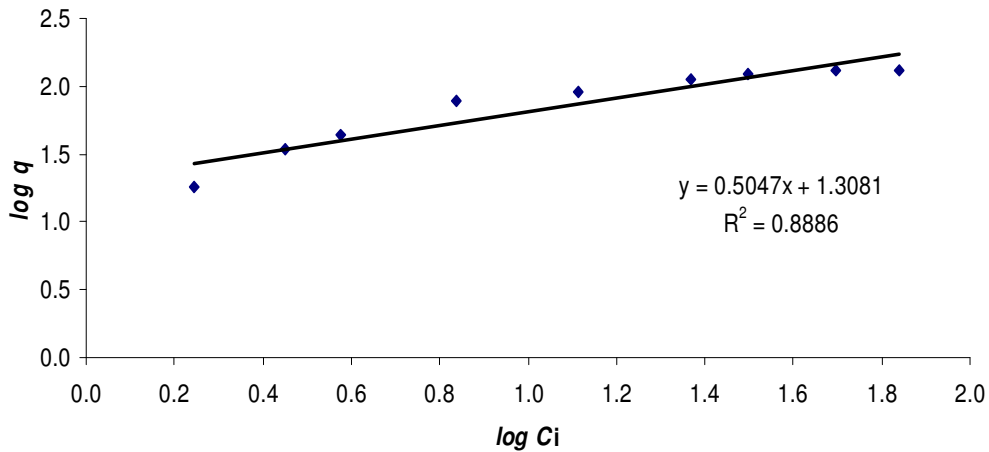


Figure A2 Transformed data fitted to the Freundlich model.

Substitution of the relevant information from the graphs into the linearized model equations allows for the calculation of the equilibrium parameters shown in Table B2.

Table A1 Equilibrium parameters calculated from the transformed and linearized data shown in **Table B1** and **Figures A1** and **A2**.

Q_{\max}	$1/b$	K	$1/n$
151.52	0.11	20.33	0.51

APPENDIX B WASTEWATER CHARACTERIZATION

The wastewater was characterized in order to identify the physical and chemical characteristics, and the concentration of these components in the wastewater.

Solids content (suspended and settleable) and acidity were measured according to Standard Methods (APHA *et al.*, 1998). Further measurements were made using colorimetric methods based on the principles of Standard Methods (APHA *et al.*, 1998): ammonia (Spectroquant kit 1.14752, analogous to method 4500-NH₃ G), chloride (Spectroquant kit 1.14897, analogous to method 4500-Cl E), COD (Spectroquant reagents 1.14679 and 1.14680, analogous to method 5220-COD D), nitrate (Spectroquant kit 1.14773) and sulphate (Spectroquant kit 1.14791). All kits were obtained from Merck, South Africa, and used according to their instructions. Results were obtained by using a Spectroquant Nova 60 photometer (South Africa). pH was measured using a Cyberscan 2500 meter (Eutech Instruments, Singapore). All metal concentration determinations were made using atomic absorption spectrophotometry (GBC 909 AA, Avanta, Australia). All metal standard solutions were prepared from 1000 mg/l stock solutions (EC Labs, South Africa) diluted with deionized water to the relevant concentrations. For all analyzes the reagents were of laboratory grade. All glassware was acid washed in 5 % HNO₃ and rinsed in distilled water before use.

Table B1 indicates the concentration of the inorganic non-metal and metal ion concentrations of a number of the components found within the wastewater. Of the non-metal components, the high concentration of chloride and sulphate and the high ammonium concentration are of most interest. In general, there is only a very small concentration of metal ions other than platinum in the wastewater. The high concentration of sodium along with the high concentration of chloride and sulphate indicate the high ionic strength of the wastewater.

Table B.1 Concentration of non-metal and metal components in the PMR wastewater (\pm SD, $n = 3$).

Non-metal Characteristic	Wastewater	Metal (mg/l)	Wastewater
Acidity (gCaCO ₃ /l)	3.67 \pm 0.12	Rhodium	< 0.1
Ammonium (g/l)	12.05 \pm 2.25	Gold	< 1
Chloride (M)	0.77 \pm 0.01	Palladium	< 0.1
COD (g/l)	6.85 \pm 0.85	Platinum	18.14 \pm 0.87
Nitrate (mg/l)	0.01 \pm 6.8 $\times 10^{-4}$	Cobalt	< 0.1
pH	1.2 – 1.5	Copper	0.325 \pm 0.09
Sulphate (M)	0.06 \pm 4.4 $\times 10^{-3}$	Iron	0.136 \pm 0.05
Settleable solids (mg/l)	4.00 \pm 0.5	Nickel	0.584 \pm 0.12
Suspended solids (mg/l)	166.10 \pm 0.02	Sodium (g/l)	2.08 \pm 0.16
		Lead	0
		Cadmium	0
		Zinc	4.41 \pm 0.08

The low pH and low contaminant metal concentration of the wastewater are advantageous to the sorption process. No pH adjustment is necessary prior to contacting the wastewater with the sorbent, and the metal ion sorbed in the highest proportion will be platinum. The inorganic content, however, may decrease the efficiency of the platinum sorption. The high ammonium concentration (a possible consequence of the amine extractant used in platinum solvent extraction) could influence the sorption of platinum by complexing with the platinum chlorocomplexes, producing species with severely reduced affinity for the sorbent. The nitrate and sulphate components, which carry negative charge, will compete directly with platinum for positively charged binding sites, and their relatively smaller size may further enhance their sorption over that of platinum. The chloride ions will act in a similar fashion to that of nitrate and sulphate ions, with one addition; the chloride concentration of the wastewater affects the speciation of the platinum chlorocomplexes within the wastewater, and so the high concentration may produce platinum chloro species with lower affinity for the sorbent than that of the platinum in a synthetic solution.